

2009

## Update to ANSI/ANS-6.4.3-1991 for low-Z and compound materials and review of particle transport theory

Luis Durani  
*University of Nevada Las Vegas*

Follow this and additional works at: <https://digitalscholarship.unlv.edu/thesesdissertations>



Part of the [Nuclear Engineering Commons](#)

---

### Repository Citation

Durani, Luis, "Update to ANSI/ANS-6.4.3-1991 for low-Z and compound materials and review of particle transport theory" (2009). *UNLV Theses, Dissertations, Professional Papers, and Capstones*. 43.  
<https://digitalscholarship.unlv.edu/thesesdissertations/43>

This Thesis is protected by copyright and/or related rights. It has been brought to you by Digital Scholarship@UNLV with permission from the rights-holder(s). You are free to use this Thesis in any way that is permitted by the copyright and related rights legislation that applies to your use. For other uses you need to obtain permission from the rights-holder(s) directly, unless additional rights are indicated by a Creative Commons license in the record and/or on the work itself.

This Thesis has been accepted for inclusion in UNLV Theses, Dissertations, Professional Papers, and Capstones by an authorized administrator of Digital Scholarship@UNLV. For more information, please contact [digitalscholarship@unlv.edu](mailto:digitalscholarship@unlv.edu).

UPDATE TO ANSI/ANS-6.4.3-1991 FOR LOW-Z AND  
COMPOUND MATERIALS AND REVIEW OF  
PARTICLE TRANSPORT THEORY

by

Luis A. Durani

Bachelor of Science, Mechanical Engineering  
Bachelor of Arts, Political Science  
University of Nevada, Las Vegas  
2008

A thesis submitted in partial fulfillment  
of the requirements for the

**Master of Science Degree in Materials and Nuclear Engineering**  
**Department of Mechanical Engineering**  
**Howard R. Hughes College of Engineering**

**Graduate College**  
**University of Nevada, Las Vegas**  
**August 2009**

## ABSTRACT

### **Update to ANSI/ANS-6.4.3-1991 for Low-Z Materials and Compound Materials and Review of Particle Transport Theory**

by

Luis A. Durani

Dr. Charlotta Sanders, Examination Committee Co-Chair  
Professor of Nuclear Engineering  
University of Nevada, Las Vegas

Dr. Brendan O'Toole, Examination Committee Co-Chair  
Professor of Mechanical Engineering  
University of Nevada, Las Vegas

The ANSI/ANS-6.4.3-1991 Gamma-Ray Attenuation Coefficients and Buildup Factors for Engineering Materials Standard (herein known as ANS Standard), contains derived gamma-ray attenuation coefficients and buildup factors for selected engineering materials and elements for use in shielding calculations (ANSI/ANS-6.1.1, 1991). The current status of the ANS Standard is withdrawn due to the lack of any updates since its last publication. Since the last update of the ANS standard, more accurate codes for particle transport and cross sectional data have become available. As a result, this study was carried out to update gamma-ray buildup factors for iron and water as a function of source energy that are presented in ANS Standard by using ENDF/B-VI.8 photo-atomic cross-section library data in Monte Carlo N Particle 5 (MCNP5) version 1.40. Another code, Anisotropic Source-Flux Iteration Technique (ASFIT), was used as a benchmarking tool to validate the MCNP5 results. The results from MCNP5 did vary from those of the ANS Standard with the greatest differences for iron and water being 10.48% and 13.83%, respectively. These differences can be attributed to the following:

- Differences in cross section libraries
- Method of solution for the codes
- Physics Assumptions
  - Bremsstrahlung
  - Coherent Scattering
- Calculation methods
- Standard deviation

To obtain buildup factors for points not calculated, fittings were calculated using a fitting function technique. After the buildup factor for each source energy was plotted as a function of mean free path (mfp), the data was fitted via Microsoft Excel. The fitting method chosen for each was a polynomial of the sixth order to ensure the highest accuracy and closest to 1 value for the regression coefficient,  $R^2$ . Tables and figures representing energy absorption buildup factors and fitting functions are attached to this study.

## TABLE OF CONTENTS

ABSTRACT .....	iii
ACKNOWLEDGEMENTS .....	xv
CHAPTER 1 INTRODUCTION .....	1
Purpose of the Study .....	1
Concepts and Terms.....	2
Significance of the Study .....	9
Buildup Factors .....	10
Buildup Factor Calculations .....	10
Energy Absorption Coefficient .....	15
Boltzmann Transport Equation.....	19
Transport Equation for Photons .....	22
ASFIT .....	23
MCNP5 .....	27
Differences between ASFIT and MCNP5 .....	31
Photon Interactions .....	32
Cross-Section Data Libraries .....	32
CHAPTER 2 REVIEW OF RELATED LITERATURE .....	34
Literature Review.....	34
CHAPTER 3 METHODOLOGY .....	44
Literature Review Criteria .....	44
Approach to Computations .....	45
Computations .....	45
Fitting Functions .....	52
CHAPTER 4 FINDINGS OF THE STUDY .....	54
Analysis of Data.....	54
CHAPTER 5 SUMMARY, CONCLUSIONS, AND RECOMMENDATIONS.....	59
Discussion of Results .....	59
Conclusions.....	64
Recommendations for Further Study .....	64
REFERENCES .....	66
APPENDICES	
Appendix I Photon Mass Attenuation Coefficients, Coherent Scattering Included .....	69
Appendix II Photon Mass Attenuation Coefficients, Coherent Scattering Not Included .....	71
Appendix III Absorbed Dose Response Functions.....	73

Appendix IV	Comparison of Hubbell and ENDF/B-VII.0 in ASFIT-VARI .....	76
Appendix V	Comparison of NIST and Hubbell Data .....	78
Appendix VI	Comparison of XCOM and ENDF Cross Sections.....	79
Appendix VII	MCNP5 Energy Absorption Buildup Factor.....	80
Appendix VIII	Comparison of Calculated Buildup Factor .....	146
Appendix IX	Fittings Function for Calculated Buildup Factor .....	154
Appendix X	Calculation of MFP.....	187
Appendix XI	Calculated Buildup Factor without Bremsstrahlung.....	188
Appendix XII	Sample Input Files .....	198
Appendix XIII	User's Guide to ASFIT-VARI.....	203
VITA.....		205

## LIST OF TABLES

Table 1	Photon Mass Attenuation Coefficient for Iron Coherent Scattering Included .....	69
Table 2	Photon Mass Attenuation Coefficient for Water Coherent Scattering Included.....	70
Table 3	Photon Mass Attenuation Coefficient for Iron Coherent Scattering Not Included.....	71
Table 4	Photon Mass Attenuation Coefficient for Water Coherent Scattering Not Included.....	72
Table 5	Absorbed Dose Response Functions-Iron.....	73
Table 6	Absorbed Dose Response Functions-Water.....	74
Table 6a	Comparison of Hubbell & ENDF in ASFIT, 0.10 MeV-Water .....	76
Table 6b	Comparison of Hubbell & ENDF in ASFIT, 1.00 MeV-Water .....	76
Table 6c	Comparison of Hubbell & ENDF in ASFIT, 10.0 MeV-Water .....	77
Table 7	Comparison of NIST and Hubbell Data.....	78
Table 8	Comparison of XCOM and ENDF Cross Sections.....	79
Table 9a	Buildup Factor w/o Coherent scattering Iron-0.015 MeV .....	80
Table 9b	Buildup Factor w/Coherent scattering Iron-0.015 MeV .....	81
Table 9c	Buildup Factor w/o Coherent scattering Iron-0.020 MeV .....	82
Table 9d	Buildup Factor w/Coherent scattering Iron-0.020 MeV .....	83
Table 9e	Buildup Factor w/o Coherent scattering Iron-0.030 MeV .....	84
Table 9f	Buildup Factor w/Coherent scattering Iron-0.030 MeV .....	85
Table 9g	Buildup Factor w/o Coherent scattering Iron-0.040 MeV .....	86
Table 9h	Buildup Factor w/Coherent scattering Iron-0.040 MeV .....	87
Table 9i	Buildup Factor w/o Coherent scattering Iron-0.050 MeV .....	88
Table 9j	Buildup Factor w/Coherent scattering Iron-0.050 MeV .....	89
Table 9k	Buildup Factor w/o Coherent scattering Iron-0.060 MeV .....	90
Table 9l	Buildup Factor w/Coherent scattering Iron-0.060 MeV .....	91
Table 9m	Buildup Factor w/o Coherent scattering Iron-0.080 MeV .....	92
Table 9n	Buildup Factor w/Coherent scattering Iron-0.080 MeV .....	93
Table 9o	Buildup Factor w/o Coherent scattering Iron-0.10 MeV .....	94
Table 9p	Buildup Factor w/Coherent scattering Iron-0.10 MeV .....	95
Table 9q	Buildup Factor w/o Coherent scattering Iron-0.15 MeV .....	96
Table 9r	Buildup Factor w/Coherent scattering Iron-0.15 MeV .....	97
Table 9s	Buildup Factor w/o Coherent scattering Iron-0.20 MeV .....	98
Table 9t	Buildup Factor w/Coherent scattering Iron-0.20 MeV .....	99
Table 9u	Buildup Factor w/o Coherent scattering Iron-0.30 MeV .....	100
Table 9v	Buildup Factor w/Coherent scattering Iron-0.30 MeV .....	101
Table 9w	Buildup Factor w/o Coherent scattering Iron-0.40 MeV .....	102
Table 9x	Buildup Factor w/Coherent scattering Iron-0.40 MeV .....	103
Table 9y	Buildup Factor w/o Coherent scattering Iron-0.50 MeV .....	104
Table 9z	Buildup Factor w/Coherent scattering Iron-0.50 MeV .....	105

Table 9aa	Buildup Factor w/o Coherent scattering Iron-0.60 MeV .....	106
Table 9bb	Buildup Factor w/Coherent scattering Iron-0.60 MeV .....	107
Table 9cc	Buildup Factor w/o Coherent scattering Iron-0.80 MeV .....	108
Table 9dd	Buildup Factor w/Coherent scattering Iron-0.80 MeV .....	109
Table 9ee	Buildup Factor w/o Coherent scattering Iron-1.00 MeV .....	110
Table 9ff	Buildup Factor w/Coherent scattering Iron-1.00 MeV .....	111
Table 9gg	Buildup Factor, Iron-1.50 MeV .....	112
Table 9hh	Buildup Factor, Iron-2.00 MeV .....	113
Table 9ii	Buildup Factor, Iron-3.00 MeV .....	114
Table 9jj	Buildup Factor, Iron-4.00 MeV .....	115
Table 9kk	Buildup Factor, Iron-5.00 MeV .....	116
Table 9ll	Buildup Factor, Iron-6.00 MeV .....	117
Table 9mm	Buildup Factor, Iron-8.00 MeV .....	118
Table 9nn	Buildup Factor, Iron-10.0 MeV .....	119
Table 9oo	Buildup Factor, Iron-15.0 MeV .....	120
Table 10a	Buildup Factor, Water-0.015 MeV .....	121
Table 10b	Buildup Factor, Water-0.020 MeV .....	122
Table 10c	Buildup Factor, Water-0.030 MeV .....	123
Table 10d	Buildup Factor, Water-0.040 MeV .....	124
Table 10e	Buildup Factor, Water-0.050 MeV .....	125
Table 10f	Buildup Factor, Water-0.060 MeV .....	126
Table 10g	Buildup Factor, Water-0.080 MeV .....	127
Table 10h	Buildup Factor, Water-0.100 MeV .....	128
Table 10i	Buildup Factor, Water-0.150 MeV .....	129
Table 10j	Buildup Factor, Water-0.200 MeV .....	130
Table 10k	Buildup Factor, Water-0.300 MeV .....	131
Table 10l	Buildup Factor, Water-0.400 MeV .....	132
Table 10m	Buildup Factor, Water-0.500 MeV .....	133
Table 10n	Buildup Factor, Water-0.600 MeV .....	134
Table 10o	Buildup Factor, Water-0.800 MeV .....	135
Table 10p	Buildup Factor, Water-1.00 MeV .....	136
Table 10q	Buildup Factor, Water-1.50 MeV .....	137
Table 10r	Buildup Factor, Water-2.00 MeV .....	138
Table 10s	Buildup Factor, Water-3.00 MeV .....	139
Table 10t	Buildup Factor, Water-4.00 MeV .....	140
Table 10u	Buildup Factor, Water-5.00 MeV .....	141
Table 10v	Buildup Factor, Water-6.00 MeV .....	142
Table 10w	Buildup Factor, Water-8.00 MeV .....	143
Table 10x	Buildup Factor, Water-10.0 MeV .....	144
Table 10y	Buildup Factor, Water-15.0 MeV .....	145
Table 11a	Buildup Factor Comparison w/ no Coherent Scattering, Iron- 0.015 MeV .....	146
Table 11b	Buildup Factor Comparison w/ no Coherent Scattering, Iron- 0.15 MeV .....	147
Table 11c	Buildup Factor Comparison w/ no Coherent Scattering, Iron- 1.50 MeV .....	148



Table 11d	Buildup Factor Comparison w/ no Coherent Scattering, Iron- 15.0 MeV .....	149
Table 11e	Buildup Factor Comparison w/ no Coherent Scattering, Water- 0.015 MeV .....	150
Table 11f	Buildup Factor Comparison w/ no Coherent Scattering, Iron- 0.15 MeV .....	151
Table 11g	Buildup Factor Comparison w/ no Coherent Scattering, Iron- 1.50 MeV .....	152
Table 11h	Buildup Factor Comparison w/ no Coherent Scattering, Iron- 15.0 MeV .....	153
Table 12	Calculation of MFP .....	187
Table 13a	Calculated Buildup Factor w/o Bremsstrahlung, 0.10 MeV-Iron..	188
Table 13b	Calculated Buildup Factor w/o Bremsstrahlung, 1.50 MeV-Iron..	189
Table 13c	Calculated Buildup Factor w/o Bremsstrahlung, 5.00 MeV-Iron..	190
Table 13d	Calculated Buildup Factor w/o Bremsstrahlung, 10.0 MeV-Iron..	191
Table 13e	Calculated Buildup Factor w/o Bremsstrahlung, 15.0 MeV-Iron..	192
Table 13f	Calculated Buildup Factor w/o Bremsstrahlung, 0.10 MeV-Water	193
Table 13g	Calculated Buildup Factor w/o Bremsstrahlung, 1.50 MeV-Water	194
Table 13h	Calculated Buildup Factor w/o Bremsstrahlung, 5.00 MeV-Water	195
Table 13i	Calculated Buildup Factor w/o Bremsstrahlung, 10.0 MeV-Water	196
Table 13j	Calculated Buildup Factor w/o Bremsstrahlung, 15.0 MeV-Water	197
Table 14	Description of Cards .....	203

## LIST OF FIGURES

Figure 1	Bremsstrahlung .....	3
Figure 2	Compton Scattering .....	4
Figure 3	Elastic Scattering .....	5
Figure 4	Pair Production.....	7
Figure 5	Photoelectric Absorption .....	8
Figure 6	Energy Shifts from Protons to Electrons .....	16
Figure 7	Energy Flux vs. Energy.....	26
Figure 8	Energy Buildup Factor vs. System Thickness .....	26
Figure 9	Life of a Neutron.....	29
Figure 10	Effects w/ and w/o Coherent Scattering.....	40
Figure 11a	MCNP5 vs. ANS Buildup Factor w/o Coherent Scattering, 0.015 MeV .....	80
Figure 11b	MCNP5 vs. ANS Buildup Factor w/Coherent Scattering, 0.015 MeV .....	81
Figure 11c	MCNP5 vs. ANS Buildup Factor w/o Coherent Scattering, 0.020 MeV .....	82
Figure 11d	MCNP5 vs. ANS Buildup Factor w/Coherent Scattering, 0.020 MeV .....	83
Figure 11e	MCNP5 vs. ANS Buildup Factor w/o Coherent Scattering, 0.030 MeV .....	84
Figure 11f	MCNP5 vs. ANS Buildup Factor w/ Coherent Scattering, 0.030 MeV .....	85
Figure 11g	MCNP5 vs. ANS Buildup Factor w/o Coherent Scattering, 0.040 MeV .....	86
Figure 11h	MCNP5 vs. ANS Buildup Factor w/Coherent Scattering, 0.040 MeV .....	87
Figure 11i	MCNP5 vs. ANS Buildup Factor w/o Coherent Scattering, 0.050 MeV .....	88
Figure 11j	MCNP5 vs. ANS Buildup Factor w/Coherent Scattering, 0.050 MeV .....	89
Figure 11k	MCNP5 vs. ANS Buildup Factor w/o Coherent Scattering, 0.060 MeV .....	90
Figure 11l	MCNP5 vs. ANS Buildup Factor w/ Coherent Scattering, 0.060 MeV .....	91
Figure 11m	MCNP5 vs. ANS Buildup Factor w/o Coherent Scattering, 0.080 MeV .....	92
Figure 11n	MCNP5 vs. ANS Buildup Factor w/ Coherent Scattering, 0.080 MeV .....	93
Figure 11o	MCNP5 vs. ANS Buildup Factor w/o Coherent Scattering, 0.10 MeV .....	94
Figure 11p	MCNP5 vs. ANS Buildup Factor w/ Coherent Scattering, 0.10 MeV .....	95
Figure 11q	MCNP5 vs. ANS Buildup Factor w/o Coherent Scattering,	

	0.15 MeV .....	96
Figure 11r	MCNP5 vs. ANS Buildup Factor w/Coherent Scattering, 0.15 MeV .....	97
Figure 11s	MCNP5 vs. ANS Buildup Factor w/o Coherent Scattering, 0.20 MeV .....	98
Figure 11t	MCNP5 vs. ANS Buildup Factor w/Coherent Scattering, 0.20 MeV .....	99
Figure 11u	MCNP5 vs. ANS Buildup Factor w/o Coherent Scattering, 0.30 MeV .....	100
Figure 11v	MCNP5 vs. ANS Buildup Factor w/Coherent Scattering, 0.30 MeV .....	101
Figure 11w	MCNP5 vs. ANS Buildup Factor w/o Coherent Scattering, 0.40 MeV .....	102
Figure 11x	MCNP5 vs. ANS Buildup Factor w/Coherent Scattering, 0.40 MeV .....	103
Figure 11y	MCNP5 vs. ANS Buildup Factor w/o Coherent Scattering, 0.50 MeV .....	104
Figure 11z	MCNP5 vs. ANS Buildup Factor w/Coherent Scattering, 0.50 MeV .....	105
Figure 11aa	MCNP5 vs. ANS Buildup Factor w/o Coherent Scattering, 0.60 MeV .....	106
Figure 11bb	MCNP5 vs. ANS Buildup Factor w/Coherent Scattering, 0.60 MeV .....	107
Figure 11cc	MCNP5 vs. ANS Buildup Factor w/o Coherent Scattering, 0.80 MeV .....	108
Figure 11dd	MCNP5 vs. ANS Buildup Factor w/Coherent Scattering, 0.80 MeV .....	109
Figure 11ee	MCNP5 vs. ANS Buildup Factor w/o Coherent Scattering, 1.00 MeV .....	110
Figure 11ff	MCNP5 vs. ANS Buildup Factor w/Coherent Scattering, 1.00 MeV .....	111
Figure 11gg	MCNP5 vs. ANS Buildup Factor, 1.50 MeV .....	112
Figure 11hh	MCNP5 vs. ANS Buildup Factor, 2.00 MeV .....	113
Figure 11ii	MCNP5 vs. ANS Buildup Factor, 3.00 MeV .....	114
Figure 11jj	MCNP5 vs. ANS Buildup Factor, 4.00 MeV .....	115
Figure 11kk	MCNP5 vs. ANS Buildup Factor, 5.00 MeV .....	116
Figure 11ll	MCNP5 vs. ANS Buildup Factor, 6.00 MeV .....	117
Figure 11mm	MCNP5 vs. ANS Buildup Factor, 8.00 MeV .....	118
Figure 11nn	MCNP5 vs. ANS Buildup Factor, 10.0 MeV .....	119
Figure 11oo	MCNP5 vs. ANS Buildup Factor, 15.0 MeV .....	120
Figure 12a	MCNP5 vs. ANS Buildup Factor, 0.015 MeV .....	121
Figure 12b	MCNP5 vs. ANS Buildup Factor, 0.020 MeV .....	122
Figure 12c	MCNP5 vs. ANS Buildup Factor, 0.030 MeV .....	123
Figure 12d	MCNP5 vs. ANS Buildup Factor, 0.040 MeV .....	124
Figure 12e	MCNP5 vs. ANS Buildup Factor, 0.050 MeV .....	125
Figure 12f	MCNP5 vs. ANS Buildup Factor, 0.060 MeV .....	126

Figure 12g	MCNP5 vs. ANS Buildup Factor, 0.080 MeV .....	127
Figure 12h	MCNP5 vs. ANS Buildup Factor, 0.100 MeV .....	128
Figure 12i	MCNP5 vs. ANS Buildup Factor, 0.150 MeV .....	129
Figure 12j	MCNP5 vs. ANS Buildup Factor, 0.200 MeV .....	130
Figure 12k	MCNP5 vs. ANS Buildup Factor, 0.300 MeV .....	131
Figure 12l	MCNP5 vs. ANS Buildup Factor, 0.400 MeV .....	132
Figure 12m	MCNP5 vs. ANS Buildup Factor, 0.500 MeV .....	133
Figure 12n	MCNP5 vs. ANS Buildup Factor, 0.600 MeV .....	134
Figure 12o	MCNP5 vs. ANS Buildup Factor, 0.800 MeV .....	135
Figure 12p	MCNP5 vs. ANS Buildup Factor, 1.00 MeV .....	136
Figure 12q	MCNP5 vs. ANS Buildup Factor, 1.50 MeV .....	137
Figure 12r	MCNP5 vs. ANS Buildup Factor, 2.00 MeV .....	138
Figure 12s	MCNP5 vs. ANS Buildup Factor, 3.00 MeV .....	139
Figure 12t	MCNP5 vs. ANS Buildup Factor, 4.00 MeV .....	140
Figure 12u	MCNP5 vs. ANS Buildup Factor, 5.00 MeV .....	141
Figure 12v	MCNP5 vs. ANS Buildup Factor, 6.00 MeV .....	142
Figure 12w	MCNP5 vs. ANS Buildup Factor, 8.00 MeV .....	143
Figure 12x	MCNP5 vs. ANS Buildup Factor, 10.0 MeV .....	144
Figure 12y	MCNP5 vs. ANS Buildup Factor, 15.0 MeV .....	145
Figure 13a	Buildup Factor Comparison w/ no Coherent Scattering, Iron- 0.015 MeV .....	146
Figure 13b	Buildup Factor Comparison w/ no Coherent Scattering, Iron- 0.15 MeV .....	147
Figure 13c	Buildup Factor Comparison w/ no Coherent Scattering, Iron- 1.50 MeV .....	148
Figure 13d	Buildup Factor Comparison w/ no Coherent Scattering, Iron- 15.0 MeV .....	149
Figure 13e	Buildup Factor Comparison w/ no Coherent Scattering, Water- 0.015 MeV .....	150
Figure 13f	Buildup Factor Comparison w/ no Coherent Scattering, Water 0.15 MeV .....	151
Figure 13g	Buildup Factor Comparison w/ no Coherent Scattering, Water 1.50 MeV .....	152
Figure 13h	Buildup Factor Comparison w/ no Coherent Scattering, Water- 15.0 MeV .....	153
Figure 14a	Fitting Function for Buildup Factor w/o Coherent Scattering, Iron- 0.015 MeV .....	154
Figure 14b	Fitting Function for Buildup Factor w/Coherent Scattering, Iron- 0.015 MeV .....	154
Figure 14c	Fitting Function for Buildup Factor w/o Coherent Scattering, Iron- 0.020 MeV .....	155
Figure 14d	Fitting Function for Buildup Factor w/ Coherent Scattering, Iron- 0.020 MeV .....	155
Figure 14e	Fitting Function for Buildup Factor w/o Coherent Scattering, Iron- 0.030 MeV .....	156

Figure 14f	Fitting Function for Buildup Factor w/Coherent Scattering, Iron-0.030 MeV .....	156
Figure 14g	Fitting Function for Buildup Factor w/o Coherent Scattering, Iron-0.040 MeV .....	157
Figure 14h	Fitting Function for Buildup Factor w/Coherent Scattering, Iron-0.040 MeV .....	157
Figure 14i	Fitting Function for Buildup Factor w/o Coherent Scattering, Iron-0.050 MeV .....	158
Figure 14j	Fitting Function for Buildup Factor w/ Coherent Scattering, Iron-0.050 MeV .....	158
Figure 14k	Fitting Function for Buildup Factor w/o Coherent Scattering, Iron-0.060 MeV .....	159
Figure 14l	Fitting Function for Buildup Factor w/ Coherent Scattering, Iron-0.060 MeV .....	159
Figure 14m	Fitting Function for Buildup Factor w/o Coherent Scattering, Iron-0.080 MeV .....	160
Figure 14n	Fitting Function for Buildup Factor w/Coherent Scattering, Iron-0.080 MeV .....	160
Figure 14o	Fitting Function for Buildup Factor w/o Coherent Scattering, Iron-0.10 MeV .....	161
Figure 14p	Fitting Function for Buildup Factor w/Coherent Scattering, Iron-0.10 MeV .....	161
Figure 14q	Fitting Function for Buildup Factor w/o Coherent Scattering, Iron-0.15 MeV .....	162
Figure 14r	Fitting Function for Buildup Factor w/Coherent Scattering, Iron-0.15 MeV .....	162
Figure 14s	Fitting Function for Buildup Factor w/o Coherent Scattering, Iron-0.20 MeV .....	163
Figure 14t	Fitting Function for Buildup Factor w/Coherent Scattering, Iron-0.20 MeV .....	163
Figure 14u	Fitting Function for Buildup Factor w/o Coherent Scattering, Iron-0.30 MeV .....	164
Figure 14v	Fitting Function for Buildup Factor w/o Coherent Scattering, Iron-0.30 MeV .....	164
Figure 14w	Fitting Function for Buildup Factor w/o Coherent Scattering, Iron-0.40 MeV .....	165
Figure 14x	Fitting Function for Buildup Factor w/o Coherent Scattering, Iron-0.40 MeV .....	165
Figure 14y	Fitting Function for Buildup Factor w/o Coherent Scattering, Iron-0.50 MeV .....	166
Figure 14z	Fitting Function for Buildup Factor w/o Coherent Scattering, Iron-0.50 MeV .....	166
Figure 14aa	Fitting Function for Buildup Factor w/o Coherent Scattering, Iron-0.60 MeV .....	167
Figure 14bb	Fitting Function for Buildup Factor w/o Coherent Scattering, Iron-0.60 MeV .....	167

Figure 14cc	Fitting Function for Buildup Factor w/o Coherent Scattering, Iron-0.80 MeV .....	168
Figure 14dd	Fitting Function for Buildup Factor w/o Coherent Scattering, Iron-0.80 MeV .....	168
Figure 14ee	Fitting Function for Buildup Factor w/o Coherent Scattering, Iron-1.00 MeV .....	169
Figure 14ff	Fitting Function for Buildup Factor w/o Coherent Scattering, Iron-1.00 MeV .....	169
Figure 14gg	Fitting Function for Buildup Factor, Iron- 1.50 MeV.....	170
Figure 14hh	Fitting Function for Buildup Factor, Iron- 2.00 MeV.....	170
Figure 14ii	Fitting Function for Buildup Factor, Iron- 3.00 MeV.....	171
Figure 14jj	Fitting Function for Buildup Factor, Iron- 4.00 MeV.....	171
Figure 14kk	Fitting Function for Buildup Factor, Iron- 5.00 MeV.....	172
Figure 14ll	Fitting Function for Buildup Factor, Iron- 6.00 MeV.....	172
Figure 14mm	Fitting Function for Buildup Factor, Iron- 8.00 MeV.....	173
Figure 14nn	Fitting Function for Buildup Factor, Iron- 10.0 MeV.....	173
Figure 14oo	Fitting Function for Buildup Factor, Iron- 15.0 MeV.....	174
Figure 14pp	Fitting Function for Buildup Factor, Water-0.015 MeV.....	174
Figure 14qq	Fitting Function for Buildup Factor, Water-0.020 MeV.....	175
Figure 14rr	Fitting Function for Buildup Factor, Water-0.030 MeV.....	175
Figure 14ss	Fitting Function for Buildup Factor, Water-0.040 MeV.....	176
Figure 14tt	Fitting Function for Buildup Factor, Water-0.050 MeV.....	176
Figure 14uu	Fitting Function for Buildup Factor, Water-0.060MeV.....	177
Figure 14vv	Fitting Function for Buildup Factor, Water-0.080 MeV.....	177
Figure 14ww	Fitting Function for Buildup Factor, Water-0.100 MeV.....	178
Figure 14xx	Fitting Function for Buildup Factor, Water-0.150 MeV.....	178
Figure 14yy	Fitting Function for Buildup Factor, Water-0.20 MeV.....	179
Figure 14zz	Fitting Function for Buildup Factor, Water-0.30 MeV.....	179
Figure 14ab	Fitting Function for Buildup Factor, Water-0.40 MeV.....	180
Figure 14ac	Fitting Function for Buildup Factor, Water-0.50 MeV.....	180
Figure 14ad	Fitting Function for Buildup Factor, Water-0.60 MeV.....	181
Figure 14ae	Fitting Function for Buildup Factor, Water-0.80 MeV.....	181
Figure 14af	Fitting Function for Buildup Factor, Water-1.00 MeV.....	182
Figure 14ag	Fitting Function for Buildup Factor, Water-1.50MeV.....	182
Figure 14ah	Fitting Function for Buildup Factor, Water-2.00 MeV.....	183
Figure 14ai	Fitting Function for Buildup Factor, Water-3.00 MeV.....	183
Figure 14aj	Fitting Function for Buildup Factor, Water-4.00 MeV.....	184
Figure 14ak	Fitting Function for Buildup Factor, Water-5.00 MeV.....	184
Figure 14al	Fitting Function for Buildup Factor, Water-6.00 MeV.....	185
Figure 14am	Fitting Function for Buildup Factor, Water-8.00 MeV.....	185
Figure 14an	Fitting Function for Buildup Factor, Water-10.0 MeV.....	186
Figure 14ao	Fitting Function for Buildup Factor, Water-15.0 MeV.....	186
Figure 15a	Comparison of Buildup Factor w/ and w/o Bremsstrahlung, 0.10 MeV-Iron .....	188
Figure 15b	Comparison of Buildup Factor w/ and w/o Bremsstrahlung, 1.50 MeV-Iron .....	189

Figure 15c	Comparison of Buildup Factor w/ and w/o Bremsstrahlung, 5.00 MeV-Iron.....	190
Figure 15d	Comparison of Buildup Factor w/ and w/o Bremsstrahlung, 10.0 MeV-Iron.....	191
Figure 15e	Comparison of Buildup Factor w/ and w/o Bremsstrahlung, 15.0 MeV-Iron.....	192
Figure 15f	Comparison of Buildup Factor w/ and w/o Bremsstrahlung, 0.10 MeV-Water.....	193
Figure 15g	Comparison of Buildup Factor w/ and w/o Bremsstrahlung, 1.50 MeV-Water.....	194
Figure 15h	Comparison of Buildup Factor w/ and w/o Bremsstrahlung, 5.00 MeV-Iron.....	195
Figure 15i	Comparison of Buildup Factor w/ and w/o Bremsstrahlung, 10.0 MeV-Water.....	196
Figure 15j	Comparison of Buildup Factor w/ and w/o Bremsstrahlung, 15.0 MeV-Water.....	197

## ACKNOWLEDGEMENTS

I would like to thank Dr. Charlotta Sanders for her patience, support, and guidance. Dr. Sanders was there for me throughout the study as an instructor, friend, and mentor. I could not have asked for a better advisor. I am also thankful to Mark Sanders, whose cooking and patience was an inspiration for me to finish. I would also like to thank Drs. Robert Boehm, Brendan O'Toole, and Ralf Sudowe for their interest in my research and participating in my advisory committee.

I would like to thank Dr. Evgeny Stankovskiy for his contributions to this project, especially his help with getting ASFIT up and running as well as MCNP5 support. I would like to thank Dr. Jeff Ryman who helped develop and shape this project.

I would like to acknowledge and thank my friends and colleagues Larry Ruggieri and Kamran Haq who have been instrumental to this study and supportive in many areas. I would like to thank Larry especially for his advice and collaboration, which was an inherent part of my completion. Special thanks to Dr. Yukio Sakamoto, Dr. Yoshiko Harima, Adam Davis, and Dr. Jabo Tang. They have provided much needed information, and guidance that was beyond my expectations. Their patience, cooperation, and imparting knowledge have aided the study in many ways.

I would like to thank my parents for always pushing me to do my best and further my education. I dedicate this thesis to them. Without their support and encouraging words, the light at the end of the tunnel would have never been reached. I dedicate this study and degree to them. I would also like to thank my two brothers and my lovely little sister, whose amusement and visits helped me get through this laborious trek.



# CHAPTER 1

## INTRODUCTION

### Purpose of the Study

ANSI/ANS-6.4.3-1991 Gamma-Ray Attenuation Coefficients and Buildup Factors for Engineering Materials Standard (herein known as the ANS Standard) sets forth physical and nuclear properties that are appropriate for a particular application in order to form the basis for the selection of radiation shielding materials. The ANS standard presents evaluated gamma-ray attenuation coefficients and single-material buildup factors for selected engineering materials for use in shielding calculations of structures in power plants and other nuclear facilities. The data covers an energy range of 0.015-15 MeV and depth of 0-40 mean free path (mfp). The information herein are standard reference data for use in radiation analysis.

The data presented in the ANS Standard is derived from data that is at least eighteen years old. Within the last eighteen years, new data has been derived that will allow the ANS standard to be updated and become more accurate. Over the past eighteen years, cross section data and accuracy has greatly improved, which allows for more accurate buildup factors to be calculated. Computer technology has also significantly improved, which will allow these intricate codes to be utilized. As a result, new codes model radiation transport more accurately than older codes. Providing new buildup factor data allows for validation of published values and increases the accuracy of the information that is available to include in the next revision of the ANS Standard. This study will attempt to provide the ground for a transition to a more current code, MCNP5.

## Concepts and Terms

Absorption – Process in which photons, as they pass through a medium, are absorbed in the material.

Annihilation photons – The process that occurs when a subatomic particle collides with its respective antiparticle. Since energy and momentum must be conserved, the particles are not made into nothing, but rather into new particles. Antiparticles have exactly opposite additive quantum numbers from particles, so the sums of all quantum numbers of the original pair are zero. Therefore, any set of particles may be produced whose total quantum numbers are also zero as long as conservation of energy and momentum are obeyed.

When a low-energy electron annihilates a low-energy positron (anti-electron), they can only produce two or more gamma ray photons, since the electron and positron do not carry enough mass-energy to produce heavier particles. However, if one or both particles carry a larger amount of kinetic energy; various other particles pairs can be produced.

Attenuation – Gradual loss in intensity of any kind of flux through a medium via interactions and energy depositions.

Binding Energy- The energy required to separate particles which are bound by electromagnetic or nuclear forces (infinitely far apart). In the case of the nucleus of an atom, these particles are protons and neutrons held together by the nuclear binding energy. The neutron and proton binding energies are the energies necessary to release a

neutron or proton from the nucleus. Electron binding energy is the energy required to completely remove an electron from an atom or a molecule.

Bremsstrahlung – Known as braking radiation. Electromagnetic radiation that is produced by the deceleration or acceleration of a charged particle, such as an electron, when deflected by another charged particle, such as a proton. (See Figure1).

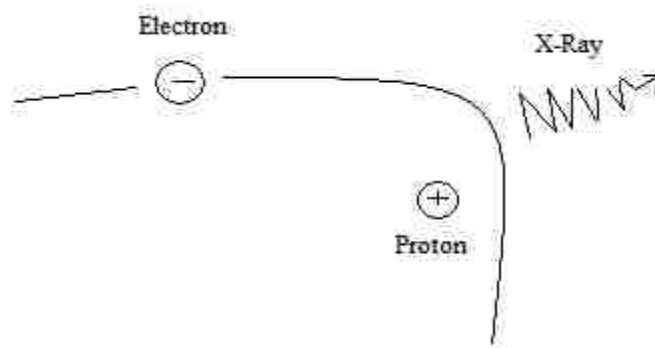


Figure 1. Bremsstrahlung

Compton scattering – The process of elastic scattering of a photon by an electron, in which both energy and momentum are conserved. The incident photon with energy  $E$  and wavelength  $\lambda_i$ , is scattered through an angle  $\theta$  and the struck electron recoils. Since the recoiling electron acquires some kinetic energy, the energy  $E'$  of the scattered photon is less than  $E$ , and since the wavelength of a photon is inversely proportional to its energy, the wavelength  $\lambda_f$  of the scattered photon is larger than  $\lambda_i$ . (See Figure 2).

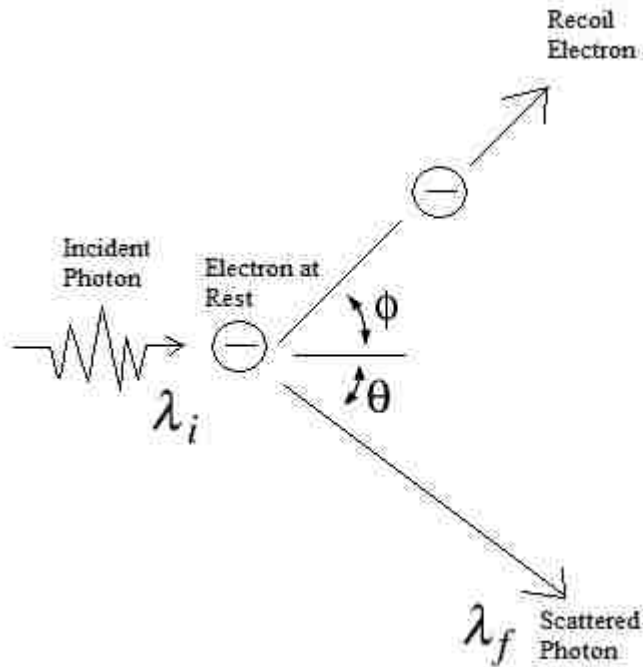


Figure 2. Compton Scattering

Dose (Absorbed) – A measure of the amount of energy from an ionizing radiation deposited in a medium.

Evaluated Nuclear Data File (ENDF)- The ENDF is a core nuclear reaction database containing evaluated (recommended) cross sections, spectra, angular distributions, fission product yields, thermal neutron scattering, photo-atomic and other data, with emphasis on neutron-induced reactions.

Elastic Scattering - In this process, the energy (kinetic energy) of the incident particles is conserved, only the direction of propagation is modified (by interaction with other particles and/or a potential). An example of a neutron engaging in this process is shown below:

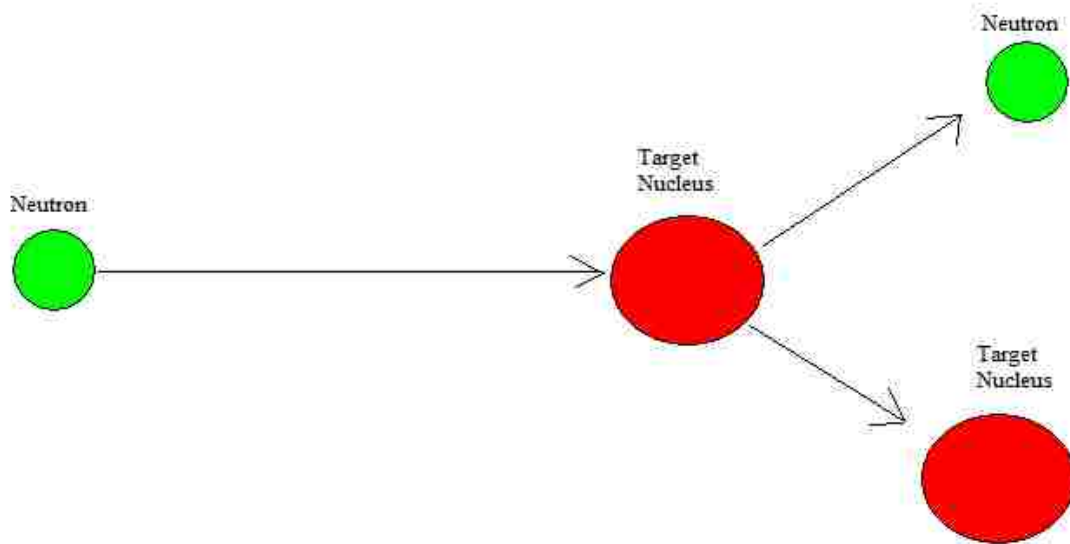


Figure 3. Elastic Scattering

Energy Absorption Coefficient- This coefficient takes into account all possible modes of energy transfer to electrons in a medium. This variable takes into account the escape of fluorescence, Compton scattered, annihilation, and Bremsstrahlung photons.

Exposure (photon) – A radiation measurement quantity which is proportional to the electric charge of either sign that is created in air as a result of ionization by secondary charged particles resulting from photon interactions in a unit mass of air.

Fluorescence – The emission of characteristic secondary (or fluorescent) photons (X-rays) from a material that has been excited by bombardment of high-energy (higher) X-rays or gamma-rays. The term is applied to a phenomenon in which the absorption of higher-energy radiation results in the re-emission of lower-energy radiation.

Flux- The amount of particles that travels through a unit area per unit time,  $\frac{\text{Particles}}{\text{cm}^2\text{s}}$ .

Fluence- Is the integrated flux or the number of particles that intersect a unit area over time.

Isotropic radiation – Radiation that is emitted by a source in all directions with equal intensity or which reaches a location from all directions with equal intensity.

K-edge – This phenomena describes a sudden increase in the attenuation coefficient of photons occurring at photon energy just above the binding energy of the K shell electron of the atoms interacting with the photons. The sudden increase in attenuation is due to photoelectric absorption of the photons. For this interaction to occur, the photons must have more energy than the binding energy of the K Shell electrons. A photon having energy just above the binding energy of the electron is therefore more likely to be absorbed than a photon having energy just below this binding energy.

Linear attenuation coefficient – Probability of interaction per unit distance traveled by a photon. It is a function of particle energy and is usually expressed in units of  $\text{cm}^{-1}$ .

Linear Energy Transfer (LET) – Is a measure of the energy transferred to a medium as an ionizing particle travels through it. Typically, this measure is used to quantify the effects of ionizing radiation on biological specimens or electronic devices.

Mean Free Path (mfp) – The average distance covered by a particle (photon) between two successive interactions. It is the inverse of the linear attenuation coefficient.

Pair production – An absorption process for photons of energies greater than 1.02 MeV in which the creation of an elementary particle and its antiparticle (electron and positron, respectively) occur, usually from a photon. This only occurs provided there is enough energy available to create the pair, at least the total rest mass energy of the two particles and that the condition allows both energy and momentum to be conserved, see figure 4.

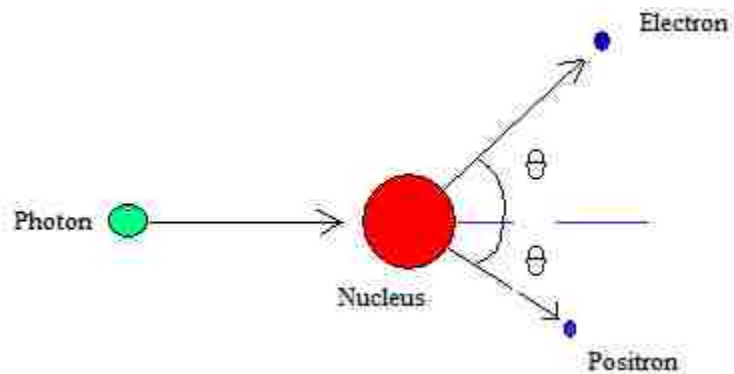


Figure 4. Pair Production

Photoelectric absorption – An absorption process for photon energies that occur below 0.5 MeV. In the process the photon loses all of its energy to an atomic electron. The electron leaves its atomic orbit and continues to move through the material, see figure 5.

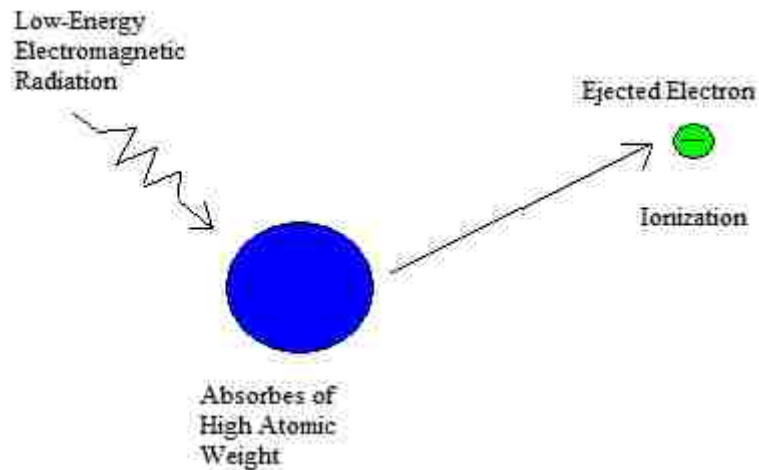


Figure 5. Photoelectric Absorption

Photon – The quantum of electromagnetic energy, regarded as a discrete particle having zero mass and no electric charge, which travels in a vacuum at only the speed of light. Examples of photons in decreasing order of energy are gamma-rays, X-rays, ultraviolet light, visible light, infrared light, microwaves, and radio waves. In this study, our focus is upon gamma-rays.

Point source – The most fundamental type of radiation source which is theoretical but is often used as an approximation to a real source provided that the real source's volume is sufficiently small compared to the volume of the attenuating medium and there is



negligible interaction of radiation with the matter in the source volume. A point source does not have any volume and is modeled as a point in space. In general, it can be characterized as being dependent on energy, direction, and time [Shultis and Faw, 2000].

### Significance of the Study

The buildup factor values that are provided in ANSI/ANS-6.4.3-1991 are derived from data that is approximately a couple decades old. The initial introduction of buildup factor was by White in 1950, (Harima, 1993) to express penetration of  $^{60}\text{Co}$   $\gamma$ -rays in water. After that Goldstein and Wilkins published a comprehensive set of  $\gamma$ -ray buildup factors calculated with a moments method code in 1954 (Harima, 1993). Following this, buildup factors for point isotropic sources were employed in point kernel method and were widely used in  $\gamma$ -ray attenuation calculations. In spite of the development of rigorous methods of transport calculations, the above data has been used as a standard for more than 30 years. Since the last update of the standard, the cross section data that is used has been updated. Since 1991, computer technology has significantly improved, allowing for more intricate and complex computationally demanding codes to be utilized. Consequently, new codes model radiation transport more accurately than older codes. Providing new buildup factor data allows for validation of published values and will increase the accuracy of the information that is available. This study was performed for the ANS-6.4.3 working group and the results will be reviewed for possible inclusion in the next revision of the ANS Standard. Since the last publication of the standard there has been no revision and as a result it has become outdated and inactive. In order to help alter

the status and allow for the standard to be used again, this study is carried out with the intent of updating the values and helping the ANS-6.4.3 group reactivate the standard.

### Buildup Factors

The practical calculation of  $\gamma$ -ray attenuation is a complex process, which is greatly simplified by buildup factors. The buildup factor is a correction factor that considers the influence of the scattered radiation plus any secondary particles in the medium during shielding calculations. The buildup factor is then a multiplicative factor which accounts for the response to the uncollided photons so as to include the contribution of the scattered photons. Thus, the buildup factor can be obtained as a ratio of the total dose to the response for uncollided dose. This study will help contribute to the buildup factor data by modeling a point isotropic source of monoenergetic photons in an infinite homogenous medium. Conventionally, buildup factors have been compiled as a function of mfp. In this study, the buildup factors will be observed in materials up to 40 mfp.

### Buildup Factor Calculations

The calculation of buildup factors is based upon the flow of a photon through a medium and the number of interactions it partakes in. Whenever energy is used in reference to a gamma-ray, it is indicative of the total energy of the photon, which is described by the following

$$E = h\nu \tag{1}$$

Where,

$E$  = Energy of the photon,  $eV$

$h$  = Plank's constant,  $4.135 \times 10^{-15} \text{ eV*s}$

$\nu$  = Frequency of electromagnetic wave of the photon,  $s^{-1}$

The mfp is the inverse of the linear attenuation coefficient, which indicates the probability of interactions per unit path length. The linear attenuation coefficient is a function of the particle energy before and after the collision/scatter, the energy recoil of the target particle, angles of deflection of the incident photon and target particles, and the angles of emission of secondary particles following certain interactions. The linear attenuation coefficient is described by the atom density and cross section of the interaction, which is seen by the following equation

$$\mu = N \times \sigma \quad (2)$$

Where,

$\mu$  = Linear attenuation coefficient,  $cm^{-1}$

$N$  = Atom density,  $\frac{atoms}{cm^3}$

$\sigma$  = Microscopic cross section, *barns or  $cm^2$*

The atom density for a single element is calculated by the following

$$N = \frac{\rho}{A} \times N_a \quad (3)$$

Where,

$N$  = Atom density,  $\frac{atoms}{(cm^3)mol}$

$\rho$  = Density,  $\frac{gram}{cm^3}$

$A$  = Atomic mass of element, *gram*

$N_a$  = Avogadro's constant,  $6.022 \times 10^{23} \text{ mol}^{-1}$

The microscopic cross section is a probability that a certain type of interaction will take place based on the target atom and incident particle energy (Lamarsh, 2001). The cross section is a function of many things such as the material, particle direction, and energy of incident particle. The values for cross sections are tabulated in a file known as the cross section data library. The data used in this study is the latest cross section library, ENDF/B-VI.8, which is distributed by National Nuclear Data Center (NNDC), which is a part of Brookhaven National Laboratory.

The buildup factor can be obtained by experiment, but since the attenuation and scattering cross section are known, it can be solved for through the solution of photon transport equation. The total value of a specified radiation at some point in space is predicted by the corresponding response of some type of detector at that point in space, that is, the detector response  $R$ .  $R$  is represented by a flux density  $\phi(r, E)$  multiplied by the detector response function  $\mathfrak{R}(E)$ , where  $r$  is the distance from a source.

The detector response provides a relationship between flux and dose. This study employs two types of response functions; absorbed dose and exposure. The response function for absorbed dose,  $\text{Gy cm}^2$ , is captured by the following

$$\mathfrak{R}_D(E) = 1.602 \times 10^{-10} E \left( \frac{\mu_{en}(E)}{\rho} \right) \quad (4)$$

Where,

$\mathfrak{R}_D(E)$  = Response for absorbed dose,  $\text{Gy cm}^2$

$E$  = Energy, eV

$\mu_{en}(E)$  = Energy absorption coefficient,  $\frac{\text{cm}^2}{\text{g}}$

$\rho$  = Density,  $\frac{g}{cm^3}$

To solve for the dose, the response function is multiplied by the flux at the detector. The flux is set number of particles that penetrate a surface (spherical) of interest over time. The following equation captures it

$$\phi^o(r) = \frac{S_p}{4\pi r^2} \quad (5)$$

Where,

$\phi(r)$  = Flux,  $\frac{Particles}{cm^2 s}$

$S_p$  = Source strength,  $\frac{particles}{time}$

$r$  = Distance, cm

The uncollided dose from a point monoenergetic isotropic source in an infinite homogenous medium is given by the following

$$D^o(r) = \frac{S_p \mathfrak{R}_D}{4\pi r^2} e^{-\mu r} \quad (5)$$

Where,

$D^o(r)$  = Uncollided dose,  $\frac{Gy}{time}$

$\mathfrak{R}_D(E)$  = Response for absorbed dose,  $Gy cm^2$

$S_p$  = Source strength,  $\frac{particles}{time}$

$r$  = Distance, cm

$e^{-\mu r}$  = Attenuation factor, *unitless*

The total dose for the same monoenergetic geometry is given by

$$D(r) = \int_{E_L}^{E_U} \phi(E) \mathfrak{R}_D(E) dE \quad (6)$$

Where,

$$D(r) = \text{Total dose, } \frac{\text{Gy}}{\text{time}}$$

$$E_U = \text{Upper energy boundary, eV}$$

$$E_L = \text{Lower energy boundary, eV}$$

$$\phi(r, E) = \text{Flux for total dose, } \frac{\text{Particles}}{\text{cm}^2 \text{s}}$$

$$\mathfrak{R}_D(E) = \text{Response for absorbed dose, } \text{Gy cm}^2$$

The energy absorption buildup factors is given by the following

$$B(r) = \frac{D(r)}{D^o(r)} = \frac{\int_0^{E_o} dE \mathfrak{R}(E) \phi(r, E)}{\mathfrak{R}(E_o) \phi^o(r)} \quad (7)$$

Where,

$$B(r) = \text{Buildup Factor}$$

$$D(r) = \text{Total dose, } \frac{\text{Gy}}{\text{time}}$$

$$D^o(r) = \text{Uncollided dose, } \frac{\text{Gy}}{\text{time}}$$

$$\mathfrak{R}(E) = \text{Response for total dose, } \text{Gy cm}^2$$

$$\phi(r, E) = \text{Flux for total dose, } \frac{\text{Particles}}{\text{cm}^2 \text{s}}$$

$$\mathfrak{R}(E_o) = \text{Response for uncollided dose, } \text{Gy cm}^2$$

$$\phi^o(r, E) = \text{Flux for uncollided dose, } \frac{\text{Particles}}{\text{cm}^2 \text{s}}$$

Buildup factors are not constant, but vary with the following parameters:

1. The type of detector response function
2. The geometric configuration of the source
3. The material of the attenuating medium
4. The energy of the source photon
5. Distance of penetration through the attenuating medium

#### Energy-Absorption Coefficient

The energy absorption coefficient is an important variable in the deciphering of interactions pertaining to photons in a medium. The amount of energy absorbed per unit mass of the medium (absorbed dose) is a significant parameter which provides a basis for discussing radiation effects. The effects of gamma rays on irradiated media are largely indirect, since they occur via electrons that are initiated as a result of gamma ray interactions with matter. They also dissipate energy as they are brought to rest. The shift of energy from photons to electrons and vice versa occurs in an intricate chain of events as shown in the Figure 6. A complete energy deposition should take into account all indicated energy transfer routes leading to electron collision losses and associated typical effects (Hubbell, 1969).

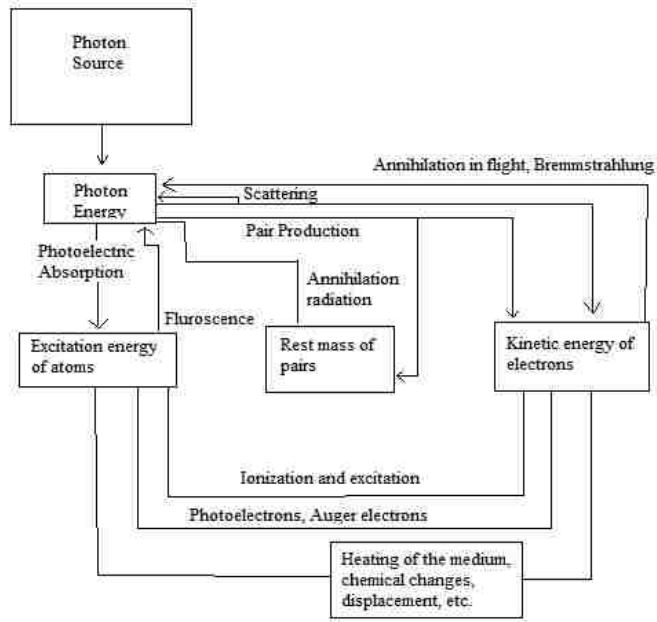


Figure 6. Energy Shift from Protons to Electrons

The significance of the interactions is based on it being a function of energy. At high energies such as 10 MeV, the range of secondary electrons tends to become comparable with the  $\gamma$ -ray mfp. Under these conditions the derivation of the energy deposition in a medium requires a cascade calculation involving the transport equations. But at energies lower than 10 MeV, where electron travel loses significance, it is sufficient to address issues in terms of flux or the energy absorption coefficient or any other coefficient as deemed appropriate (Hubbell, 1969).

The mass energy absorption coefficient is the energy absorption coefficient divided by the density of the medium. This coefficient takes into account all the modes of energy transfer to electrons such as the escape of Compton-scattered, fluorescence, annihilation, and Bremsstrahlung photons. While other coefficients account for certain types of



interactions, the mass energy transfer coefficient accounts for the interactions listed above except Bremsstrahlung photons. While the mass absorption coefficient accounts for the escape of Compton-scattered photons only. The mass energy absorption coefficient is a more encompassing variable that results in accurate results compared to the other two coefficients. Equation 8 captures the calculation approach for the three coefficients and weighting factors are inserted to show the significance of the principal interactions.

$$\left. \begin{aligned} \frac{\mu_{en}}{\rho} &= \\ \frac{\mu_K}{\rho} &= \left( \frac{\mu_\tau}{\rho} \right) f_\tau + \left( \frac{\mu_C}{\rho} \right) f_C + \left( \frac{\mu_K}{\rho} \right) f_K \\ \frac{\mu_a}{\rho} &= \end{aligned} \right\} \quad (8)$$

Where,

$$\frac{\mu_{en}}{\rho} = \text{Mass energy absorption coefficient, } \frac{cm^2}{g}$$

$$\frac{\mu_K}{\rho} = \text{Mass energy transfer coefficient, } \frac{cm^2}{g}$$

$$\frac{\mu_a}{\rho} = \text{Mass absorption coefficient, } \frac{cm^2}{g}$$

$$\frac{\mu_\tau}{\rho} = \text{Photoelectric absorption, } \frac{cm^2}{g}$$

$f_\tau$  = Average fraction of photon energy converted to photoelectric absorption

$$\frac{\mu_C}{\rho} = \text{Compton collision absorption, } \frac{cm^2}{g}$$

$f_C$  = Average fraction of photon energy converted to Compton collision

$$\frac{\mu_K}{\rho} = \text{Pair production, } \frac{cm^2}{g}$$

$f_K$  = Average fraction of photon energy converted to pair production

The methods used to calculate the mass energy-absorption coefficient are described more clearly through the use of an intermediate quantity, the mass energy-transfer coefficient. The mass energy transfer coefficient accounts only for the escape of secondary photons produced at the point of interaction and the quanta of radiation from the annihilation of positrons (NIST, 1996).

The mass energy transfer coefficient is related to the mass energy absorption coefficient by the following equation:

$$\frac{\mu_{en}}{\rho} = \frac{(1-g)\mu_{tr}}{\rho} \quad (9)$$

Where,

$$\frac{\mu_{en}}{\rho} = \text{Mass energy absorption coefficient, } \frac{cm^2}{g}$$

$$\frac{\mu_{tr}}{\rho} = \text{Mass energy transfer coefficient, } \frac{cm^2}{g}$$

$g$  = Average fraction of the kinetic energy of secondary charged particles

The calculation of  $g$  is an intricate process of integration of cross sections related to the radiative process of interest over the differential track length distribution established by the particles in the course of slowing down. When the quantitative values of  $g$  are relatively small, the errors are truncated in the mass energy absorption coefficient. The evaluation of  $g$  takes into account the following interactions:

- Emission of Bremsstrahlung
- Positron annihilation in flight
- Fluorescence emission as result of electron and positron interaction
- Energy loss straggling and knock on electron production as the secondary particles slow down

#### Boltzmann Transport Equation

The behavior of individual neutrons and nuclei cannot be determined; however the average behavior of a large population of neutrons can be described if information about neutron fluxes, cross-sections, and reaction rates are known. This phenomenon is known as Transport Theory and is based on the solution of the Boltzmann transport equation. Due to the intricacies involved in the equation, it can be only solved purely analytically if certain restrictions are placed. But a negative consequence of this approach is that the restrictions limit the usefulness of the solutions obtained. To obtain physically realistic solutions to the transport equation, a numerical technique approach is necessary. Numerical techniques are capable of providing solutions of certain accuracy based upon computer time. These outputs are fundamentally more accurate than those obtained via the diffusion theory approximation of the Boltzmann transport equation. The Boltzmann

transport equation is a conservation equation of particles in space. It is simply a bookkeeping process of particles. The basic form that the equation takes is:

$$\begin{aligned} \Omega \cdot \nabla \phi(r, E, \Omega) + \mu(r, E)\phi(r, E, \Omega) = \\ \int_0^\infty dE' \int_{4\pi} d\Omega' \mu_s(r, E' \rightarrow E, \Omega' \rightarrow \Omega)\phi(r, E', \Omega') + S(r, E, \Omega) \end{aligned} \quad (10)$$

The Boltzmann transport equation is a powerful tool for analyzing transport phenomena within systems that involve temperature and density gradients. The equation above is a general solution for particles, either photons or neutrons, and accounts for all type of interactions that are encompassed by the variables. It is considered an *integrodifferential* equation due to the fact it has derivative (Duderstadt, 1976).

The steady-state version of equation 10 can be written as follows:

$$\frac{d}{dR} \phi(r, \Omega) dr d\Omega + \mu(r)\phi(r, \Omega) dr d\Omega = S(r, \Omega) dr d\Omega \quad (11)$$

where  $dR$  is the differential length along the direction  $\Omega$  (i.e.,  $\Omega \cdot \nabla = d / dR$ ). This equation may be integrated along the direction  $\Omega$  from  $r_0$  to  $r$ , to obtain

$$\phi(r, \Omega) dr = e^{-\alpha(r_0, r)} \phi(r_0, \Omega) dr_0 + \int_{r_0}^r e^{-\alpha(r', r)} S(r', \Omega) dr' \quad (12)$$

where  $\alpha(r', r)$  is the total number of mean-free path lengths along the direction  $\Omega$  between  $r'$  and  $r$ :

$$\alpha(r', r) \equiv \left| \int_{r'}^r \mu(R) dR \right| \quad (13)$$

Given an isotropic point source of strength  $S_0$  (particles/s) located at  $r_0$ , the directional flux outward through the cone  $d\Omega$  about direction  $\Omega$  is  $S_0 (d\Omega / 4\pi)$ . The volume element  $dr$  subtended by this cone at distance  $R = |r - r'|$  away is  $4\pi d\Omega R^2 dr$ .

The directional flux at  $r$  of uncollided particles from an isotropic point source at  $r'$  (such that the direction from  $r'$  to  $r$  is  $\Omega$ ) is given by

$$\phi_{pi}(R) = \phi(|r - r'|, \Omega) = \frac{S_0 e^{-\alpha(r,r')}}{4\pi|r - r'|^2} = \frac{S_0 e^{-\alpha(R,0)}}{4\pi R^2} \quad (14)$$

This set up for an isotropic point source is what this study will entail and be modeled for.

There are two classes of computational techniques that are used to solve the transport equation numerically. In the first class, deterministic method, the transport equation is discretized using a variety of methods and then solved directly or iteratively. Different types of discretization give rise to different deterministic methods such as discrete ordinates, spherical harmonics, collision probabilities, nodal methods, and others. The second class of techniques, Monte Carlo methods, constructs a stochastic model in which the expected value of a random variable is equivalent to the value of a physical quantity to be determined. The expected value is estimated by the average of many independent samples representing the random variable. Random numbers, following the distributions of the variable to be estimated, are used to construct these independent samples. There are two different ways to construct a stochastic model for Monte Carlo calculations. In the first case the physical process is stochastic and the Monte Carlo calculation involves a computational simulation of the real physical process. In the other case, a stochastic model is constructed artificially, such as the solution of deterministic equations by Monte Carlo.

## Transport Equation for Photons

For most photon-transport calculations the quantity of interest is the doubly differential energy flux density  $I(r, E, \Omega) \equiv E\phi(r, E, \Omega)$ . The Boltzmann transport equation in integro-differential form multiplied by  $E$  on both sides may be written as:

$$\Omega \nabla(r, E, \Omega) + \mu(r, E)I(r, E, \Omega) = \int_0^\infty dE' \int_{4\pi} d\Omega' \frac{E}{E'} \mu_s(r, E'-E, \Omega'-\Omega) x I(r, E', \Omega') + ES(r, E, \Omega) \quad (15)$$

Where,

$\mu$  = Total interaction coefficient,

$\mu_s(r, E' \rightarrow E, \Omega' \rightarrow \Omega) dE' d\Omega'$  = The probable number of secondary photons at a point  $r$  with energies in  $dE$  about  $E'$  in direction  $d\Omega$  about  $\Omega'$

$S(r, E, \Omega)$  = The product rate of photons.

The secondary photon production kernel  $\mu_s$  can be written as the sum of the contributions from the three dominant photon-medium interactions as (Harima, 1993):

$$\mu_s(r, E' \rightarrow E, \Omega' \rightarrow \Omega) dE' d\Omega' = \mu_c(r, E' \rightarrow E, \Omega' \rightarrow \Omega) + \frac{1}{4\pi} \mu_{pp}(r, E') 2\delta(E - mc^2) + \frac{1}{4\pi} \mu_{ph}(r, E') N(r, E, E') \quad (16)$$

Where,

$\mu_c$  = Compton scattering

$\mu_{pp}$  = pair production

$\mu_{ph}$  = photoelectric absorption coefficient

$N(r, E, E')$  = The number of photons in unit energy about  $E$  per photon of energy  $E'$  absorbed in a photoelectric interaction at  $r$ . (The equation assumes that fluorescence and annihilation radiation are emitted isotropically at the point where the primary photon is absorbed).

## ANISTROPIC SOURCE FLUX ITERATION

### (ASFIT)

ASFIT-VARI solves problems of gamma-ray transport in slab geometry. The method is applicable to energy-dependent, multiple region radiation transport with arbitrary degree of anisotropy. Buildup factors and energy-angular distributions at the spatial mesh points are calculated. The code sets up a monoenergetic source and is either normal or isotropically incident at the surface or in a region. The code accounts for secondary sources such as annihilation, Bremsstrahlung, and fluorescence but coherent scattering is not accounted for in this version.

The method of solution for ASFIT is that the transport equation is written in the form of a coupled integral equation in which two terms are separated, the spatial and energy-angular transmission. For the radiation source and flux, the Legendre polynomial is used for the approximation in the direction cosine and discrete ordinate representation in energy and spatial domain. The space and energy-angle transmission kernels are evaluated analytically and the integral equations are solved by a rapid converging iterative technique. Quadratic interpolation of the sources between space nodes is used for spatial integration. The only cross section input needed from the user is the pair production and total cross sections. The Compton cross sections are computed internally

(RSICC Computer Code CCC-336). The program is operated in the computing language of Fortran 77 and a tutorial on how to write a sample input is enclosed in Appendix XII and XIII.

ASFIT is a semi-analytical method that is derived on the probabilities of collision for energy dependent radiation transport calculations. Essentially the equation is not solved directly but rather combinations of certain terms are solved directly and others are converged upon by successive iterations. The equation for radiation transport, one dimension setting, for ASFIT is written as follows:

$$\phi(x, E, \mu) = \int S(x', E, \mu) T(E, \mu, x' - x) \frac{dx'}{\mu} \quad (17)$$

$$\int S(x', E, \mu) = \int d\Omega' \int dE' \phi(x, E', \Omega') G(E' - E, \Omega' - \Omega) + S'(x, E, \mu) \quad (18)$$

Where,

$\phi$  = Flux densities

$S$  = Source densities

$S'$  = External source

$T$  = Spatial transmission kernels

$G$  = Energy angle transmission kernels

Employing discrete ordinate representation in space and energy along with the Legendre polynomial expansion in  $\mu$  in equation 17 and 18, and the following is given:

$$\phi_{j,g,n} = \sum_{n'} \sum_{j'} S_{j',g,n'} T(g, n' - n, j' - j) \quad (19)$$

$$S_{j,g,n} = \sum_{g'} \phi_{j,g',n} G(n, g' - g) \quad (20)$$

Where,



$\phi_{j,g,n} = n$ 'th Legendre coefficient for flux terms at the  $g$ 'th and  $j$ 'th spatial nodes

$S_{j,g,n} = n$ 'th Legendre coefficient for source terms at the  $g$ 'th and  $j$ 'th spatial nodes

From equation 19 and 20, the spatial and energy-angle transfer matrices T and G are evaluated iteratively (Gopinath, 1973). The T matrices are used to define the movement of the photon with respect to its spatial direction. The G matrices described the energy angle transmission of a photon or the interaction and travel of a certain photon in the angular direction which is a direct function of its source energy. The Legendre polynomial expansion of the flux with respect to the angular dependencies is appropriate for the derivation of the collision integral with anisotropic scattering. Discretization in the direction cosine abridges the spatial transmission computation. To include the benefits of both techniques, ASFIT was modified to ASFIT-VARI. This code will employed for the determination of buildup factors in this study.

The model setup angular sources at the zeros of a given order polynomial and calculates the fluxes at these given angles. Taking these calculated fluxes, the Legendre coefficients of the resultant flux is obtained via Gaussian quadrature. Then from there, the collision integral is evaluated for the Legendre coefficients of the source. Now working backwards, from the source coefficients the actual sources terms at the required angles are computed and this process is iterated.

An ensuing study was followed for convergence at different orders of Gaussian quadrature for the angular flux. From this study two figures, see below, were created that essentially give the perturbations of the reflected spectrum and buildup factors of a typical system with the order of the approximation,  $n$ . It is shown that beyond  $n = 4$  there is no change at all and that even at  $n = 2$  convergence to within a percent is obtained. The

significance of these graphs is that with alterations the computing time is reduced anywhere from a factor 2 to 3 (Gopinath, 1973).

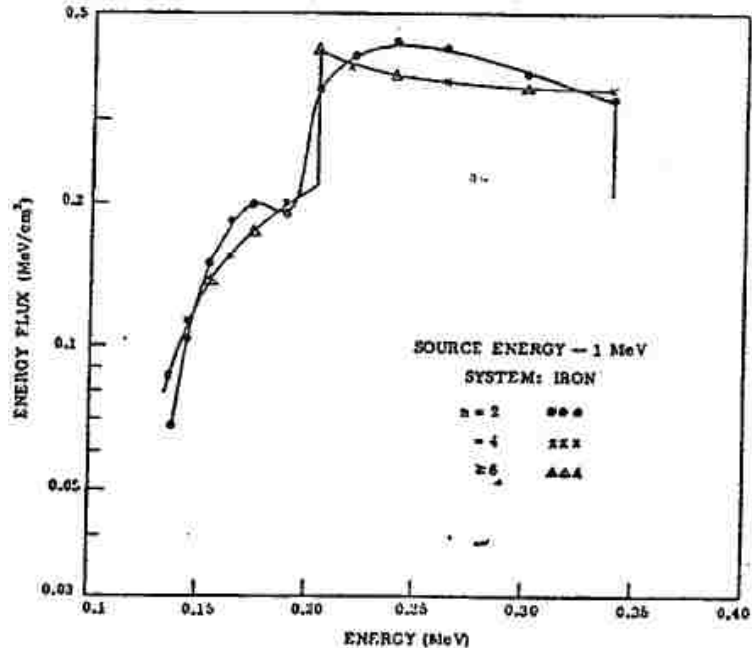


Figure 7. Energy Flux vs. Energy

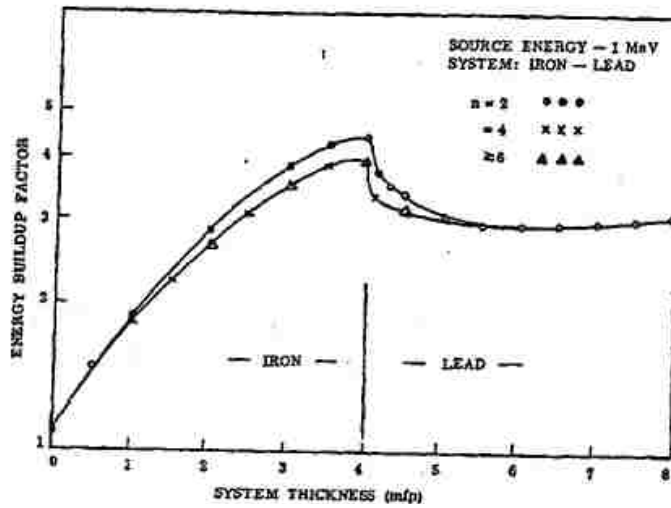


Figure 8. Energy Buildup Factor vs. System Thickness

An issue that arises with ASFIT is that it calculates the buildup factor for a plane isotropic source whereas for the ANS standard a point source is needed. To make this conversion the following relations is needed for the calculated buildup factors from ASFIT (Harima, 1993):

$$B^{Pt}(x) = B^{Pl}(x) - x * \exp(x) E_1(x) \frac{d}{dx} B^{Pl}(x) \quad (21)$$

Where,

$B^{Pt}$  = Point source buildup factor

$B^{Pl}$  = Plane isotropic source buildup factor

$x$  = distance in mfp

$E_1$  = Energy buildup factors is being evaluated at, eV

#### Monte Carlo N-Particle 5 (MCNP5)

The Monte Carlo method for solving transport problems was compiled at Los Alamos National Laboratory (LANL) during World War II. The technique is generally attributed to Fermi, von Neumann, Ulam, Metropolis, and Richtmyer. MCNP, released in 1977, is the progeny of their work and has been under incessant development for the past quarter of a century. MCNP5 is a product of the Diagnostic Applications Group (X-5) in the Applied Physics Division (X division) at LANL (X-5 Monte Carlo Team, 2005).

MCNP5 is a general purpose, continuous-energy, generalized-geometry, time-dependent, coupled neutron/photon/electron Monte Carlo transport code. MCNP5 is a code used for neutron, photon, or electron transport, including the capacity to calculate eigenvalue for critical systems. Essential features of MCNP5 make it adaptable and flexible and easy to use which include a powerful general source, criticality source and

surface source, geometry and output tally plotters, numerous variance reduction methods, versatile structure, and an all encompassing cross section library (X-5 Monte Carlo Team, 2005).

The user inputs certain information into MCNP5. The text file entails the following information:

- Geometry Specification
- Material description & Cross-Section Evaluations
- Location and Characteristics of Neutron, Proton, and Electron Source
- Types of Tallies Desired
- Variance Reduction Techniques to Improve Efficiency

MCNP5, as denoted by its name, employs the Monte Carlo method of solving intricate problems. This technique is used to reproduce a statistical process and particularly expedient for involved problems that cannot be modeled and solved using codes that utilize deterministic methods. Each probabilistic event that combines a process is simulated sequentially. The probability distributions governing these events are statistically sampled to describe the total phenomenon. Due to the exorbitant number of trials necessary to adequately simulate a phenomenon the method is performed on computers. The arbitrary sampling process is based on the selection of random numbers. The method is analogous to gambling games such as throwing a dice, hence the name “Monte Carlo.” In transport of particles, MCNP is a numerical experiment. It starts with a source emitting particles and actually following each of many of those particles from its beginning to its termination in a certain type of interaction, i.e. absorption, escape, capture, etc. Probability distributions are sampled indiscriminately using transport

information to decipher the consequence of each stage of its life. The figure below is a visual demonstration of the random phases of a particle incident on a slab that can result in fission. The process steps below the figure show the random events that can occur in the process entering the slab (X-5 Monte Carlo Team, 2005).

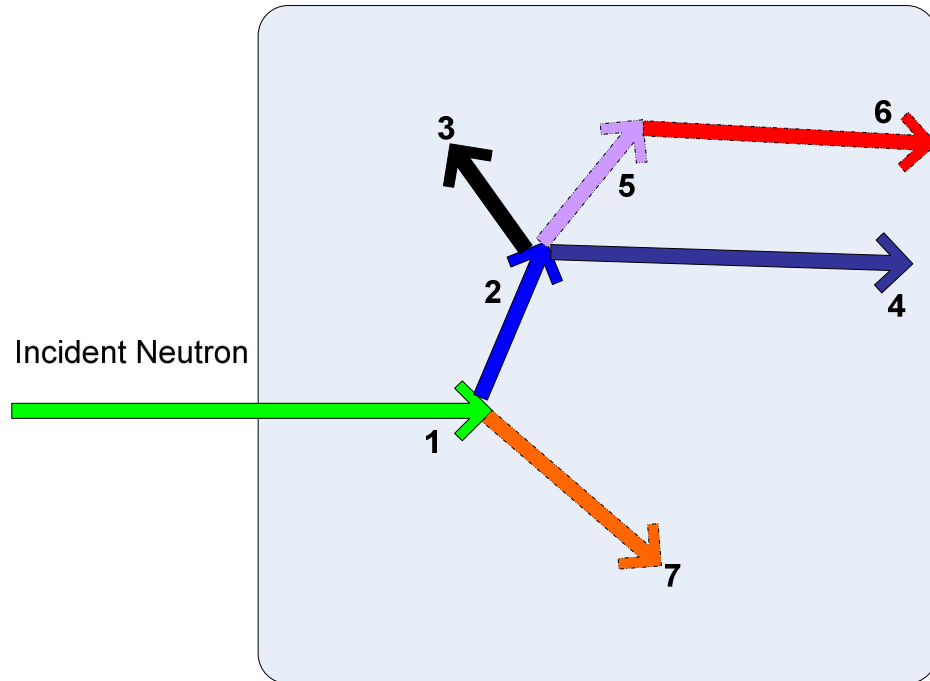


Figure 9. Life of a Neutron

#### Process Steps

1. Neutron scatter; photon produced
2. Fission; photon produced
3. Neutron capture
4. Neutron leakage
5. Photon scatter

6. Photon leakage

7. Photon capture

Even with all these very useful applications that MCNP5 offers to users it may not be considered ideal for deep penetrations because of the statistical nature and for that reason a transition to ASFIT was done, which is a deterministic code and can be used as a validation reference for our MCNP5 results. Another issue is the convergence rate, for novice users this causes the software to appear to be slow. To create an efficient run one must have a plethora of experience in the employment of variance reduction. It is considered an “art” to utilize and create an effective variance reduction technique.

Cross sections for photon interaction is required for all photon problems. Photon interactions in this current version of MCNP5 are able to account for both photoatomic and photonuclear events. Due to the difference of events in real world such as elemental versus isotopic, the data are stored on separate tables.

Directions and energies of atomically scattered photons information from sets of angular and energy distributions can be found on neutron interactions tables. The angular distribution for different interactions such as fluorescence x-rays from the relaxation cascade after a photoelectric event is isotropic. The angular categorization for coherent and incoherent scattering comes from sampling the Thomson and Klein-Nishina formulas, respectively. The default setting of MCNP causes sampling for the form factor and scattering function data at incident energies below 100 MeV. Anything above that energy level that data is ignored, this is a conservative and reasonable approximation for high-energy photons. Incoherent scattered photons have their energy calculated from the sampled scattered angle. If necessary and available, the energy is modified to account for

the momentum of the bound electrons (X-5 Monte Carlo Team, 2005). MCNP5 was chosen to be the primary code used for this study because it is currently supported by the Radiation Safety Information Computational Center (RSICC) and is widely used by professionals in the nuclear industry whereas ASFIT is not commonly used.

#### Differences between MCNP5 and ASFIT

For this study these two codes were employed due to the differences in their method of calculation of the particle transport equation. ASFIT employs a deterministic method; specifically discrete ordinates method and therefore solves the transport equation for the approximately. By contrast, MCNP5 using the Monte Carlo method simulates individual particles and utilizing the tallies records different aspects of their *average* behavior..

ASFIT outputs the buildup factor if desired while MCNP5 only gives out the total and uncollided dose via the tallies and from there calculates it by dividing the former by the latter. MCNP5 only gives out information based on the specific tallies inputted by the user. ASFIT in deriving the solution uses quadratic interpolation whereas MCNP5 employs logarithmic interpolations. The logarithmic interpolation is considered more accurate for most applications. Another differences lies in the modeling of sources, MCNP5 can treat a point source or any type of geometry as long as modeled as such but ASFIT is designed for a plane slab source and equation 21 can be used to convert it to a point source (X-5 Monte Carlo Team, 2005).

### Photon Interactions

The majority of buildup-factor data is for point, isotropic, and monoenergetic sources of photons in infinite homogeneous media. The initial data was based upon moment-method codes such as GAMMOM and only accounted for Compton scattering. Early data sets were based on moments-method calculations and accounted only for buildup of Compton-scattered photons. The buildup of annihilation photons was accounted for in subsequent moments-method calculations (Harima, 1993). Buildup-factor calculations using ASFIT-VARI code account for Compton-scattered photons, annihilation photons, fluorescence, and Bremsstrahlung. (Harima, 1993) Buildup factors in the ANS Standard exclude coherently scattered photons and treat Compton scattering according to the Klein-Nishina cross-section for photon scattering with free electrons. There is a provided correction factor in the back for each table to account for coherent scattering. (ANSI/ANS-6.4.3, 1991).

Dose to medium response functions used for the current ANS Standard shall be used in this study by MCNP5; however, the cross-section data shall be from different sources. (Hubbell, 1969).

### Cross-Section Data Libraries

Various cross-section data libraries are available for radiation transport computations. PHOTX cross-section and Hubbell cross section data libraries were used for the calculation of buildup factors for the ANS Standard (ANSI/ANS-6.4.3, 1991). Since the publication of the ANS Standard, a new data library has been developed. ENDF has become a primary choice for data cross sections. ENDF has provided a medium for



representations for cross sections and distributions, photon production from neutron reactions, a limited amount of charged particle production from nuclear reactions, photo-atomic interaction data, thermal neutron scattering data, and radionuclide production and decay data, which include fission product (Chadwick et al., 2006). The ENDF system was created for the storage and retrieval of evaluated nuclear data to be used in nuclear technology applications. ENDF/B data sets are revised or replaced only after extensive review and testing.

## CHAPTER 2

### REVIEW OF RELATED LITERATURE

#### Literature Review

Since its origin, the compilation, precision, and methods of calculating buildup factors have been debated. According to Harima, the practical calculation of gamma ray attenuations is often abridged by the use of buildup factor, whose origins are shrouded in the beginning of the Manhattan Project (1993). The term buildup factor was coined by White in 1950 to express penetration of  $^{60}\text{Co}$  gamma rays in water. Its magnitude was acknowledged by Fano in 1953. From there the premise of buildup factors took off starting with an extensive set of tables for buildup factors in 1954 by Goldstein and Wilkins, which were derived using the moment's method. Their study had included data for 6 elements and water; buildup factors for other elements were obtained via interpolation between the atomic numbers. Despite the progress of computers and transport calculations methods, this data has been used as the *de facto* standard for more than more than 30 years (Harima, 1993). A tremendous amount of work has gone into the study of gamma-ray buildup factors in the last 40 years. Tanaka *l.* of the Gamma-Ray Buildup Factor Working group of the Japan Atomic Energy Society performed a literature review encompassing all the works pertaining to this subject from 1950 to 1987, almost a span of four decades. The result can be divided into three categories (Harima, 1993). The initial category includes numerous amounts of buildup factor calculations that are based on the transport equation and compared to decipher the differences among the different solutions to the transport equation. Impediments have arose in the calculations

that usually cast a shadow of doubt in their accuracy and hence their usefulness. In reaction to this, excellent experiments have been conducted that supplement these calculations and help stimulate improvements within them. The second category of results is for the numerous approximations of buildup factors by empirical formulas. The final category is for the application of buildup factors (Harima, 1993). During the 1980s, a working group ANS-6.4.3 was formed to develop a standard on buildup factors following the Three Mile Island Accident. But before the group was created to form the standard, an available set of buildup factors existed in National Bureau of Standards (NBS), which is now renamed as the National Institute of Standards and Technology (NIST), of which only concrete, air, water, and iron has been published. Again, this data set was derived using the moments method. These early data sets only took account of Compton Scattering in their codes. But the NBS data set attempted to take into account contribution from the secondary sources such as annihilation and fluorescence, yet left Bremsstrahlung out of the loop (Harima, 1993). The NBS data was contrasted with a Monte Carlo method code and other transport codes to help further validate the data and modifications were made accordingly by the working group. The PALLAS code was utilized for inclusion of the contribution of secondary particles including Bremsstrahlung for high Z materials. One thing that has been ignored in the buildup factor data was coherent scattering (Harima, 1993). The rationale for this exclusion was that coherent scattering of photons were seen as not affecting buildup factors because there is no energy change and only a miniscule change in direction with coherent scattering. The odds of a photon being coherently scattered at a relatively large angle increases significantly below a few hundred keV, especially for high Z elements (Harima, 1993).

Correction factors accounting for coherent scattering, even though they maybe small or negligible, has been included in the standard.

In a study conducted by Shimizu et al. (2003), a comprehensive work was carried out to help generate a new data set for buildup factors for a point isotropic source in an infinite medium using the Invariant Embedding (IE) method. Its point of comparison was the ANS Standard, which was setup in a similar manner.. The observations for improvement were that an expansion in terms of buildup factor depths for interaction or mfps had been conducted. The ANS standard values are based upon a 40 mfp distance for the gamma-ray attenuation, whereas this study went up to 100 mfp for evaluation purposes but claims it had initially calculated values up to 300 mfp (Shimizu et al., 2003). The rationale behind this extension was intended for severe accidents that required buildup factors beyond the depths of 40 mfp which corresponds to an average distance of 2 meters (m) where the current extension of up to 100 mfp is equivalent to approximately 5 m. This would make the gamma ray buildup factors more practical in the real world. It was demonstrated in a previous paper, according to Shimizu et al. that the IE method is very efficient and accurate in providing the buildup factors of depths to a 100 mfp and more (Shimizu et al. 2003). Another point of development that this study shows is that full effects of Bremsstrahlung were taken into account whereas for the ANS standard, which was calculated using the moments method, buildup factors for low-Z materials neglected the effects of Bremsstrahlung. High-Z materials were calculated by a discrete ordinate integral code, PALLAS, which did account for Bremsstrahlung but its assumption was a simple model assuming that all the secondary photons are emitted in the same direction as the primary photon. The IE method used in this study is based on an

energy-angle distribution of the secondary photons in contrast to the initial code that Hirayama utilized, EGS4, which simulated generation and transport of electron and positron. The IE method is used for calculating gamma-ray buildup factors for both low-Z and high-Z elements. The buildup factors for all elements are computed with the effects of Bremsstrahlung of electron and positron along with the annihilation of positrons (Shimizu et al. 2003). The buildup factors for high-Z elements were calculated with fluorescence in the locality of the K-edge. Instead the K X-rays were used. A third point of enhancement in comparison to the ANS standard is the notion of consistency in terms of the gamma ray cross sections used for materials. In the ANS standard, the buildup factor of low-Z materials were calculated with the gamma-ray cross section NBS29 while PHOTX was used for high-Z elements. But in their study all buildup factors were calculated using PHOTX for all Z elements. The total cross section is the sum of Compton scattering, photoelectric effect, and pair production while neglecting coherent scattering (Shimizu et al. 2003). The current study does not account for coherent scattering and electron binding effects in incoherent scattering. The last two points of improvement over the ANS standard with this study is that three types of buildup factors are calculated: effective dose, exposure, and energy absorption. Also the exactness of the transport calculation is quantitatively assessed (Shimizu et al 2003).

In a study conducted by Ahmet Bozkurt and Nicholas Tsoulfanidis, the calculation of exposure buildup factors for reactor fuels using MCNP is conducted. The premise behind the study is that attenuation of gamma rays in irradiated fuel rods cannot be ignored and their product, which is secondary gamma rays must not be neglected. Their method of calculation was to locate a point isotropic and monoenergetic gamma source in an infinite

UO<sub>2</sub> medium which extends to 40 mfp thick (Bozkurt and Tsoufanidis, 1996). Around this source, ten concentric spheres were placed at certain radii for tallying reasons. As a result, ten different source energies were studied. Coherent and Bremsstrahlung effects were included in the computation. The study goes on to describe how to use the tallying output in MCNP along with other data to derive the buildup factor at each distance examined (Bozkurt and Tsoufanidis, 1996). This paper was a great forerunner in terms of modeling for the current study, which emulated the geometries and attempted to solve for the buildup factors in a similar fashion.

In the calculation of buildup factors for gamma-ray transport calculations, the coherent scattering process is not included due to its inability to reduce the energy of the photon. From studies that have included the coherent scattering into their collision process, it has been argued that the scattered flux escalates by an amount that reimburses for the sudden attenuation of the beam due to the addition of the coherent scattering process (Subbaiah et al. 1989). In their study, Subbaiah et al. note that some general observations have been made. The first is with respect to the practice of typically ignoring the coherent scattering process, which can be rightly substantiated if there is no alteration in the direction of the photon after a scattering incident has taken place. It can still be approximated and valid for very small angular deflections. Yet, in the study by Subbaiah et al. the coherent scattering process shows a considerable angular spread in spite of the dominant peaking in the forward direction. Another observation deals with the notion that even though the process may cause only small angular deflections, a large number of such collisions occurring could increase the path length traversed by the photons and as a result increase the possibility of termination in terms of absorption. Due

to these general observations, Subbaiah et al. carried out their study to evaluate the effects of coherent scattering on transport properties of gamma rays. These authors focused mainly on the transport code ASFIT. Adjustments to the computation scheme of the existing slab geometry gamma-ray transport code ASFIT are introduced to include the effects and influence of coherent scattering. The altered code is then validated against two model problems in their study and consequently used to investigate quantitatively the transport effects of coherent scattering as a function of the incident photon energy and the atomic number  $Z$  of the medium (Subbaiah et al. 1989). The materials under study for their paper were an array of low and high- $Z$  elements for photon energies ranging from 0.015 and 0.3 MeV. The system they created is a 48 mfp thick slab, which has entrenched a strip of isotropic source located 4 mfp from the left boundary. The results have been reported in the form of scattered flux spectra and dose rates, both well deep in the media. Due to the limited availability of transport codes that account for coherent scattering, the modified ASFIT code is utilized in their study as a function of incident photon energy and atomic number of the medium. For the contributions of any type of scattering, the influence can be significantly determined by the ratio of the respective scattering cross section, in this case coherent scattering, to the total cross section (Subbaiah et al. 1989). From this study, a few observations arose, first at any given distance or mfps, the spectral shape is almost untouched by the inclusion of the coherent scattering. The shape of the total cross section curve forms the shape of the scattered gamma spectra and since the shape of the total cross section is not modified significantly by the addition of coherent scattering, hence the spectral shapes are identical with or without including the coherent scattering process. The major difference is noted by Subbaiah et al. in their other

observation, which pertained to the difference in magnitudes of the fluxes with and without coherent scattering. The addition of the coherent scattering leads to a marginal increase in the flux for points close to the incident face, while anything beyond 4 mfp it leads to a reduction, which increases marginally with depth. The consequence of coherent scattering is to deflect the photons from their direction, which as a result increase the path length between the source and any point of observation in that geometry. The figure below illustrates the inclusion and exclusion of coherent scattering to a system (Subbaiah et al. 1989).

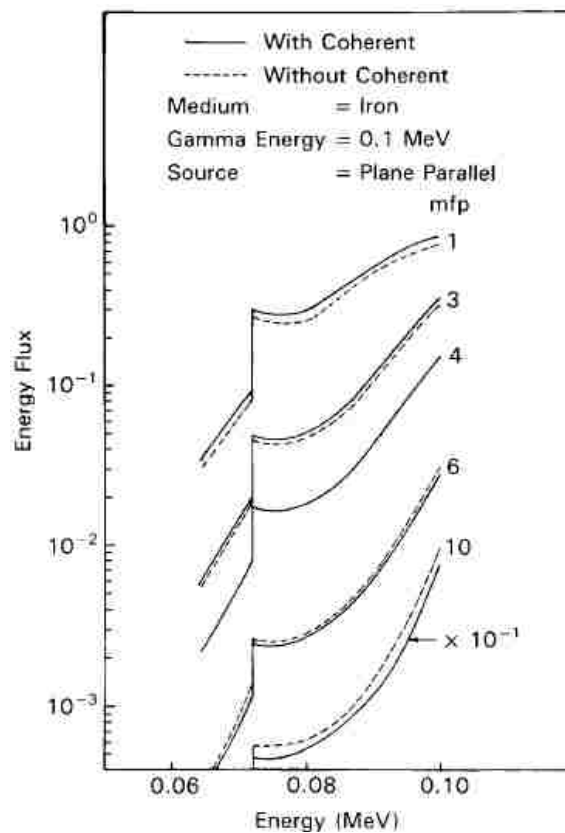


Figure 10. Effects of w/ and w/o Coherent Scattering



Customarily, buildup factor have been derived as a function of mfp, this approach has some disadvantages in assessing coherent scattering, since the physical/linear length associated with mfp differs depending on the total cross section and its exclusion or inclusion of coherent scattering. The earlier works had not accounted for coherent scattering and therefore the ratios of buildup factors with and without the process can serve as a correction factor for the earlier values. Hirayama and Trubey carried out some work in this respect using EGS4, a Monte Carlo method code. Their works were compared with ASFIT values and agreed within 10% of any energy or depth (Subbaiah et al. 1989). The study conducted by Subbaiah et al. was the initial attempt to use a discrete ordinates code to account for the influence of coherent scattering via a modified version of ASFIT. It can be summarized that Subbaiah et al. found that the inclusion of coherent scattering in the gamma-ray calculations lead to an enormous reduction in flux and dose in the deep penetration problems and essential to all materials in low energy zones. A crucial finding in the study was that the spectral shape is relatively unaffected by coherent scattering, which lays the foundation for the use of correction factors to earlier buildup factors to account for coherent scattering. But the unchanging spectrum's magnitude is decided by the ratio of coherent scattering to the total cross section. This also gives insight to energy regions where coherent scattering is important and wherever these vital energy regions exist are where the bound electron Compton scattering are vital also.

In the study by Harima et al. the PALLAS code was enhanced to include the effects of secondary sources such as Bremsstrahlung and fluorescence in the gamma ray transport calculations. The buildup factors for low-Z materials in the low energy range,

were calculated and were validated by the comparison with the results of the EGS4 code and ANISN code. The EGS4 code was improved to take into account the influence of coherent scattering, which was evaluated by including both coherent and bound electron incoherent scattering cross section in low energy range. In Harima et al. the fitting formula, geometric progression is developed. The employment of this fitting function can replicate the data over the full range of distance, energy and atomic number with a very high accuracy (Harima et al. 1991). The attenuation coefficient expands as the photon energy decreases by the successive scattering. It was found by them that coherent scattering can be neglected for most calculation under the condition that the total attenuation coefficient used to the calculation does not include it, since there is no energy change essentially and only a small change in direction with coherent scattering. This is applicable to only photons above a few hundred keV, especially in high Z materials.

Harima found in her study that the inclusion of annihilation radiation enhances exposure buildup factors by 4-5% and 5-6% enhancement of the energy absorption buildup factor. From Harima's study the effect of Bremsstrahlung radiations has impacted buildup factors by 7%. The contribution of Bremsstrahlung has a small and wide bump within a few mfp from the source and decrease with increasing penetrating depth for water, concrete, and iron (Harima, 1993).

Yoshida carried out a study to find and develop a method for a fitting function for gamma ray buildup factors. The fitting functions, Taylor and Geometric Progression (GP), parameters are in the ANS standard. Out of many fitting functions, GP is considered the most accurate but requires an extraordinary level of fitting technique. As a result of this, Yoshida points out that the GP formula was separated into a curved line and

a part representing the base values. Yoshida examined a plethora of methods ranging from Taylor, Berger, parabolic, Harima formulae, and the GP method but it was found that the GP method was more accurate (2006).

## CHAPTER 3

### METHODOLOGY

#### Literature Review Criteria

The technical papers cited in this study were all referenced in the ANS standard or part of a search criteria set forth per the authors' scope. For the study at hand, technical papers that were related to MCNP, ASFIT, low-Z material buildup factor calculations, and fitting technique were searched for this was the scope of the work. The literature review helped establish an understanding of the subject matter at hand, buildup factors, and its history. In addition, it helps shed light on many techniques and codes utilized to derive the buildup factors along with the different fitting techniques used. This allowed one to determine a viable code to use as a validation point against MCNP5 and what type of fitting to employ to help create an accurate fit. The literature review was limited to English language publications and documents that pertained to the study at hand. The standard of acceptance was established as the following:

- The document is a journal, academic, or scholarly publication that is peer-reviewed and credible.
- Examines the gamma-ray transport equation, buildup factors, ASFIT, MCNP5, ANS Standard, Geometric Progression fitting function, and/or transport codes.

The results that were encountered as part of this search were reviewed and applied under this criterion article by article. The internet was the primary medium to help track down plenty of articles and other pertinent data but academic textbooks and online data sources

were used in addition to the articles. To maintain the credibility and legitimacy of the online data sources they were limited to government affiliated organization such as national labs, scientific institutes, and any international scientific organizations.

### Approach to Computation

For this calculation, the buildup factor is calculated and validated in the following way:

- Run ASFIT cases to ensure it works on the new operating platform by recreating the same values in the ANS Standard.
- Update the ASFIT input cross section with ENDF library to calculate new buildup factors and use as a benchmarking code.
- Compare a deterministic code, ASFIT, and a stochastic code, MCNP5, on a one to one basis to evaluate buildup factors.
- Due to the old standard lacking the interactions of Bremsstrahlung, cases were executed in MCNP5 without Bremsstrahlung to account for some of the differences between the production runs and the ANS Standard.
- All the MCNP5 results for the assorted source energy are considered to be the official results.

### Computations

The focus of this study is to compute buildup factor values for low-Z materials and compounds. The material that shall be examined in this study that is considered a low-Z material by the ANS standard is iron and the compound is water. The photon cross

section, attenuation coefficients, and energy absorption coefficients data that was published by the NBS will be used in ASFIT program to calculate the gamma-ray buildup factors (Hubbell, 1969). Using the differences that exist between the NIST data and Hubbell, which were miniscule, it was deemed that the NIST cross sections can be used in conjunction with the Hubbell data to complete the input for ASFIT (Appendix V). Due to the lack of the difference in mass energy coefficients in the NIST data, the data from Hubbell will be used to help supplement the updated cross section values. Table 7 of Appendix V outlines the differences between Hubbell and NIST. The techniques that shall be laid out to calculate iron and water buildup factors may be applied to derive the buildup factors for all low-Z materials and compounds in the ANS standard. For this study a point, isotropic, and monoenergetic source of photons in an infinite homogenous medium was modeled for each energy level using MCNP5 and ASFIT which is consistent with the ANS standard.

Photon mass attenuation coefficients ( $\text{cm}^2/\text{g}$ ) with and without coherent scattering were calculated using ENDF/B-VI.8 photo-atomic interaction cross-sections for energies within the range of .010 to 30.000, which are consistent with the ANS Standard. Not only are these values included in the ANS Standard, they are also necessary for the calculation of mean-free path values and dose card response function that are used in the input section of MCNP5. A comparison between the new ENDF/B-VI.8 photon mass attenuation coefficients and those of the ANS Standard for iron and water without and with coherent scattering are provided in Appendix I, II, III, and IV respectively.

The buildup factor data in the ANS standard was generated using Hubbell's data for cross section for low-Z materials (ANSI/ANS-6.1.1, 1991). Per the author's decision, the

ENDF/B-VII.0 library would be the choice for generation of the new data. The election of this library is that it is the latest version to be officially released. The gamma ray data that is used in this study is the same as that which is used in ENDF/B-VI.8. Since the data for the latter is identical in terms of gamma ray values, it is sufficient to employ here and also would be in line with the latest version of ENDF which is not released yet. The photo-atomic interaction data used in ENDF/B-VI.8 are that of the EPDL97 (Evaluated Photon Interaction Data Library-1997) (Cullen, 1997). The ENDF library series was the first version to employ EPDL97 data, while the previous release used a decade old EPDL data, EPDL89. The ENDF/B-VI.8 are ACE-formatted (ASCII) and their files are readily available whereas ENDF/B-VII.0 ACE-formatted files for photo-atomic interactions are not available yet (Cullen, 1997).

To study the effects of using the ENDF/B-VI.8 photo-atomic data and Hubbell's photon cross section, the cross sections were compared one to another, see Appendix IV. The following bullets explain the rationale for comparing the two different sets:

- First, the use of Hubbell's cross section was to validate the code and reproduce the same values as those in ANS and account for any difference if they do exist.
- Second, compare the differences in Hubbell's cross section and the ENDF/B-VI.8 cross section, which will be used to update the buildup factor data, to record the explicit difference that exists in the input values.
- Third, use the ENDF cross section to compute updated buildup factors and compare those to the ANS Standard, account for differences that exist by the pure difference in the old and new cross section and the physics of the updated cross section.

The ENDF/B-VI.8 data were converted into a format that is readable by the softwares through elementary equations which convert cross-sections (barns) to attenuation coefficients ( $\text{cm}^2/\text{g}$ ). Appendix IV shows the percentage difference between the Hubbell data and the ENDF/B-VI.8 data at each energy value. Mass energy-absorption and mass energy-transfer coefficients using ENDF/B-VI.8 (or ENDF/B-VII.0) data were not found. To provide mass energy coefficient values that are more current than those previously used, data from the National Institute of Standards and Technology (NIST) (Hubbell & Seltzer, 2004) were used (Appendix X).

To study the effects of using two different computational codes, the ASFIT program was operated with the same values to simulate the same effects but with a different method of solving the transport equation. The results were expected to show some differences due to the two different methods of solution that were employed. The NIST values for the mass energy coefficients were used indirectly in MCNP5 via the dose card which incorporates the NIST data in its derivation. Ideally, ENDF/B-VI.8 values would be used for the mass energy coefficients to be consistent; however, ENDF/B-VI.8 mass energy coefficients are outside the scope of this study and for purposes here the NIST values are the most current that were found. The results and differences between the two programs are shown in Appendix VIII.

MCNP5 was used to calculate a new table of buildup factors for iron and water. The energies examined were the same as those used in the ANS Standard and as follows: 0.015, 0.02, 0.03, 0.04, 0.05, 0.06, 0.08, 0.1, 0.15, 0.2, 0.3, 0.4, 0.5, 0.6, 0.8, 1.0, 1.5, 2.0, 3.0, 4.0, 5.0, 6.0, 8.0, 10.0, and 15.0 MeV. Iron and water were chosen as the materials of interest and mfp thickness values from 0.5 to 40 were used, which is consistent with what



had been done in the ANS Standard. All mfp values were calculated manually using the total microscopic cross-section data from ENDF/B-VI.8 (Appendix X). An isotropic monoenergetic point source was used in all input files. For ASFIT, the results were computed for a planar monoenergetic isotropic source but converted to a point source by using the equation 21 outlined by Harima (1993). The variance reduction technique known as importance mapping, specifically geometry splitting (LANL, 2005), was used to improve statistics. Hirayama's studies shows that the technique of particle splitting is a very effective variance reduction method for buildup factors that demonstrate deep penetrations (1995). Total absorbed dose and uncollided absorbed dose calculations were performed simultaneously by the use of energy bins. The same method may be used for total exposure and uncollided exposure calculations. Absorbed dose card values were calculated using NIST values and can be seen in Table 3 of Appendix III. The values used in the absorbed dose cards are logarithmically interpolated when values fall between the discrete values that are given in the cards. To provide acceptable statistics without excessively long run times,  $10^6$  source particle histories were used for each input card. In a few instances where the source energy was above 10 MeV, more source particle histories were run to improve results.

Surface tallies (f2) were used to calculate flux rather than point detectors or ring detectors. Next event estimators such as point and ring detectors are known to be unreliable when calculating the flux at large numbers of mean-free-paths in scattering medium. If next event estimators are used, the user risks under-sampling coherent scattering which is characterized by many low scores to the detector when the photon trajectory is away from the detector and a very few, enormously large scores when the

trajectory is nearly aimed at the detector. Such under-sampled events cause a sudden increase in both the tally and the variance, and a failure to pass the statistical checks for the tally (X-5 Monte Carlo Team, 2003).

Concentric spheres were used with the point source located at the origin (0 0 0) similar to a study carried out by Bozkurt and Tsoufanidis (1996). The radius of each concentric sphere was determined by the mfp value and they were manually calculated (Appendix X). In order to simulate an infinite homogenous medium, the thickness of the material went beyond 40 mfp, which was designated as a void. An example of an input file used in MCNP5 is shown in Appendix XII. Once the surface tally outputted both total and uncollided dose, those were taken and used to calculate the buildup factor at each mfp. The buildup factor was calculated by dividing the total dose by the uncollided dose.

The values generated by MCNP5 were then compared to the published values in the ANS Standard and are shown in Appendix VII. ASFIT was the other code used to compare and benchmark buildup factor values with that of MCNP5. ASFIT was designed to calculate buildup factor and angular energy distribution. The input required for ASFIT is the pair production and total cross sections. It computes internally the scattering cross sections. The code is setup for slab geometry and the user defines how the source will interact with the slab. The mesh points at which the buildup factors are to be specified and whether they should be in mfps or cm. The source energy is specified. The user also specifies what type of secondary interactions will take place.

The input to ASFIT is divided into two files. In the first file, the user has to define what kind of cross section they will input, whether it is point or group cross sections. For this study point cross section was chosen, The user needs to specify the order of Legendre

polynomial and the number of angular nodes, which for this study was 6 and 10, respectively. These values can be altered to help converge better. The energy and space nodes need to be specified. This helps the resolution of the calculation but can slow down the calculation time. The number of material regions must be specified and in this study single layered materials are being analyzed. For the input a plane isotropic flux, this will be converted to a point isotropic simulation by equation 21. The units of defining the space nodes are in cm rather than mfp. After this the user specifies the necessary secondary interactions that shall partake in the model... The user will go on to define what information to print in the output. Finally the user goes on to define what source energy the model will have and at what mesh points the buildup factor will be calculated at.

The second input file contains the cross section data. The user defines the title followed by the units being specified for the cross section. The user goes on to define the description of the material such as density, atomic number, and atomic weight of the material of interest. For compounds, this can be an issue and iterations are needed. For water, the buildup factors at the higher mfps were deviating greatly and this was due to the fact that water does not have an atomic number. The atomic number of Hydrogen was proved to reproduce the most accurate results where as the atomic number of Oxygen or the summation of the atomic numbers resulted in skewed results. The rest of the inputs are the photoelectric cross sections, total cross sections, and the energy absorption coefficients.

For a more detail discussion and description of the input requirements please see Appendix XII and XIII. The results of the comparison are seen in Appendix VIII.

## Fitting Functions

Generated buildup factor data are commonly fitted to curves to provide a method of determining buildup factor for values that fall between generated data points. Buildup factor coefficients using both Geometric Progression (GP) method and Taylor fitting function coefficients were presented in data tables in the ANS Standard. To maintain the consistency with ANS Standard, the data generated by MCNP5 shall be fitted to a curve. (Yoshida, 2006).

The buildup factor is a comparison of gross gamma-rays to an uncollided gamma ray. When a gamma ray transverses through a medium and reaches a desired point, it always exceeds unity (Yoshida, 2006). The mathematical derivation for the GP method is derived by the premise that when a thickness  $X$  (mfp) is added to a similar medium,  $dX$  (mfp), and the gamma-ray buildup factor  $x$  is  $B(x)$  and that  $X + dX$  then the build up factor can be established to be  $B(X+dX)$ , as a result of following is ascertained:

$$B(X + dX) \geq B(x) \quad (22)$$

Essentially, eqn. 22 is stating that the buildup factor remains constant and only increases proportionally to penetration depth of a single material. Assuming the buildup factor is  $B(E,1)$  at a certain gamma ray energy,  $E$  and unit penetration depth,  $X_1$ . An increment of the buildup factor at a certain penetration depth is supposed to be expressed by the sum of the geometric progression of geometric ratio  $K$ , with initial term  $(B(E,1)-1)$ :

$$\begin{aligned} \Delta B(E, x) &= (B(E,1) - 1) \frac{K^x - 1}{K - 1}; K \neq 1 \\ \Delta B(E, x) &= (B(E,1) - 1)x; K = 1 \end{aligned} \quad (23)$$

Where,

$\Delta B(E, x)$  = Change in Buildup factor

K = Geometric ratio

x = Ratio of the penetration depth, X, to the unit penetration depth  $X_1$ ,  $x=X/X_1$

The geometric progression ratio, K is defined as follows:

$$K(E, x) = cx^a + d \frac{\tanh\left(\frac{x}{X_k} - 2\right) - \tanh(-2)}{1 - \tanh(-2)} \quad (24)$$

Where,

K(E,x)= Geometric Ratio

c,a, $X_k$ ,d= GP parameters

The sum of geometric progression is assumed to increase by the geometric ratio from the initial term. Curve fitting shall be completed to an extent by this study and completed by members of the ANS-6.4.3 working group. The employment of geometric progression would be implemented by the ANS-6.4.3 working group. For this study, the fitting function used is a polynomial that goes to the 6<sup>th</sup> order to derive the fitting. The 6<sup>th</sup> order polynomial provides the highest accuracy provided by the Excel program. The equation for the fitting function and the linear regression coefficient,  $R^2$ , is given in each graph. Almost all the fittings had a regression coefficient of 0.99 or greater, deeming the function very accurate. These function can be used to find buildup factors at those sources energies at mfps deeper than 40.

## CHAPTER 4

### FINDINGS OF THE STUDY

#### Analysis of Data

The comparison between the ENDF/B-VI.8 derived photon mass attenuation coefficients and the ANS standard showed slight discrepancy for iron and water, see Appendix I and II.

There was a maximum percentage difference of 2.47% (at 0.100 MeV) and a minimum percentage difference of 0.01% (at 4.000 MeV) between the ENDF/B-VI.8 photon mass attenuation coefficients without coherent scattering for iron, which was used to calculate mfp values for MCNP5, compared to those of the ANS Standard.

There was a maximum percentage difference of 0.61% (at 0.080 MeV) and the minimum percentage difference was in exact agreement between the ENDF/B-VI.8 photon mass attenuation coefficients with coherent scattering for iron, which was used to calculate mfp values for MCNP5, compared to those of the ANS Standard.

There was a maximum percentage difference of 4.78% (at 0.030 MeV) and a minimum percentage difference of 0.05% (at 5.000 MeV) between the ENDF/B-VI.8 photon mass attenuation coefficients without coherent scattering for water, which was used to calculate mfp values for MCNP5, compared to those of the ANS Standard.

There was a maximum percentage difference of 0.33% (at 0.150 MeV) and the minimum percentage difference was in exact agreement between the ENDF/B-VI.8 photon mass attenuation coefficients with coherent scattering for water, which was used to calculate mfp values for MCNP5, compared to those of the ANS Standard.

There was a maximum percentage difference of 3.59% (at 0.010 MeV) and the minimum percentage difference was in exact agreement between the NIST data library and Hubbell library photon mass attenuation coefficients for iron. There was a maximum percentage difference of 3.59% (at 0.010 MeV) and the minimum percentage difference was in exact agreement between the NIST data library and Hubbell library absorbed dose response function.

There was a maximum percentage difference of 10.48% (at 35 mfp for 0.015 MeV) and the minimum percentage difference was in exact agreement between the energy absorption buildup factors for iron calculated in ASFIT-VARI and MCNP5 using ENDF/B-VI.8 data library cross-sections.

There was a maximum percentage difference of 13.83 (at 40.0 mfp for 1.50 MeV) and the minimum percentage difference was in exact agreement between the energy absorption buildup factors for water calculated in ASFIT-VARI and MCNP5 using ENDF/B-VI.8 data library cross-sections.

The percentage difference in the range of 0.500 to 40.000 mfp at various energies in the range of 0.015 MeV to 15.000 MeV were calculated to compare the energy absorption buildup factors calculated in MCNP5 with those of the ANS Standard. The energy absorption buildup factors calculated within MCNP5 and from the ANS Standard are provided along with their percentage differences in Appendix VI.

Due to the statistical nature of MCNP5, each tally output has been solved for in a statistical manner. Therefore associated with each output is a statistical error. This is given in the standard deviation associated with each dose value, total and uncollided. Now from a review of the statistical deviation associated with each dose a few

observations were noted. The overwhelming majority of values related to the standard deviation were under 1.5% except for the cases that will be stated. All the higher values of deviation occurred at the higher interval of mfps, 25-40 mfp. All the cases of which the standard deviation was higher than 1.5% occurred for the uncollided dose whereas the total dose standard deviation was less than 1.5%. The standard deviation is a partial attribute and explanation of the some of the differences that exist between the ANS Standard and the calculated buildup factor.

The cases in which iron exceeded 1.5% for the standard deviation occurred in three source energies. The first was at 0.5 MeV for 35 and 40 mfp in which the deviation was no greater than 3%. The next case was for a 1.5 MeV source and it occurred at the range of 25-40 mfp in which the standard deviation was less than 3%.

For water, the following cases exceeded 1.5%. The first occurs at 0.02 MeV for 30-40 mfp in which the standard deviation did not exceed 3.00%. For 0.04 MeV at 25 mfp the deviation was 3.77%. For a 0.1 MeV source the standard deviation did not exceed 4% for the range of 30-40 mfp . For a 0.5 MeV the standard deviation occurred at 35 and 40 mfp in which it was no more than 3.00% Another case that this occurred at was at 1.5 MeV for 35 and 40 mfp which the standard deviation did not go higher than 2.50% The final case was for 2.0 MeV at 35 and 40 mfp the deviation it did not exceed 2.50%.

In order to capture a physical visualization of the results from all of these tables one needs to examine what kind of interactions occur in what energy interval and what their effects are on the buildup factor. There are three effects that take place in terms of interactions. The first is the Compton scattering which causes an increase in the buildup factor and the other two are photoelectric effect and pair production. These latter two



interactions have absorption effects on a material. For low-Z materials at low energy the Compton scattering is more pronounced and as a result there should be higher buildup factors at the lower energy intervals for the most part. The photoelectric effect is dependent on the material but usually observed below 0.5 MeV. No matter what type of scattering takes place the effects on the buildup factor is that it will increase in magnitude, whereas absorption diminishes the magnitude of the buildup factor.

The MCNP5 calculated buildup factors showed trends that matched the interactions in the respective energy intervals. To demonstrate these effects the calculated buildup factors were divided into two energy intervals, 0.015 -1.00 MeV and 2.00 -15.0 MeV for both iron and water. In the first interval set, the effects of scattering are more pronounced and as a result the buildup factors should reflect this by a high value but below 0.5 MeV the photoelectric effect is observed. This is noticed in how the buildup factors are low in the initial part of the lower energy spectrum but pick up in magnitude as the Compton scattering takes more effect. Whereas in the second interval set, the effects of pair production takes hold and the buildup factor diminishes in value. For iron in the lower energy interval, it is shown that the MCNP5 values are higher and the magnitude in comparison to the higher energy interval is much greater. When coherent scattering which is accounted for in this lower energy interval is taken into consideration that magnitude only rises as expected. The higher energy interval of 2.00 -15.0 MeV demonstrates the effects of absorption. Past 1.02 MeV the effects of pair production come into play and as a result there is a decrease in the magnitude of the buildup factor which is observed in the tables representing that energy interval.

The effects of scattering are much greater in water, as one notices by the sheer magnitude of the buildup factor in the lower energy interval. As one notices the calculated buildup factor from 0.015 MeV to 1.00 MeV is significant. The buildup factor increases from about 1.91 at 40 mfp at 0.015 MeV to almost 19,000 at 40 mfp at a source energy of 0.15 MeV (Table 10a and Table 10i). This is due to the effect of Compton scattering but also during this lower energy interval there is a diminishing effect on the value of the buildup factor that is attributed to the photoelectric effect, which occurs at the lower energy interval also. Then the effects of photoelectric absorption kick in and the buildup factor diminishes. In the higher energy interval the buildup factor begins to diminish greatly due to the fact that pair production absorption effect is taking place and it has a pronounced effect on the buildup factor.

The ANS standard demonstrates these physical interactions in its values as the shift from a lower energy source to a higher one see the drop in buildup factors especially for water. The values that have been calculated for the most part are aligned or close to the values, first demonstrating that it reflects the interactions partaking correctly. Secondly the differences for the most part in the results tend to be skewed more towards the reflection of the interaction.

## CHAPTER 5

### SUMMARY, CONCLUSIONS, AND RECOMMENDATIONS

#### Discussion of Results

The photon mass attenuation coefficients derived from ENDF/B-VI.8 for the case when coherent scattering is considered as well as the case where coherent scattering is omitted showed good agreement with the values of the ANS Standard. The percentage difference between the values was relatively small for the case for iron and water. Although the latter showed a bit more difference and these relatively small differences can produce large differences in the final results. This was explicit in the difference water had, especially in higher mfps, in comparison to the ANS, MCNP5, and ASFIT. This acceptable difference was necessary to ensure that the mass attenuation coefficients, which were used to calculate the mfps for the buildup factor, were accurate. The reason for this was the lack of updated data for the mass energy coefficients. Analysis of the output data was viewed in three intervals, which are defined as:

- Low Energy, 0.015 to 0.80 MeV
- Intermediate Energy, 1.0-8.0 MeV
- High Energy, 10.0-15.0 MeV

In the lower energy range a defining trend was not observed that is explicit in all energy sources but one that is common is in the lower end of the lower energy bracket is that as the photon goes to higher mfp the divergence between the MCNP5 and ANS standard is more pronounced but within the acceptable limits. But within the lower

energy range as the transition occurs to the middle and higher end of the range what is observed is that the two data sets becomes more aligned even at higher mfps. This divergence of values at higher mfps is due to the inherent uncertainties that each interaction has. Each mfp represents an occurrence of interaction and as one travels through the medium further and further the incident of interactions increases and thus the uncertainties propagate and compound which results in the divergences that is observed at higher mfps. Due to the low source energy, the attenuation that occurs throughout the medium has a higher uncertainty associated with it. The higher energy intervals, the photon has more power to attenuate further with greater accuracy. While the inclusion of coherent scattering appears to decrease the value of the buildup factor at higher mfps just like the ANS Standard and is more align with the standard.

In the intermediate interval, there is not a distinct trend that emerges between the different energies or in the mfps. The only thing that was common was that the calculated buildup factor and ANS buildup factor were very closely align and no divergence emerged at any rates.

In the higher energy range, as the same as above there is no definite trend that emerges but only that the values that were calculated by MCNP5 are similar to those of the ANS Standard and there is no divergence that would make one suspicious of the values.

The difference that exists between the calculated buildup factor and the ANS Standard is partly due to differences in cross section input. The cross section values that were used in the ANS standard were updated and latest data, ENDF/B-VI.8, are necessary to input to ensure the latest and most accurate buildup factor values is

calculated. The reason for the upgrade from the previous cross section is that more empirical experiments and new computing capabilities has allowed for far more accurate cross section to be derived. The differences in cross section are due to three essential reasons:

1. There have been improvements in our nuclear data. Today's data has become more detailed than it was a decade ago let alone two decades. There is new measurements and methods of analysis, as well as angular and energy distributions. Also it is common today to include double differential data to describe the information more accurately.
2. The application code that they use to derive the cross sections has greatly improved in accuracy and ability to handle newer types of data in newer evaluations.
3. Lastly the exponential increase in computing speed has allowed analysts to run problems they would never have a few years ago. An example of this is the TART Monte Carlo code run to output cross sections would take 8-10 hours in 1996 to run but today on a regular personal computer (PC) it only takes about 47 seconds. Allowing for more intricate codes to be processed and netting more accurate data.

These factors have allowed the newer cross section to give us more accurate data and therefore a difference compared to the previous data used in the ANS Standard, which is a partial cause of the differences that exist (Cullen, 1997).

The difference between ASFIT and MCNP5 when both codes used the ENDF/B-VI.8 values demonstrates that the solution method for the transport equation that both codes

employ cause the discrepancy. Some of these differences can be accounted for in the physics models used by each code while others are probably due to differences in the computational techniques.

Another factor that can be attributed is the equation used to convert the ASFIT-VARI results, which are outputted for a planar source to a point source like the one used in the ANS standard. Some of the factors employed in the transformation equation had inaccuracies which were further compounded when outputting the buildup factors for point source. The equation itself is an approximation than accurate conversion (Harima, 1993).

Another reason for the difference between the ANS Standard and the calculated buildup factor is that the ANS Standard did not account for Bremsstrahlung for low-Z materials and compound materials whereas the calculated buildup factor did account for Bremsstrahlung (Shimizu, 2004). Appendix XI shows calculated buildup factor that did not account for Bremsstrahlung like the ANS standard and from these runs, a noticeable trend emerges over the 40 mfps, the differences drop by a half or more. Therefore, the lack of Bremsstrahlung interactions in the ANS standard can be accounted for the major difference between the calculated buildup factor and the ANS Standard.

As discussed before, ASFIT allows the user to define the space nodes in either cm or mfp. In the course of this study an issue was discovered in regards to this option. When employing ASFIT to calculate buildup factors at certain mfps, ensure that the calculation of mfp at those space nodes is performed using the cm equivalent of the mfp rather than the mfp itself. The reason for this is that when mfps were chosen to describe the space nodes, its equivalent distance in cm did not match the calculated value of mfps in cm.

This discrepancy will not allow a one to one comparison. There was a difference noted if one was to use the mfp option instead of inputting the equivalent cm value for the space nodes. If the mfp is used for the space nodes there will be a difference of less than 1% for iron's buildup factor and difference of 3% for water's buildup factor.

As stated above, the standard deviation is another source of divergence for the buildup factors that were calculated. Since the MCNP5 code is statistical in nature, it has inherent uncertainties with it in the form of the standard deviation. For the most part, these deviations were under 1.5% but for some cases that were documented in Chapter 4, they exceeded 1.5%. But a review of all the standard deviation deemed them acceptable.

For the most part, the energy absorption buildup factors calculated in MCNP5 had good agreement (<10%) with those of the ANS Standard. There were large relative errors for values near at deep mfp lengths.

The large relative errors can at least partially be explained by the stack-up of uncertainty as particles scatter within the medium and travel to deeper mfp depths. The increase in the photoelectric cross-section is proportional to an increase in the number of interactions. There is uncertainty associated with each interaction and with more interactions comes more uncertainty. The mfp is defined as the distance between two successive interactions. Each interaction has an inherent uncertainty associated with it. As the code ventures deeper in the medium to higher mfps, the uncertainties are compounded at each mfp and propagated it out. This can be seen as one of the rationales behind the higher relative differences in the upper mfp region. There were no general trends noticed in the calculated values except that on average the MCNP5 values were greater than those of the ANS Standard.

## Conclusions

Updating the ANS Standard buildup factors using the latest cross section library is a necessity to obtain more accurate values. The differences between the energy absorption buildup factors calculated in this study and those of the ANS Standard can be explained by differences in cross-section data libraries, calculation methods, and physics assumptions. Also the two methods of solution for the software is another explanation of the discrepancies. While some inaccuracies were observed in the new data, it is believed that most of the new values (other than those previously noted as being inaccurate) are more accurate than those published in the ANS Standard. MCNP5 performs calculations with much greater detail and resolution than ASFIT-VARI, due to it being relative antiquated and not updated and maintained. The combination of using a detailed computational code with more accurate cross-section data than was used in the ANS Standard justifies the proposed use of the data in ANS Standard.

## Recommendations for further Study

Seltzer's method (1993) should be reviewed to see if it is applicable for use with ENDF/B-VI.8 cross-sections. Calculation of these values from ENDF/B-VI.8 will provide the most accurate data available for buildup factor calculations and consequently will increase the accuracy of results as well as show good consistency in the calculation method. When new mass energy-absorption and mass energy-transfer coefficients that are derived from ENDF/B-VI.8 (EPDL97) data become available, the calculations performed in this study should be repeated to improve their consistency and accuracy. It is essential to the success of the newest revision of the ANS Standard that mass energy-



Absorption and mass energy-transfer coefficients from ENDF/B-VI.8 data be calculated. Following the step by step explanation in NIST, a reevaluation of the coefficients and recalculation of them are imperative to reactivating the ANS Standard. Curve fitting should be performed using GP due to the accuracy and level of detail it provides.

A comparison between the data from this study should be made with data from recent studies (studies performed after the 1991 ANS Standard was published) which include new codes such as EBUF (a new Monte Carlo code) and new methods of calculating buildup factors such as the Method of Invariant Embedding and the Angular Eigen value Method. (Chibani, 2001; Shimizu, 2004; Shimizu, 2000)

Data should be generated for some of the “new” shielding materials that are not included in the ANS Standard. Many of these “new” materials are used in the medical industry and it would be of great value to have them added to the ANS Standard.

In addition to current data contained in the ANS Standard, consideration should be given to adding a section for values pertinent to layered shields.

## REFERENCES

1. **ANSI/ANS-6.1.1-1991**, *American National Standard for Neutron and Gamma-Ray Fluence-to-Dose Factors*, American Nuclear Society, La Grange Park (1991)
2. **ANSI/ANS-6.4.3-1991**, *Gamma-Ray Attenuation Coefficients and Buildup Factors for Engineering Materials*, American Nuclear Society, La Grange Park (1991)
3. **Bozkurt A**, Tsoufanidis N. Exposure Buildup Factors of UO<sub>2</sub> Using the Monte Carlo Method. *Nuclear Technology* 1996;116:257-260
4. **Chadwick M**, Oblozinsky P, Herman M, *et al.* ENDF/B-VII.0: Next Generation Evaluated Nuclear Data Library For Nuclear Science and Technology. *Nuclear Data Sheets* 2006;107:2931-3060
5. **Chibani O**. New Photon Exposure Buildup Factors. *Nuclear Science and Engineering* 2001;137:215-225
6. **Cullen D**, Hubbell J, *et al.* "The Evaluated Photon Data Library, '97 version," UCRL-50400, Vol. 6, Rev. 5 (1997).
7. **Duderstadt J**, Hamilton L. (1976). *Nuclear Reactor Analysis* (1st ed.). New York: John Wiley & Sons, Inc.
8. **Goldstein H**, Wilkins J. Calculations of the Penetration of Gamma Rays. *Nuclear Development Associates, Inc.* 1954;NYO-3075
9. **Harima Y**. An Historical Review and Current Status of Buildup Factor Calculations and Applications. *Radiation Physics and Chemistry* 1993;41:631-672
10. **Harima Y**, Trubey D, *et al.* Gamma-Ray Attenuation in the Vicinity of the K Edge in Molybdenum, Tin, Lanthanum, Gadolinium, Tungsten, Lead, and Uranium. *Nuclear Science and Engineering* 1991;107:385-393
11. **Harima Y**, Hirayama H, *et al.* A Comparison of Gamma-Ray Buildup Factors for Low-Z Material and for Low Energies Using Discrete Ordinates and Point Monte Carlo Methods. *Nuclear Science and Engineering* 1987;96:241-252
12. **Hirayama H**. Calculation of Gamma-ray Exposure Buildup Factors up to 40 mfp using the EGS4 Monte Carlo Code with a Particle Splitting. *Journal of Nuclear Science and Technology* 1995;32:1201-1207
13. **Hubbell J**, Seltzer S. Tables of X-Ray Mass Attenuation Coefficients and Mass Energy-Absorption Coefficients (version 1.4). 2004 [Online] Available:

- <http://physics.nist.gov/xaamdi> [2008, November 3]. National Institute of Standards and Technology, Gaithersburg, MD.
14. **Hubbell J.** Photon Cross-sections, Attenuation Coefficients, and Energy Absorption Coefficients from 10 keV to 100 GeV," NSRDS-NBS-29, National Standard Reference Data Systems, U.S. National Bureau of Standards (1969).
  15. **Lamarsh J, Baratta A.** (2001). *Introduction to Nuclear Engineering* (3rd ed.). New Jersey: Prentice-Hall, Inc.
  16. **LANL** (Regents of the University of California at Los Alamos National Laboratory). MCNP5 User's Manual, Version 2.5.0, **LA-CP-05-0369**, Los Alamos National Laboratory, Los Alamos (2005).
  17. **NIST** (National Institute of Standards and Technology). PHOTX: Photon Interaction Cross-Sections, **DLC-136**, Radiation Shielding Information Center Data Package
  18. **Seltzer S.** Calculation of Photon Mass Energy-Transfer and Mass Energy-Absorption Coefficients. *Radiation Research* 1993;136:147-170
  19. **Shimizu A, Onda T, et al.** Calculation of Gamma-Ray Buildup Factors up to Depths of 100 mfp by the Method of Invariant Embedding, (III) Generation of an Improved Data Set. *Nuclear Science and Technology* 2004;41:413-424
  20. **Shimizu A.** Development of Angular Eigenvalue Method for Radiation Transport Problems in Slabs and Its Application to Penetration of Gamma-rays. *Nuclear Science and Technology* 2000;37:15-25
  21. **Shultis K, Faw R.** (2000). *Radiation Shielding* (1st ed.). Illinois: American Nuclear Society, Inc.
  22. **Storm E, Israel H.** Photon Cross-Sections from 1keV to 100 MeV for Elements Z=1 to Z=100. *Nuclear Data Tables* 1970;A7:565
  23. **Subbaiah K, Natarajan A, et al.** Impact of Coherent Scattering on the Spectra and Energy Deposition of Gamma Rays in Bulk Media. *Nuclear Science and Engineering* 1989;101:352-370
  24. **Subbaiah K, Natarajan A, et al.** Effect of Fluorescence in Deep Penetration of Gamma Rays. *Nuclear Science and Engineering* 1987;96:330-342
  25. **Subbaiah K, Natarajan A, et al.** Effect of Fluorescence, Bremsstrahlung, and Annihilation Radiation on the Spectra and Energy Deposition of Gamma-rays in Bulk Media. *Nuclear Science and Engineering* 1982;81:172-195

26. **Gopination, D.V., Subbaiah, K.V.** ASFIT-VARI: Gamma-Ray Transport Code System for One-Dimensional Finite Systems. *Indira Gandhi Centre for Atomic Reasearch and Oak Ridge National Laboratory* 1989; CCC-336.
27. **X-5 Monte Carlo Team.** MCNP – A General Monte Carlo N-Particle Transport Code, Version 5, Los Alamos National Laboratory, Los Alamos (2003).
28. **Zaidi H.** Comparative Evaluation of Photon Cross-Section Libraries for Materials of Interest in PET Monte Carlo Simulations. *IEEE Transactions on Nuclear Science* 2000;77:2722-2735

APPENDIX I

PHOTON MASS ATTENUATION COEFFICIENTS,  
COHERENT SCATTERING INCLUDED

Table 1. Photon Mass Attenuation Coefficient for Iron Coherent Scattering Included

Energy (MeV)	MCNP5 Photon Mass Attenuation Coefficient (cm <sup>2</sup> /g)	ANS-6.4.3-1991 Photon Mass Attenuation Coefficient (cm <sup>2</sup> /g)	Difference (%)
0.010	170.110	170.700	0.35%
0.015	56.749	57.080	0.58%
0.020	25.678	25.680	0.01%
0.030	8.177	8.176	0.01%
0.040	3.632	3.629	0.07%
0.050	1.959	1.957	0.12%
0.060	1.206	1.205	0.05%
0.080	0.596	0.592	0.61%
0.100	0.372	0.372	0.07%
0.150	0.196	0.196	0.00%
0.200	0.146	0.146	0.04%
0.300	0.110	0.110	0.16%
0.400	0.094	0.094	0.11%
0.500	0.084	0.084	0.12%
0.600	0.077	0.077	0.21%
0.800	0.067	0.067	0.15%
1.000	0.060	0.060	0.10%
1.500	0.049	0.049	0.25%
2.000	0.043	0.043	0.23%
3.000	0.036	0.036	0.29%
4.000	0.033	0.033	0.29%
5.000	0.031	0.031	0.27%
6.000	0.030	0.031	0.26%
8.000	0.030	0.030	0.22%
10.000	0.030	0.030	0.21%
15.000	0.031	0.031	0.20%
20.000	0.032	0.032	0.18%
30.000	0.035	0.035	0.17%

Table 2. Photon Mass Attenuation Coefficient for Water, Coherent Scattering Included

Energy (MeV)	MCNP5 Photon Mass Attenuation Coefficient (cm <sup>2</sup> /g)	ANS-6.4.3-1991 Photon Mass Atenuation Coefficient (cm <sup>2</sup> /g)	Difference (%)
0.010	5.33E+00	5.328E+00	0.04%
0.015	1.67E+00	1.673E+00	0.18%
0.020	8.10E-01	8.098E-01	0.02%
0.030	3.76E-01	3.756E-01	0.11%
0.040	2.68E-01	2.683E-01	0.11%
0.050	2.27E-01	2.269E-01	0.04%
0.060	2.06E-01	2.058E-01	0.10%
0.080	1.84E-01	1.836E-01	0.22%
0.100	1.71E-01	1.707E-01	0.18%
0.150	1.51E-01	1.505E-01	0.33%
0.200	1.37E-01	1.370E-01	0.00%
0.300	1.19E-01	1.187E-01	0.25%
0.400	1.06E-01	1.061E-01	0.09%
0.500	9.69E-02	9.687E-02	0.03%
0.600	8.96E-02	8.956E-02	0.04%
0.800	7.87E-02	7.866E-02	0.05%
1.000	7.07E-02	7.072E-02	0.03%
1.500	5.75E-02	5.754E-02	0.07%
2.000	4.94E-02	4.941E-02	0.02%
3.000	3.97E-02	3.969E-02	0.03%
4.000	3.40E-02	3.403E-02	0.09%
5.000	3.03E-02	3.031E-02	0.03%
6.000	2.77E-02	2.770E-02	0.00%
8.000	2.43E-02	2.429E-02	0.04%
10.000	2.22E-02	2.214E-02	0.27%
15.000	1.94E-02	1.936E-02	0.21%
20.000	1.81E-02	1.808E-02	0.11%
30.000	0.017	1.706E-02	0.23%

APPENDIX II

PHOTON MASS ATTENUATION COEFFICIENTS,  
COHERENT SCATTERING NOT INCLUDED

Table 3. Photon Mass Attenuation Coefficient for Iron Coherent Scattering Not Included

<b>Energy (MeV)</b>	<b>MCNP5 Photon Mass Attenuation Coefficient (cm<sup>2</sup>/g)</b>	<b>ANS-6.4.3-1991 Photon Mass Attenuation Coefficient (cm<sup>2</sup>/g)</b>	<b>Difference (%)</b>
0.010	168.883	169.600	0.42%
0.015	55.957	56.410	0.80%
0.020	25.130	25.220	0.36%
0.030	7.881	7.930	0.62%
0.040	3.446	3.478	0.92%
0.050	1.832	1.854	1.19%
0.060	1.112	1.131	1.67%
0.080	0.539	0.551	2.18%
0.100	0.334	0.343	2.47%
0.150	0.179	0.183	2.36%
0.200	0.136	0.138	1.92%
0.300	0.105	0.106	1.29%
0.400	0.091	0.092	0.85%
0.500	0.082	0.083	0.61%
0.600	0.076	0.076	0.56%
0.800	0.066	0.066	0.34%
1.000	0.059	0.060	0.28%
1.500	0.049	0.049	0.22%
2.000	0.042	0.043	0.13%
3.000	0.036	0.036	0.14%
4.000	0.033	0.033	0.01%
5.000	0.031	0.031	0.10%
6.000	0.030	0.031	0.07%
8.000	0.030	0.030	0.04%
10.000	0.030	0.030	0.06%
15.000	0.031	0.031	0.08%
20.000	0.032	0.032	0.06%
30.000	0.035	0.035	0.06%

Table 4. Photon Mass Attenuation Coefficient for Water, Coherent Scattering Not Included

Energy (MeV)	MCNP5 Photon Mass Attenuation Coefficient (cm <sup>2</sup> /g)	ANS-6.4.3-1991 Photon Mass Atenuation Coefficient (cm <sup>2</sup> /g)	Difference (%)
0.010	5.100	5.157	1.11%
0.015	1.54E+00	1.579	2.47%
0.020	7.21E-01	0.751	3.93%
0.030	3.29E-01	0.346	4.78%
0.040	2.40E-01	0.250	4.08%
0.050	2.08E-01	0.215	3.21%
0.060	1.92E-01	0.197	2.69%
0.080	1.75E-01	0.179	2.02%
0.100	1.65E-01	0.167	1.43%
0.150	1.48E-01	0.149	0.67%
0.200	1.36E-01	0.136	0.07%
0.300	1.18E-01	0.118	0.25%
0.400	1.06E-01	0.106	0.09%
0.500	9.66E-02	0.097	0.07%
0.600	8.94E-02	0.089	0.03%
0.800	7.86E-02	0.079	0.05%
1.000	7.07E-02	0.071	0.11%
1.500	5.75E-02	0.057	0.05%
2.000	4.94E-02	0.049	0.16%
3.000	3.97E-02	0.040	0.23%
4.000	3.40E-02	0.034	0.15%
5.000	3.03E-02	0.030	0.20%
6.000	2.77E-02	0.028	0.25%
8.000	2.43E-02	0.024	0.29%
10.000	2.22E-02	0.022	0.27%
15.000	1.94E-02	0.019	0.21%
20.000	1.81E-02	0.018	0.11%
30.000	0.017	0.017	0.23%



APPENDIX III

ABSORPED DOSE RESPONSE FUNCTIONS

Table 5. Absorbed Dose Response Functions-Iron

<b>Energy (MeV)</b>	<b>Photon Mass Energy- Absorption Coefficient (cm<sup>2</sup>/g) (NIST)</b>	<b>Absorbed Dose Response Function (Gy*cm<sup>2</sup>)</b>
0.01	1.369E+02	2.19E-10
0.015	4.896E+01	1.18E-10
0.020	2.260E+01	7.24E-11
0.030	7.251E+00	3.48E-11
0.040	3.155E+00	2.02E-11
0.050	1.638E+00	1.31E-11
0.060	9.555E-01	9.18E-12
0.080	4.104E-01	5.26E-12
0.100	2.177E-01	3.49E-12
0.150	7.961E-02	1.91E-12
0.200	4.825E-02	1.55E-12
0.300	3.361E-02	1.62E-12
0.350	3.184E-02	1.79E-12
0.400	3.039E-02	1.95E-12
0.450	2.972E-02	2.14E-12
0.500	2.914E-02	2.33E-12
0.550	2.872E-02	2.53E-12
0.600	2.836E-02	2.73E-12
0.650	2.802E-02	2.92E-12
0.700	2.770E-02	3.11E-12
0.800	2.714E-02	3.48E-12
1.000	2.603E-02	4.17E-12
1.400	2.400E-02	5.38E-12
1.500	2.360E-02	5.67E-12
1.800	2.257E-02	6.51E-12
2.000	2.199E-02	7.05E-12
2.200	2.161E-02	7.62E-12
2.600	2.096E-02	8.73E-12
2.800	2.068E-02	9.28E-12
3.000	2.042E-02	9.81E-12
3.250	2.027E-02	1.06E-11
3.750	2.002E-02	1.20E-11
4.000	1.990E-02	1.28E-11
4.250	1.988E-02	1.35E-11
4.750	1.985E-02	1.51E-11

5.000	1.983E-02	1.59E-11
5.250	1.987E-02	1.67E-11
5.500	1.987E-02	1.75E-11
6.000	1.997E-02	1.92E-11
6.310	2.006E-02	2.03E-11
6.750	2.019E-02	2.18E-11
7.000	2.025E-02	2.27E-11
8.000	2.050E-02	2.63E-11
9.000	2.080E-02	3.00E-11
10.000	2.108E-02	3.38E-11
11.000	2.134E-02	3.76E-11
13.000	2.180E-02	4.54E-11
15.000	2.221E-02	5.34E-11
20.000	2.400E-02	7.69E-11

Table 6. Absorbed Dose Response Functions-Water

<b>Energy (MeV)</b>	<b>Photon Mass Energy-Absorption Coefficient (cm<sup>2</sup>/g) (NIST)</b>	<b>Absorbed Dose Response Function (Gy*cm<sup>2</sup>) (Shielding Text 5.26)</b>
0.01	4.07E+03	6.51E-09
0.015	1.37E+00	3.30E-12
0.020	5.50E-01	1.76E-12
0.030	1.56E-01	7.48E-13
0.040	6.95E-02	4.45E-13
0.050	4.22E-02	3.38E-13
0.060	3.19E-02	3.07E-13
0.080	2.60E-02	3.33E-13
0.100	2.55E-02	4.08E-13
0.150	2.76E-02	6.64E-13
0.200	2.97E-02	9.51E-13
0.300	3.19E-02	1.53E-12
0.350	3.24E-02	1.82E-12
0.400	3.28E-02	2.10E-12
0.450	3.29E-02	2.37E-12
0.500	3.30E-02	2.64E-12
0.550	3.29E-02	2.90E-12
0.600	3.28E-02	3.16E-12
0.650	3.26E-02	3.39E-12
0.700	3.25E-02	3.63E-12
0.800	3.21E-02	4.11E-12
1.000	3.10E-02	4.97E-12
1.400	2.80E-02	7.95E-12
1.500	2.83E-02	6.81E-12

1.800	2.70E-02	7.74E-12
2.000	2.61E-02	8.36E-12
2.200	2.54E-02	8.88E-12
2.600	2.41E-02	9.92E-12
2.800	2.35E-02	1.04E-11
3.000	2.28E-02	1.10E-11
3.250	2.23E-02	1.15E-11
3.750	2.12E-02	1.27E-11
4.000	2.07E-02	1.32E-11
4.250	2.03E-02	1.38E-11
4.750	1.95E-02	1.48E-11
5.000	1.92E-02	1.53E-11
5.250	1.89E-02	1.58E-11
5.500	1.86E-02	1.63E-11
6.000	1.81E-02	1.74E-11
6.310	1.78E-02	1.80E-11
6.750	1.75E-02	1.88E-11
7.000	1.73E-02	1.93E-11
8.000	1.66E-02	2.12E-11
9.000	1.61E-02	2.32E-11
10.000	1.57E-02	2.51E-11
11.000	1.52E-02	2.83E-11
13.000	1.44E-02	3.46E-11
15.000	1.44E-02	3.46E-11
20.000	1.38E-02	4.43E-11

APPENDIX IV

**COMPARISON OF HUBBELL AND ENDF/B-VI.8 IN ASFIT-VARI**

Table 6a. Comparison of Hubbell & ENDF in ASFIT, 0.10 MeV-Water

<b>MFP</b>	<b>ANS Standard</b>	<b>Hubbell Buildup Factor</b>	<b>ENDF/B-VI.8 Buildup Factor</b>	<b>% Difference between Hubbell &amp; ENDF/B-VI.8</b>
0.50	2.36	2.37	2.41	1.70%
1.00	4.52	4.53	4.59	1.31%
2.00	11.70	11.81	12.04	1.92%
3.00	23.50	23.63	25.02	5.55%
4.00	40.60	40.74	42.14	3.33%
5.00	64.00	65.02	67.13	3.14%
6.00	94.80	95.84	99.21	3.40%
7.00	134.00	136.21	143.21	4.89%
8.00	183.00	184.13	191.21	3.70%
10.00	314.00	315.12	328.12	3.96%
15.00	917.00	917.52	921.87	0.47%
20.00	2120.00	2148.21	2201.31	2.41%
25.00	4260.00	4271.19	4397.19	2.87%
30.00	7780.00	7821.12	8039.78	2.72%
35.00	13100.00	13002.12	13753.21	5.46%
40.00	20300.00	19983.63	20932.46	4.53%

Table 6b. Comparison of Hubbell & ENDF in ASFIT, 1.00 MeV-Water

<b>MFP</b>	<b>ANS Standard</b>	<b>Hubbell Buildup Factor</b>	<b>ENDF/B-VI.8 Buildup Factor</b>	<b>% Difference between Hubbell &amp; ENDF/B-VI.8</b>
0.50	1.47	1.49	1.52	1.89%
1.00	2.08	2.09	2.15	2.83%
2.00	3.62	3.65	3.78	3.33%
3.00	5.50	5.53	5.64	1.89%
4.00	7.66	7.69	7.81	1.55%
5.00	10.10	10.12	10.34	2.12%
6.00	12.80	12.93	13.01	0.62%
7.00	15.70	15.72	16.02	1.87%
8.00	18.90	19.01	19.45	2.28%
10.00	26.00	26.25	27.78	5.52%

15.00	47.40	48.12	50.32	4.37%
20.00	73.50	74.01	76.12	2.78%
25.00	104.00	105.23	107.61	2.21%
30.00	138.00	139.62	141.14	1.89%
35.00	175.00	176.83	183.42	1.89%
40.00	214.00	216.12	231.23	6.53%

Table 6c. Comparison of Hubbell & ENDF in ASFIT, 10.0 MeV-Water

<b>MFP</b>	<b>ANS Standard</b>	<b>Hubbell Buildup Factor</b>	<b>ENDF/B-VI.8 Buildup Factor</b>	<b>% Difference between Hubbell &amp; ENDF/B-VI.8</b>
0.50	1.21	1.23	1.28	4.05%
1.00	1.38	1.40	1.44	2.30%
2.00	1.70	1.72	1.79	3.75%
3.00	2.00	2.04	2.10	2.51%
4.00	2.29	2.34	2.41	2.98%
5.00	2.57	2.61	2.74	4.72%
6.00	2.85	2.98	3.08	3.14%
7.00	3.13	3.19	3.35	4.57%
8.00	3.40	3.63	3.81	4.73%
10.00	3.94	4.02	4.32	6.94%
15.00	5.24	5.47	5.81	5.87%
20.00	6.51	6.68	6.83	2.21%
25.00	7.75	7.91	8.12	2.60%
30.00	8.97	9.07	9.93	8.66%
35.00	10.20	10.78	11.42	5.59%
40.00	11.30	11.81	12.32	4.13%

APPENDIX V

**COMPARISON OF NIST AND HUBBELL DATA**

Table 7. Comparison of NIST and Hubbell Data

<b>Energy (MeV)</b>	<b>Photon Mass Energy- Absorption Coefficient (cm<sup>2</sup>/g) (NIST)</b>	<b>Photon Mass Energy- Absorption Coefficient (cm<sup>2</sup>/g) (Hubbell)</b>	<b>Diff (%)</b>	<b>Absorbed Dose Response Function (NIST) (Gy*cm<sup>2</sup>) (Shielding Text 5.26)</b>	<b>Absorbed Dose Response Function (Hubbell) (Gy*cm<sup>2</sup>) (Shielding Text 5.26)</b>	<b>Diff (%)</b>
0.01	136.90	142.00	3.59%	2.19E-10	2.27E-10	3.59%
0.02	48.96	49.30	0.69%	1.18E-10	1.18E-10	0.69%
0.02	22.60	22.80	0.88%	7.24E-11	7.31E-11	0.88%
0.03	7.25	7.28	0.40%	3.48E-11	3.50E-11	0.40%
0.04	3.16	3.17	0.47%	2.02E-11	2.03E-11	0.47%
0.05	1.64	1.64	0.12%	1.31E-11	1.31E-11	0.12%
0.06	0.96	0.96	0.57%	9.18E-12	9.24E-12	0.57%
0.08	0.41	0.41	0.87%	5.26E-12	5.31E-12	0.87%
0.10	0.22	0.22	0.59%	3.49E-12	3.51E-12	0.59%
0.15	0.08	0.08	2.20%	1.91E-12	1.96E-12	2.20%
0.20	0.05	0.05	2.53%	1.55E-12	1.59E-12	2.53%
0.30	0.03	0.03	0.33%	1.62E-12	1.61E-12	0.33%
0.40	0.03	0.03	0.36%	1.95E-12	1.95E-12	0.36%
0.50	0.03	0.03	0.55%	2.33E-12	2.35E-12	0.55%
0.60	0.03	0.03	0.84%	2.73E-12	2.75E-12	0.84%
0.80	0.03	0.03	0.59%	3.48E-12	3.50E-12	0.59%
1.00	0.03	0.03	0.65%	4.17E-12	4.20E-12	0.65%
1.50	0.02	0.02	0.42%	5.67E-12	5.70E-12	0.42%
2.00	0.02	0.02	0.05%	7.05E-12	7.05E-12	0.05%
3.00	0.02	0.02	0.10%	9.81E-12	9.80E-12	0.10%
4.00	0.02	0.02	0.00%	1.28E-11	1.28E-11	0.00%
5.00	0.02	0.02	0.15%	1.59E-11	1.59E-11	0.15%
6.00	0.02	0.02	0.35%	1.92E-11	1.91E-11	0.35%
8.00	0.02	0.02	0.49%	2.63E-11	2.61E-11	0.49%
10.00	0.02	0.02	0.86%	3.38E-11	3.35E-11	0.86%

APPENDIX VI

**COMPARISON OF XCOM AND ENDF DATA**

Table 8. Comparison of XCOM and ENDF Cross Sections

Photon Energy (MeV)	Total microscopic cross-sections (cm <sup>2</sup> ) XCOM data	Total microscopic cross-sections (cm <sup>2</sup> )-ENDF data	Difference (%)
0.015	5.29779E-21	5.26523E-21	0.61%
0.020	2.38447E-21	2.38241E-21	0.09%
0.030	7.58948E-22	7.58673E-22	0.04%
0.040	3.36795E-22	3.36943E-22	0.04%
0.050	1.81851E-22	1.81785E-22	0.04%
0.060	1.11337E-22	1.11855E-22	0.47%
0.080	5.52047E-23	5.5259E-23	0.10%
0.100	3.45145E-23	3.451E-23	0.01%
0.150	1.81851E-23	1.82215E-23	0.20%
0.200	1.3546E-23	1.354E-23	0.04%
0.300	1.02059E-23	1.018E-23	0.25%
0.400	8.72141E-24	8.71158E-24	0.11%
0.500	7.80288E-24	7.79688E-24	0.08%
0.600	7.14413E-24	7.133E-24	0.16%
0.800	6.21632E-24	6.206E-24	0.17%
1.000	5.55758E-24	5.552E-24	0.10%
1.500	4.52771E-24	4.519E-24	0.19%
2.000	3.95247E-24	3.948E-24	0.11%
3.000	3.35867E-24	3.35E-24	0.26%
4.000	3.07105E-24	3.064E-24	0.23%
5.000	2.9226E-24	2.911E-24	0.40%
6.000	2.8391E-24	2.829E-24	0.36%
7.000	2.79271E-24	2.786E-24	0.24%
8.000	2.77415E-24	2.769E-24	0.19%
9.000	2.77415E-24	2.765E-24	0.33%
10.000	2.77415E-24	2.772E-24	0.08%
11.000	2.79271E-24	2.783E-24	0.35%
13.000	2.82054E-24	2.819E-24	0.05%
15.000	2.86693E-24	2.863E-24	0.14%
20.000	2.98755E-24	2.986E-24	0.05%

APPENDIX VII

**MCNP5 CALCULATED BUILDUP FACTORS –IRON**

Table 9a. Buildup Factor w/o Coherent scattering Iron-0.015 MeV

MFP	ANS Standard	Calculated Buildup Factor	% Difference
0.5	1	1.05	4.76%
1	1	1.05	5.05%
2	1.01	1.06	5.01%
3	1.01	1.06	5.12%
4	1.01	1.07	5.23%
5	1.01	1.07	5.34%
6	1.01	1.07	5.44%
7	1.01	1.08	6.72%
8	1.01	1.08	6.83%
10	1.01	1.09	6.94%
15	1.01	1.09	7.04%
20	1.01	1.09	7.15%
25	1.01	1.10	8.28%
30	1.01	1.10	8.38%
35	1.01	1.10	8.49%
40	1.01	1.10	8.59%

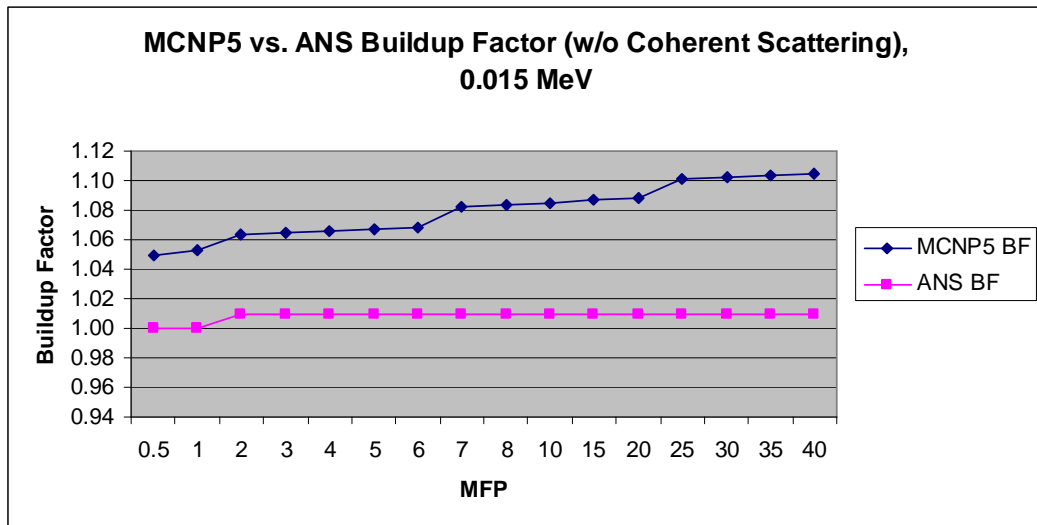


Figure 11a. MCNP5 vs. ANS Buildup Factor w/o Coherent Scattering, 0.015 MeV



Table 9b. Buildup Factor w/Coherent scattering Iron-0.015 MeV

MFP	Corr. Factor	ANS Standard	ANS W/CS	Calculated Buildup Factor	% Difference
0.5	1	1	1	1.02	2.06%
1	1.01	1	1.01	1.02	1.42%
2	1	1.01	1.01	1.05	3.38%
3	0.99	1.01	0.9999	1.05	4.56%
4	0.99	1.01	0.9999	1.05	4.77%
5	0.98	1.01	0.9898	1.05	5.94%
6	0.98	1.01	0.9898	1.05	6.14%
7	0.97	1.01	0.9797	1.06	7.30%
8	0.96	1.01	0.9696	1.06	8.46%
10	0.95	1.01	0.9595	1.06	9.61%
15	0.91	1.01	0.9191	1.06	13.60%
20	0.87	1.01	0.8787	1.09	19.39%
25	0.83	1.01	0.8383	1.09	23.25%
30	0.79	1.01	0.7979	1.09	27.11%
35	0.75	1.01	0.7575	1.10	30.94%
40	0.71	1.01	0.7171	1.10	34.52%

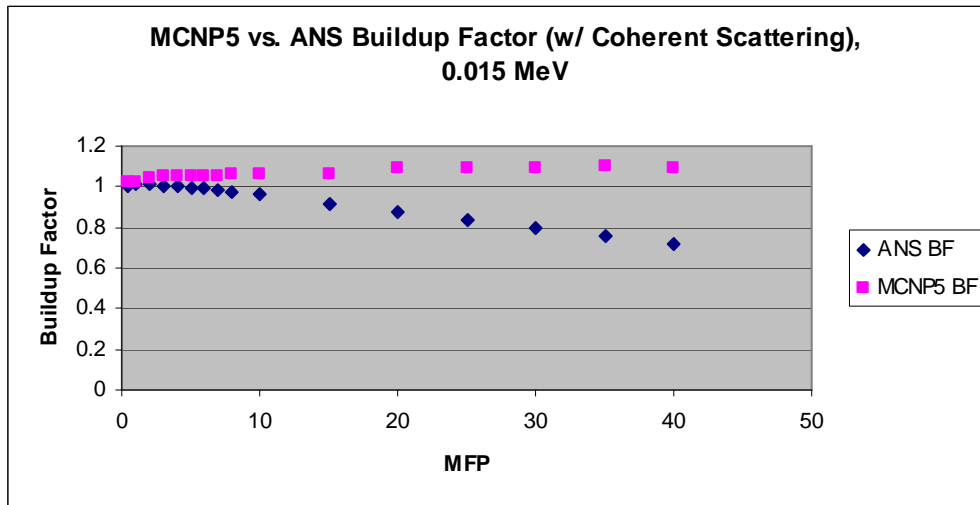


Figure 11b. MCNP5 vs. ANS Buildup Factor w/Coherent Scattering, 0.015 MeV

Table 9c. Buildup Factor w/o Coherent scattering Iron-0.02 MeV

<b>.02 MeV Buildup Factors (No Coherent Scattering)</b>			
<b>MFP</b>	<b>ANS Standard</b>	<b>Calculated Buildup Factor</b>	<b>% Difference</b>
0.50	1.01	1.03	1.94%
1.00	1.01	1.03	2.20%
2.00	1.01	1.04	2.79%
3.00	1.01	1.04	3.00%
4.00	1.02	1.07	4.43%
5.00	1.02	1.07	4.66%
6.00	1.02	1.07	4.78%
7.00	1.02	1.09	6.70%
8.00	1.02	1.10	7.17%
10.00	1.02	1.10	7.45%
15.00	1.02	1.11	7.74%
20.00	1.03	1.11	7.12%
25.00	1.03	1.11	7.41%
30.00	1.03	1.12	7.69%
35.00	1.03	1.12	7.97%
40.00	1.03	1.12	8.26%

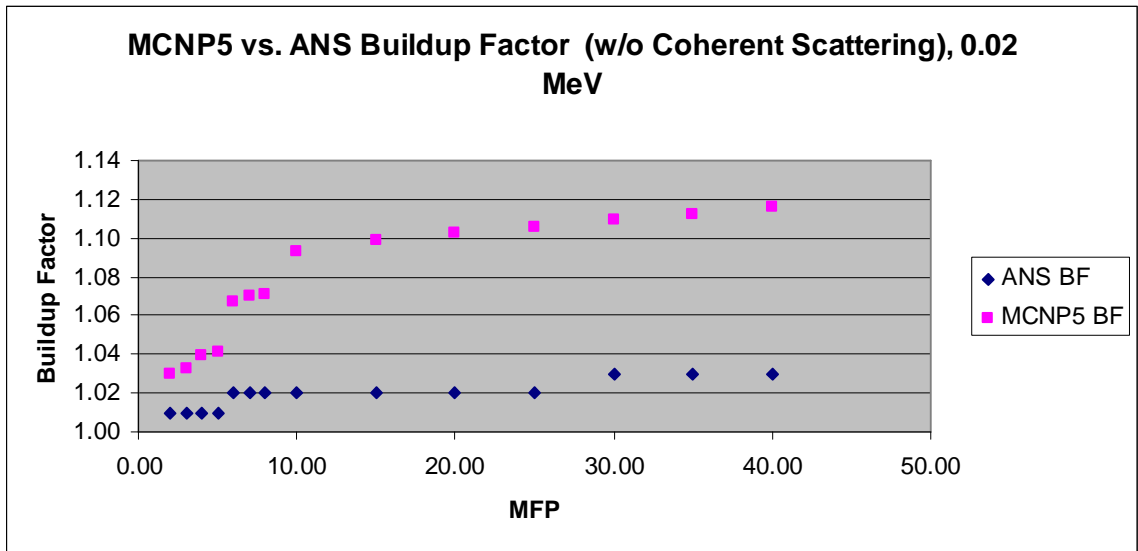


Figure 11c. MCNP5 vs. ANS Buildup Factor w/o Coherent Scattering, 0.020 MeV

Table 9d. Buildup Factor w/ Coherent scattering Iron-0.02 MeV

MFP	Corr. Factor	ANS Standard	ANS W/CS	Calculated Buildup Factor	% Difference
0.50	1.00	1.01	1.01	1.06	4.54%
1.00	1.00	1.01	1.01	1.07	5.61%
2.00	1.00	1.01	1.01	1.09	7.17%
3.00	1.00	1.01	1.01	1.08	6.31%
4.00	0.98	1.02	1.00	1.05	4.80%
5.00	0.98	1.02	1.00	1.04	3.88%
6.00	0.97	1.02	0.99	1.05	5.68%
7.00	0.96	1.02	0.98	1.05	6.65%
8.00	0.95	1.02	0.97	1.06	8.50%
10.00	0.93	1.02	0.95	1.01	6.08%
15.00	0.88	1.02	0.90	0.93	3.48%
20.00	0.82	1.03	0.84	0.92	7.95%
25.00	0.77	1.03	0.79	0.84	5.58%
30.00	0.71	1.03	0.73	0.80	8.73%
35.00	0.66	1.03	0.68	0.74	8.42%
40.00	0.61	1.03	0.63	0.68	7.91%

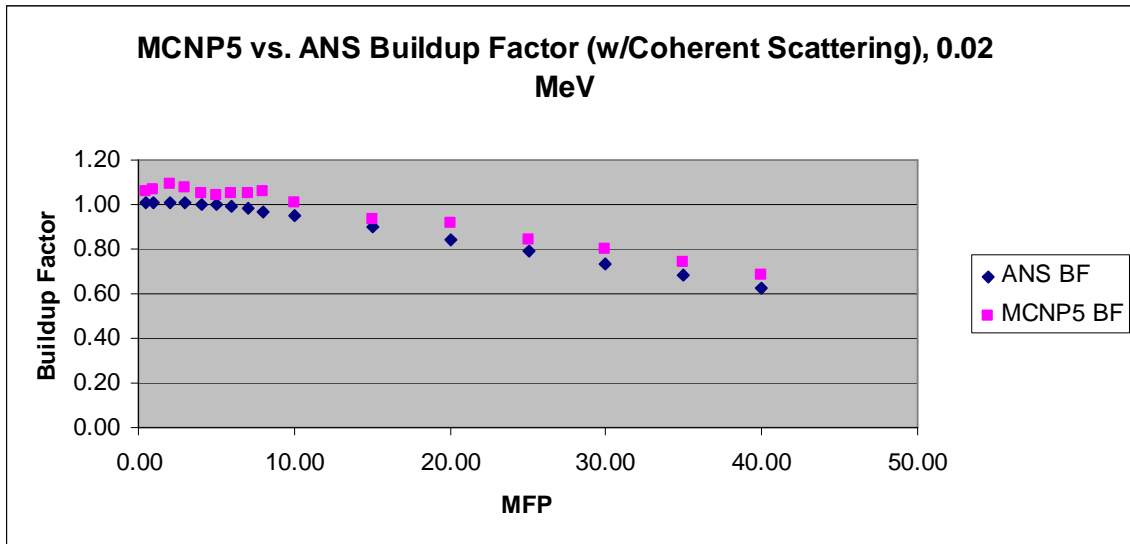


Figure 11d. MCNP5 vs. ANS Buildup Factor w/Coherent Scattering, 0.020 MeV

Table 9e. Buildup Factor w/o Coherent scattering Iron-0.03 MeV

MFP	ANS Standard	Calculated Buildup Factor	% Difference
0.5	1.02	1.04	1.59%
1	1.03	1.03	0.16%
2	1.03	1.04	0.55%
3	1.04	1.04	0.16%
4	1.05	1.04	0.85%
5	1.05	1.04	0.86%
6	1.05	1.05	0.42%
7	1.06	1.07	0.52%
8	1.06	1.09	2.36%
10	1.06	1.10	3.84%
15	1.07	1.12	4.66%
20	1.08	1.13	4.78%
25	1.08	1.15	6.26%
30	1.09	1.16	6.20%
35	1.09	1.18	7.89%
40	1.09	1.20	8.83%

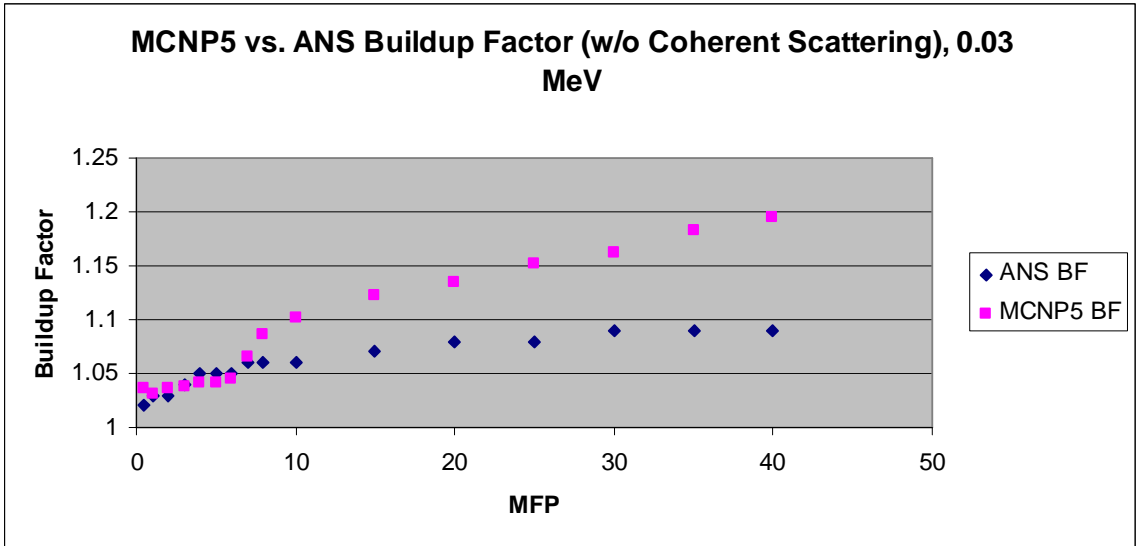


Figure 11e. MCNP5 vs. ANS Buildup Factor w/o Coherent Scattering, 0.03 MeV

Table 9f. Buildup Factor w/Coherent scattering Iron-0.03 MeV

MFP	Corr. Factor	ANS Standard	ANS W/CS	Calculated Buildup Factor	% Difference
0.5	1.00E+00	1.02	1.02	0.96	6.47%
1	1.00E+00	1.03	1.03	0.97	6.19%
2	1.00E+00	1.03	1.03	0.99	4.25%
3	9.90E-01	1.04	1.03	0.98	5.28%
4	9.80E-01	1.05	1.03	0.95	8.32%
5	9.70E-01	1.05	1.02	0.94	8.35%
6	9.60E-01	1.05	1.01	0.93	8.15%
7	9.40E-01	1.06	1.00	0.90	10.15%
8	9.30E-01	1.06	0.99	0.88	12.15%
10	9.10E-01	1.06	0.96	0.87	11.51%
15	8.30E-01	1.07	0.89	0.84	6.11%
20	7.50E-01	1.08	0.81	0.75	7.86%
25	6.70E-01	1.08	0.72	0.68	6.41%
30	6.00E-01	1.09	0.65	0.62	6.00%
35	5.30E-01	1.09	0.58	0.64	9.73%
40	4.70E-01	1.09	0.51	0.55	6.00%

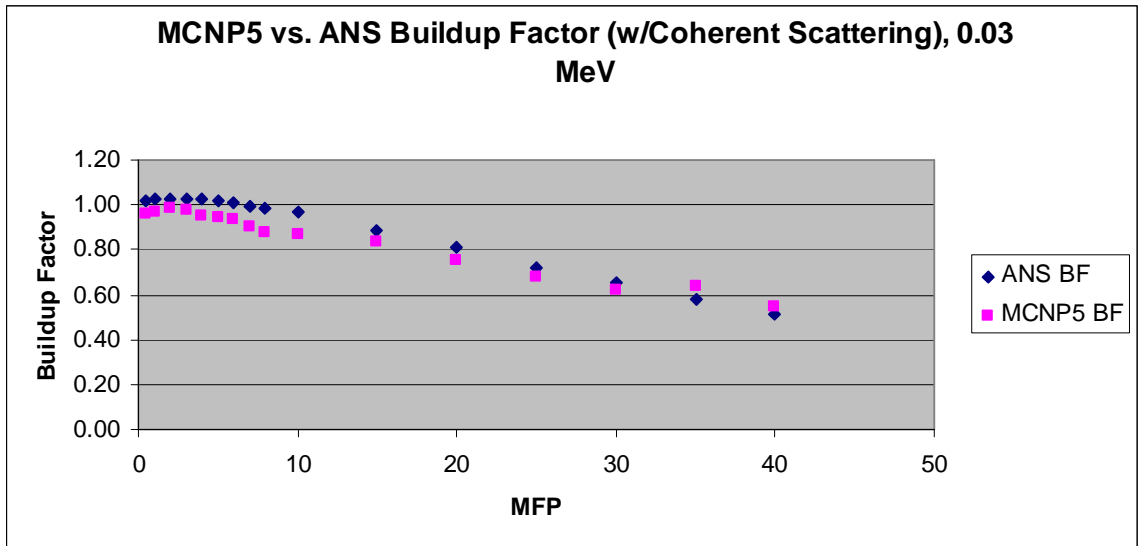


Figure 11f. MCNP5 vs. ANS Buildup Factor w/Coherent Scattering, 0.03 MeV

Table 9g. Buildup Factor w/o Coherent scattering Iron-0.04 MeV

MFP	ANS Standard	Calculated Buildup Factor	% Difference
0.5	1.04	1.10	5.08%
1	1.06	1.11	4.90%
2	1.08	1.13	4.04%
3	1.09	1.14	4.00%
4	1.10	1.14	3.73%
5	1.11	1.15	3.41%
6	1.12	1.15	2.89%
7	1.12	1.16	3.33%
8	1.12	1.16	3.41%
10	1.14	1.26	9.76%
15	1.16	1.27	8.67%
20	1.17	1.28	8.30%
25	1.18	1.28	7.54%
30	1.19	1.28	6.78%
35	1.20	1.27	5.78%
40	1.20	1.27	5.83%

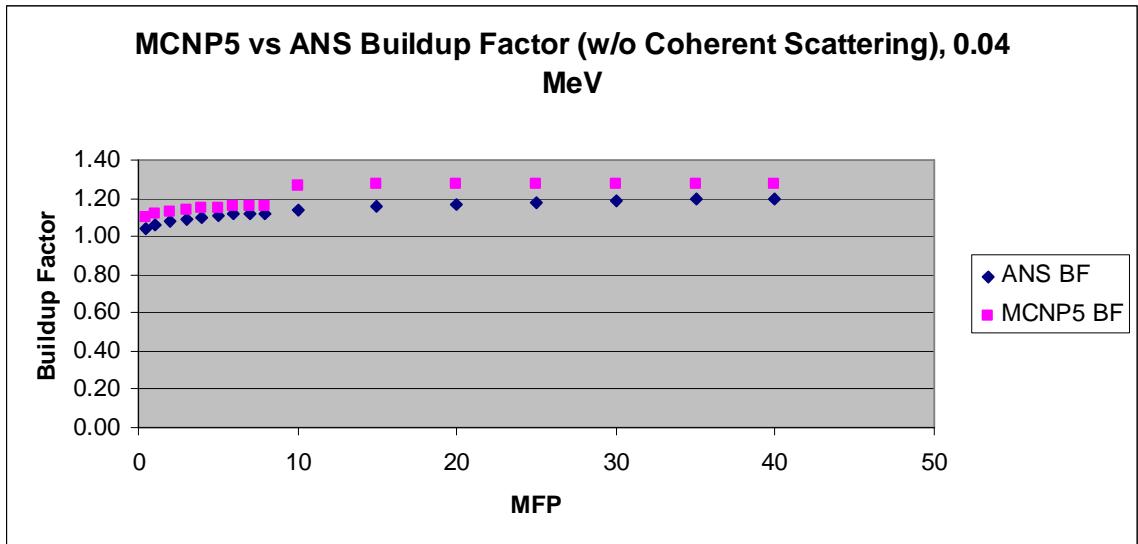


Figure 11g. MCNP5 vs. ANS Buildup Factor w/o Coherent Scattering, 0.04 MeV

Table 9h. Buildup Factor w/ Coherent scattering Iron-0.04 MeV

MFP	Corr. Factor	ANS Standard	ANS W/CS	Calculated Buildup Factor	% Difference
0.5	1.01	1.04	1.05	1.07	1.57%
1	1.00	1.06	1.06	1.09	2.38%
2	1.00	1.08	1.08	1.05	2.60%
3	0.99	1.09	1.08	1.06	1.64%
4	0.98	1.10	1.08	1.07	0.80%
5	0.96	1.11	1.07	1.07	0.81%
6	0.95	1.12	1.06	1.03	3.30%
7	0.94	1.12	1.05	1.02	3.11%
8	0.92	1.12	1.03	1.01	2.02%
10	0.89	1.14	1.01	0.98	3.74%
15	0.79	1.16	0.92	0.86	6.81%
20	0.70	1.17	0.82	0.84	2.27%
25	0.61	1.18	0.72	0.76	5.71%
30	0.53	1.19	0.63	0.68	7.56%
35	0.45	1.20	0.54	0.58	7.23%
40	0.39	1.20	0.47	0.53	12.05%

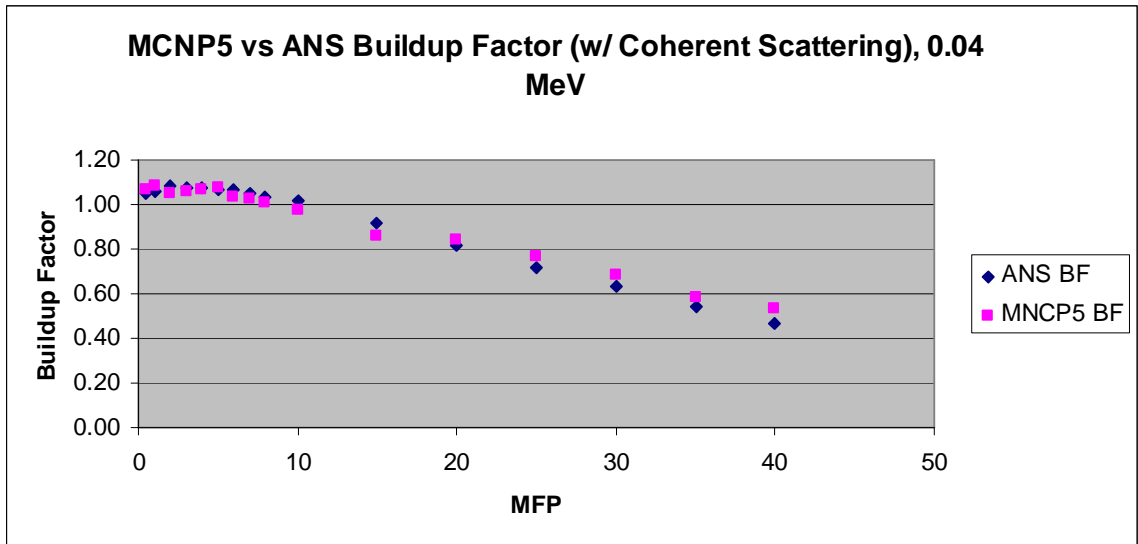


Figure 11h. MCNP5 vs. ANS Buildup Factor w/ Coherent Scattering, 0.04 MeV

Table 9i. Buildup Factor w/o Coherent scattering Iron-0.05 MeV

MFP	ANS Standard	Calculated Buildup Factor	% Difference
0.5	1.08	1.14	5.52%
1	1.10	1.18	6.54%
2	1.14	1.21	5.49%
3	1.17	1.22	4.37%
4	1.19	1.24	3.84%
5	1.21	1.25	3.07%
6	1.22	1.26	2.92%
7	1.23	1.26	2.64%
8	1.24	1.27	2.60%
10	1.26	1.28	1.57%
15	1.30	1.35	3.70%
20	1.33	1.36	2.17%
25	1.35	1.36	1.05%
30	1.37	1.37	0.27%
35	1.38	1.37	0.79%
40	1.39	1.37	1.61%

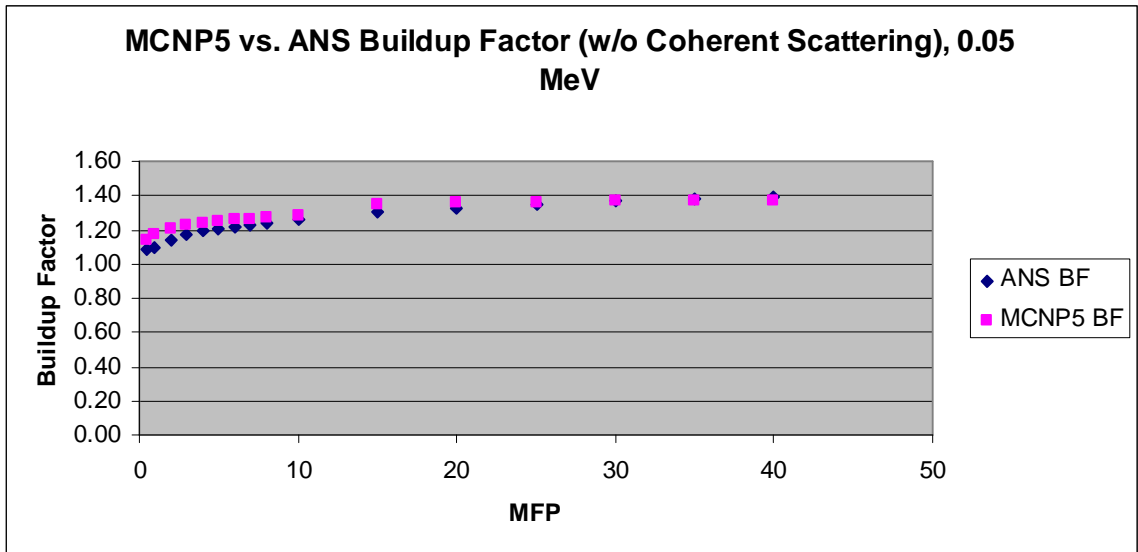


Figure 11i. MCNP5 vs. ANS Buildup Factor w/o Coherent Scattering, 0.05 MeV



Table 9j. Buildup Factor w/ Coherent scattering Iron-0.05 MeV

MFP	Corr. Factor	ANS Standard	ANS W/CS	Calculated Buildup Factor	% Difference
0.5	1.01	1.08	1.09	1.19	8.38%
1	1.01	1.10	1.11	1.22	8.95%
2	1.01	1.14	1.15	1.25	8.20%
3	0.99	1.17	1.16	1.27	9.04%
4	0.98	1.19	1.17	1.29	9.36%
5	0.97	1.21	1.17	1.30	9.66%
6	0.95	1.22	1.16	1.25	7.22%
7	0.93	1.23	1.14	1.20	4.61%
8	0.91	1.24	1.13	1.15	1.81%
10	0.87	1.26	1.10	1.14	3.84%
15	0.77	1.30	1.00	1.09	8.17%
20	0.67	1.33	0.89	0.96	7.50%
25	0.57	1.35	0.77	0.82	6.27%
30	0.48	1.37	0.66	0.70	6.50%
35	0.40	1.38	0.55	0.60	8.19%
40	0.33	1.39	0.46	0.54	15.37%

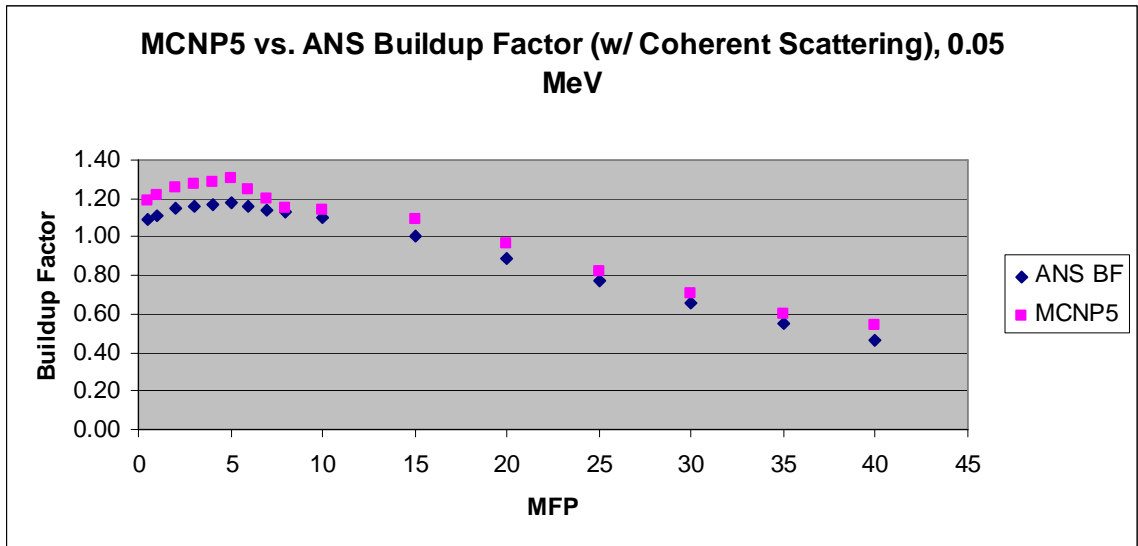


Figure 11j. MCNP5 vs. ANS Buildup Factor w/ Coherent Scattering, 0.05 MeV

Table 9k. Buildup Factor w/o Coherent scattering Iron-0.06 MeV

MFP	ANS Standard	Calculated Buildup Factor	% Difference
0.5	1.12	1.22	8.01%
1	1.17	1.26	7.04%
2	1.23	1.32	6.60%
3	1.28	1.35	5.14%
4	1.31	1.38	5.12%
5	1.34	1.40	4.23%
6	1.37	1.42	3.32%
7	1.39	1.43	2.81%
8	1.41	1.44	2.13%
10	1.45	1.46	0.83%
15	1.52	1.50	1.23%
20	1.57	1.52	3.58%
25	1.61	1.53	5.25%
30	1.65	1.55	6.79%
35	1.67	1.55	7.77%
40	1.68	1.56	7.85%

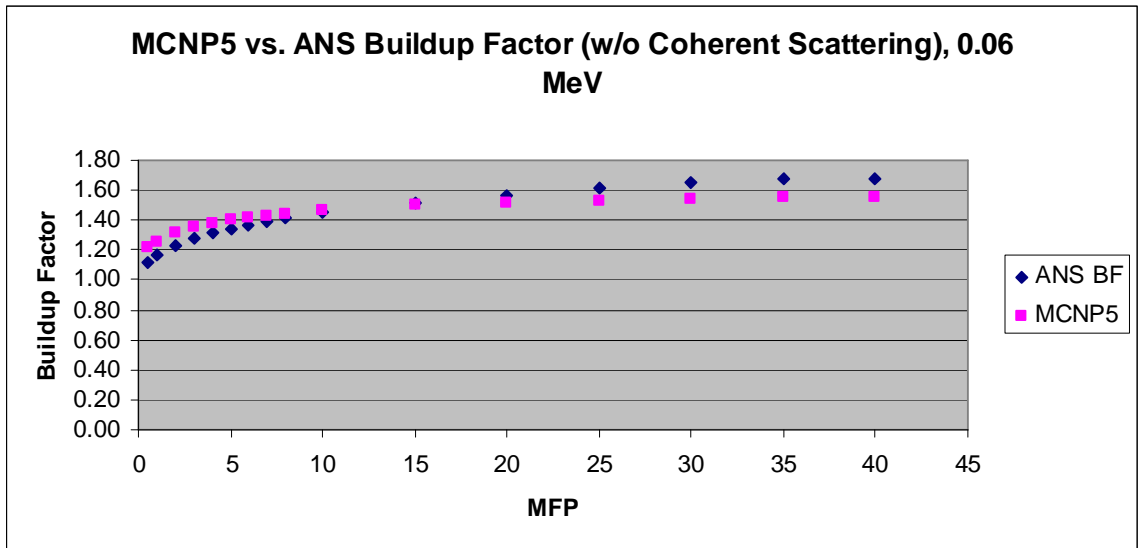


Figure 11k. MCNP5 vs. ANS Buildup Factor w/o Coherent Scattering, 0.06 MeV

Table 91. Buildup Factor w/ Coherent scattering Iron-0.06 MeV

MFP	Corr. Factor	ANS Standard	ANS W/CS	Calculated Buildup Factor	% Difference
0.5	1.01	1.22	1.23	1.21	1.26%
1	1.01	1.26	1.27	1.26	0.70%
2	1.01	1.32	1.33	1.32	1.02%
3	0.99	1.35	1.34	1.35	1.19%
4	0.98	1.38	1.35	1.38	1.81%
5	0.97	1.40	1.36	1.40	2.92%
6	0.95	1.42	1.35	1.42	5.03%
7	0.93	1.43	1.33	1.37	2.74%
8	0.91	1.44	1.31	1.37	4.03%
10	0.87	1.46	1.27	1.36	6.74%
15	0.76	1.50	1.14	1.21	6.00%
20	0.65	1.52	0.99	1.00	1.87%
25	0.55	1.53	0.84	0.88	4.40%
30	0.46	1.55	0.71	0.75	5.24%
35	0.37	1.55	0.57	0.61	6.31%
40	0.31	1.56	0.48	0.51	6.05%

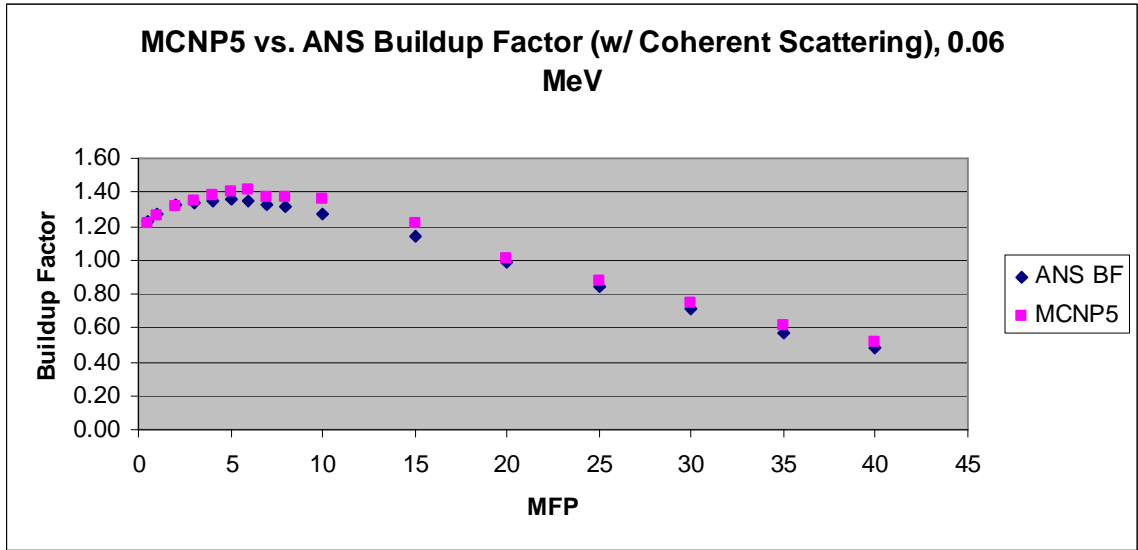


Figure 111. MCNP5 vs. ANS Buildup Factor w/ Coherent Scattering, 0.06 MeV

Table 9m. Buildup Factor w/o Coherent scattering Iron-0.08 MeV

MFP	ANS Standard	Calculated Buildup Factor	% Difference
0.5	1.23	1.31	6.02%
1	1.34	1.42	5.62%
2	1.51	1.55	2.32%
3	1.61	1.64	1.75%
4	1.70	1.71	0.47%
5	1.78	1.76	1.15%
6	1.84	1.82	1.28%
7	1.91	1.86	2.42%
8	1.96	1.89	3.49%
10	2.06	1.96	5.10%
15	2.26	2.08	8.84%
20	2.41	2.39	0.84%
25	2.54	2.51	1.20%
30	2.65	2.58	2.71%
35	2.73	2.68	2.06%
40	2.77	2.72	1.73%

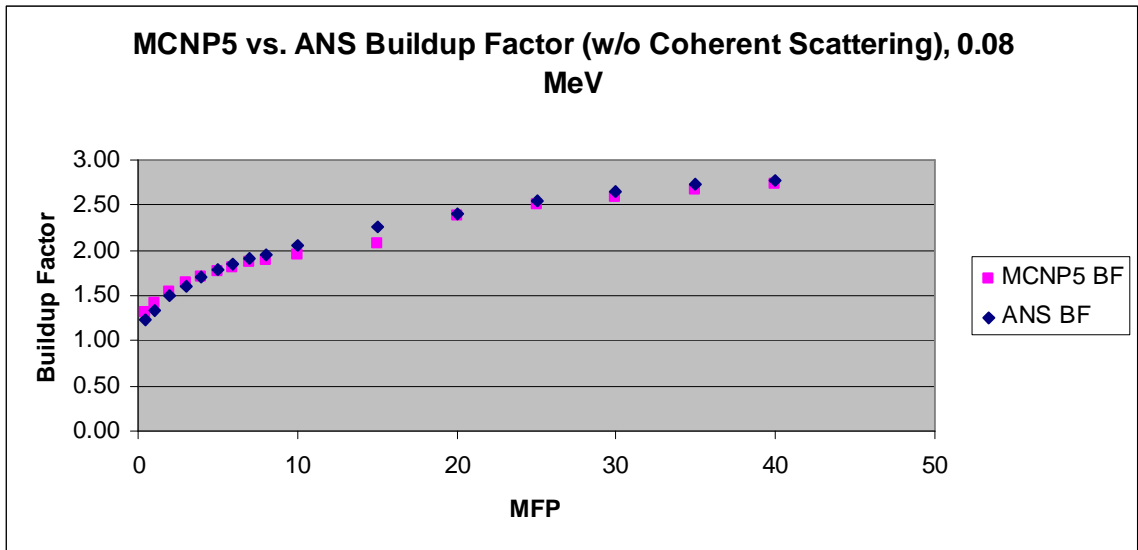


Figure 11m. MCNP5 vs. ANS Buildup Factor w/o Coherent Scattering, 0.08 MeV

Table 9n. Buildup Factor w/ Coherent scattering Iron-0.08 MeV

MFP	Corr. Factor	ANS Standard	ANS W/CS	Calculated Buildup Factor	% Difference
0.5	1.01	1.23	1.24	1.31	5.08%
1	1.01	1.34	1.35	1.42	4.88%
2	1.00	1.51	1.51	1.55	2.61%
3	0.99	1.61	1.59	1.64	2.56%
4	0.98	1.70	1.67	1.71	2.46%
5	0.96	1.78	1.71	1.76	2.96%
6	0.95	1.84	1.75	1.81	3.54%
7	0.93	1.91	1.78	1.85	4.16%
8	0.91	1.96	1.78	1.89	5.87%
10	0.87	2.06	1.79	1.81	0.98%
15	0.75	2.26	1.70	1.69	0.09%
20	0.64	2.41	1.54	1.57	1.66%
25	0.53	2.54	1.35	1.37	1.70%
30	0.44	2.65	1.17	1.17	0.22%
35	0.36	2.73	0.98	0.94	4.20%
40	0.29	2.77	0.80	0.83	2.81%

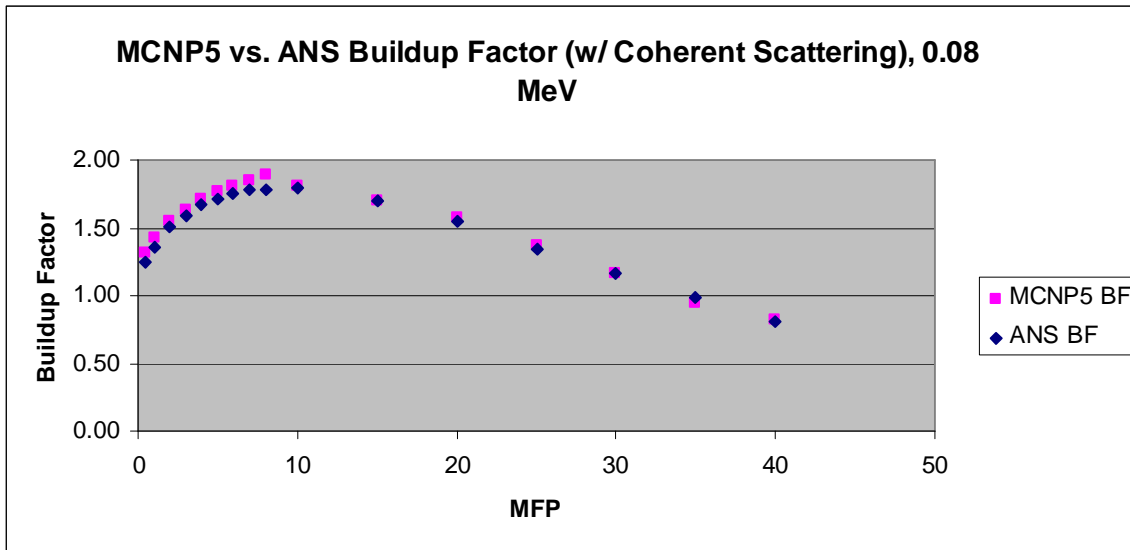


Figure 11n. MCNP5 vs. ANS Buildup Factor w/ Coherent Scattering, 0.08 MeV

Table 9o. Buildup Factor w/o Coherent scattering Iron-0.10 MeV

MFP	ANS Standard	Calculated Buildup Factor	% Difference
0.5	1.38	1.44	4.14%
1	1.60	1.62	1.33%
2	1.94	1.86	4.20%
3	2.13	2.02	5.27%
4	2.31	2.15	7.59%
5	2.48	2.36	5.21%
6	2.63	2.57	2.45%
7	2.77	2.78	0.26%
8	2.90	2.99	2.92%
10	3.13	3.15	0.74%
15	3.61	3.59	0.53%
20	4.00	3.89	2.89%
25	4.34	4.29	1.19%
30	4.63	4.72	2.16%
35	4.85	4.72	2.69%
40	4.98	4.88	2.05%

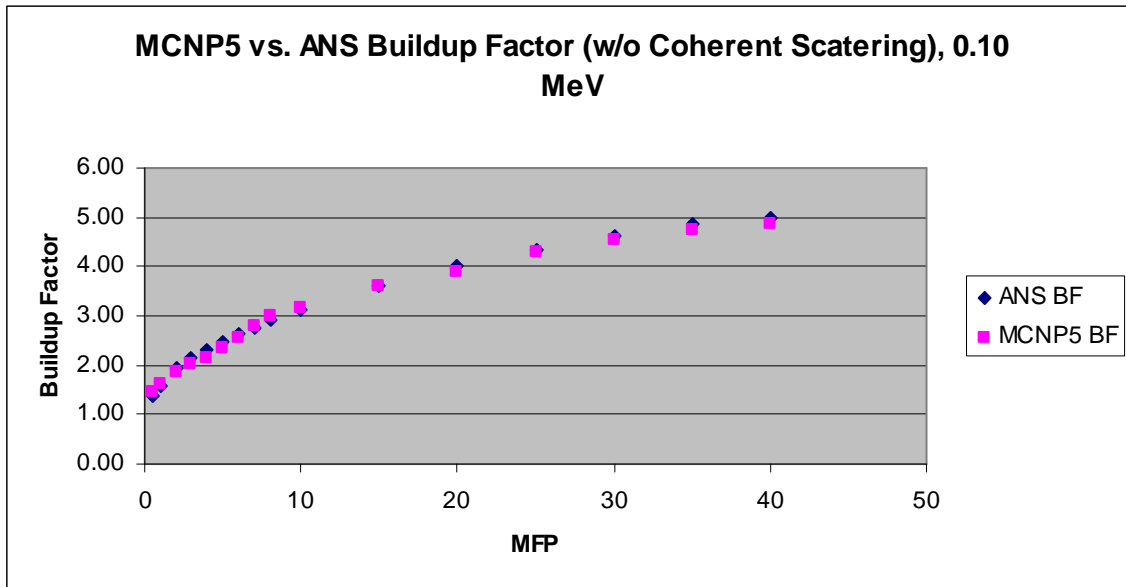


Figure 11o. MCNP5 vs. ANS Buildup Factor w/o Coherent Scattering, 0.10 MeV

Table 9p. Buildup Factor w/ Coherent scattering Iron-0.10 MeV

MFP	Corr. Factor	ANS Standard	ANS W/CS	Calculated Buildup Factor	% Difference
0.5	1.02	1.38	1.41	1.44	2.22%
1	1.01	1.60	1.62	1.62	0.34%
2	1.00	1.94	1.94	1.86	4.20%
3	0.99	2.13	2.11	2.02	4.22%
4	0.98	2.31	2.26	2.15	5.44%
5	0.97	2.48	2.41	2.37	1.63%
6	0.95	2.63	2.50	2.59	3.42%
7	0.94	2.77	2.60	2.81	7.24%
8	0.91	2.90	2.64	2.73	3.41%
10	0.88	3.13	2.75	2.79	1.32%
15	0.77	3.61	2.78	2.74	1.37%
20	0.66	4.00	2.64	2.68	1.54%
25	0.56	4.34	2.43	2.51	3.26%
30	0.47	4.63	2.18	2.31	5.88%
35	0.39	4.85	1.89	2.01	5.90%
40	0.31	4.98	1.54	1.68	8.17%

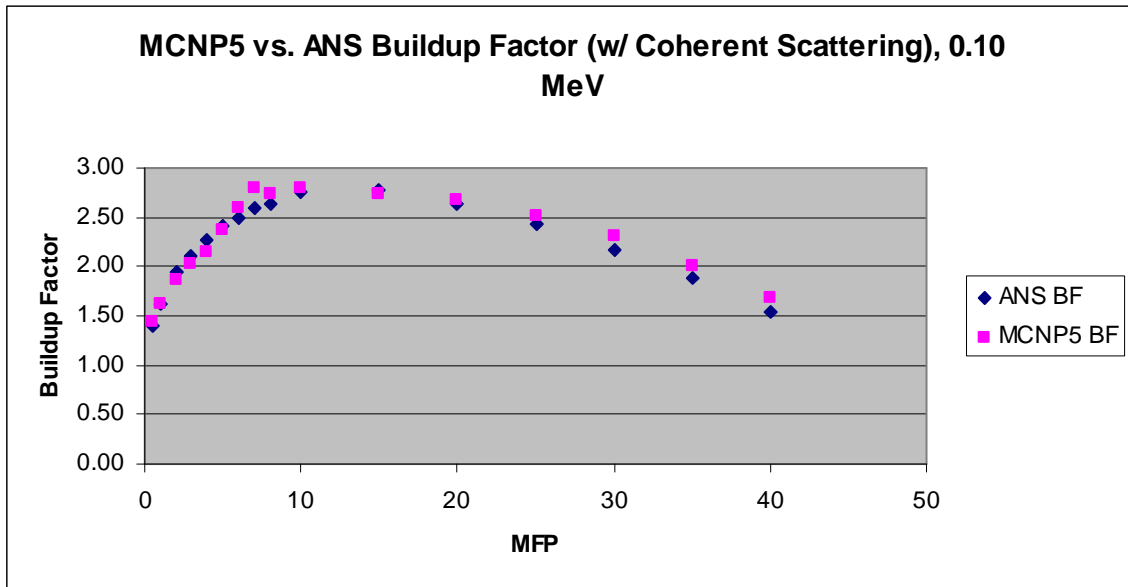


Figure 11p. MCNP5 vs. ANS Buildup Factor w/ Coherent Scattering, 0.10 MeV

Table 9q. Buildup Factor w/o Coherent scattering Iron-0.15 MeV

MFP	ANS Standard	Calculated Buildup Factor	% Difference
0.5	1.93	1.86	3.51%
1	2.46	2.37	3.94%
2	3.22	3.11	3.45%
3	3.93	3.74	5.14%
4	4.60	4.32	6.58%
5	5.23	4.84	8.16%
6	5.84	5.31	9.96%
7	6.42	6.04	6.24%
8	6.98	6.58	6.06%
10	8.07	7.69	4.98%
15	10.60	10.13	4.62%
20	12.90	12.25	5.30%
25	15.00	14.69	2.12%
30	16.90	16.34	3.41%
35	19.40	18.15	6.92%
40	21.70	20.97	3.50%

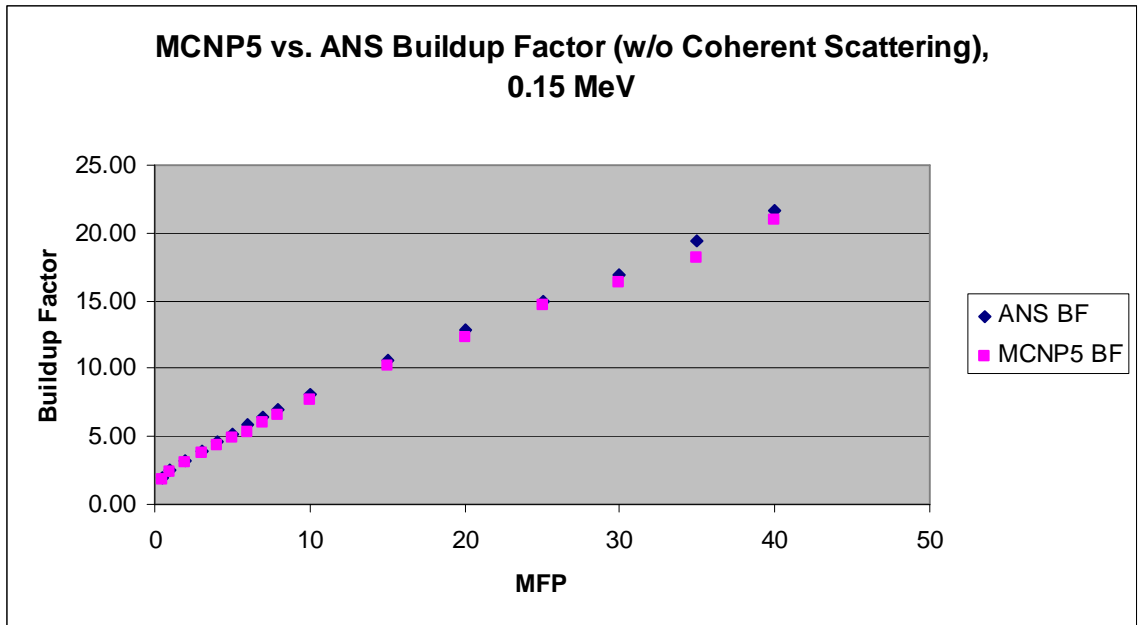


Figure 11q. MCNP5 vs. ANS Buildup Factor w/o Coherent Scattering, 0.15 MeV



Table 9r. Buildup Factor w/ Coherent scattering Iron-0.15 MeV

MFP	Corr. Factor	ANS Standard	ANS W/CS	Calculated Buildup Factor	% Difference
0.5	1.01	1.93	1.95	1.86	4.79%
1	1.01	2.46	2.48	2.37	4.78%
2	1.01	3.22	3.25	3.12	4.18%
3	1.00	3.93	3.93	3.75	4.93%
4	0.99	4.60	4.55	4.31	5.75%
5	0.99	5.23	5.18	4.82	7.45%
6	0.97	5.84	5.66	5.30	6.95%
7	0.96	6.42	6.16	5.73	7.47%
8	0.95	6.98	6.63	6.16	7.57%
10	0.92	8.07	7.42	7.24	2.50%
15	0.85	10.60	9.01	8.91	1.10%
20	0.77	12.90	9.93	9.67	2.71%
25	0.70	15.00	10.50	10.12	3.72%
30	0.62	16.90	10.48	10.68	1.89%
35	0.55	19.40	10.67	10.82	1.43%
40	0.48	21.70	10.42	10.97	5.01%

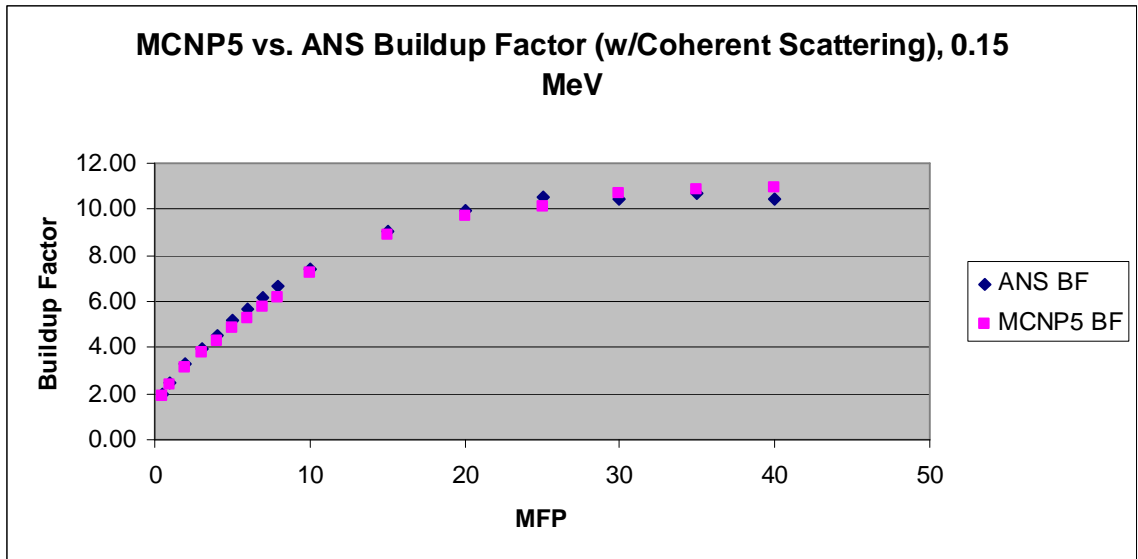


Figure 11r. MCNP5 vs. ANS Buildup Factor w/ Coherent Scattering, 0.15 MeV

Table 9s. Buildup Factor w/o Coherent scattering Iron-0.20 MeV

MFP	ANS Standard	Calculated Buildup Factor	% Difference
0.5	2.13	2.08	2.32%
1	2.94	2.89	1.68%
2	4.34	4.24	2.34%
3	5.72	5.50	4.05%
4	7.14	6.71	6.41%
5	8.58	8.38	2.37%
6	10.00	9.52	5.01%
7	11.50	10.87	5.80%
8	13.10	12.78	2.50%
10	16.10	15.99	0.68%
15	24.20	23.13	4.62%
20	32.50	30.31	7.21%
25	41.00	39.83	2.95%
30	49.80	48.74	2.18%
35	58.80	57.25	2.71%
40	68.10	65.81	3.48%

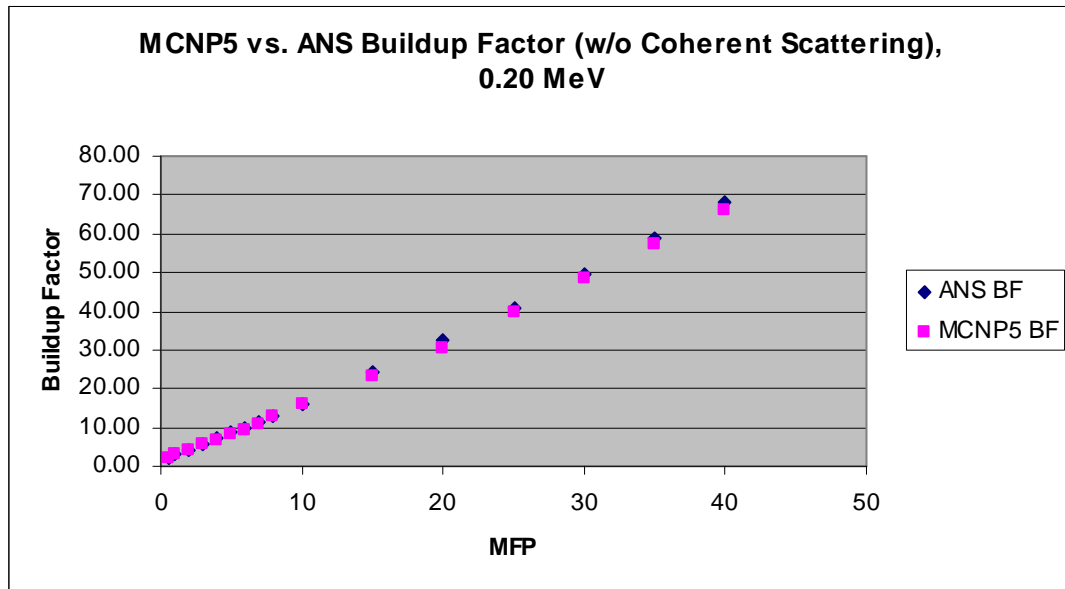


Figure 11s. MCNP5 vs. ANS Buildup Factor w/o Coherent Scattering, 0.20 MeV

Table 9t. Buildup Factor w/ Coherent scattering Iron-0.20 MeV

MFP	Corr. Factor	ANS Standard	ANS W/CS	Calculated Buildup Factor	% Difference
0.5	1.01	2.13	2.15	2.10	2.47%
1	1.00	2.94	2.94	2.89	1.69%
2	1.00	4.34	4.34	4.24	2.28%
3	1.00	5.72	5.72	5.49	4.10%
4	1.00	7.14	7.14	6.72	6.31%
5	0.99	8.58	8.49	7.92	7.22%
6	0.99	10.00	9.90	9.17	7.93%
7	0.98	11.50	11.27	10.38	8.61%
8	0.97	13.10	12.71	12.52	1.49%
10	0.96	16.10	15.46	15.01	2.99%
15	0.92	24.20	22.26	21.77	2.28%
20	0.86	32.50	27.95	26.89	3.94%
25	0.81	41.00	33.21	32.48	2.23%
30	0.75	49.80	37.35	36.85	1.36%
35	0.70	58.80	41.16	40.20	2.38%
40	0.64	68.10	43.58	42.90	1.59%

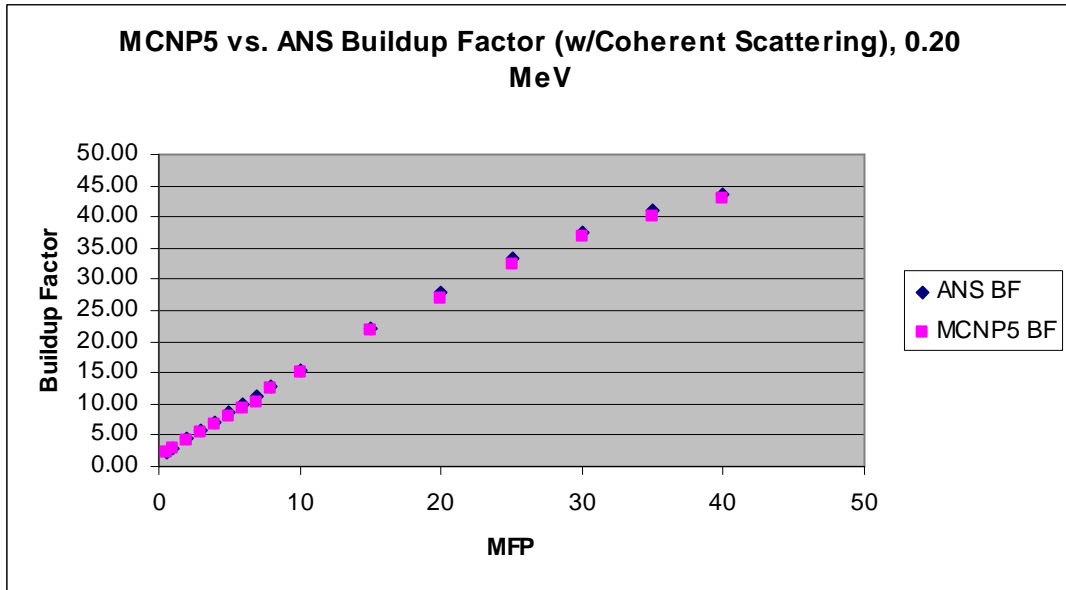


Figure 11t. MCNP5 vs. ANS Buildup Factor w/ Coherent Scattering, 0.20 MeV

Table 9u. Buildup Factor w/o Coherent scattering Iron-0.30 MeV

MFP	ANS Standard	Calculated Buildup Factor	% Difference
0.5	2.07	2.10	1.40%
1	3.08	3.09	0.30%
2	5.09	5.04	1.05%
3	7.23	7.08	2.06%
4	9.58	9.32	2.81%
5	12.10	11.73	3.15%
6	14.90	14.31	4.15%
7	17.90	17.06	4.95%
8	21.00	19.90	5.52%
10	27.80	26.11	6.47%
15	47.60	46.61	2.12%
20	70.80	66.33	6.74%
25	97.20	96.83	0.38%
30	126.00	125.58	0.34%
35	158.00	154.72	2.12%
40	192.00	189.80	1.16%

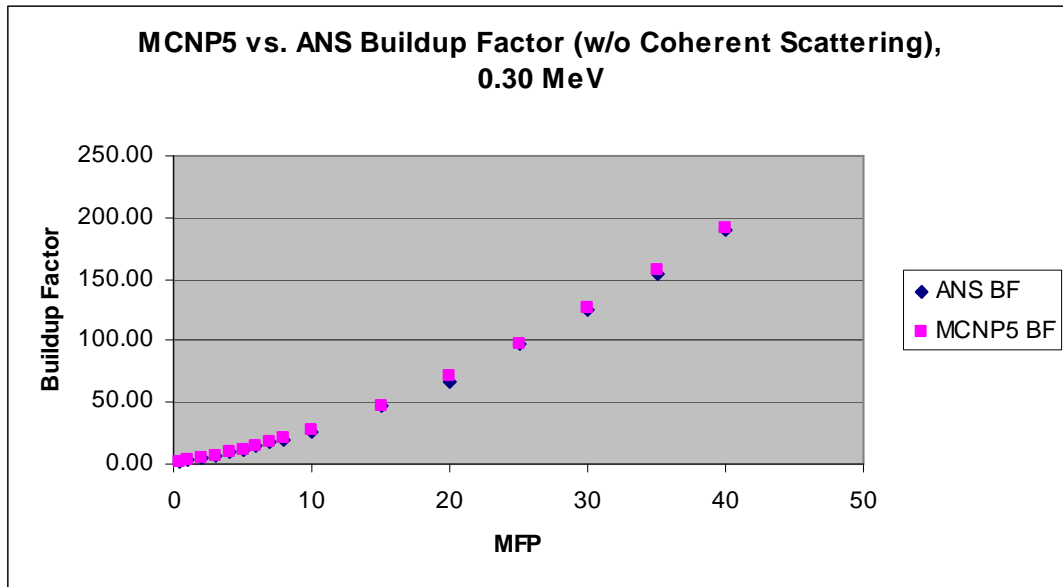


Figure 11u. MCNP5 vs. ANS Buildup Factor w/o Coherent Scattering, 0.30 MeV

Table 9v. Buildup Factor w/ Coherent scattering Iron-0.30 MeV

MFP	Corr. Factor	ANS Standard	ANS W/CS	Calculated Buildup Factor	% Difference
0.5	1.01	2.07	2.09	2.09	0.21%
1	1.00	3.08	3.08	3.07	0.18%
2	1.00	5.09	5.09	5.02	1.36%
3	1.00	7.23	7.23	7.09	1.98%
4	1.00	9.58	9.58	9.31	2.92%
5	1.00	12.10	12.10	11.72	3.22%
6	0.99	14.90	14.75	14.30	3.13%
7	0.99	17.90	17.72	17.01	4.16%
8	0.99	21.00	20.79	19.90	4.45%
10	0.98	27.80	27.24	25.99	4.82%
15	0.96	47.60	45.70	43.14	5.92%
20	0.94	70.80	66.55	62.90	5.81%
25	0.92	97.20	89.42	87.36	2.36%
30	0.89	126.00	112.14	110.35	1.62%
35	0.87	158.00	137.46	134.31	2.34%
40	0.84	192.00	161.28	159.24	1.28%

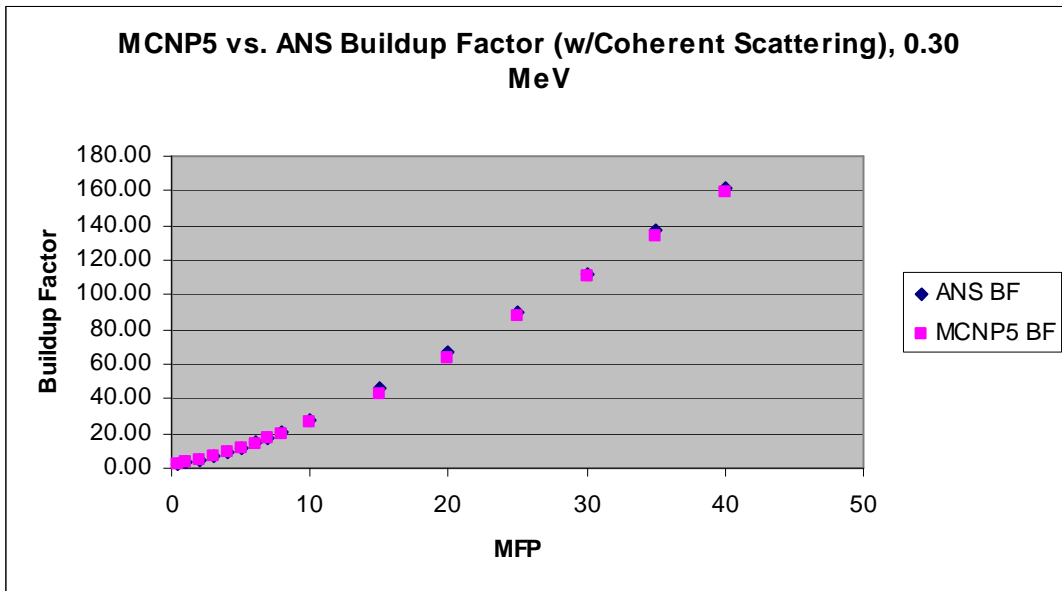


Figure 11v. MCNP5 vs. ANS Buildup Factor w/ Coherent Scattering, 0.30 MeV

Table 9w. Buildup Factor w/o Coherent scattering Iron-0.40 MeV

MFP	ANS Standard	Calculated Buildup Factor	% Difference
0.5	1.91	1.95	2.26%
1	2.86	2.90	1.54%
2	4.90	4.88	0.39%
3	7.17	7.11	0.82%
4	9.75	9.62	1.36%
5	12.70	12.45	1.99%
6	15.90	15.51	2.53%
7	19.40	18.88	2.77%
8	23.30	22.54	3.38%
10	31.90	30.55	4.41%
15	58.60	56.49	3.73%
20	92.30	89.81	2.77%
25	133.00	129.92	2.37%
30	180.00	176.25	2.13%
35	233.00	224.19	3.93%
40	292.00	281.23	3.83%

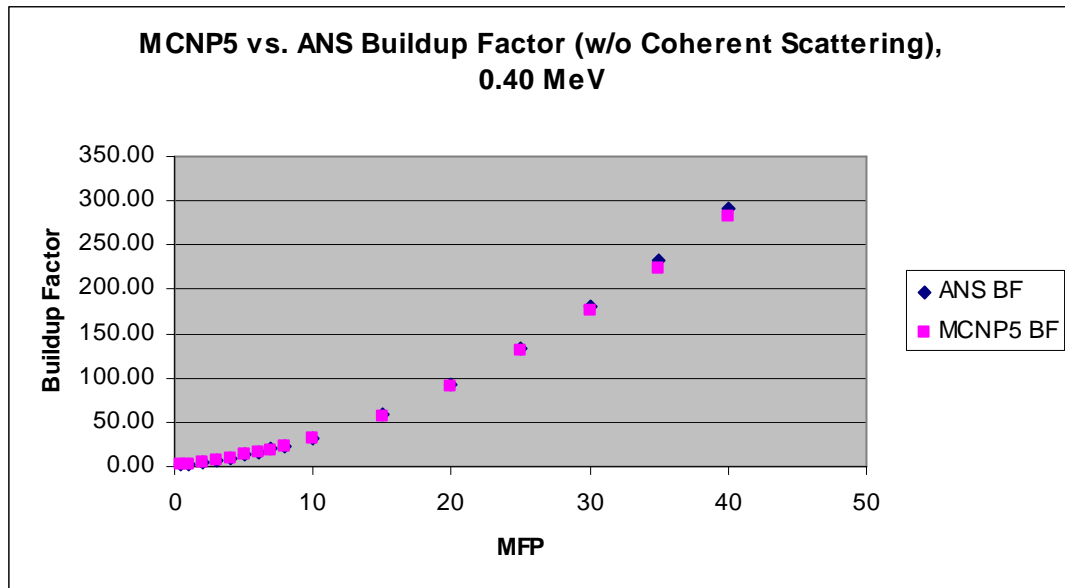


Figure 11w. MCNP5 vs. ANS Buildup Factor w/o Coherent Scattering, 0.40 MeV

Table 9x. Buildup Factor w/ Coherent scattering Iron-0.40 MeV

MFP	Corr. Factor	ANS Standard	ANS W/CS	Calculated Buildup Factor	% Difference
0.5	1.01	1.91	1.93	1.95	1.31%
1	1.00	2.86	2.86	2.88	0.78%
2	1.00	4.90	4.90	4.88	0.33%
3	1.00	7.17	7.17	7.13	0.54%
4	1.00	9.75	9.75	9.61	1.42%
5	1.00	12.70	12.70	12.48	1.78%
6	1.00	15.90	15.90	15.54	2.33%
7	1.00	19.40	19.40	18.90	2.65%
8	1.00	23.30	23.30	22.61	3.07%
10	0.99	31.90	31.58	30.66	3.01%
15	0.99	58.60	58.01	54.58	6.29%
20	0.97	92.30	89.53	84.87	5.49%
25	0.96	133.00	127.68	118.25	7.98%
30	0.95	180.00	171.00	167.43	2.13%
35	0.95	233.00	221.35	217.61	1.72%
40	0.94	292.00	274.48	268.92	2.07%

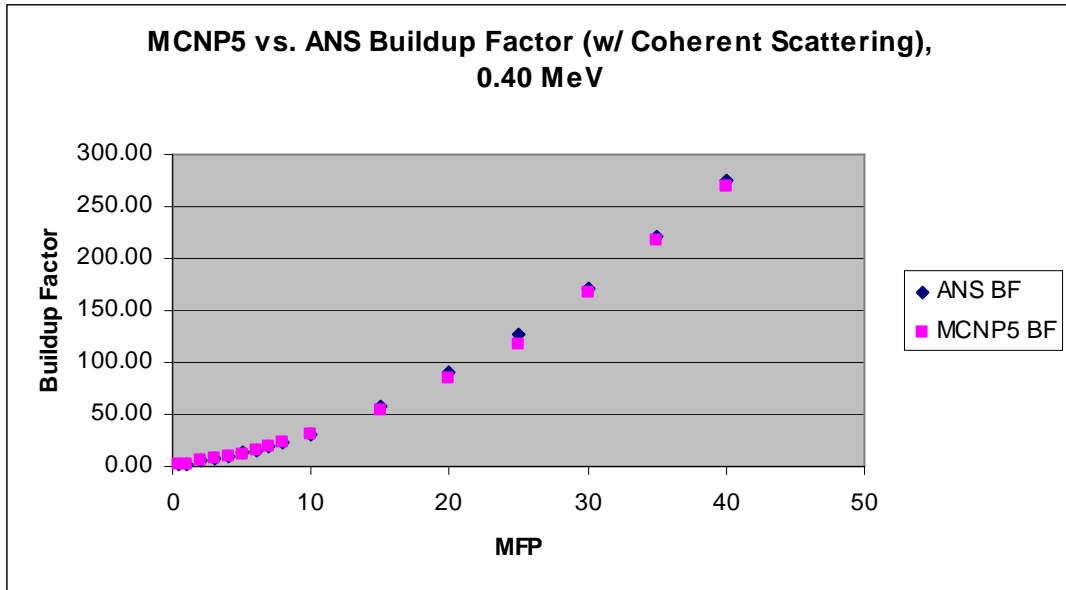


Figure 11x. MCNP5 vs. ANS Buildup Factor w/ Coherent Scattering, 0.40 MeV

Table 9y. Buildup Factor w/o Coherent scattering Iron-0.50 MeV

MFP	ANS Standard	Calculated Buildup Factor	% Difference
0.5	1.79	1.84	2.65%
1	2.66	2.70	1.62%
2	4.57	4.59	0.51%
3	6.75	6.77	0.22%
4	9.25	9.25	0.01%
5	12.10	12.06	0.35%
6	15.30	15.16	0.92%
7	18.80	18.63	0.92%
8	22.70	22.26	1.97%
10	31.40	30.46	3.09%
15	58.80	56.05	4.90%
20	93.90	92.17	1.88%
25	136.00	134.43	1.17%
30	186.00	183.47	1.38%
35	242.00	238.53	1.45%
40	305.00	298.12	2.31%

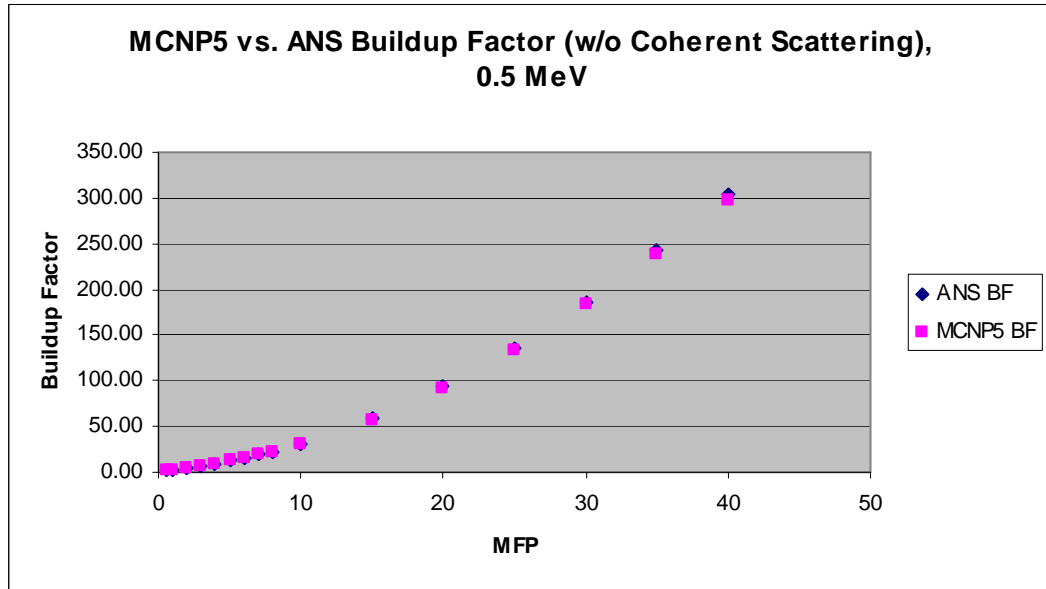


Figure 11y. MCNP5 vs. ANS Buildup Factor w/o Coherent Scattering, 0.50 MeV



Table 9z. Buildup Factor w/ Coherent scattering Iron-0.50 MeV

MFP	Corr. Factor	ANS Standard	ANS W/CS	Calculated Buildup Factor	% Difference
0.5	1.00	1.79	1.79	1.84	2.96%
1	1.00	2.66	2.66	2.70	1.51%
2	1.00	4.57	4.57	4.59	0.53%
3	1.00	6.75	6.75	6.77	0.26%
4	1.00	9.25	9.25	9.24	0.07%
5	1.00	12.10	12.10	12.06	0.37%
6	1.00	15.30	15.30	15.16	0.90%
7	1.00	18.80	18.80	18.56	1.29%
8	1.00	22.70	22.70	22.20	2.25%
10	1.00	31.40	31.40	30.50	2.94%
15	0.99	58.80	58.21	55.98	3.98%
20	0.99	93.90	92.96	87.78	5.90%
25	0.98	136.00	133.28	127.19	4.79%
30	0.98	186.00	182.28	178.28	2.24%
35	0.98	242.00	237.16	234.30	1.22%
40	0.98	305.00	298.90	291.79	2.44%

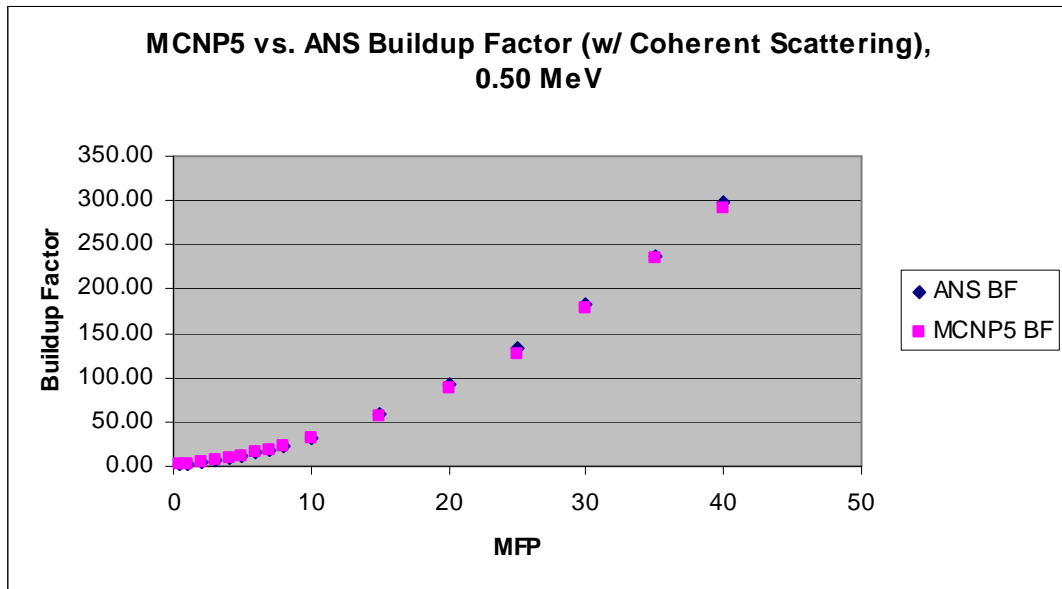


Figure 11z. MCNP5 vs. ANS Buildup Factor w/ Coherent Scattering, 0.50 MeV

Table 9aa. Buildup Factor w/o Coherent scattering Iron-0.60 MeV

MFP	ANS Standard	Calculated Buildup Factor	% Difference
0.5	1.71	1.75	2.22%
1	2.50	2.54	1.73%
2	4.27	4.30	0.65%
3	6.30	6.33	0.44%
4	8.65	8.68	0.31%
5	11.30	11.32	0.19%
6	14.30	14.23	0.49%
7	17.70	17.48	1.27%
8	21.30	21.01	1.39%
10	29.40	28.77	2.20%
15	55.00	52.66	4.45%
20	87.40	86.45	1.10%
25	127.00	124.11	2.33%
30	172.00	168.82	1.88%
35	223.00	219.28	1.70%
40	280.00	274.57	1.98%

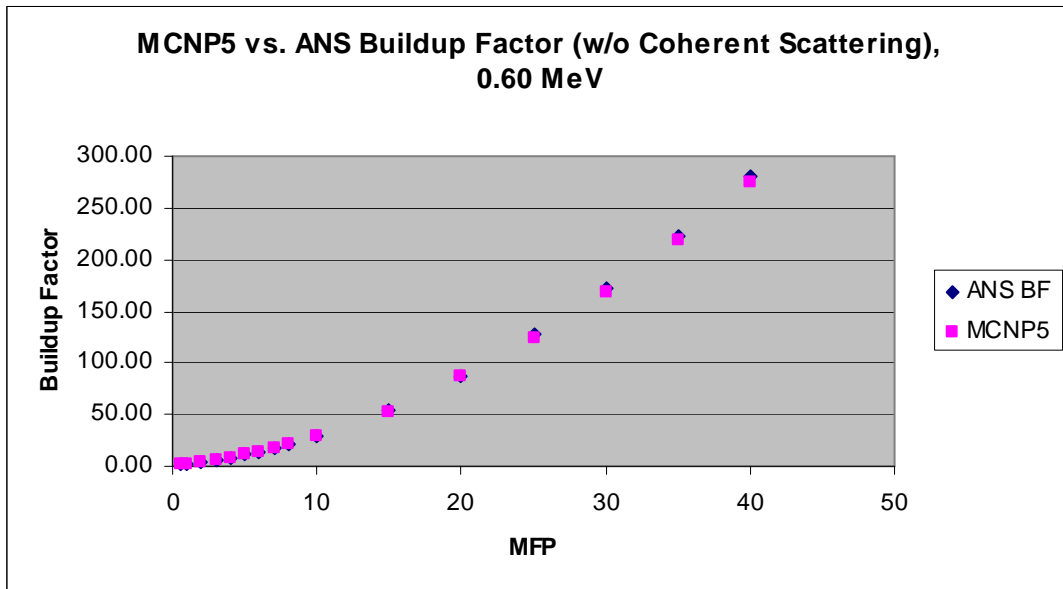


Figure 11aa. MCNP5 vs. ANS Buildup Factor w/o Coherent Scattering, 0.60 MeV

Table 9bb. Buildup Factor w/ Coherent scattering Iron-0.60 MeV

MFP	Corr. Factor	ANS Standard	ANS W/CS	Calculated Buildup Factor	% Difference
0.5	1.01	1.71	1.73	1.82	4.91%
1	1.00	2.50	2.50	2.59	3.62%
2	1.00	4.27	4.27	4.35	1.79%
3	1.00	6.30	6.30	6.38	1.22%
4	1.00	8.65	8.65	8.73	0.88%
5	1.00	11.30	11.30	11.37	0.63%
6	1.00	14.30	14.30	14.28	0.14%
7	1.00	17.70	17.70	17.53	0.98%
8	0.99	21.30	21.09	20.85	1.14%
10	1.00	29.40	29.40	28.82	2.02%
15	0.99	55.00	54.45	52.18	4.35%
20	1.00	87.40	87.40	86.50	1.04%
25	0.99	127.00	125.73	122.92	2.29%
30	0.99	172.00	170.28	167.18	1.85%
35	1.00	223.00	223.00	219.33	1.67%
40	1.01	280.00	282.80	277.37	1.96%

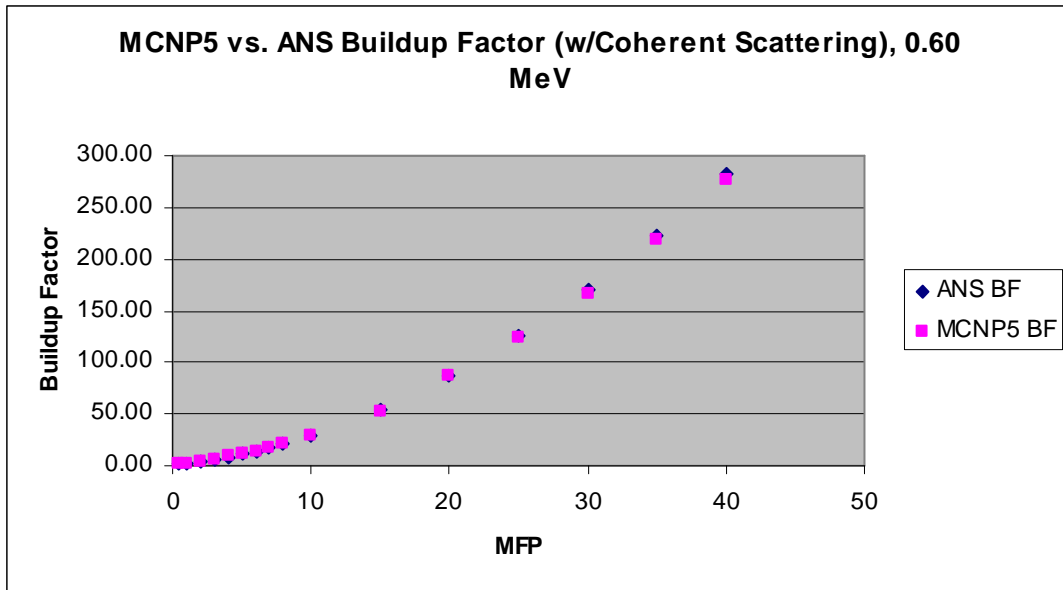


Figure 11bb. MCNP5 vs. ANS Buildup Factor w/ Coherent Scattering, 0.60 MeV

Table 9cc. Buildup Factor w/o Coherent scattering Iron-0.80 MeV

<b>0.80 MeV Buildup Factors (No Coherent Scattering)</b>			
<b>MFP</b>	<b>ANS Standard</b>	<b>Calculated BUILDUP FACTOR</b>	<b>% Difference</b>
0.5	1.60	1.56	2.56%
1	2.28	2.24	1.79%
2	3.81	3.75	1.69%
3	5.57	5.52	0.88%
4	7.60	7.52	1.05%
5	9.88	9.58	3.15%
6	12.40	12.01	3.22%
7	15.20	14.85	2.36%
8	18.20	17.14	6.17%
10	24.90	22.93	8.59%
15	45.30	43.45	4.26%
20	70.40	68.23	3.18%
25	99.80	97.67	2.18%
30	133.00	129.61	2.62%
35	170.00	167.21	1.67%
40	211.00	208.52	1.19%

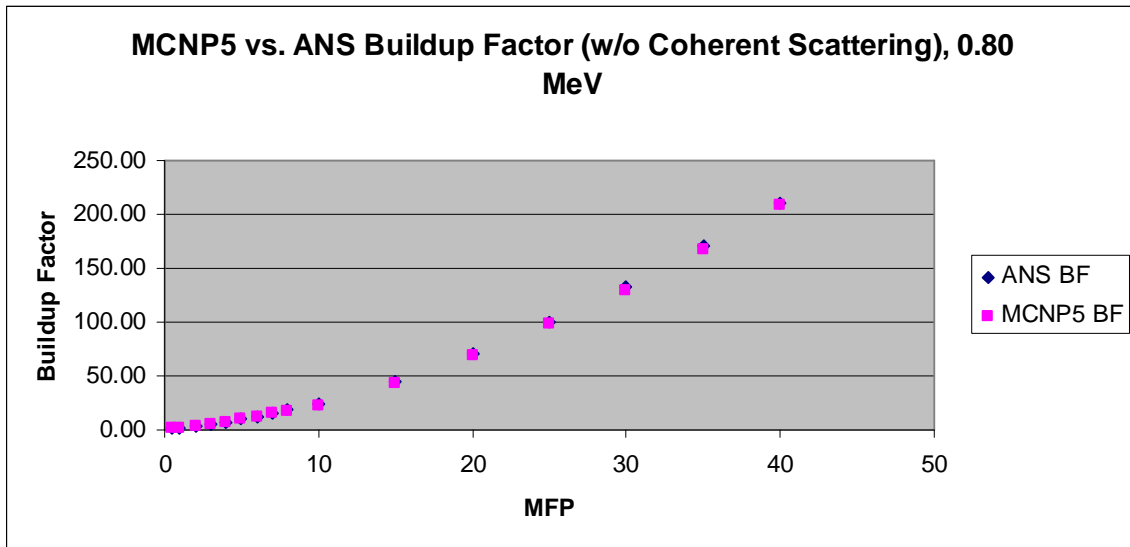


Figure 11cc. MCNP5 vs. ANS Buildup Factor w/o Coherent Scattering, 0.80 MeV

Table 9dd. Buildup Factor w/ Coherent scattering Iron-0.80 MeV

0.80 MeV Buildup Factors (Coherent Scattering)					
MFP	Corr. Factor	ANS Standard	ANS W/CS	Calculated BUILDUP FACTOR	% Difference
0.5	1.01	1.60	1.62	1.61	0.62%
1	1.00	2.28	2.28	2.26	0.88%
2	1.00	3.81	3.81	3.76	1.44%
3	1.00	5.57	5.57	5.54	0.49%
4	1.00	7.60	7.60	7.57	0.44%
5	1.00	9.88	9.88	9.65	2.43%
6	1.00	12.40	12.40	12.15	2.06%
7	1.00	15.20	15.20	14.65	3.75%
8	1.00	18.20	18.20	17.45	4.30%
10	1.00	24.90	24.90	23.89	4.23%
15	1.00	45.30	45.30	42.57	6.41%
20	1.00	70.40	70.40	68.35	3.00%
25	1.01	99.80	100.80	97.31	3.58%
30	1.01	133.00	134.33	131.28	2.32%
35	1.03	170.00	175.10	173.29	1.04%
40	1.03	211.00	217.33	213.81	1.65%

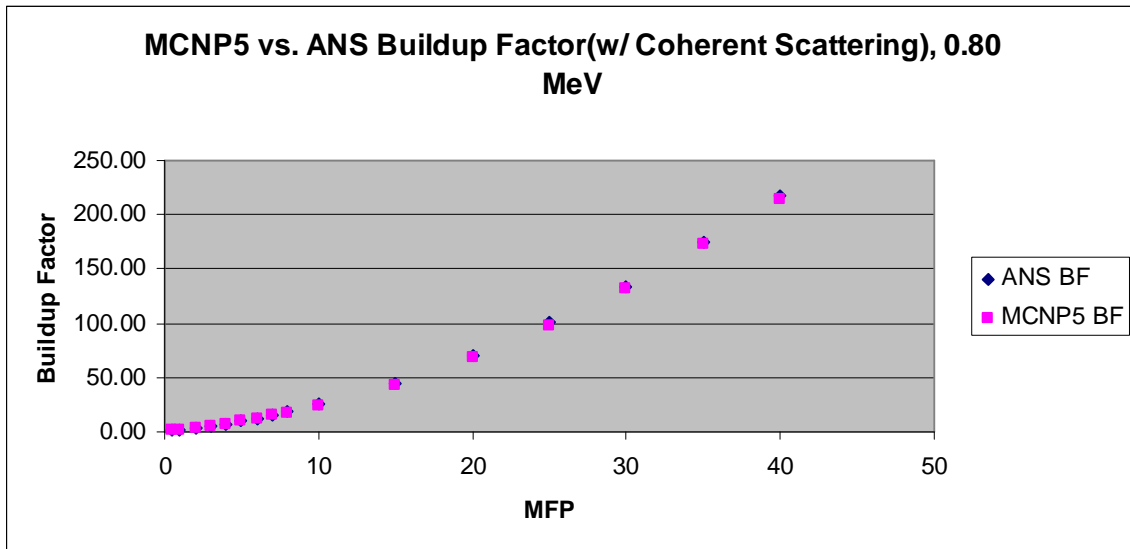


Figure 11dd. MCNP5 vs. ANS Buildup Factor w/ Coherent Scattering, 0.80 MeV

Table 9ee. Buildup Factor w/o Coherent scattering Iron-1.00 MeV

MFP	ANS Standard	Calculated Buildup Factor	% Difference
0.5	1.53	1.58	3.0%
1	2.14	2.19	2.4%
2	3.5	3.56	1.8%
3	5.04	5.13	1.8%
4	6.79	6.92	1.9%
5	8.74	8.90	1.8%
6	10.9	11.03	1.1%
7	13.2	13.36	1.2%
8	15.7	15.81	0.7%
10	21.1	21.22	0.5%
15	37.1	37.01	0.2%
20	56.2	56.03	0.3%
25	77.9	77.51	0.5%
30	102	100.03	2.0%
35	128	123.11	4.0%
40	156	148.79	4.8%

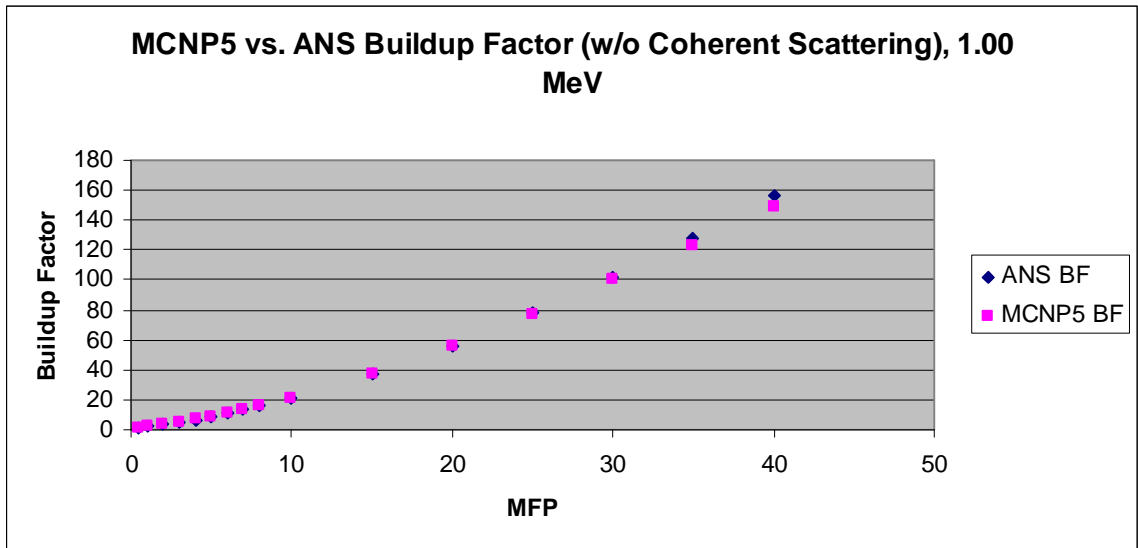


Figure 11ee. MCNP5 vs. ANS Buildup Factor w/o Coherent Scattering, 1.00 MeV

Table 9ff. Buildup Factor w/ Coherent scattering Iron-1.00 MeV

MFP	Corr. Factor	ANS Standard	ANS W/CS	Calculated Buildup Factor	% Difference
0.5	1.00	1.53	1.53	1.6	3.1%
1	1.00	2.14	2.14	2.2	2.3%
2	1.00	3.5	3.5	3.6	1.7%
3	1.00	5.04	5.04	5.1	2.0%
4	1.00	6.79	6.79	6.9	1.9%
5	1.00	8.74	8.74	8.9	1.7%
6	1.00	10.9	10.9	11.0	1.1%
7	1.00	13.2	13.2	13.4	1.3%
8	1.00	15.7	15.7	15.9	1.2%
10	1.00	21.1	21.1	21.3	1.1%
15	1.00	37.1	37.1	37.2	0.2%
20	1.00	56.2	56.2	55.5	1.2%
25	1.01	77.9	78.679	76.3	3.1%
30	1.01	102	103.02	99.6	3.4%
35	1.02	128	130.56	128.1	1.9%
40	1.03	156	160.68	154.2	4.2%

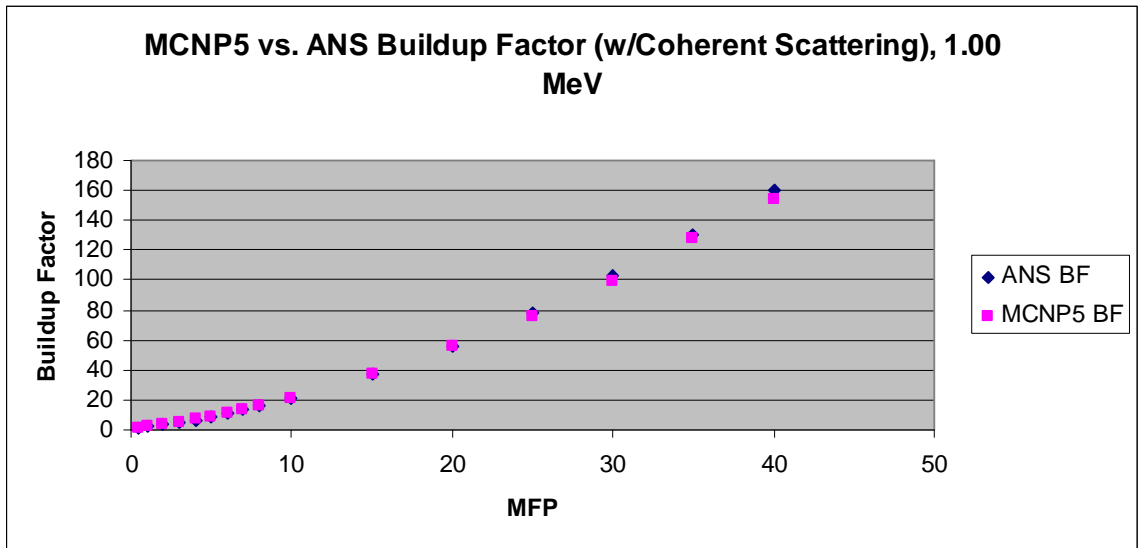


Figure 11ff. MCNP5 vs. ANS Buildup Factor w/ Coherent Scattering, 1.00 MeV

Table 9gg. Buildup Factor, Iron-1.50 MeV

MFP	ANS Standard	Calculated Buildup Factor	% Difference
0.5	1.45	1.49	2.72%
1	1.95	2.01	2.83%
2	3.03	3.12	2.85%
3	4.23	4.35	2.69%
4	5.54	5.70	2.82%
5	6.95	7.15	2.80%
6	8.47	8.69	2.54%
7	10.1	10.37	2.60%
8	11.8	12.04	1.96%
10	15.3	15.68	2.40%
15	25.4	25.91	1.95%
20	36.8	37.96	3.05%
25	49.2	50.17	1.93%
30	62.6	63.22	0.97%
35	76.8	76.95	0.20%
40	91.6	87.44	4.76%

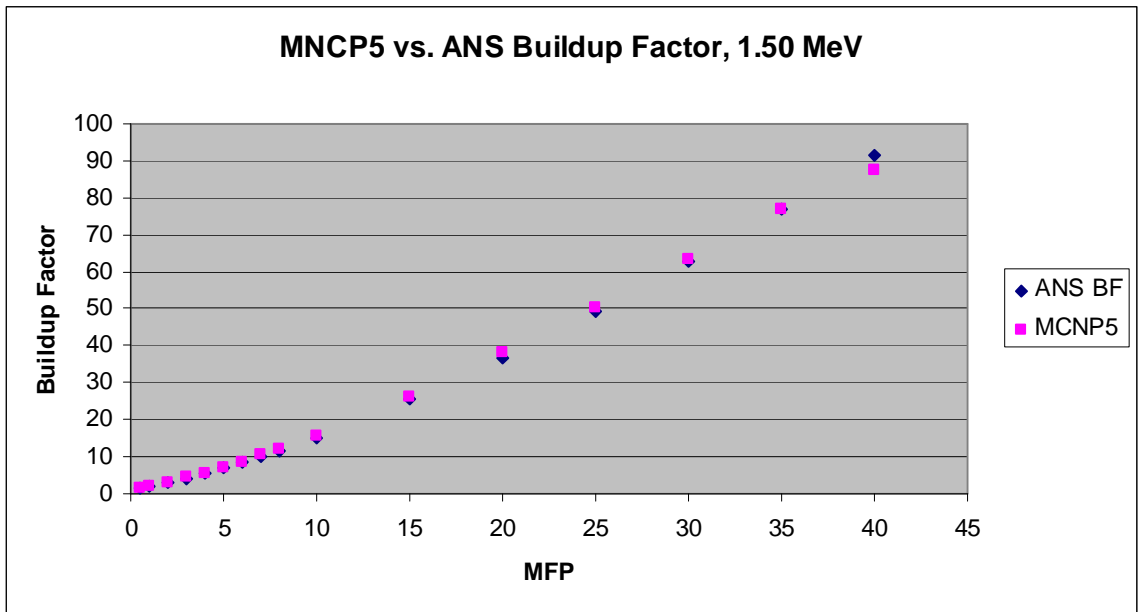


Figure 11gg. MCNP5 vs. ANS Buildup Factor, 1.50 MeV



Table 9hh. Buildup Factor, Iron-2.00 MeV

MFP	ANS Standard	Calculated Buildup Factor	% Difference
0.5	1.4	1.45	3.16%
1	1.84	1.90	3.31%
2	2.76	2.86	3.35%
3	3.74	3.88	3.54%
4	4.8	4.98	3.61%
5	5.93	6.16	3.79%
6	7.12	7.41	3.85%
7	8.37	8.70	3.80%
8	9.67	10.07	3.96%
10	12.4	12.97	4.37%
15	20	20.91	4.33%
20	28.5	29.80	4.35%
25	37.7	39.31	4.10%
30	47.4	49.90	5.01%
35	57.7	60.23	4.20%
40	68.4	68.10	0.44%

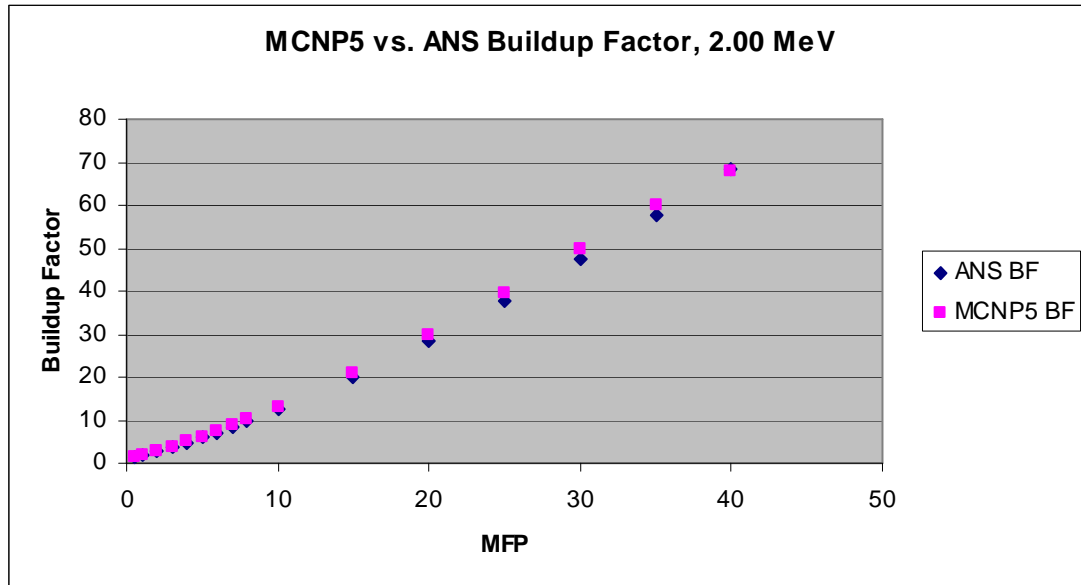


Figure 11hh MCNP5 vs. ANS Buildup Factor, 2.00 MeV

Table 9ii. Buildup Factor, Iron-3.00 MeV

MFP	ANS Standard	Calculated Buildup Factor	% Difference
0.5	1.35	1.37	1.46%
1	1.7	1.72	1.16%
2	2.39	2.43	1.65%
3	3.1	3.12	0.70%
4	3.86	3.90	1.03%
5	4.66	4.69	0.64%
6	5.51	5.55	0.72%
7	6.39	6.47	1.24%
8	7.3	7.45	2.01%
10	9.23	9.35	1.28%
15	14.5	14.95	3.01%
20	20.4	21.46	4.94%
25	26.7	27.05	1.29%
30	33.3	33.89	1.74%
35	40.4	41.02	1.51%
40	47.8	50.12	4.63%

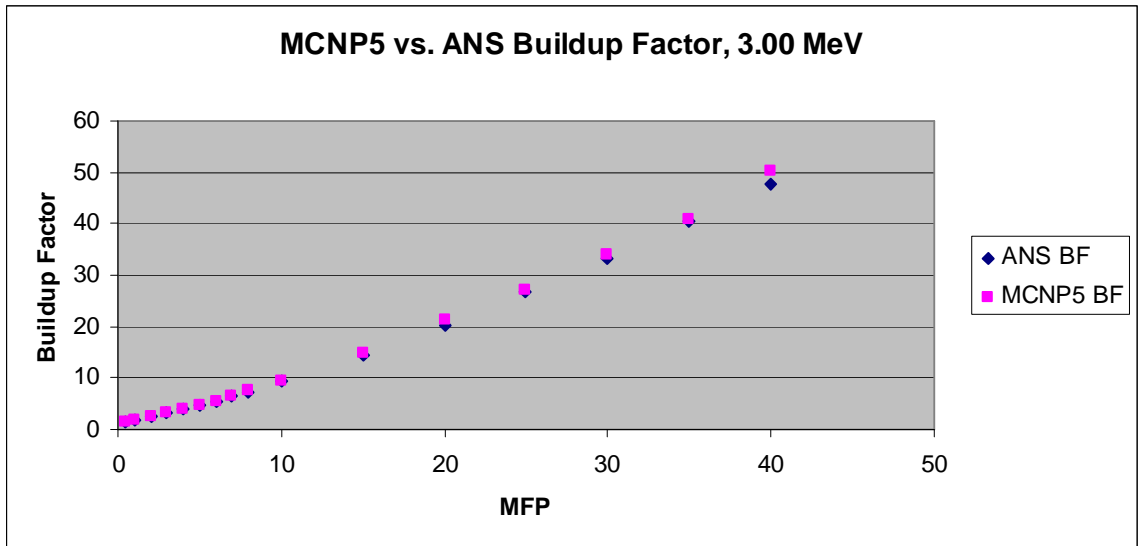


Figure 11ii. MCNP5 vs. ANS Buildup Factor, 3.00 MeV

Table 9jj. Buildup Factor, Iron- 4.00 MeV

MFP	ANS Standard	Calculated Buildup Factor	% Difference
0.5	1.31	1.33	1.84%
1	1.59	1.62	2.06%
2	2.12	2.14	1.10%
3	2.68	2.71	1.20%
4	3.27	3.32	1.62%
5	3.89	3.93	1.07%
6	4.55	4.59	0.89%
7	5.23	5.29	1.06%
8	5.95	6.13	3.00%
10	7.46	7.68	2.84%
15	11.7	12.01	2.58%
20	16.4	15.94	2.89%
25	21.6	20.67	4.48%
30	27	26.14	3.30%
35	32.5	31.33	3.73%
40	37.9	36.98	2.49%

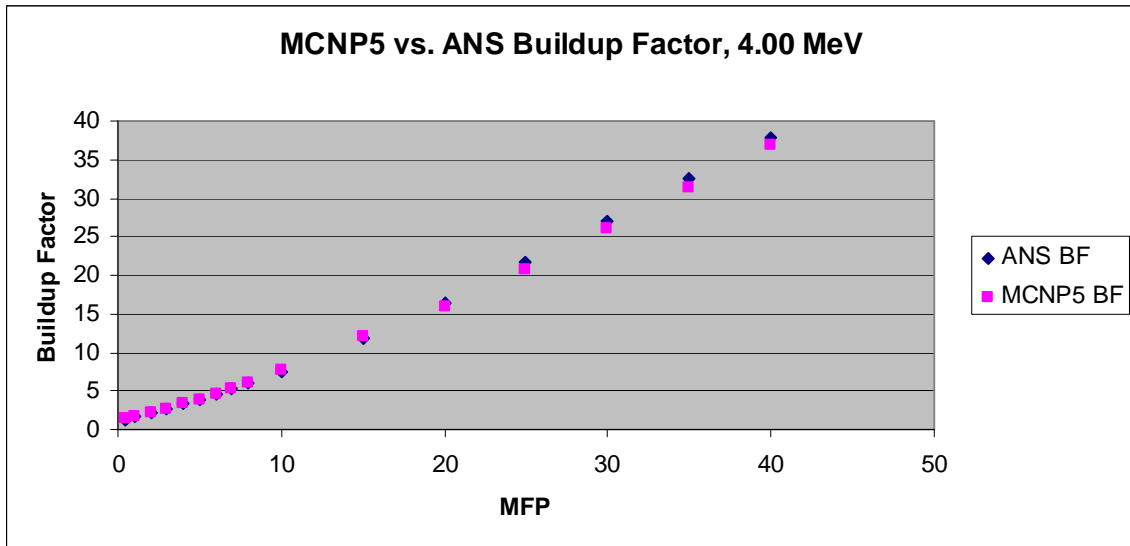


Figure 11jj. MCNP5 vs. ANS Buildup Factor, 4.00 MeV

Table 9kk. Buildup Factor, Iron-5.00 MeV

MFP	ANS Standard	Calculated Buildup Factor	% Difference
0.5	1.26	1.27	0.87%
1	1.49	1.51	1.32%
2	1.93	1.94	0.67%
3	2.39	2.43	1.65%
4	2.86	2.82	1.60%
5	3.37	3.31	1.81%
6	3.91	3.87	1.16%
7	4.47	4.41	1.31%
8	5.07	5.13	1.17%
10	6.33	6.43	1.62%
15	9.92	10.05	1.29%
20	14.1	13.88	1.62%
25	18.7	18.21	2.69%
30	23.7	23.08	2.71%
35	28.9	28.10	2.85%
40	34	33.10	2.72%

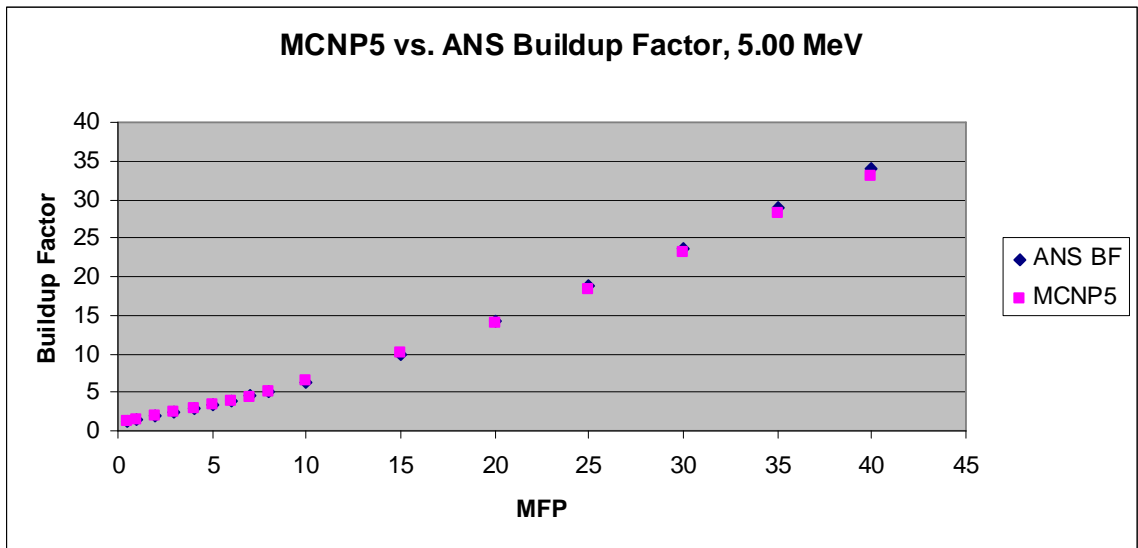


Figure 11kk. MCNP5 vs. ANS Buildup Factor, 5.00 MeV

Table 9ll. Buildup Factor, Iron-6.00 MeV

MFP	ANS Standard	Calculated Buildup Factor	% Difference
0.5	1.22	1.24	1.85%
1	1.42	1.46	3.01%
2	1.79	1.82	1.70%
3	2.17	2.21	1.90%
4	2.57	2.61	1.62%
5	2.99	3.05	1.84%
6	3.45	3.51	1.77%
7	3.93	3.98	1.33%
8	4.44	4.51	1.55%
10	5.54	5.63	1.63%
15	8.72	8.57	1.75%
20	12.5	12.22	2.29%
25	16.9	16.43	2.86%
30	21.7	21.12	2.75%
35	26.8	26.17	2.41%
40	32.1	30.90	3.88%

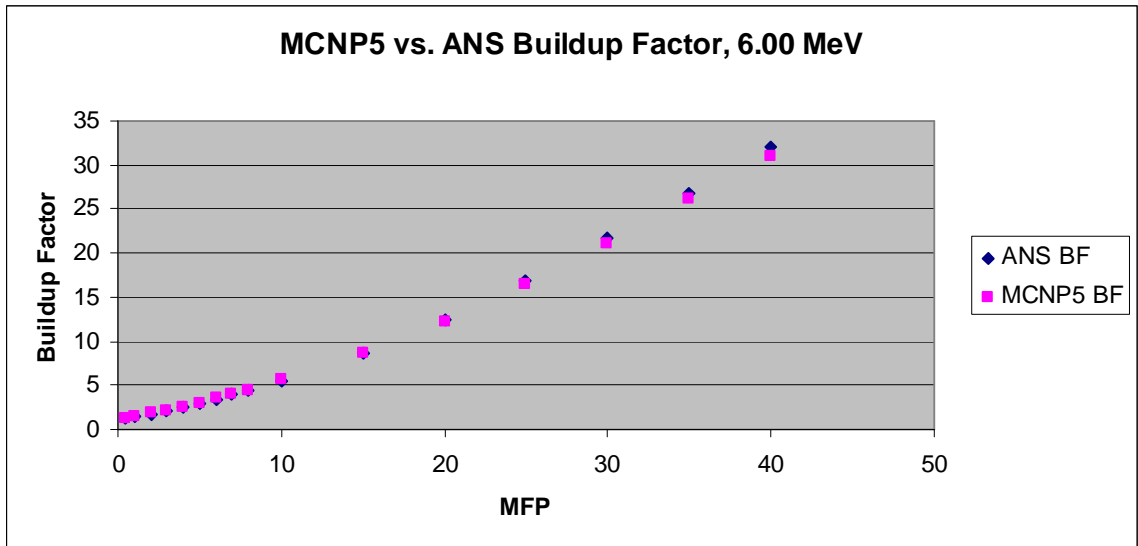


Figure 11ll. MCNP5 vs. ANS Buildup Factor, 6.00 MeV

Table 9mm. Buildup Factor, Iron-8.00 MeV

MFP	ANS Standard	Calculated Buildup Factor	% Difference
0.5	1.18	1.20	1.67%
1	1.33	1.35	1.48%
2	1.6	1.62	1.23%
3	1.88	1.90	1.05%
4	2.17	2.20	1.50%
5	2.5	2.54	1.40%
6	2.85	2.89	1.38%
7	3.22	3.26	1.23%
8	3.62	3.69	1.82%
10	4.5	4.62	2.66%
15	7.18	7.05	1.84%
20	10.6	10.45	1.41%
25	14.8	14.43	2.55%
30	19.8	19.20	3.13%
35	25.6	24.86	2.98%
40	32.4	31.45	3.02%

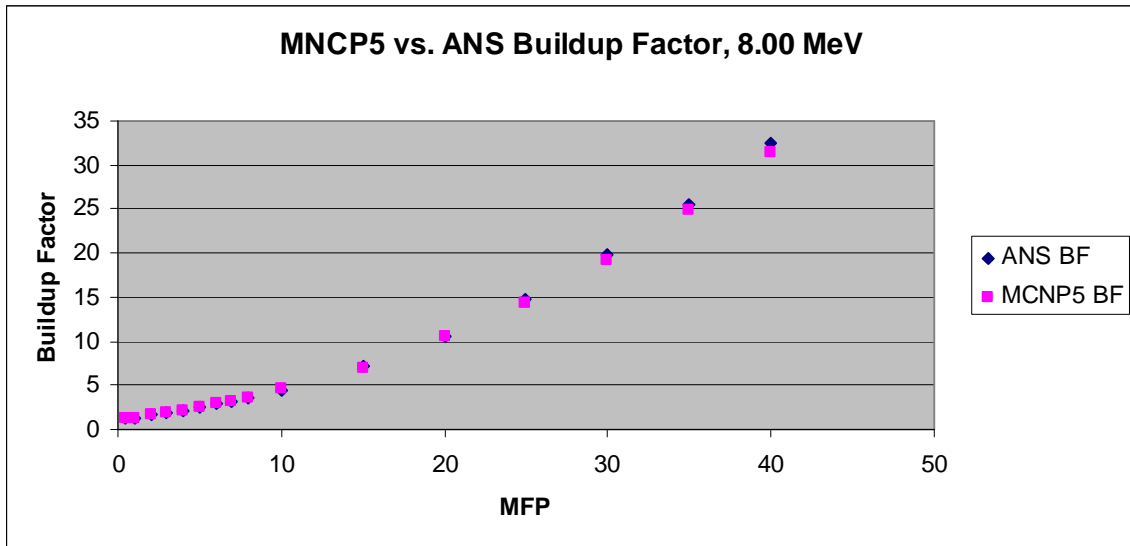


Figure 11mm. MCNP5 vs. ANS Buildup Factor, 8.00 MeV

Table 9nn. Buildup Factor, Iron-10.0 MeV

MFP	ANS Standard	Calculated Buildup Factor	% Difference
0.5	1.15	1.16	1.03%
1	1.27	1.31	3.05%
2	1.48	1.51	1.99%
3	1.69	1.72	1.74%
4	1.93	1.98	2.33%
5	2.19	2.21	0.90%
6	2.47	2.49	0.68%
7	2.78	2.80	0.71%
8	3.12	3.14	0.64%
10	3.87	3.76	2.82%
15	6.29	6.19	1.57%
20	9.59	9.48	1.20%
25	14	13.89	0.79%
30	19.6	19.20	2.08%
35	26.7	26.30	1.52%
40	35.4	34.69	2.03%

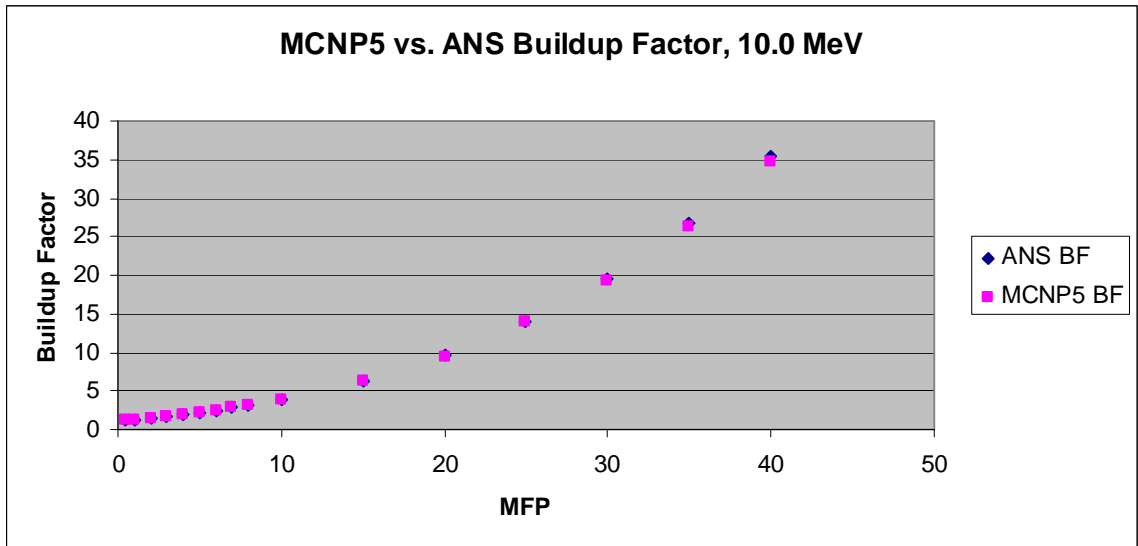


Figure 11nn. MCNP5 vs. ANS Buildup Factor, 10.0 MeV

Table 900. Buildup Factor, Iron-15.0 MeV

MFP	ANS Standard	Calculated Buildup Factor	% Difference
0.5	1.1	1.12	1.79%
1	1.18	1.21	2.48%
2	1.31	1.34	1.87%
3	1.44	1.49	3.29%
4	1.59	1.64	3.05%
5	1.76	1.80	2.11%
6	1.96	2.02	3.11%
7	2.17	2.23	2.86%
8	2.42	2.51	3.67%
10	2.99	3.13	4.59%
15	5.06	5.13	1.27%
20	8.44	8.15	3.56%
25	13.8	13.23	4.31%
30	22.2	21.24	4.51%
35	35	34.36	1.86%
40	54.1	51.24	5.58%

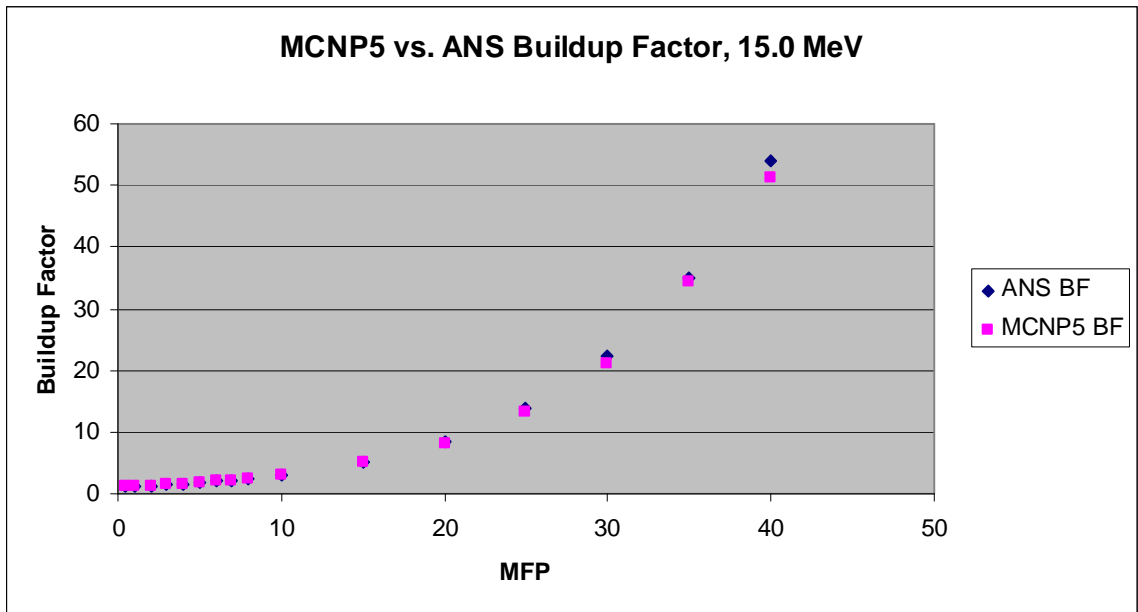


Figure 1100. MCNP5 vs. ANS Buildup Factor, 15.0 MeV



MCNP5 CALCULATED BUILDUP FACTORS –WATER

Table 10a. Buildup Factor, Water-0.015 MeV

<b>MFP</b>	<b>ANS Standard</b>	<b>Calculated Buildup Factor</b>	<b>% Difference</b>
0.5	1.13	1.13	0.39%
1	1.19	1.18	0.73%
2	1.28	1.24	3.03%
3	1.34	1.30	3.00%
4	1.4	1.38	1.58%
5	1.44	1.41	1.98%
6	1.48	1.46	1.58%
7	1.51	1.49	1.26%
8	1.54	1.52	1.01%
10	1.59	1.57	1.15%
15	1.69	1.65	2.23%
20	1.77	1.72	2.73%
25	1.83	1.79	2.12%
30	1.88	1.86	1.23%
35	1.93	1.90	1.84%
40	1.96	1.91	2.51%

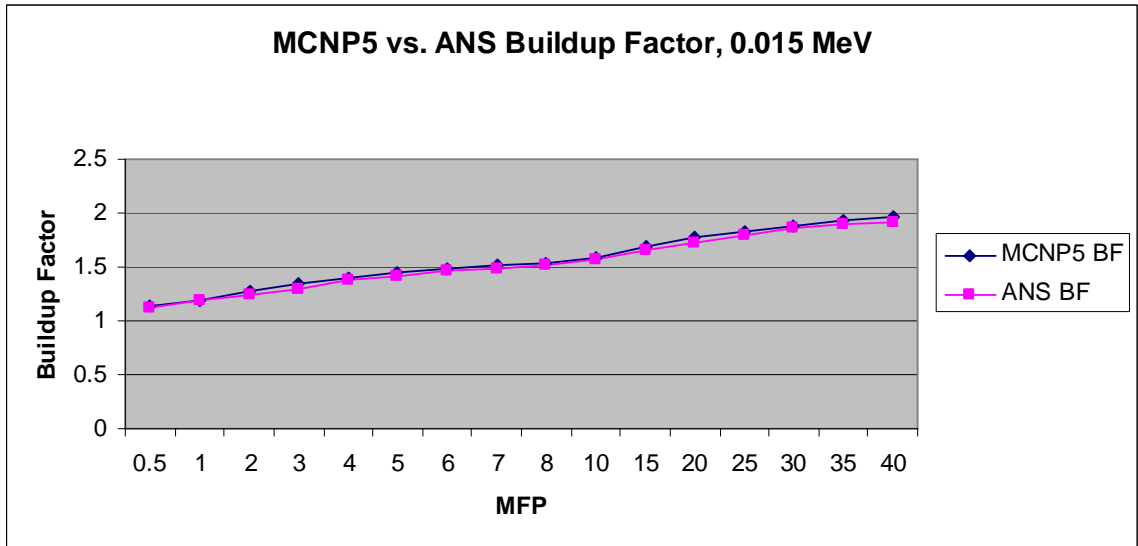


Figure 12a. MCNP5 vs. ANS Buildup Factor, 0.015 MeV

Table 10b. Buildup Factor, Water-0.02 MeV

MFP	ANS Standard	Calculated Buildup Factor	% Difference
0.5	1.29	1.31	1.68%
1	1.45	1.42	2.04%
2	1.7	1.64	3.53%
3	1.89	1.85	1.93%
4	2.05	2.01	1.88%
5	2.19	2.14	2.28%
6	2.31	2.29	0.82%
7	2.43	2.37	2.48%
8	2.53	2.41	4.98%
10	2.72	2.69	1.24%
15	3.13	2.99	4.79%
20	3.47	3.32	4.62%
25	3.76	3.56	5.58%
30	4.03	3.96	1.71%
35	4.25	4.13	2.96%
40	4.43	4.38	1.10%

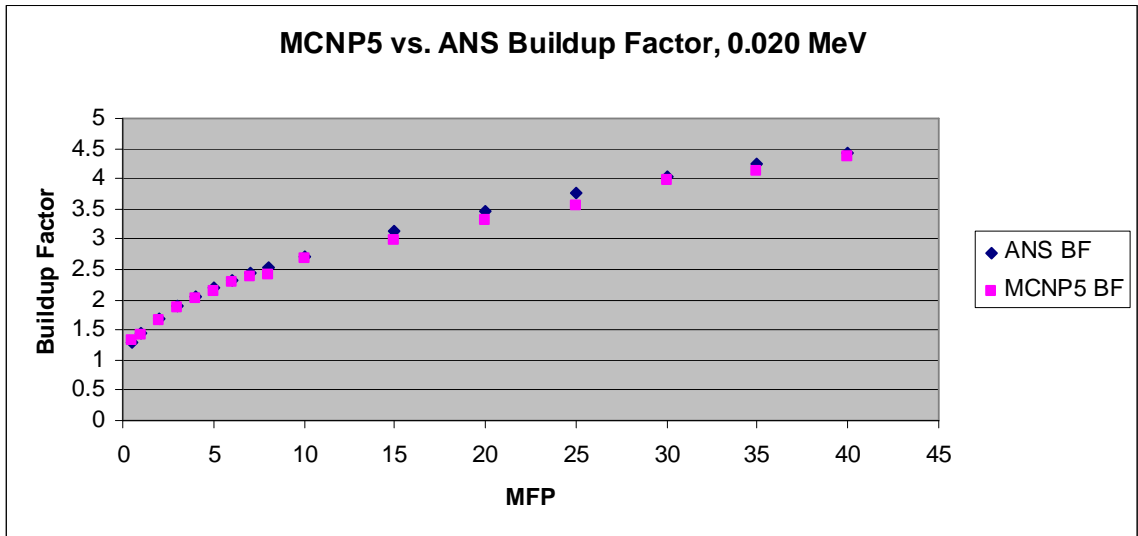


Figure 12b. MCNP5 vs. ANS Buildup Factor, 0.020 MeV

Table 10c. Buildup Factor, Water-0.03 MeV

MFP	ANS Standard	Calculated Buildup Factor	% Difference
0.5	1.81	1.78	1.69%
1	2.43	2.40	1.30%
2	3.46	3.41	1.47%
3	4.41	4.32	1.99%
4	5.32	5.21	2.05%
5	6.18	6.11	1.11%
6	7.01	6.84	2.44%
7	7.81	7.62	2.45%
8	8.61	8.32	3.47%
10	10.2	9.67	5.44%
15	14.1	13.48	4.64%
20	18.1	17.72	2.12%
25	22.3	21.13	5.54%
30	26.7	25.79	3.53%
35	31.3	29.39	6.50%
40	35.9	30.74	16.78%

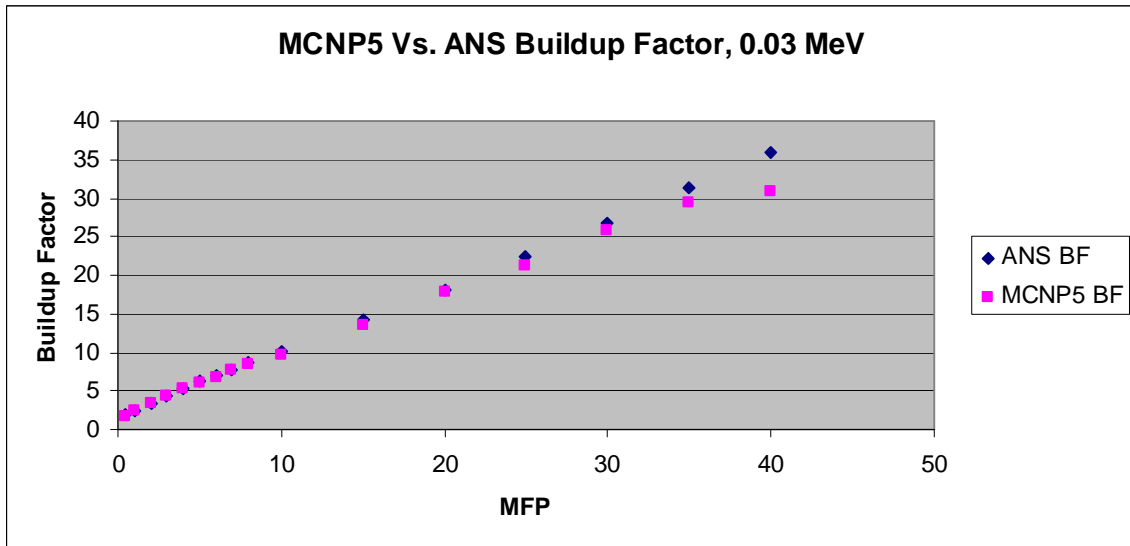


Figure 12c. MCNP5 vs. ANS Buildup Factor, 0.03 MeV

Table 10d. Buildup Factor, Water-0.04 MeV

MFP	ANS Standard	Calculated Buildup Factor	% Difference
0.5	2.27	2.21	2.71%
1	3.58	3.54	1.04%
2	6.41	6.34	1.09%
3	9.50	9.24	2.80%
4	12.80	12.51	2.32%
5	16.30	15.71	3.76%
6	19.90	19.10	4.19%
7	23.80	22.73	4.71%
8	27.80	26.79	3.76%
10	36.50	34.91	4.55%
15	61.60	58.37	5.53%
20	92.10	89.72	2.65%
25	128.00	124.83	2.54%
30	169.00	158.21	6.82%
35	216.00	208.17	3.76%
40	269.00	258.90	3.90%

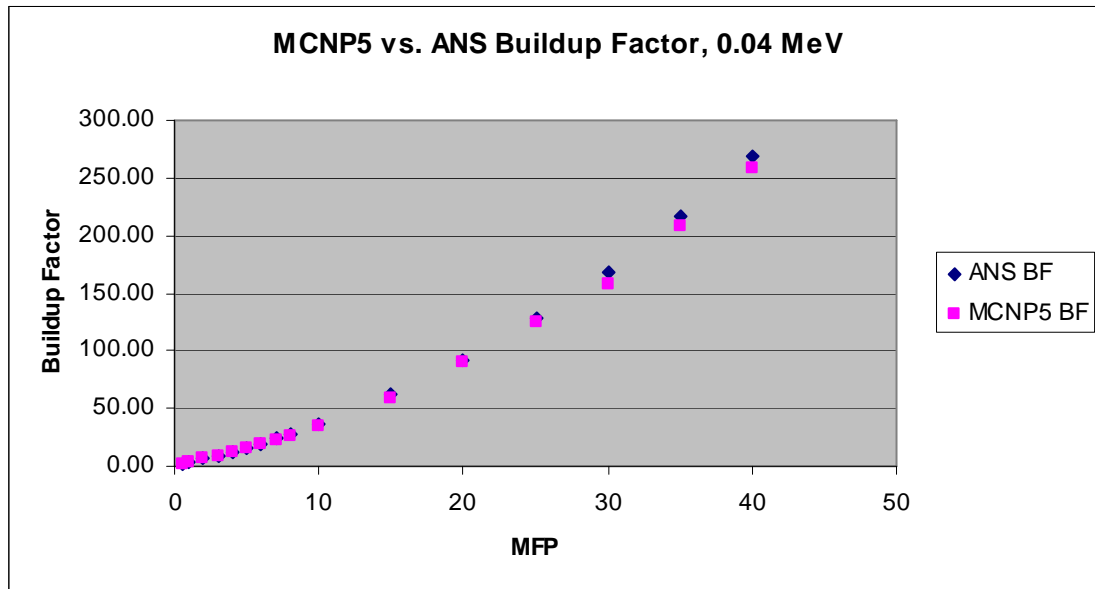


Figure 12d. MCNP5 vs. ANS Buildup Factor, 0.04 MeV

Table 10e. Buildup Factor, Water-0.05 MeV

MFP	ANS Standard	Calculated Buildup Factor	% Difference
0.5	2.55	2.45	4.08%
1	4.51	4.24	6.37%
2	9.49	8.97	5.80%
3	15.70	14.82	5.94%
4	23.20	21.92	5.84%
5	31.80	29.31	8.50%
6	41.60	38.49	8.08%
7	52.60	49.32	6.65%
8	64.90	60.13	7.93%
10	93.30	89.37	4.40%
15	190.00	182.35	4.20%
20	331.00	312.12	6.05%
25	525.00	502.43	4.49%
30	779.00	718.21	8.46%
35	1100.00	1011.73	8.72%
40	1510.00	1381.34	9.31%

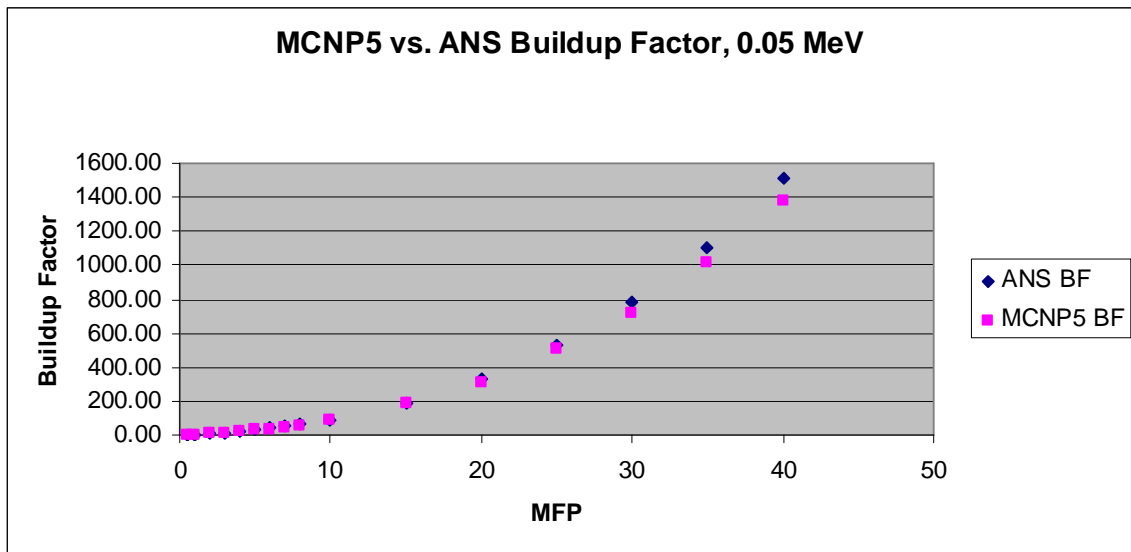


Figure 12e. MCNP5 vs. ANS Buildup Factor, 0.05 MeV

Table 10f. Buildup Factor, Water-0.06 MeV

MFP	ANS Standard	Calculated Buildup Factor	% Difference
0.5	2.63	2.59	1.39%
1	4.94	4.72	4.64%
2	1.50	1.38	8.70%
3	20.60	18.43	11.80%
4	32.40	30.23	7.20%
5	46.90	44.73	4.86%
6	64.30	62.13	3.50%
7	84.80	82.19	3.17%
8	109.00	104.28	4.53%
10	167.00	156.83	6.48%
15	390.00	365.71	6.64%
20	758.00	729.37	3.93%
25	1320.00	1283.46	2.85%
30	2140.00	1948.83	9.81%
35	3270.00	3042.13	7.49%
40	4820.00	4479.34	7.61%

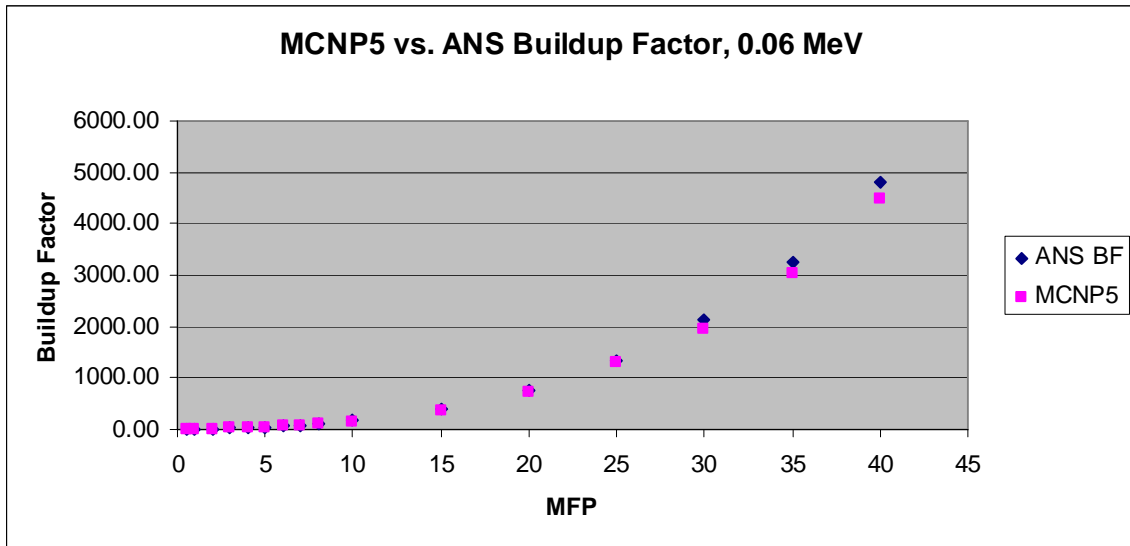


Figure 12f. MCNP5 vs. ANS Buildup Factor, 0.06 MeV

Table 10g. Buildup Factor, Water-0.08 MeV

MFP	ANS Standard	Calculated Buildup Factor	% Difference
0.5	2.54	2.49	1.89%
1	4.93	4.83	2.05%
2	12.50	11.73	6.56%
3	24.30	22.76	6.78%
4	40.80	38.42	6.19%
5	62.70	58.63	6.94%
6	90.60	84.21	7.59%
7	125.00	115.82	7.93%
8	167.00	156.32	6.83%
10	278.00	262.35	5.97%
15	754.00	716.28	5.27%
20	1650.00	1593.72	3.53%
25	3160.00	3071.73	2.87%
30	5560.00	5283.29	5.24%
35	9190.00	8783.47	4.63%
40	14500.00	13652.38	6.21%

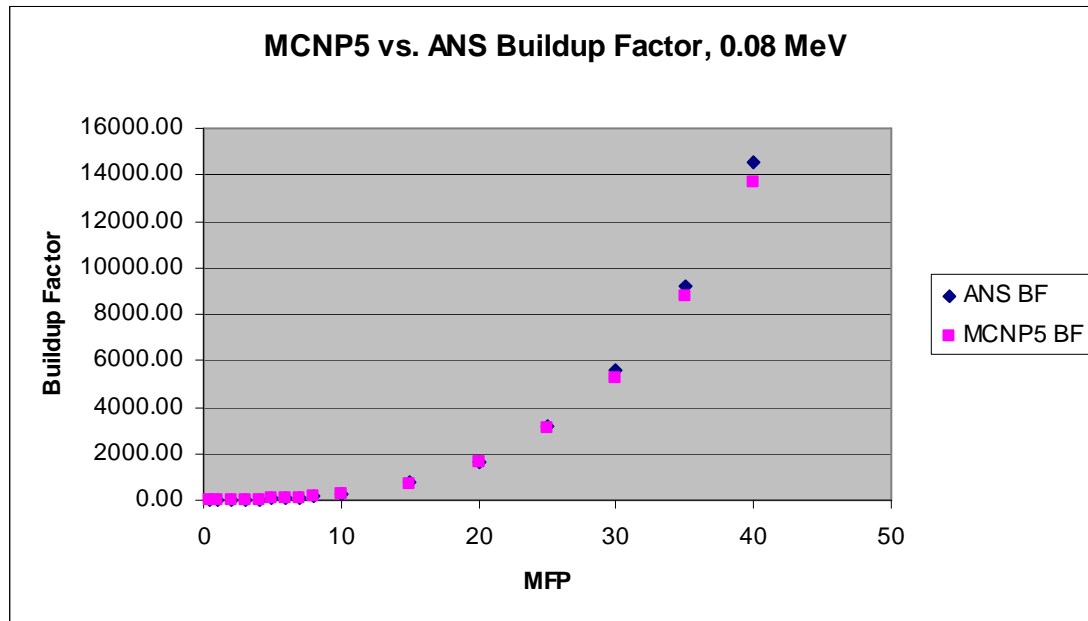


Figure 12g. MCNP5 vs. ANS Buildup Factor, 0.08 MeV

Table 10h. Buildup Factor, Water-0.10 MeV

MFP	ANS Standard	Calculated Buildup Factor	% Difference
0.5	2.36	2.34	0.89%
1	4.52	4.47	1.04%
2	11.70	11.02	5.80%
3	23.50	22.43	4.55%
4	40.60	38.76	4.53%
5	64.00	60.49	5.49%
6	94.80	89.15	5.97%
7	134.00	126.32	5.73%
8	183.00	176.23	3.70%
10	314.00	289.47	7.81%
15	917.00	892.17	2.71%
20	2120.00	2003.82	5.48%
25	4260.00	3975.25	6.68%
30	7780.00	7174.87	7.78%
35	13100.00	11993.81	8.44%
40	20300.00	18823.91	7.27%

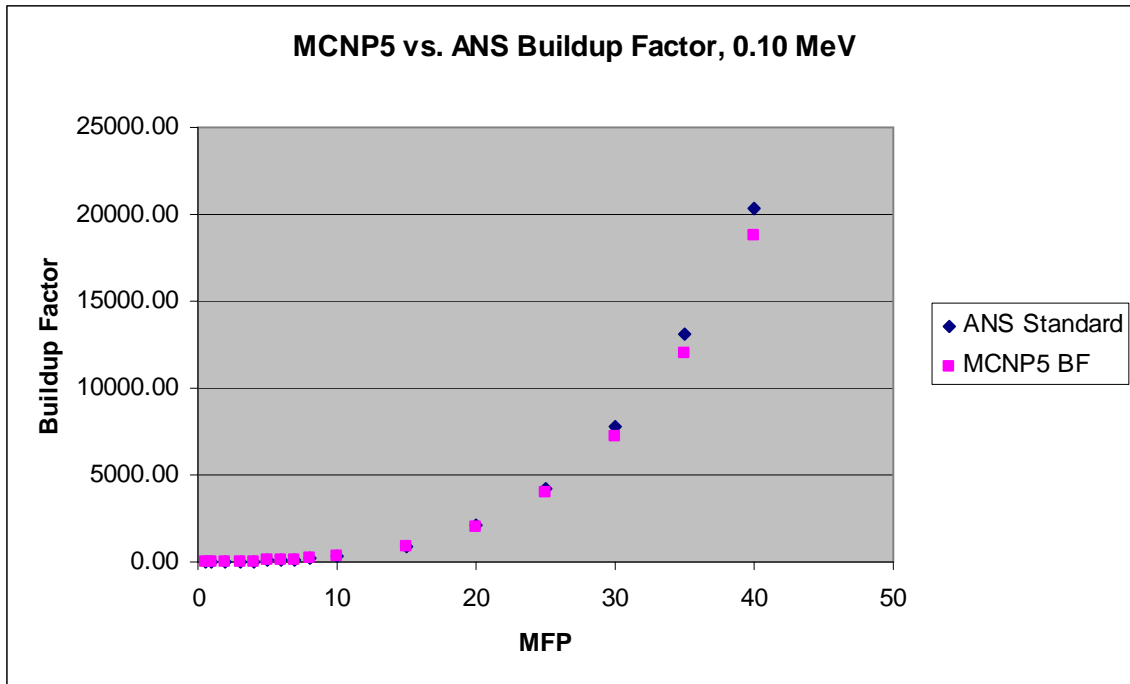


Figure 12h. MCNP5 vs. ANS Buildup Factor, 0.10 MeV



Table 10i. Buildup Factor, Water-0.15 MeV

MFP	ANS Standard	Calculated Buildup Factor	% Difference
0.5	2.07	2.12	2.24%
1	3.91	3.72	5.24%
2	9.36	9.78	4.28%
3	18.60	18.73	0.69%
4	32.50	32.32	0.56%
5	52.00	51.54	0.89%
6	77.90	77.45	0.58%
7	111.00	110.05	0.86%
8	153.00	150.87	1.41%
10	268.00	258.92	3.50%
15	805.00	745.52	7.98%
20	1890.00	1762.36	7.24%
25	3840.00	3654.91	5.06%
30	7050.00	6954.18	1.38%
35	12100.00	11889.41	1.77%
40	19600.00	18887.21	3.77%

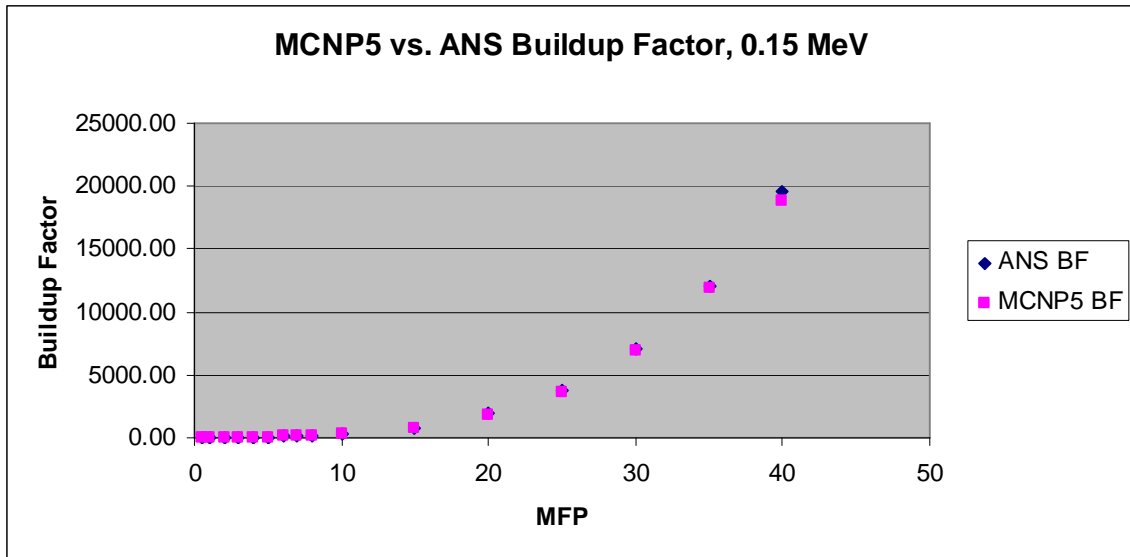


Figure 12i. MCNP5 vs. ANS Buildup Factor, 0.15 MeV

Table 10j. Buildup Factor, Water-0.2 MeV

MFP	ANS Standard	Calculated Buildup Factor	% Difference
0.5	1.92	1.96	2.05%
1	3.42	3.35	2.13%
2	8.22	7.91	3.90%
3	15.70	15.06	4.28%
4	26.40	25.25	4.56%
5	41.30	39.42	4.78%
6	61.00	58.31	4.61%
7	86.20	79.62	8.27%
8	118.00	110.10	7.18%
10	202.00	192.39	5.00%
15	582.00	569.26	2.24%
20	1310.00	1265.67	3.50%
25	2580.00	2468.31	4.52%
30	4640.00	4482.17	3.52%
35	7890.00	7562.18	4.33%
40	12800.00	11824.56	8.25%

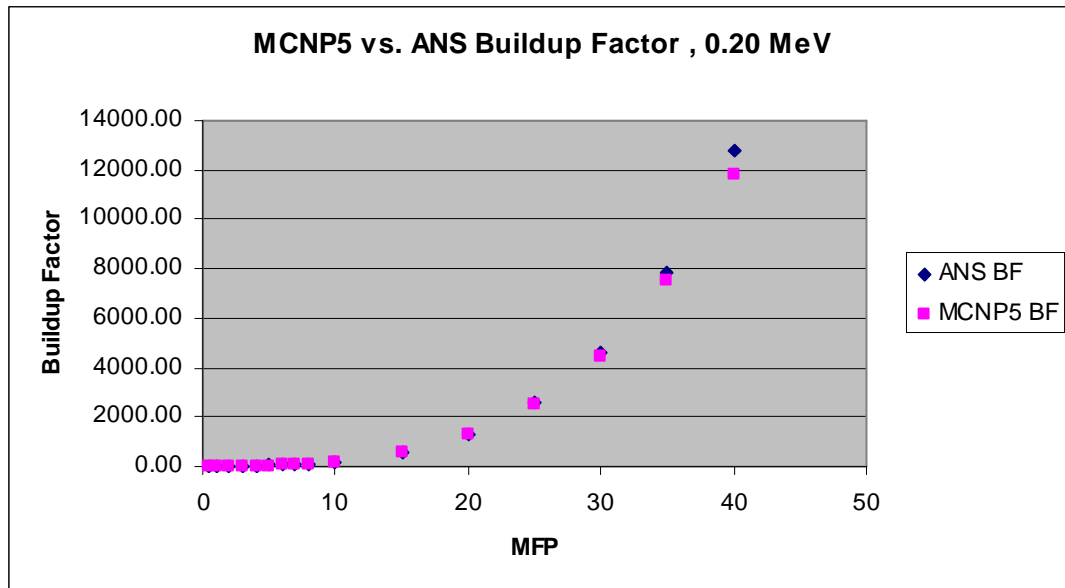


Figure 12j. MCNP5 vs. ANS Buildup Factor, 0.20 MeV

Table 10k. Buildup Factor, Water-0.30 MeV

MFP	ANS Standard	Calculated Buildup Factor	% Difference
0.5	1.75	1.69	3.31%
1	2.84	2.74	3.53%
2	6.25	5.86	6.58%
3	11.50	10.55	9.00%
4	19.00	18.05	5.26%
5	28.80	27.85	3.41%
6	41.20	40.25	2.36%
7	56.50	53.82	4.97%
8	75.00	71.92	4.28%
10	122.00	117.26	4.04%
15	318.00	308.26	3.16%
20	656.00	633.29	3.59%
25	1180.00	1134.42	4.02%
30	1930.00	1869.38	3.24%
35	2950.00	2823.42	4.48%
40	4280.00	4014.23	6.62%

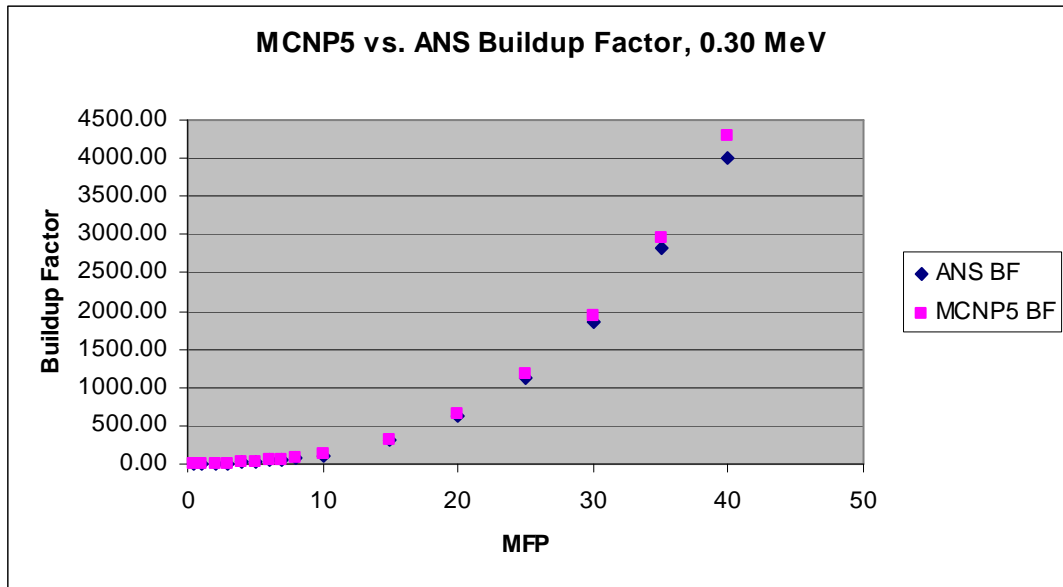


Figure 12k. MCNP5 vs. ANS Buildup Factor, 0.30 MeV

Table 10l. Buildup Factor, Water-0.40 MeV

MFP	ANS Standard	Calculated Buildup Factor	% Difference
0.5	1.66	1.62	2.41%
1	2.60	2.57	1.15%
2	5.42	5.35	1.27%
3	9.56	9.24	3.38%
4	15.10	14.29	5.36%
5	22.20	21.35	3.81%
6	30.80	29.34	4.74%
7	41.10	38.94	5.25%
8	53.20	52.01	2.24%
10	83.20	78.43	5.73%
15	197.00	189.24	3.94%
20	377.00	367.31	2.57%
25	632.00	612.42	3.10%
30	972.00	889.13	8.53%
35	1400.00	1294.21	7.56%
40	1940.00	1792.10	7.62%

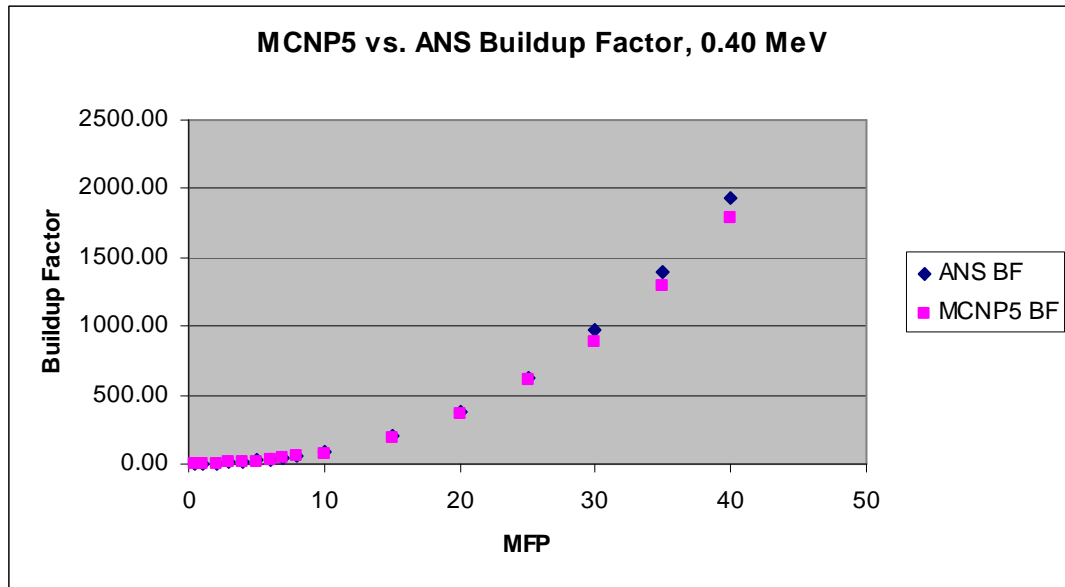


Figure 12l. MCNP5 vs. ANS Buildup Factor, 0.40 MeV

Table 10m. Buildup Factor, Water-0.50 MeV

MFP	ANS Standard	Calculated Buildup Factor	% Difference
0.5	1.61	1.66	3.30%
1	2.45	2.57	4.77%
2	4.87	5.06	3.79%
3	8.29	8.62	3.80%
4	12.70	13.18	3.64%
5	18.10	19.00	4.74%
6	24.60	25.39	3.10%
7	32.20	33.32	3.35%
8	40.80	41.51	1.72%
10	61.80	61.88	0.13%
15	137.00	136.59	0.30%
20	247.00	244.57	0.99%
25	395.00	383.86	2.90%
30	582.00	554.83	4.90%
35	809.00	820.13	1.36%
40	1080.00	1003.10	7.67%

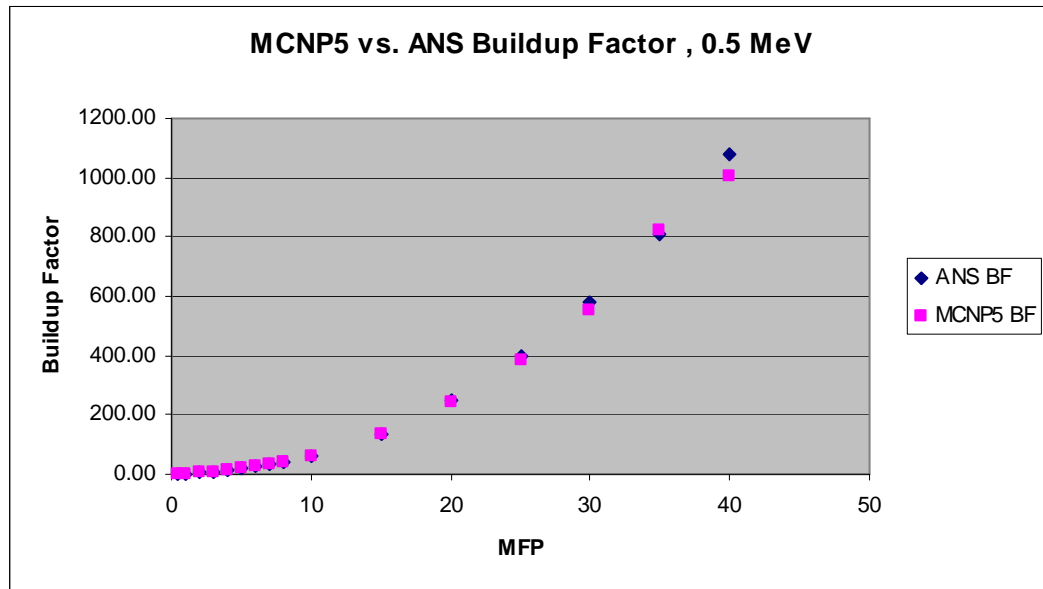


Figure 12m. MCNP5 vs. ANS Buildup Factor, 0.50 MeV

Table 10n. Buildup Factor, Water-0.60 MeV

MFP	ANS Standard	Calculated Buildup Factor	% Difference
0.5	1.71	1.58	8.23%
1	2.50	2.35	6.38%
2	4.27	4.02	6.22%
3	6.30	5.89	6.94%
4	8.65	8.02	7.86%
5	11.30	10.58	6.85%
6	14.30	13.83	3.42%
7	17.70	17.01	4.04%
8	21.30	20.87	2.06%
10	29.40	28.72	2.37%
15	55.00	52.87	4.03%
20	87.40	82.71	5.67%
25	127.00	121.81	4.26%
30	172.00	163.42	5.25%
35	223.00	212.61	4.89%
40	280.00	256.34	9.23%

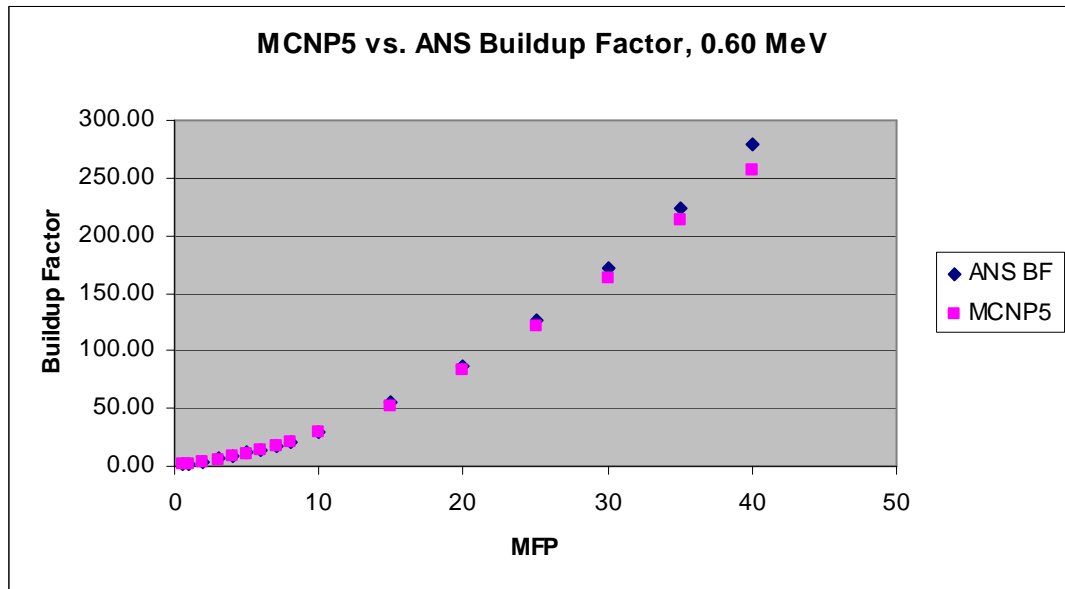


Figure 12n. MCNP5 vs. ANS Buildup Factor, 0.60 MeV

Table 10o. Buildup Factor, Water-0.80 MeV

MFP	ANS Standard	Calculated Buildup Factor	% Difference
0.5	1.51	1.56	3.21%
1	2.18	2.24	2.68%
2	3.96	3.75	5.69%
3	6.24	5.94	5.02%
4	8.96	8.64	3.68%
5	12.10	11.59	4.40%
6	15.60	14.82	5.24%
7	19.60	18.84	4.02%
8	24.00	22.89	4.84%
10	33.90	31.97	6.03%
15	65.60	61.87	6.03%
20	106.00	102.41	3.51%
25	156.00	161.62	3.48%
30	213.00	198.42	7.35%
35	277.00	259.34	6.81%
40	349.00	327.26	6.64%

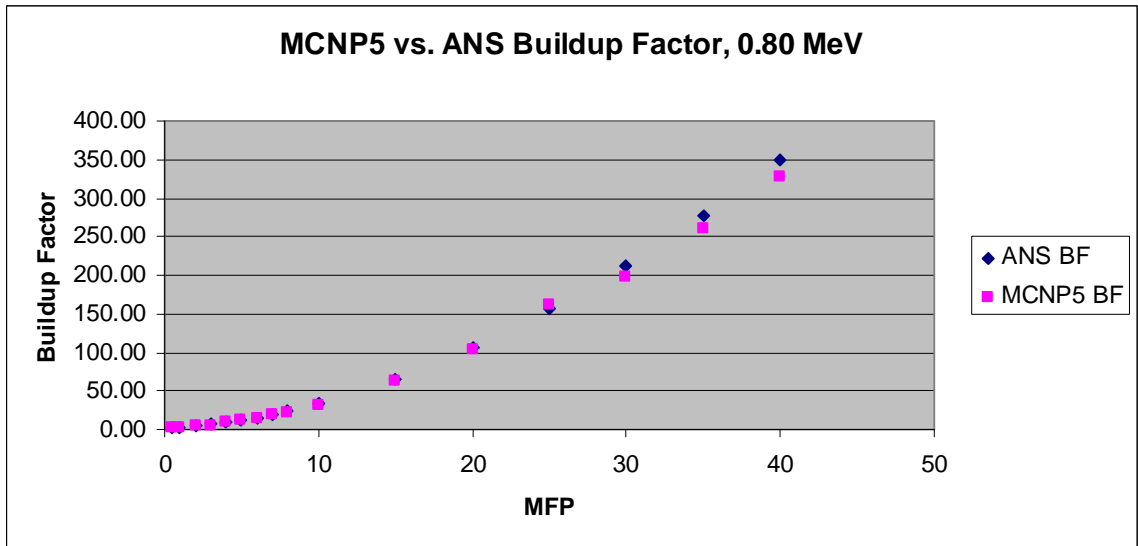


Figure 12o. MCNP5 vs. ANS Buildup Factor, 0.80 MeV

Table 10p. Buildup Factor, Water-1.00 MeV

MFP	ANS Standard	Calculated Buildup Factor	% Difference
0.5	1.47	1.61	8.58%
1	2.08	2.18	4.73%
2	3.62	3.83	5.57%
3	5.5	5.78	4.87%
4	7.66	8.12	5.64%
5	10.1	10.72	5.81%
6	12.8	13.38	4.31%
7	15.7	16.61	5.46%
8	18.9	19.66	3.88%
10	26	26.96	3.55%
15	47.4	48.66	2.60%
20	73.5	80.69	8.91%
25	104	107.59	3.33%
30	138	139.63	1.17%
35	175	176.84	1.04%
40	214	196.47	8.92%

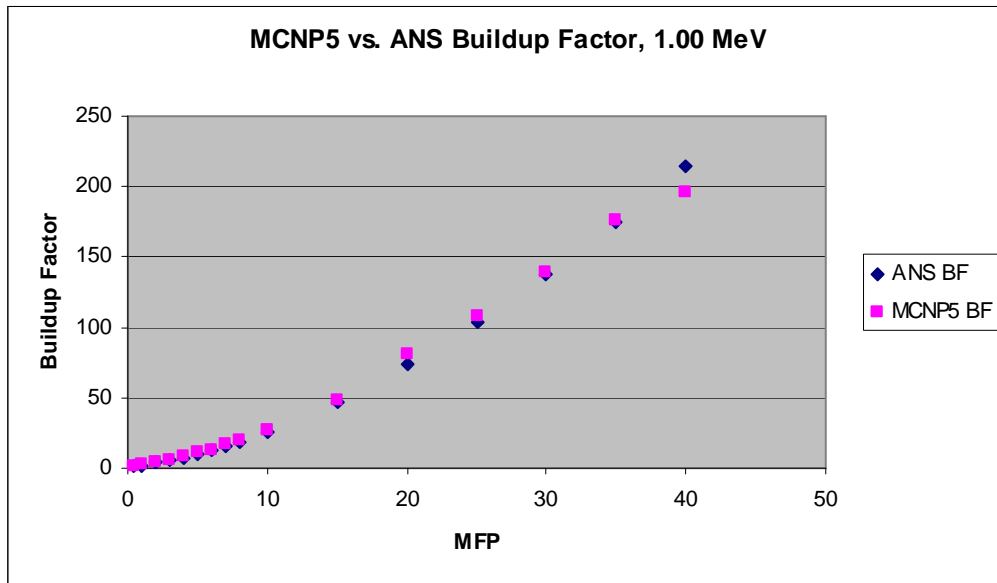


Figure 12p. MCNP5 vs. ANS Buildup Factor, 1.00 MeV



Table 10q. Buildup Factor, Water-1.50 MeV

MFP	ANS Standard	Calculated Buildup Factor	% Difference
0.5	1.42	1.49	4.74%
1	1.93	2.01	3.83%
2	3.11	3.12	0.28%
3	4.44	4.35	2.15%
4	5.9	5.70	3.50%
5	7.47	7.15	4.47%
6	9.14	8.69	5.17%
7	10.9	10.37	5.12%
8	12.8	12.04	6.35%
10	16.8	15.68	7.17%
15	27.9	25.91	7.70%
20	40.4	37.96	6.43%
25	54.1	50.17	7.84%
30	68.8	63.22	8.83%
35	84.4	76.95	9.67%
40	101	87.44	15.51%

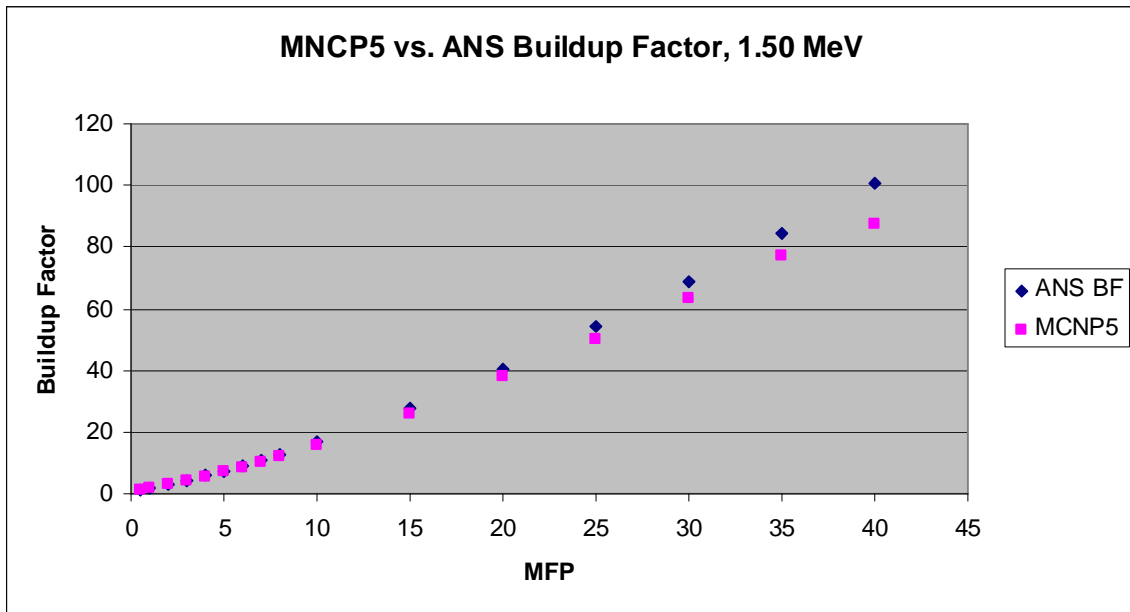


Figure 12q. MCNP5 vs. ANS Buildup Factor, 1.50 MeV

Table 10r. Buildup Factor, Water-2.00 MeV

MFP	ANS Standard	Calculated Buildup Factor	% Difference
0.5	1.38	1.45	4.55%
1	1.83	1.90	3.83%
2	2.82	2.86	1.24%
3	3.87	3.88	0.19%
4	4.99	4.98	0.20%
5	6.16	6.16	0.06%
6	7.38	7.41	0.34%
7	8.66	8.70	0.47%
8	9.97	10.07	0.98%
10	12.7	12.97	2.05%
15	20.1	20.91	3.85%
20	28	29.80	6.03%
25	36.4	39.31	7.40%
30	45.2	49.90	9.42%
35	54.3	60.23	9.85%
40	63.6	68.10	6.61%

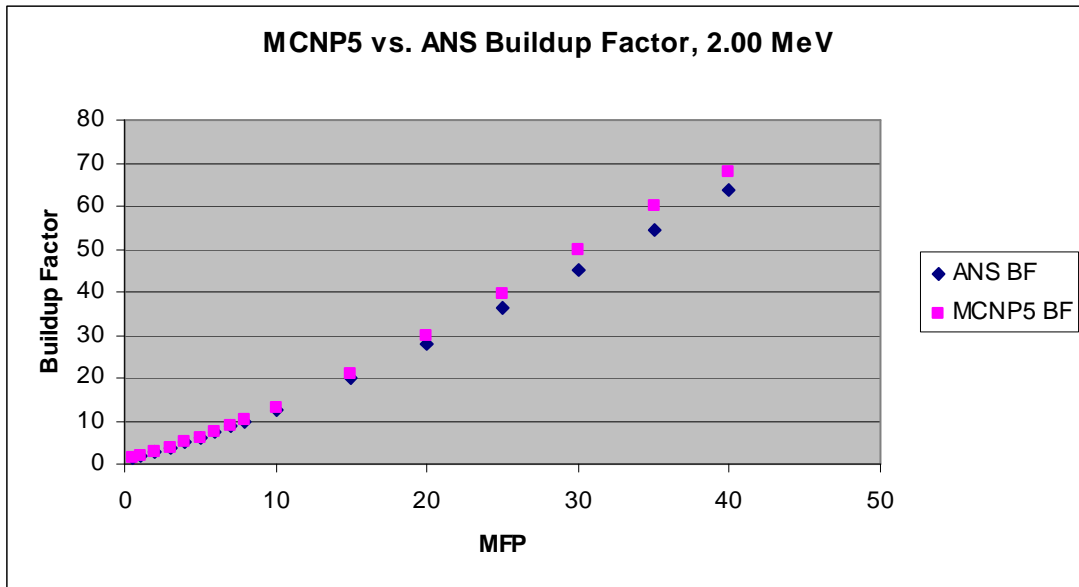


Figure 12r. MCNP5 vs. ANS Buildup Factor, 2.00 MeV

Table 10s. Buildup Factor, Water-3.00 MeV

MFP	ANS Standard	Calculated Buildup Factor	% Difference
0.5	1.34	1.37	2.19%
1	1.71	1.72	0.58%
2	2.47	2.43	1.65%
3	3.24	3.12	3.78%
4	4.01	3.90	2.82%
5	4.81	4.69	2.56%
6	5.62	5.55	1.26%
7	6.45	6.47	0.31%
8	7.28	7.45	2.28%
10	8.98	9.35	3.96%
15	13.4	13.64	1.76%
20	17.8	18.13	1.82%
25	22.4	23.19	3.41%
30	27.1	27.79	2.48%
35	31.8	33.42	4.85%
40	36.5	40.03	8.82%

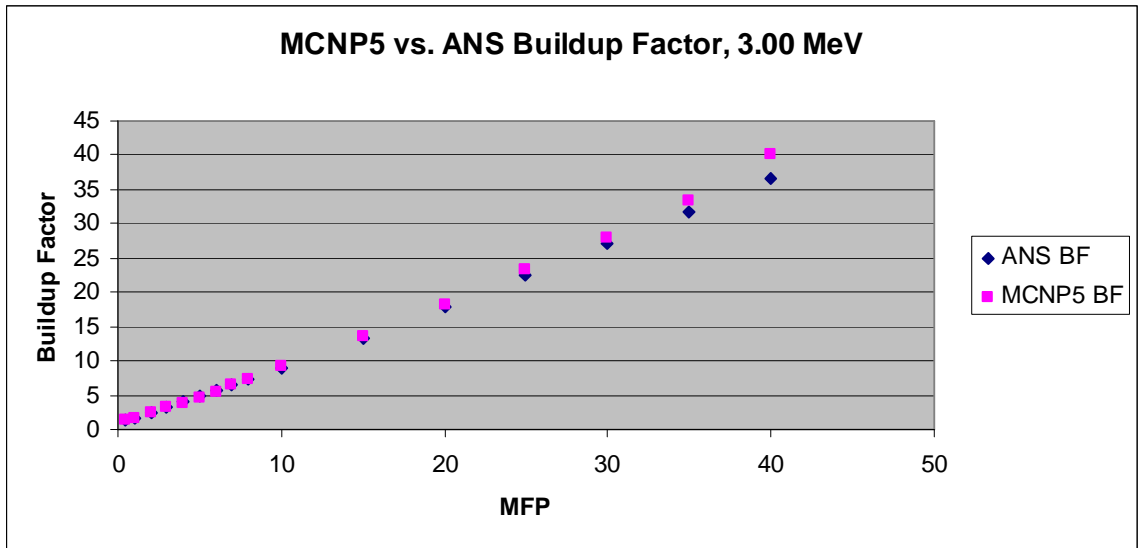


Figure 12s. MCNP5 vs. ANS Buildup Factor, 3.00 MeV

Table 10t. Buildup Factor, Water-4.00 MeV

MFP	ANS Standard	Calculated Buildup Factor	% Difference
0.5	1.31	1.33	1.84%
1	1.63	1.62	0.41%
2	2.26	2.14	5.43%
3	2.87	2.71	5.81%
4	3.48	3.32	4.69%
5	4.09	3.93	4.02%
6	4.71	4.59	2.59%
7	5.33	5.29	0.83%
8	5.95	6.13	3.00%
10	7.2	6.93	3.87%
15	10.3	10.64	3.22%
20	13.5	13.94	3.18%
25	16.6	17.63	5.84%
30	19.8	21.03	5.85%
35	23	24.37	5.62%
40	26.1	27.89	6.42%

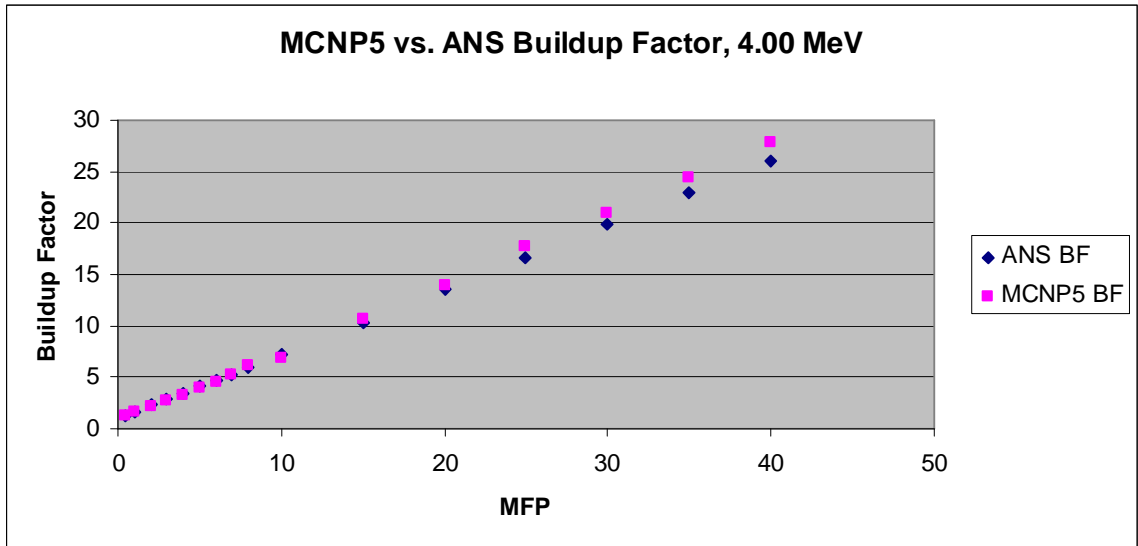


Figure 12t. MCNP5 vs. ANS Buildup Factor, 4.00 MeV

Table 10u. Buildup Factor, Water-5.00 MeV

MFP	ANS Standard	Calculated Buildup Factor	% Difference
0.5	1.29	1.35	4.39%
1	1.57	1.69	7.32%
2	2.1	2.27	7.43%
3	2.62	2.85	7.92%
4	3.12	3.31	5.87%
5	3.63	3.87	6.29%
6	4.14	4.45	6.96%
7	4.64	4.99	7.07%
8	5.14	5.55	7.46%
10	6.14	6.69	8.19%
15	8.62	9.38	8.10%
20	11.1	12.01	7.55%
25	13.5	14.87	9.19%
30	15.9	17.24	7.76%
35	18.3	20.32	9.93%
40	20.7	21.51	3.76%

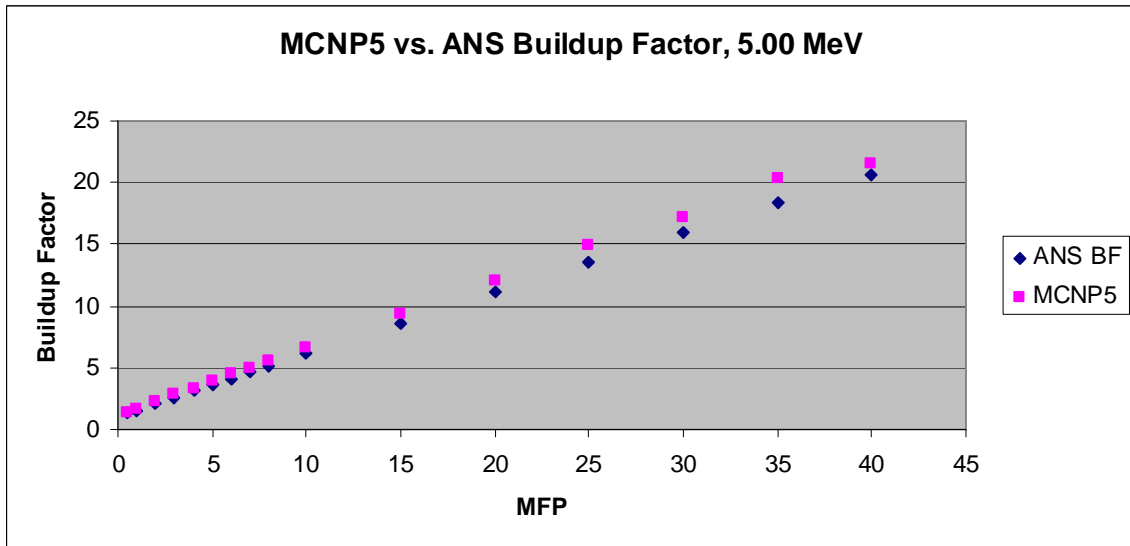


Figure 12u. MCNP5 vs. ANS Buildup Factor, 5.00 MeV

Table 10v. Buildup Factor, Water-6.00 MeV

MFP	ANS Standard	Calculated Buildup Factor	% Difference
0.5	1.27	1.24	2.17%
1	1.55	1.46	5.87%
2	1.98	1.82	8.73%
3	2.43	2.21	9.86%
4	2.87	2.61	9.86%
5	3.31	3.05	8.67%
6	3.74	3.51	6.49%
7	4.16	3.98	4.44%
8	4.59	4.51	1.77%
10	5.43	5.63	3.59%
15	7.49	7.80	3.95%
20	9.52	9.92	4.04%
25	11.5	11.68	1.56%
30	13.5	14.18	4.80%
35	15.5	16.27	4.74%
40	17.9	19.78	9.51%

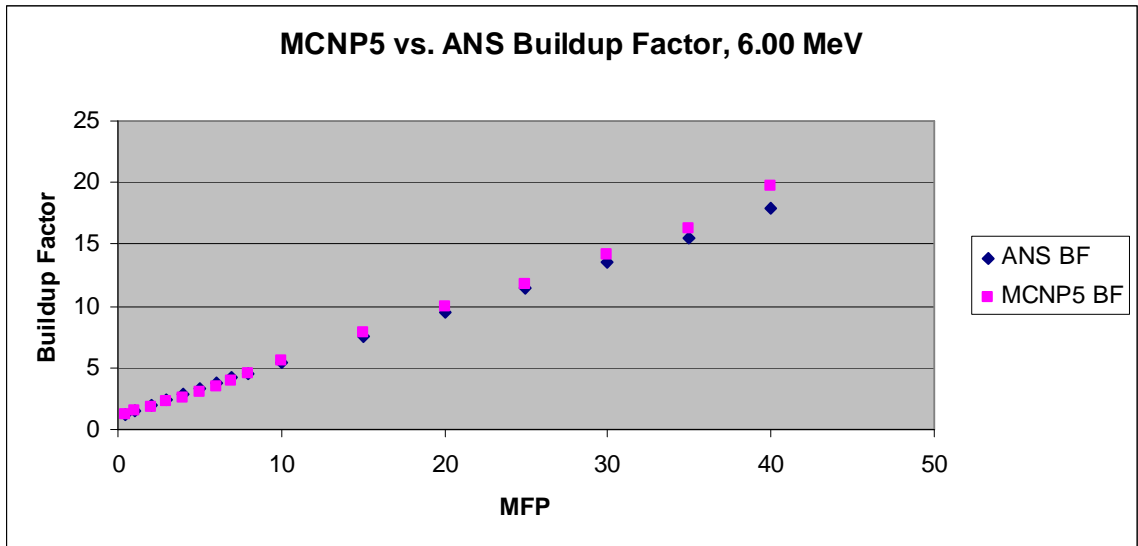


Figure 12v. MCNP5 vs. ANS Buildup Factor, 6.00 MeV

Table 10w. Buildup Factor, Water-8.00 MeV

MFP	ANS Standard	Calculated Buildup Factor	% Difference
0.5	1.23	1.25	1.60%
1	1.44	1.46	1.37%
2	1.82	1.84	1.09%
3	2.17	2.19	0.91%
4	2.52	2.20	14.39%
5	2.86	2.54	12.79%
6	3.2	3.24	1.23%
7	3.53	3.57	1.12%
8	3.86	3.69	4.69%
10	4.51	4.62	2.44%
15	6.08	6.46	5.88%
20	7.61	7.92	3.93%
25	9.1	9.80	7.14%
30	10.6	11.40	7.02%
35	12.2	13.03	6.37%
40	14.1	15.14	6.87%

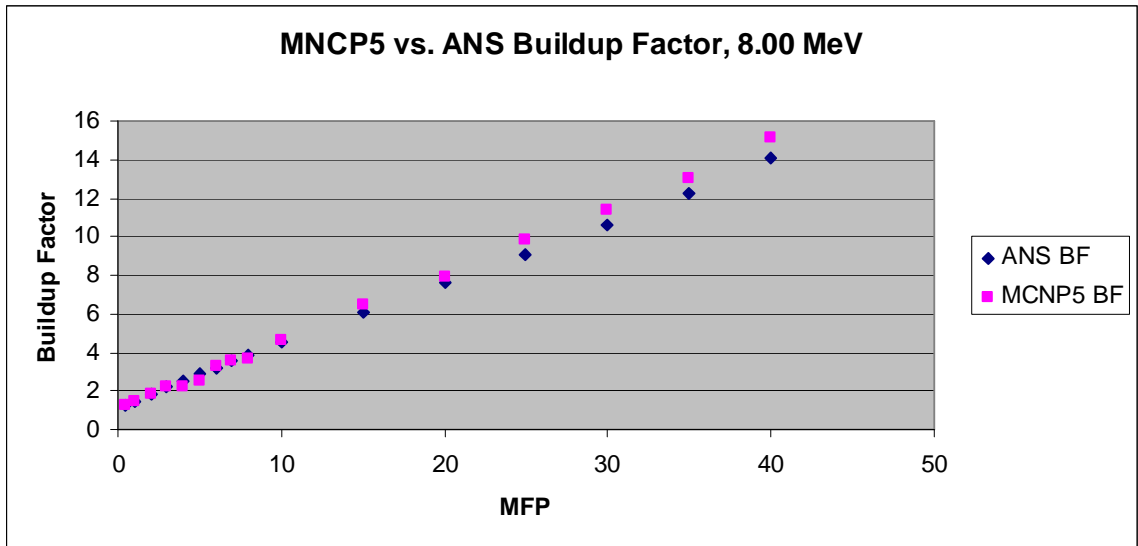


Figure 12w. MCNP5 vs. ANS Buildup Factor, 8.00 MeV

Table 10x. Buildup Factor, Water-10.0 MeV

MFP	ANS Standard	Calculated Buildup Factor	% Difference
0.5	1.21	1.23	1.76%
1	1.38	1.44	4.30%
2	1.7	1.80	5.36%
3	2	2.14	6.40%
4	2.29	2.34	2.35%
5	2.57	2.67	3.60%
6	2.85	2.98	4.46%
7	3.13	3.29	4.75%
8	3.4	3.62	6.10%
10	3.94	4.20	6.23%
15	5.24	5.64	7.14%
20	6.51	7.03	7.37%
25	7.75	8.19	5.42%
30	8.97	9.75	7.98%
35	10.2	11.03	7.49%
40	11.3	12.34	8.44%

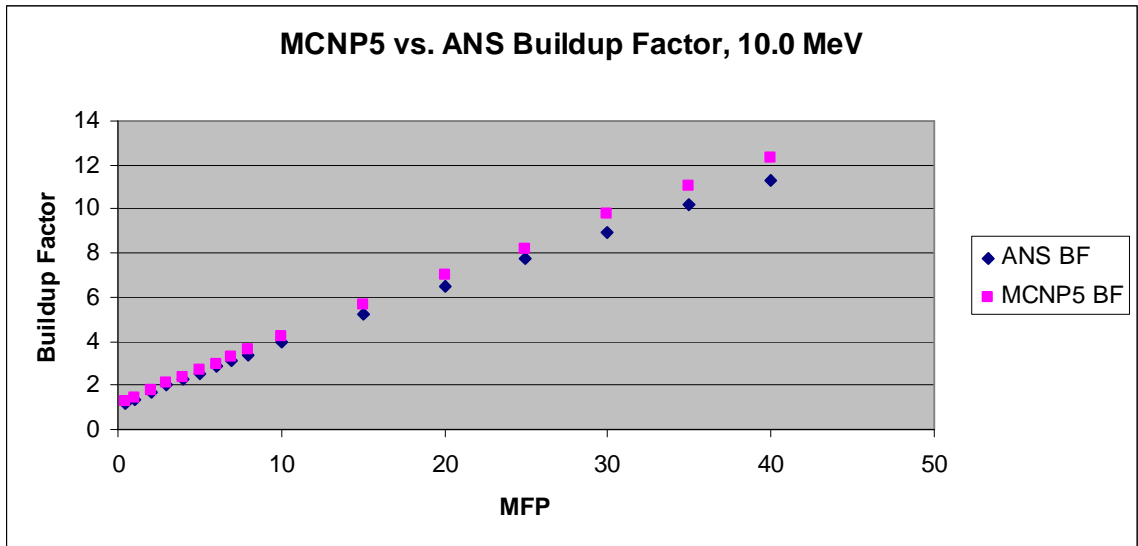


Figure 12x. MCNP5 vs. ANS Buildup Factor, 10.0 MeV



Table 10y. Buildup Factor, Water-15.0 MeV

MFP	ANS Standard	Calculated Buildup Factor	% Difference
0.5	1.16	1.15	0.94%
1	1.29	1.32	2.52%
2	1.51	1.53	1.06%
3	1.72	1.79	4.13%
4	1.93	2.06	6.20%
5	2.14	2.22	3.65%
6	2.34	2.48	5.83%
7	2.53	2.72	7.03%
8	2.73	2.98	8.38%
10	3.11	3.27	4.75%
15	4.04	4.17	3.16%
20	4.93	5.04	2.22%
25	5.81	5.95	2.39%
30	6.64	6.79	2.24%
35	7.42	7.82	5.13%
40	8.09	8.88	8.92%

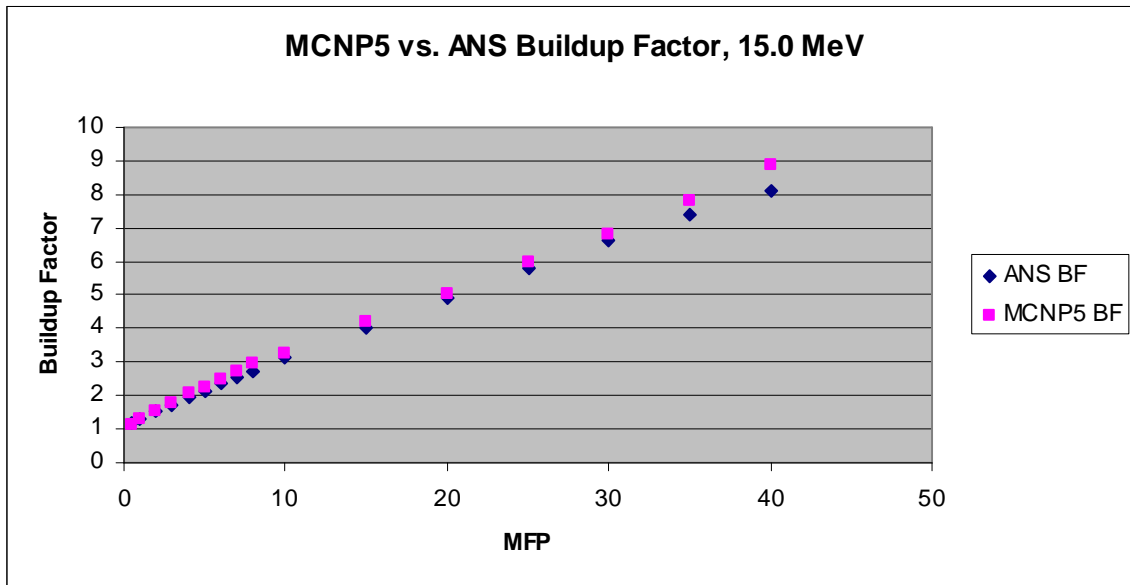


Figure 12y. MCNP5 vs. ANS Buildup Factor, 15.0 MeV

APPENDIX VIII

COMPARISON OF CALCULATED BUILDUP FACTORS

Table 11a. Buildup Factor Comparison w/ no Coherent Scattering, Iron- 0.015 MeV

No Coherent Scattering Iron-0.015 MeV						
MFP	ANS Standard	ASFIT BF	Calculated BF	% Diff of ASFIT & MCNP5	% Diff of ASFIT & ANS	% Diff of MCNP5 & ANS
0.5	1	1.000	1.05	4.76%	0.00%	4.76%
1	1	1.000	1.05	5.05%	0.00%	5.05%
2	1.01	1.001	1.06	5.85%	0.90%	5.01%
3	1.01	1.003	1.06	5.77%	0.70%	5.12%
4	1.01	1.003	1.07	5.86%	0.68%	5.23%
5	1.01	1.004	1.07	5.90%	0.60%	5.34%
6	1.01	1.005	1.07	5.91%	0.50%	5.44%
7	1.01	1.006	1.08	7.09%	0.40%	6.72%
8	1.01	1.005	1.08	7.29%	0.50%	6.83%
10	1.01	1.007	1.09	7.21%	0.30%	6.94%
15	1.01	0.989	1.09	8.97%	2.12%	7.04%
20	1.01	0.986	1.09	9.35%	2.43%	7.15%
25	1.01	0.981	1.10	10.90%	2.94%	8.28%
30	1.01	0.980	1.10	11.11%	3.06%	8.38%
35	1.01	0.980	1.10	11.20%	3.06%	8.49%
40	1.01	0.992	1.10	10.22%	1.81%	8.59%

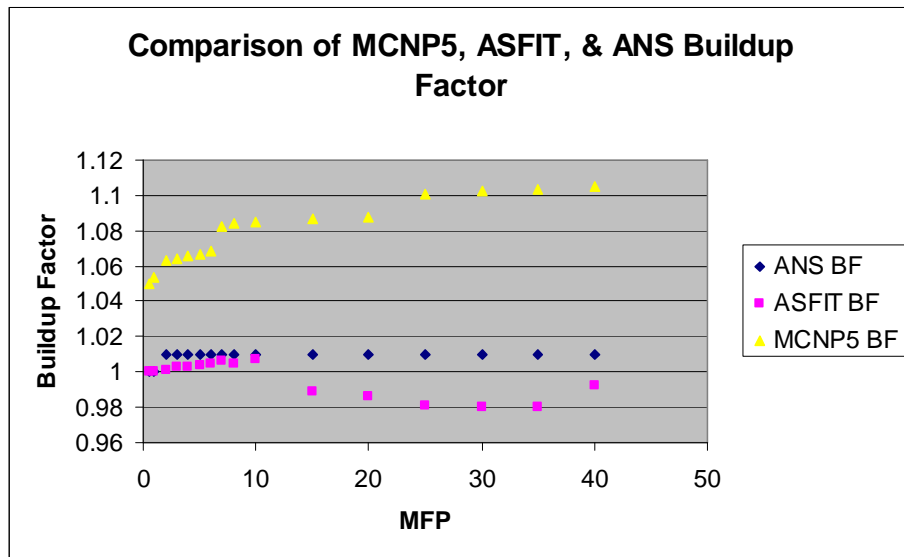


Figure 13a. Buildup Factor Comparison w/ no Coherent Scattering, Iron- 0.015 MeV

Table 11b. Buildup Factor Comparison w/ no Coherent Scattering, Iron- 0.15 MeV

No Coherent Scattering Iron-0.15 MeV						
MFP	ANS Standard	ASFIT BF	Calculated BF	% Diff of ASFIT & MCNP5	% Diff of ASFIT & ANS	% Diff of MCNP5 & ANS
0.5	1.93	1.89	1.86	1.41%	2.06%	3.51%
1	2.46	2.51	2.37	6.05%	1.99%	3.94%
2	3.22	3.18	3.11	2.10%	1.32%	3.45%
3	3.93	3.87	3.74	3.62%	1.47%	5.14%
4	4.60	4.48	4.32	3.84%	2.63%	6.58%
5	5.23	5.08	4.84	4.96%	3.05%	8.16%
6	5.84	5.69	5.31	7.18%	2.60%	9.96%
7	6.42	6.36	6.04	5.31%	0.88%	6.24%
8	6.98	7.02	6.58	6.67%	0.57%	6.06%
10	8.07	8.16	7.69	6.19%	1.14%	4.98%
15	10.60	11.27	10.13	11.23%	5.94%	4.62%
20	12.90	13.53	12.25	10.44%	4.66%	5.30%
25	15.00	15.64	14.69	6.49%	4.11%	2.12%
30	16.90	17.08	16.34	4.52%	1.05%	3.41%
35	19.40	20.09	18.15	10.72%	3.44%	6.92%
40	21.70	22.43	20.97	6.98%	3.25%	3.50%

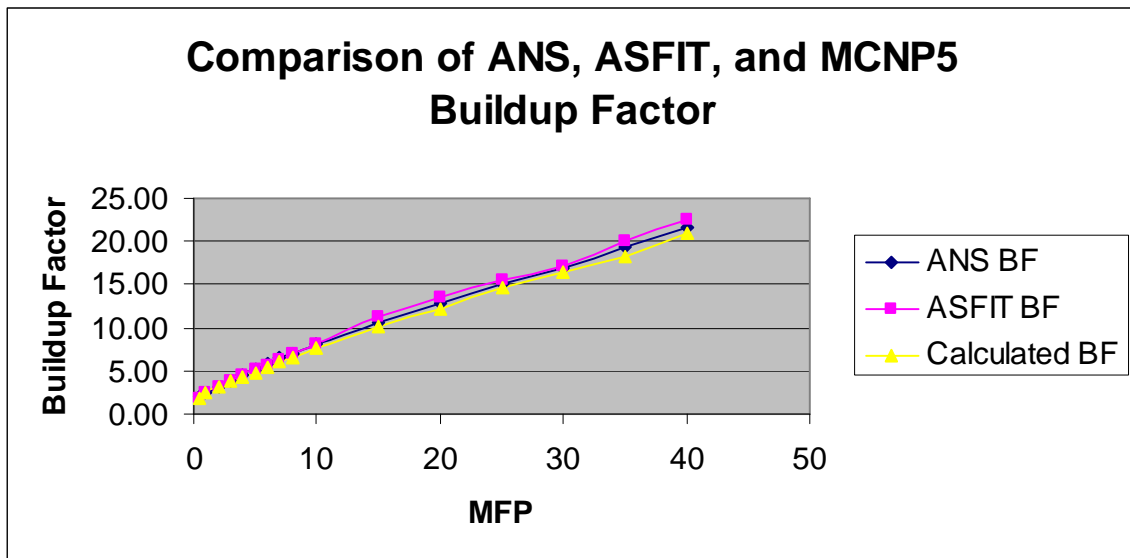


Figure 13b. Buildup Factor Comparison w/ no Coherent Scattering, Iron- 0.15 MeV

Table 11c. Buildup Factor Comparison w/ no Coherent Scattering, Iron- 1.5 MeV

No Coherent Scattering Iron-1.5 MeV						
MFP	ANS Standard	ASFIT BF	Calculated BF	% Diff of ASFIT & MCNP5	% Diff of ASFIT & ANS	% Diff of MCNP5 & ANS
0.50	1.45	1.44	1.49	3.51%	0.69%	2.72%
1.00	1.95	1.90	2.01	5.56%	2.58%	2.83%
2.00	3.03	2.97	3.12	4.90%	1.92%	2.85%
3.00	4.23	4.20	4.35	3.47%	0.69%	2.69%
4.00	5.54	5.58	5.70	2.11%	0.77%	2.82%
5.00	6.95	7.06	7.15	1.23%	1.60%	2.80%
6.00	8.47	8.56	8.69	1.53%	1.05%	2.54%
7.00	10.1	10.31	10.37	0.58%	2.04%	2.60%
8.00	11.8	12.09	12.04	0.45%	2.40%	1.96%
10.00	15.3	15.38	15.68	1.92%	0.52%	2.40%
15.00	25.4	27.12	25.91	4.48%	6.34%	1.95%
20.00	36.8	38.87	37.96	2.35%	5.33%	3.05%
25.00	49.2	51.93	50.17	3.40%	5.26%	1.93%
30.00	62.6	65.83	63.22	3.97%	4.91%	0.97%
35.00	76.8	79.65	76.95	3.38%	3.58%	0.20%
40.00	91.6	94.67	87.44	7.64%	3.24%	4.76%

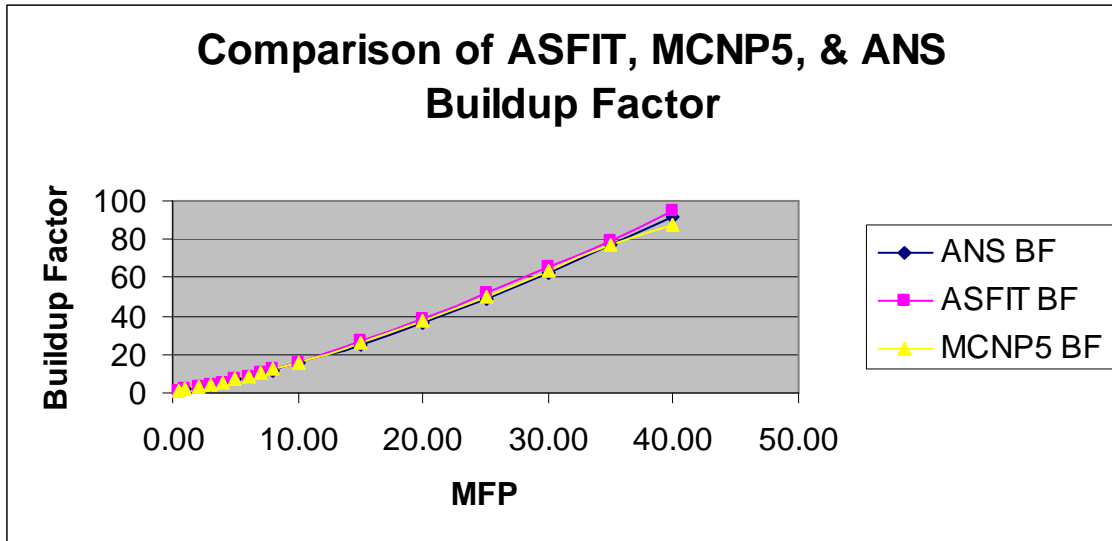


Figure 13c. Buildup Factor Comparison w/ no Coherent Scattering, Iron- 1.5 MeV

Table 11d. Buildup Factor Comparison w/ no Coherent Scattering, Iron- 15.0 MeV

Buildup Factor Comparison Iron-15.0 MeV						
MFP	ANS Standard	ASFIT BF	Calculated BF	% Diff of ASFIT & MCNP5	% Diff of ASFIT & ANS	% Diff of MCNP5 & ANS
0.50	1.1	1.07	1.12	4.73%	3.09%	1.79%
1.00	1.18	1.19	1.21	1.65%	0.84%	2.48%
2.00	1.31	1.33	1.34	0.37%	1.50%	1.87%
3.00	1.44	1.51	1.49	1.41%	4.64%	3.29%
4.00	1.59	1.62	1.64	1.22%	1.85%	3.05%
5.00	1.76	1.79	1.80	0.44%	1.68%	2.11%
6.00	1.96	2.03	2.02	0.35%	3.45%	3.11%
7.00	2.17	2.21	2.23	1.07%	1.81%	2.86%
8.00	2.42	2.45	2.51	2.32%	1.39%	3.67%
10.00	2.99	3.02	3.13	3.61%	1.03%	4.59%
15.00	5.06	5.11	5.13	0.25%	1.02%	1.27%
20.00	8.44	8.49	8.15	4.17%	0.59%	3.56%
25.00	13.8	14.12	13.23	6.73%	2.27%	4.31%
30.00	22.2	21.74	21.24	2.34%	2.12%	4.51%
35.00	35	34.08	34.36	0.81%	2.70%	1.86%
40.00	54.1	55.61	51.24	8.52%	2.72%	5.58%

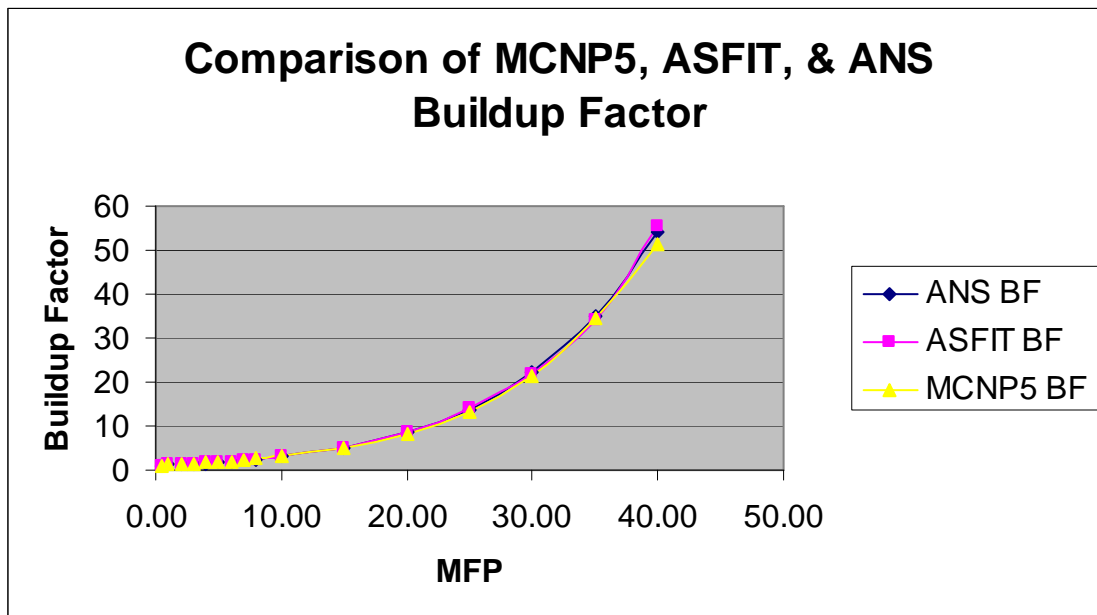


Figure 13d. Buildup Factor Comparison w/ no Coherent Scattering, Iron- 15.0 MeV

Table 11e Buildup Factor Comparison w/ no Coherent Scattering, Water- 0.015 MeV

Buildup Factor Comparison H <sub>2</sub> O-0.0150 MeV						
MFP	ANS Standard	ASFIT BF	MCNP5 BF	% Diff of ASFIT & MCNP5	% Diff of ASFIT & ANS	% Diff of MCNP5 & ANS
0.50	1.13	1.11	1.13	1.74%	2.17%	0.39%
1.00	1.19	1.20	1.18	1.23%	0.50%	0.73%
2.00	1.28	1.27	1.24	1.82%	1.19%	3.03%
3.00	1.34	1.33	1.30	2.08%	0.90%	3.00%
4.00	1.40	1.37	1.38	0.89%	2.49%	1.58%
5.00	1.44	1.40	1.41	1.13%	3.15%	1.98%
6.00	1.48	1.45	1.46	0.27%	1.86%	1.58%
7.00	1.51	1.52	1.49	1.93%	0.66%	1.26%
8.00	1.54	1.53	1.52	0.35%	0.65%	1.01%
10.00	1.59	1.61	1.57	2.42%	1.24%	1.15%
15.00	1.69	1.73	1.65	4.77%	2.42%	2.23%
20.00	1.77	1.80	1.72	4.53%	1.72%	2.73%
25.00	1.83	1.86	1.79	3.63%	1.45%	2.12%
30.00	1.88	1.90	1.86	2.30%	1.05%	1.23%
35.00	1.93	1.98	1.90	4.26%	2.33%	1.84%
40.00	1.96	2.03	1.91	6.17%	3.45%	2.51%

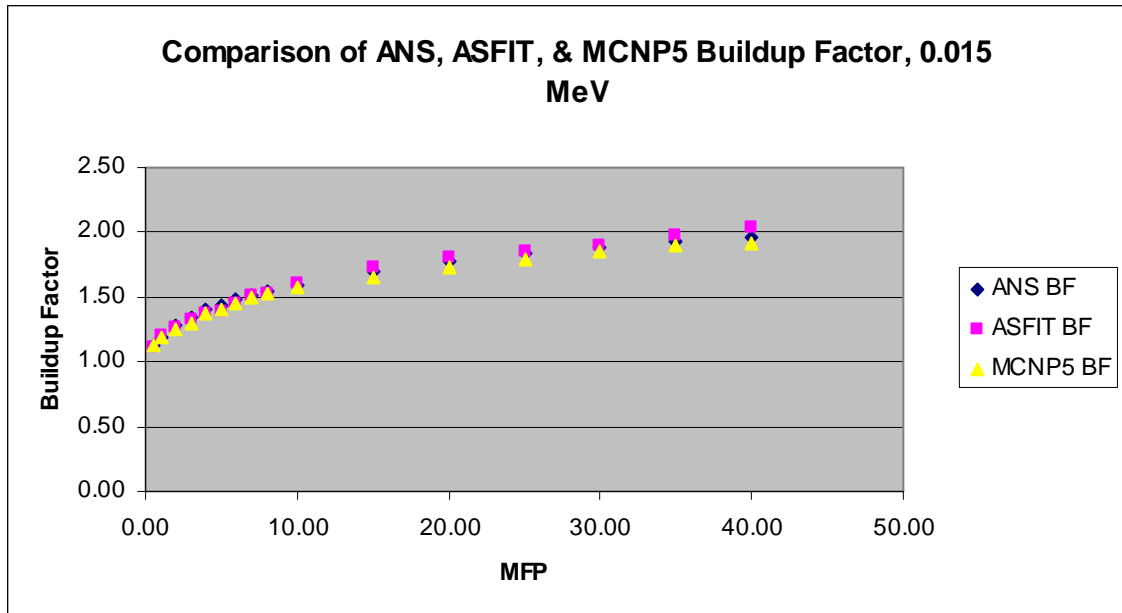


Figure 13e. Buildup Factor Comparison w/ no Coherent Scattering, Iron- 0.015 MeV

Table 11f. Buildup Factor Comparison w/ no Coherent Scattering, Water- 0.15 MeV

Buildup Factor Comparison H <sub>2</sub> O-0.150 MeV						
MFP	ANS Standard	ASFIT BF	MCNP5 BF	% Diff of ASFIT & MCNP5	% Diff of ASFIT & ANS	% Diff of MCNP5 & ANS
0.50	2.07	2.09	2.12	1.30%	0.96%	2.24%
1.00	3.91	3.92	3.72	5.51%	0.26%	5.24%
2.00	9.36	9.39	9.78	3.99%	0.31%	4.28%
3.00	18.60	18.64	18.73	0.47%	0.21%	0.69%
4.00	32.50	32.84	32.32	1.61%	1.04%	0.56%
5.00	52.00	52.14	51.54	1.15%	0.26%	0.89%
6.00	77.90	78.34	77.45	1.15%	0.56%	0.58%
7.00	111.00	113.73	110.05	3.34%	2.40%	0.86%
8.00	153.00	155.67	150.87	3.18%	1.72%	1.41%
10.00	268.00	270.01	258.92	4.28%	0.74%	3.50%
15.00	805.00	806.12	745.52	8.13%	0.14%	7.98%
20.00	1890.00	1898.83	1762.36	7.74%	0.47%	7.24%
25.00	3840.00	3764.43	3654.91	3.00%	2.01%	5.06%
30.00	7050.00	7156.44	6954.18	2.91%	1.49%	1.38%
35.00	12100.00	12278.43	11889.41	3.27%	1.45%	1.77%
40.00	19600.00	20012.33	18887.21	5.96%	2.06%	3.77%

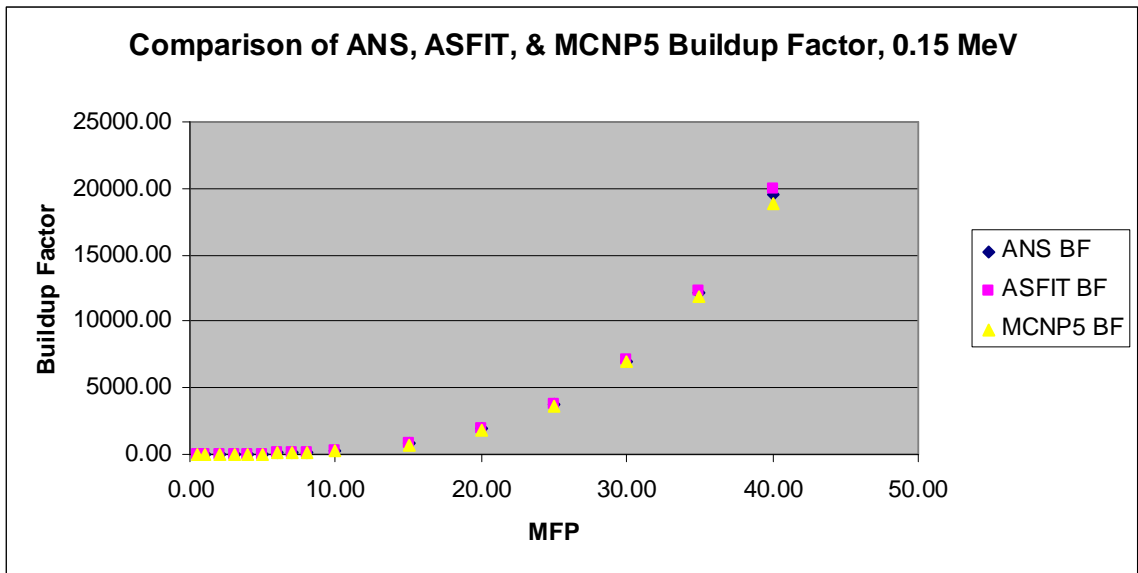


Figure 13f. Buildup Factor Comparison w/ no Coherent Scattering, Iron- 0.15 MeV

Table 11g. Buildup Factor Comparison w/ no Coherent Scattering, Water- 1.50 MeV

Buildup Factor Comparison H <sub>2</sub> O-1.50 MeV						
MFP	ANS Standard	ASFIT BF	MCNP5 BF	% Diff of ASFIT & MCNP5	% Diff of ASFIT & ANS	% Diff of MCNP5 & ANS
0.50	1.42	1.41	1.49	5.41%	0.71%	4.74%
1.00	1.93	1.94	2.01	3.33%	0.52%	3.83%
2.00	3.11	3.12	3.12	0.04%	0.32%	0.28%
3.00	4.44	4.46	4.35	2.61%	0.45%	2.15%
4.00	5.9	5.80	5.70	1.74%	1.72%	3.50%
5.00	7.47	7.40	7.15	3.44%	1.00%	4.47%
6.00	9.14	9.18	8.69	5.66%	0.47%	5.17%
7.00	10.9	11.01	10.37	6.18%	1.00%	5.12%
8.00	12.8	12.97	12.04	7.78%	1.33%	6.35%
10.00	16.8	16.31	15.68	4.05%	3.00%	7.17%
15.00	27.9	26.82	25.91	3.53%	4.03%	7.70%
20.00	40.4	40.37	37.96	6.35%	0.07%	6.43%
25.00	54.1	51.01	50.17	1.69%	6.05%	7.84%
30.00	68.8	67.24	63.22	6.37%	2.32%	8.83%
35.00	84.4	81.48	76.95	5.88%	3.58%	9.67%
40.00	101	99.12	87.44	13.36%	1.90%	15.51%

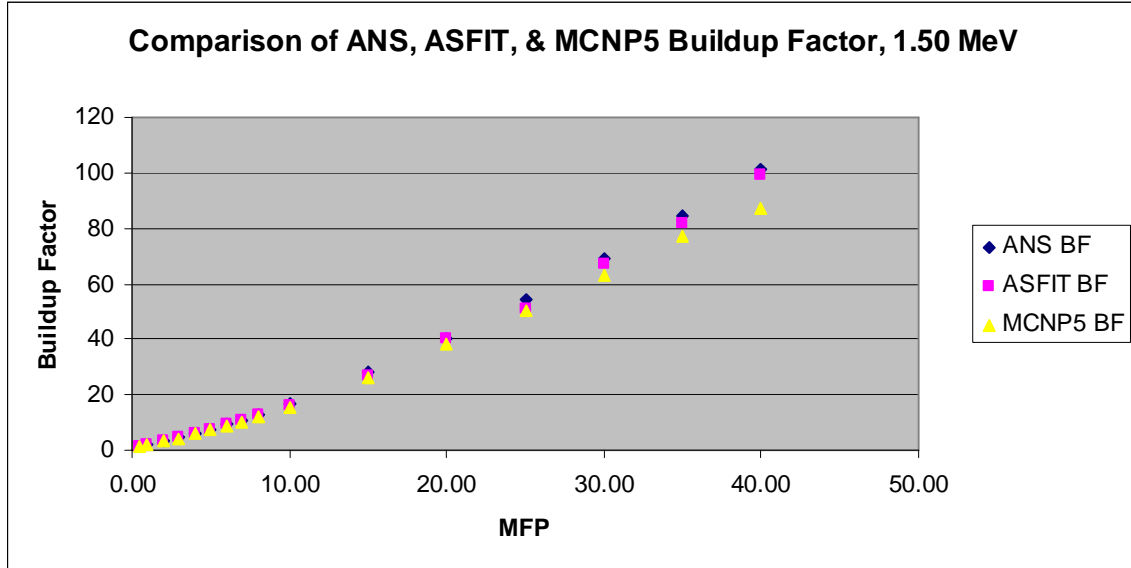


Figure 13g. Buildup Factor Comparison w/ no Coherent Scattering, Iron- 1.50 MeV



Table 11h. Buildup Factor Comparison w/ no Coherent Scattering, Water- 15.0 MeV

Buildup Factor Comparison H <sub>2</sub> O-15.0 MeV						
MFP	ANS Standard	ASFIT BF	MCNP5 BF	% Diff of ASFIT & MCNP5	% Diff of ASFIT & ANS	% Diff of MCNP5 & ANS
0.50	1.16	1.19	1.15	3.43	2.52	0.94
1.00	1.29	1.30	1.32	1.48	1.07	2.52
2.00	1.51	1.55	1.53	1.54	2.58	1.06
3.00	1.72	1.76	1.79	1.93	2.27	4.13
4.00	1.93	1.98	2.06	4.02	2.43	6.20
5.00	2.14	2.20	2.22	1.19	2.51	3.65
6.00	2.34	2.38	2.48	4.32	1.76	5.83
7.00	2.53	2.65	2.72	2.54	4.67	7.03
8.00	2.73	2.83	2.98	5.21	3.60	8.38
10.00	3.11	3.22	3.27	1.40	3.42	4.75
15.00	4.04	4.06	4.17	2.76	0.49	3.16
20.00	4.93	4.88	5.04	3.32	1.02	2.22
25.00	5.81	5.89	5.95	1.02	1.39	2.39
30.00	6.64	6.61	6.79	2.72	0.42	2.24
35.00	7.42	7.24	7.82	7.98	2.44	5.13
40.00	8.09	7.98	8.88	11.28	1.35	8.92

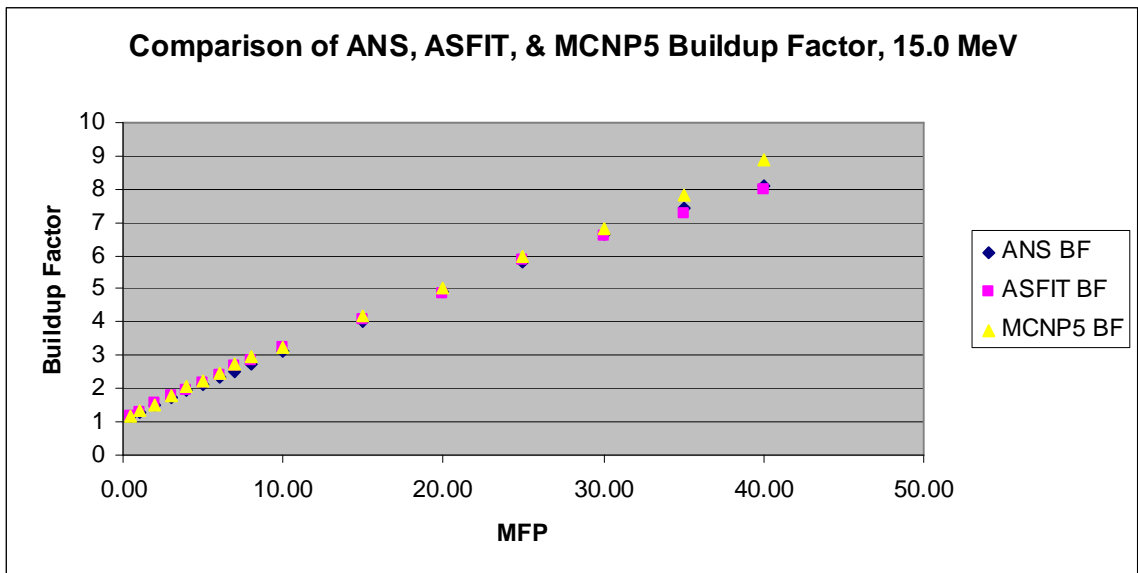


Figure 13h. Buildup Factor Comparison w/ no Coherent Scattering, Iron- 15.0 MeV

APPENDIX IX

**FITTING FUNCTION FOR CALCULATED BUILDUP FACTOR**

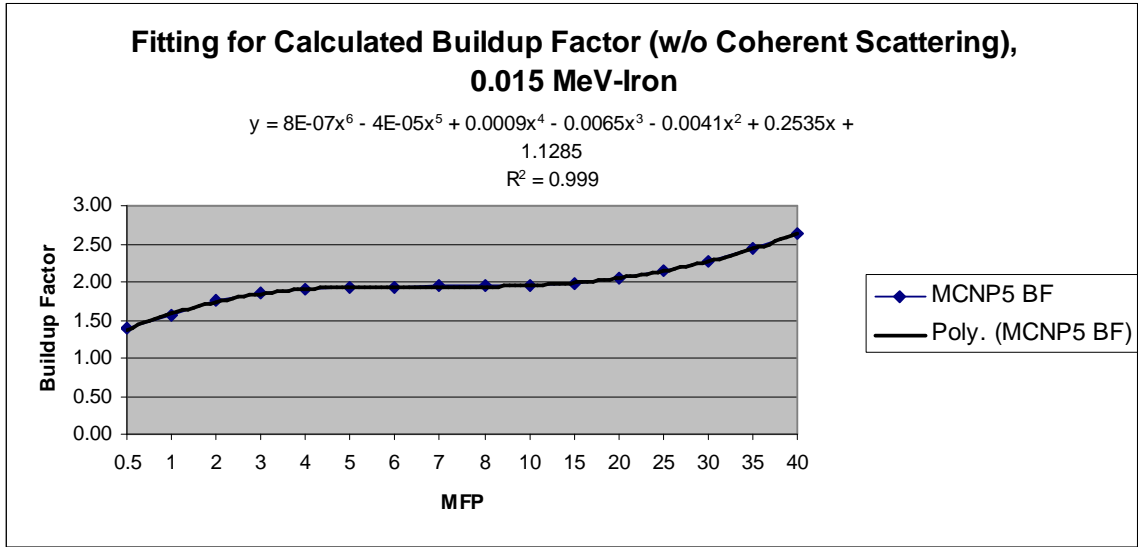


Figure 14a. Fitting Function for Buildup Factor w/o Coherent Scattering, Iron-0.015 MeV

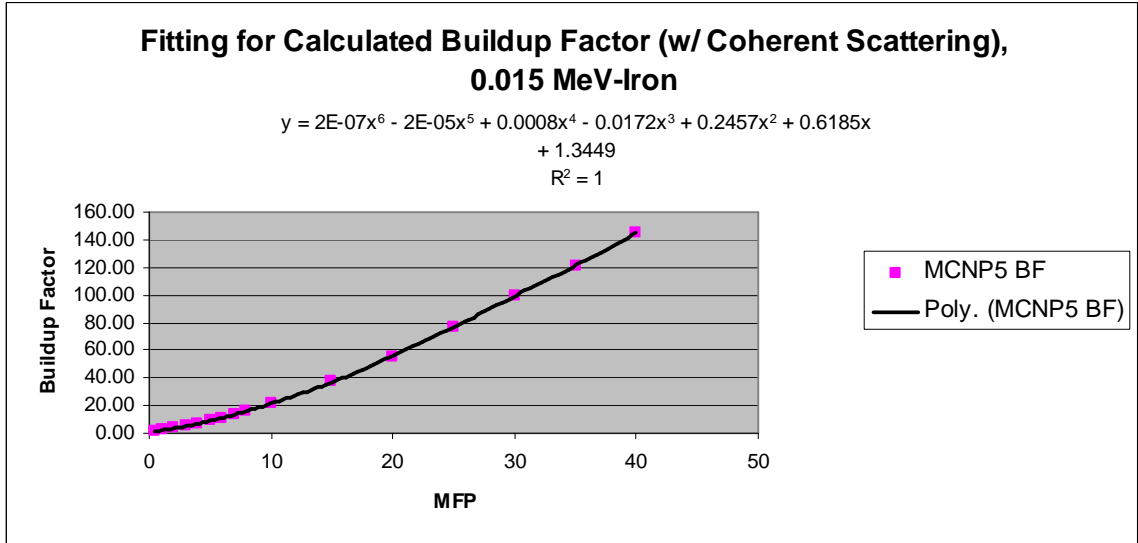


Figure 14b. Fitting Function for Buildup Factor w/ Coherent Scattering, Iron-0.015 MeV

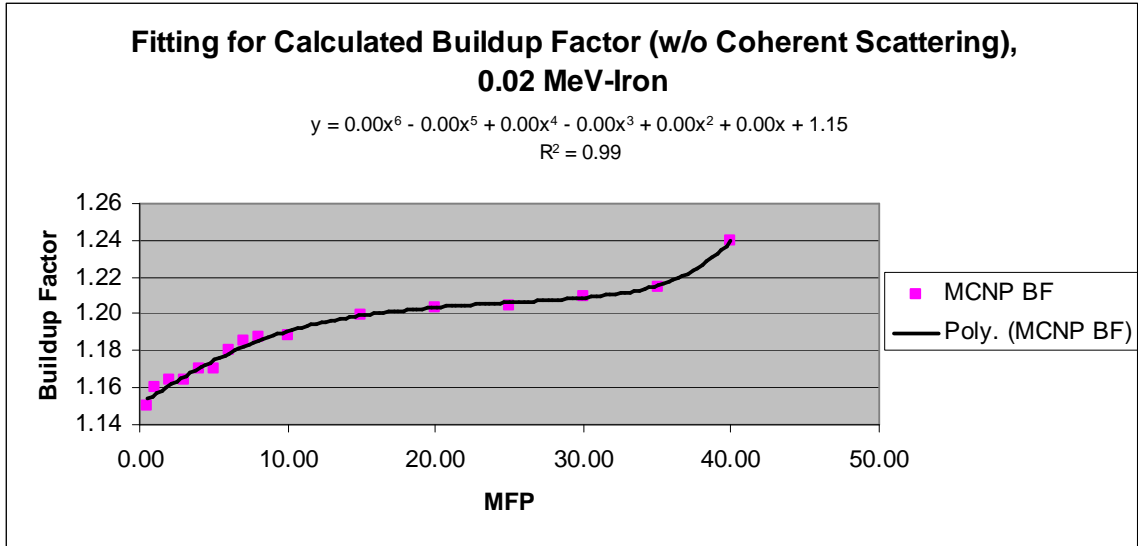


Figure 14c. Fitting Function for Buildup Factor w/o Coherent Scattering, Iron-0.02 MeV

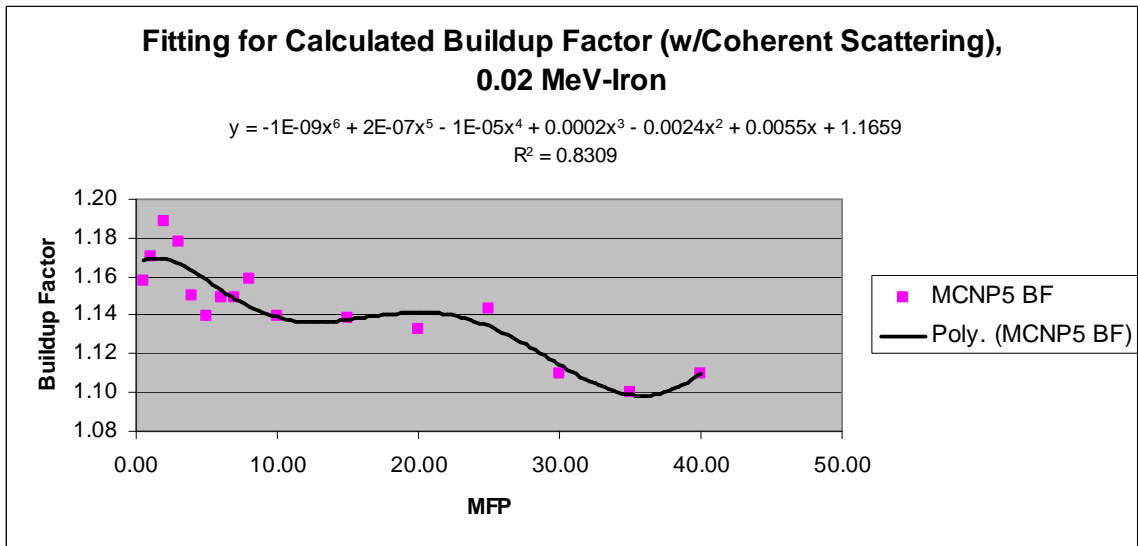


Figure 14d. Fitting Function for Buildup Factor w/ Coherent Scattering, Iron-0.02 MeV

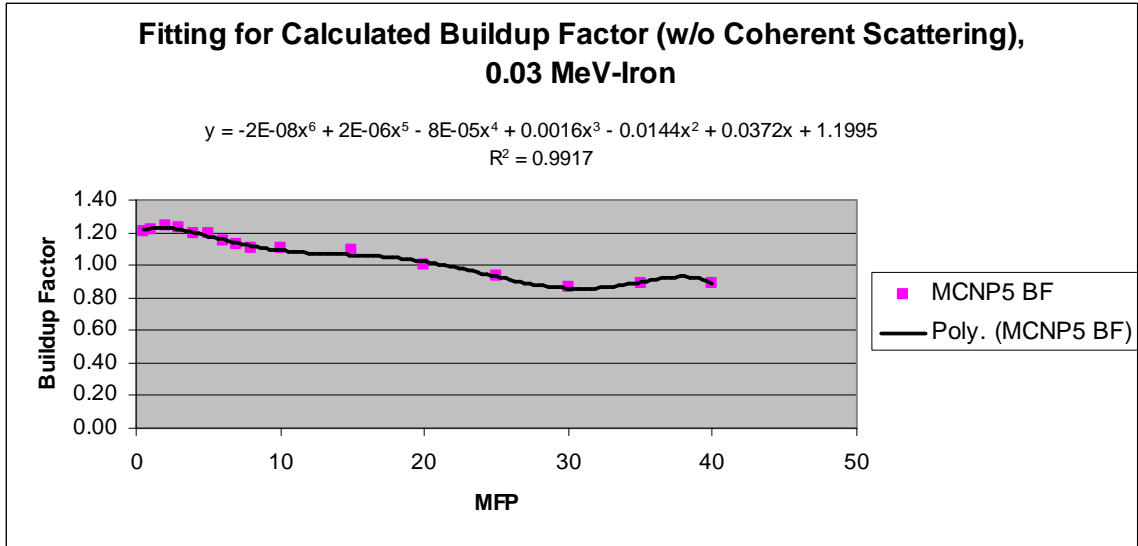


Figure 14e. Fitting Function for Buildup Factor w/o Coherent Scattering, Iron-0.03 MeV

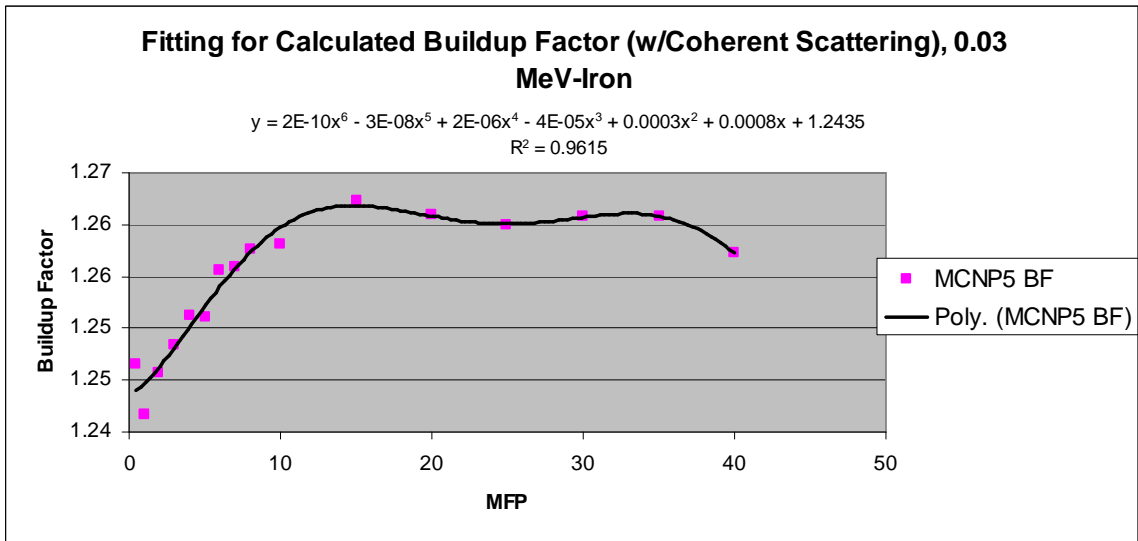


Figure 14f. Fitting Function for Buildup Factor w/Coherent Scattering, Iron-0.03 MeV

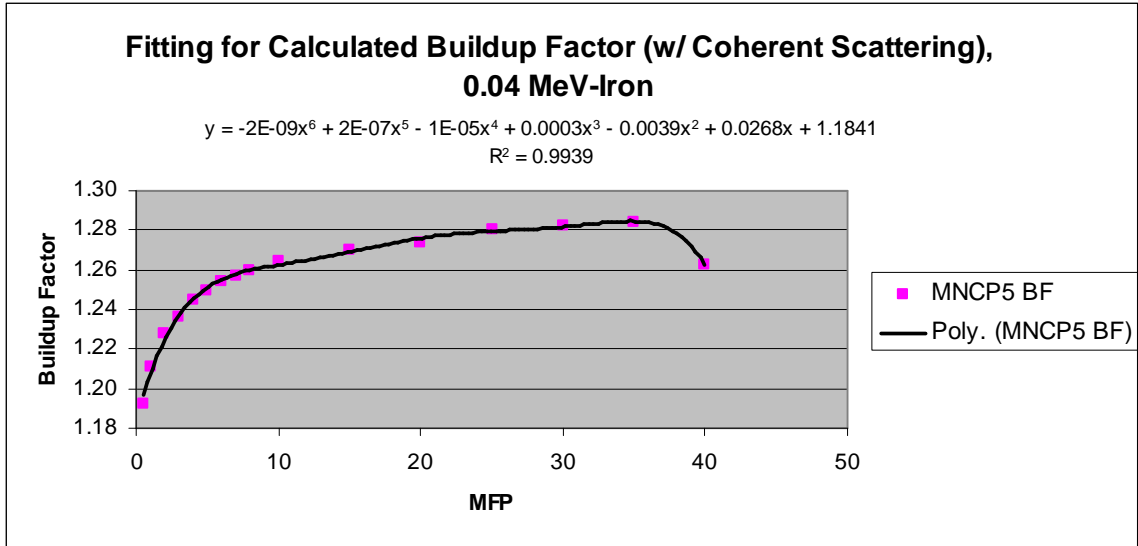


Figure 14g. Fitting Function for Buildup Factor w/Coherent Scattering, Iron-0.04 MeV

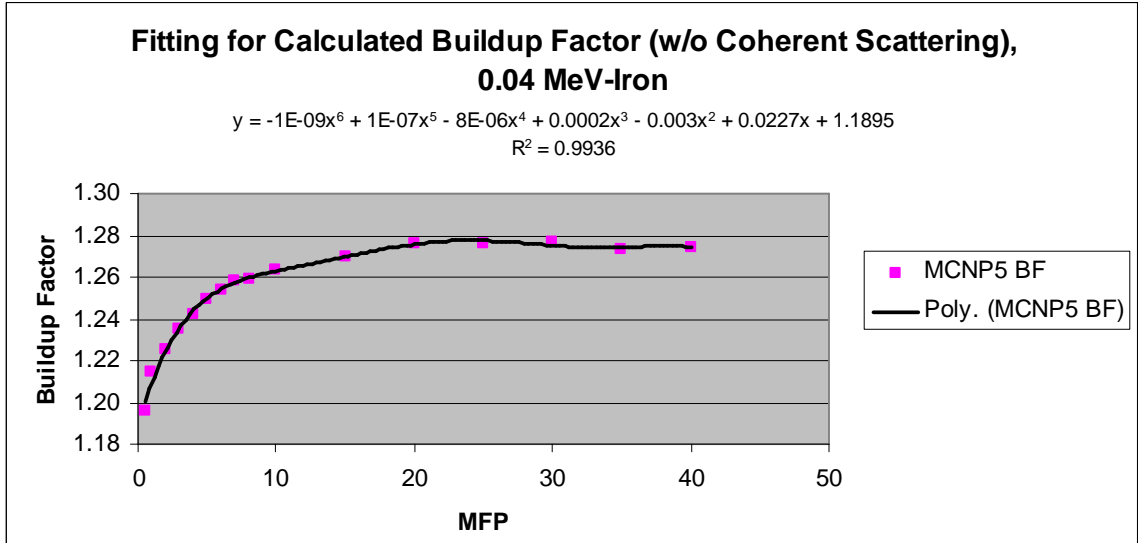


Figure 14h. Fitting Function for Buildup Factor w/o Coherent Scattering, Iron-0.04 MeV

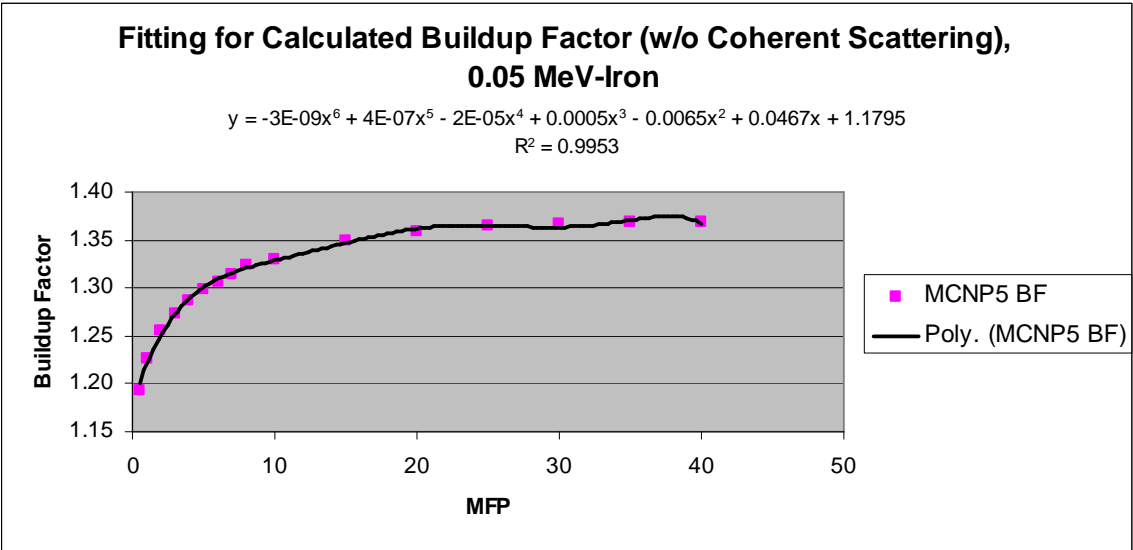


Figure 14i. Fitting Function for Buildup Factor w/o Coherent Scattering, Iron-0.05 MeV

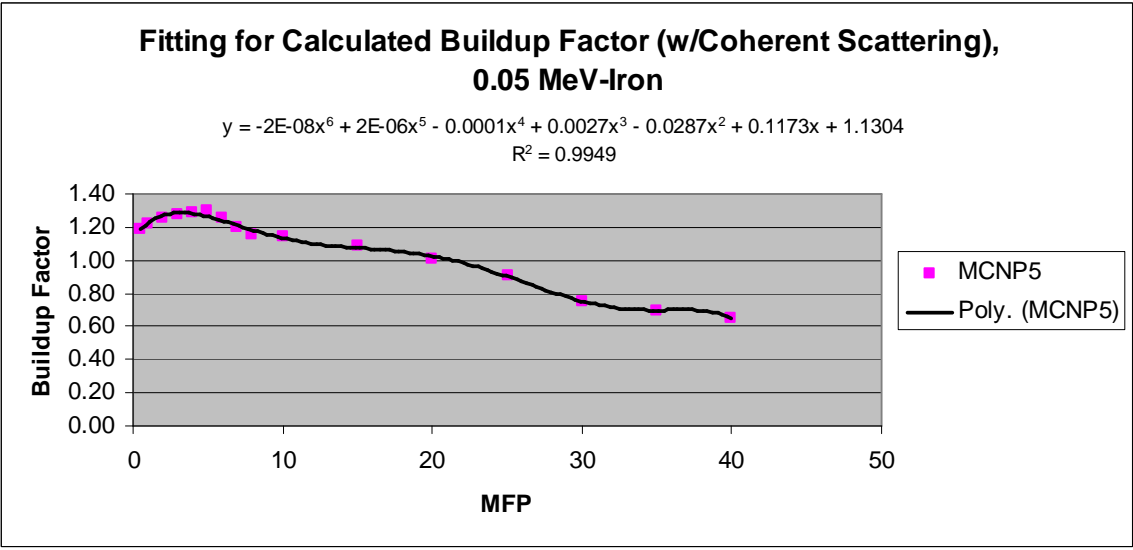


Figure 14j. Fitting Function for Buildup Factor w/Coherent Scattering, Iron-0.05 MeV

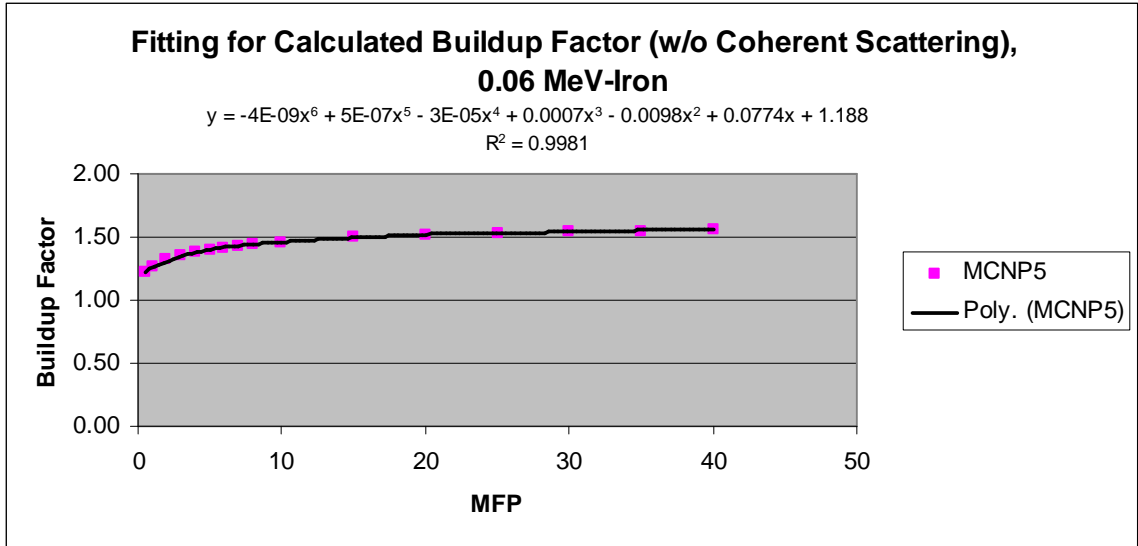


Figure 14k. Fitting Function for Buildup Factor w/o Coherent Scattering, Iron-0.06 MeV

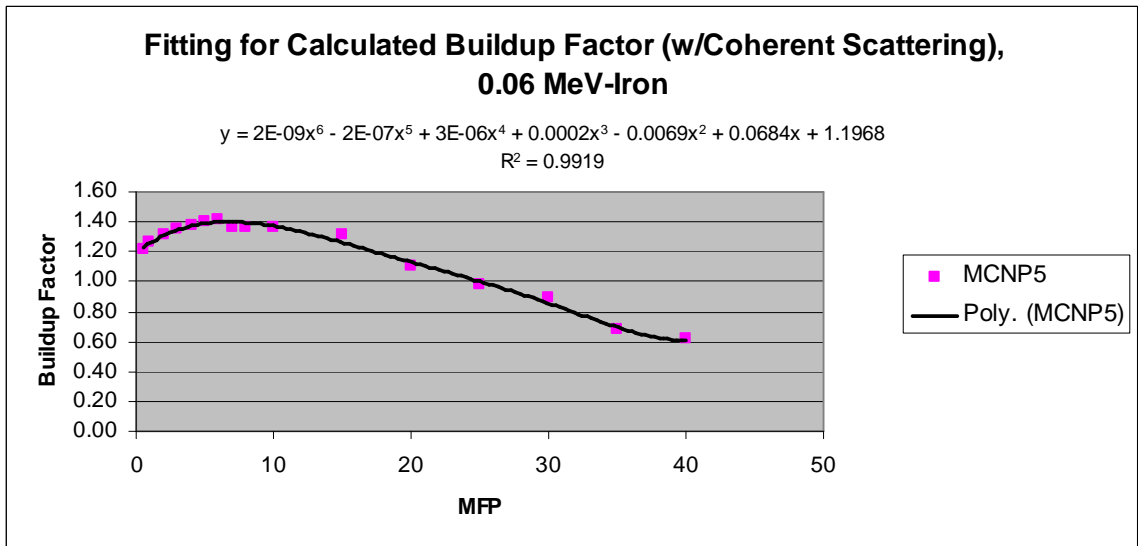


Figure 14l. Fitting Function for Buildup Factor w/ Coherent Scattering, Iron-0.06 MeV

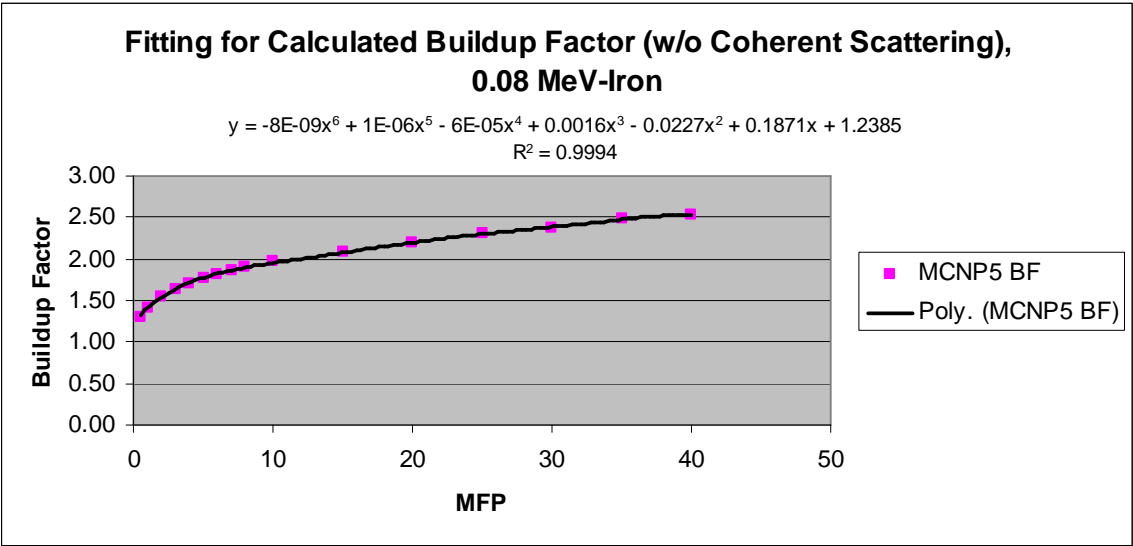


Figure 14m. Fitting Function for Buildup Factor w/o Coherent Scattering, Iron-0.08 MeV

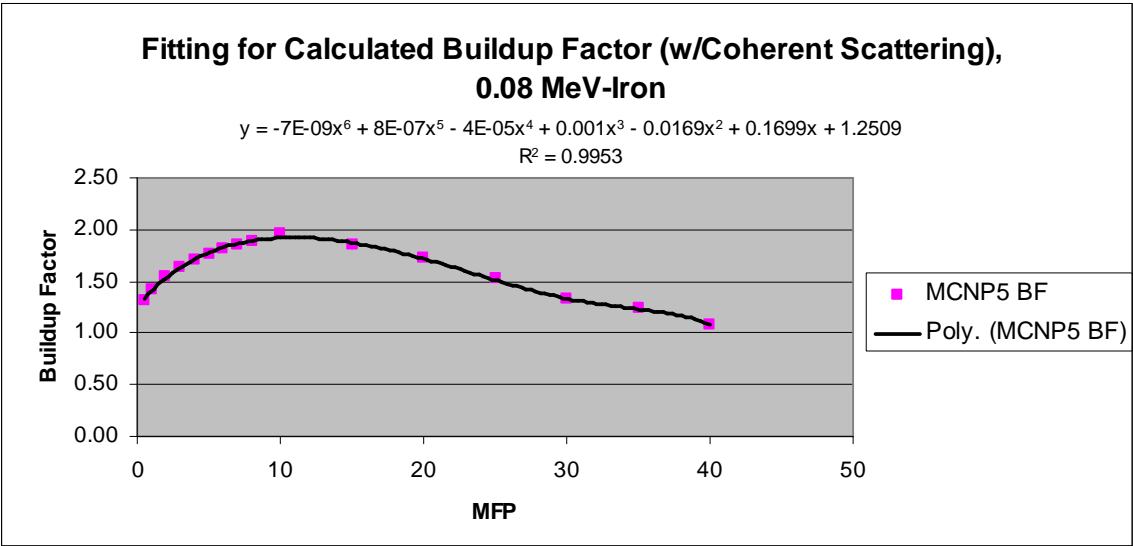


Figure 14n. Fitting Function for Buildup Factor w/ Coherent Scattering, Iron-0.08 MeV



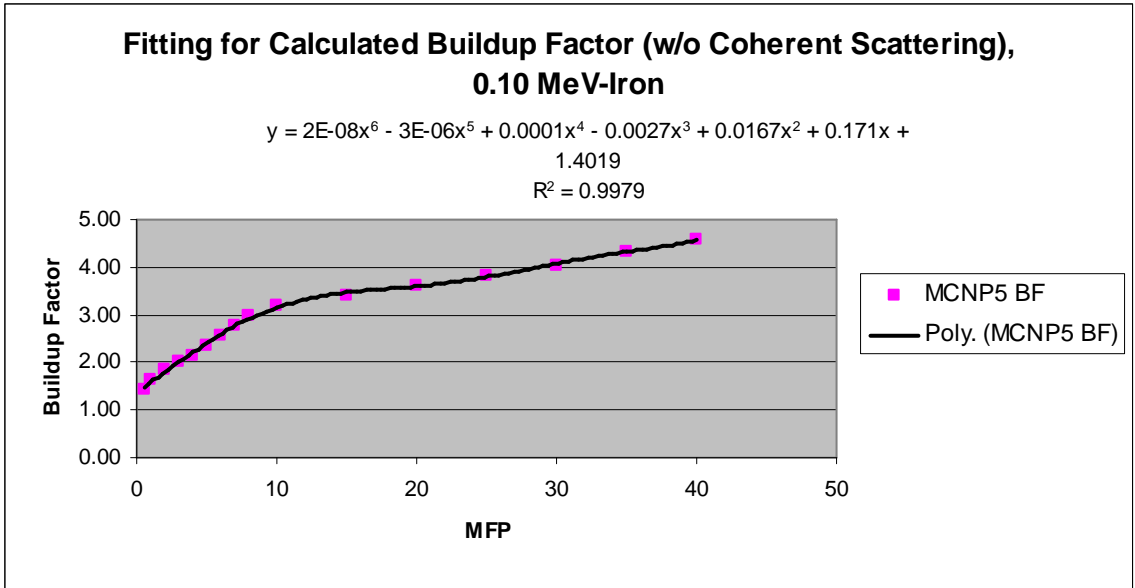


Figure 14o. Fitting Function for Buildup Factor w/o Coherent Scattering, Iron-0.10 MeV

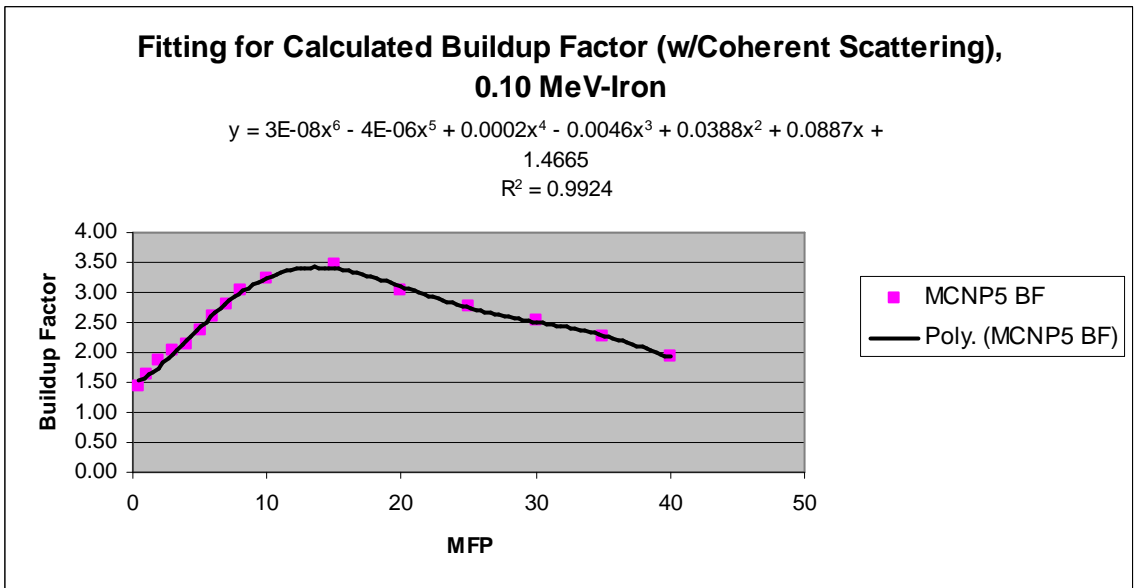


Figure 14p. Fitting Function for Buildup Factor w/ Coherent Scattering, Iron-0.10 MeV

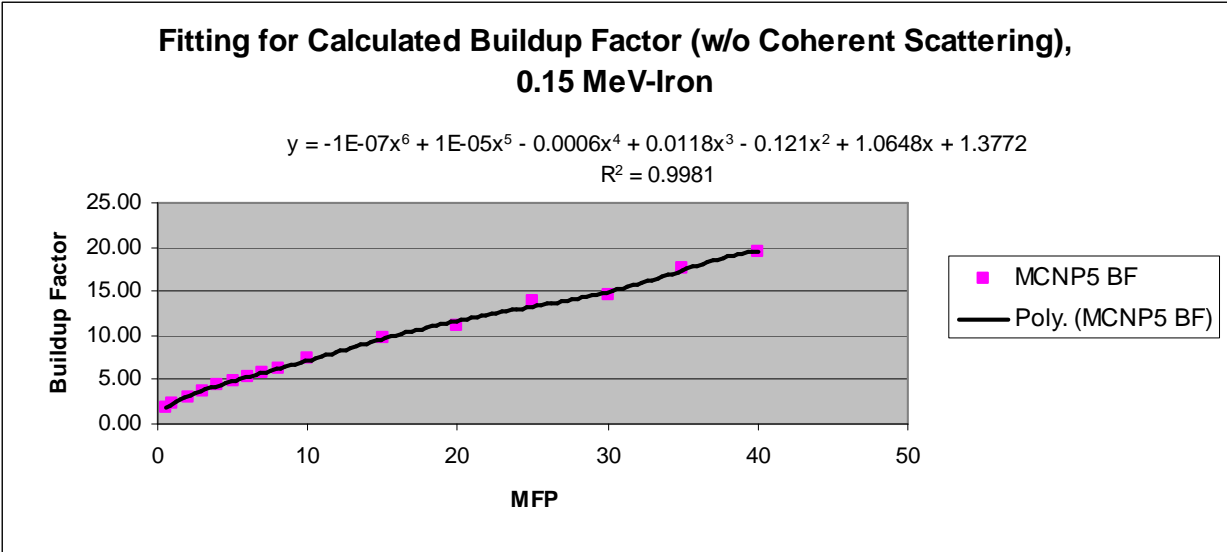


Figure 14q. Fitting Function for Buildup Factor w/o Coherent Scattering, Iron-0.15 MeV

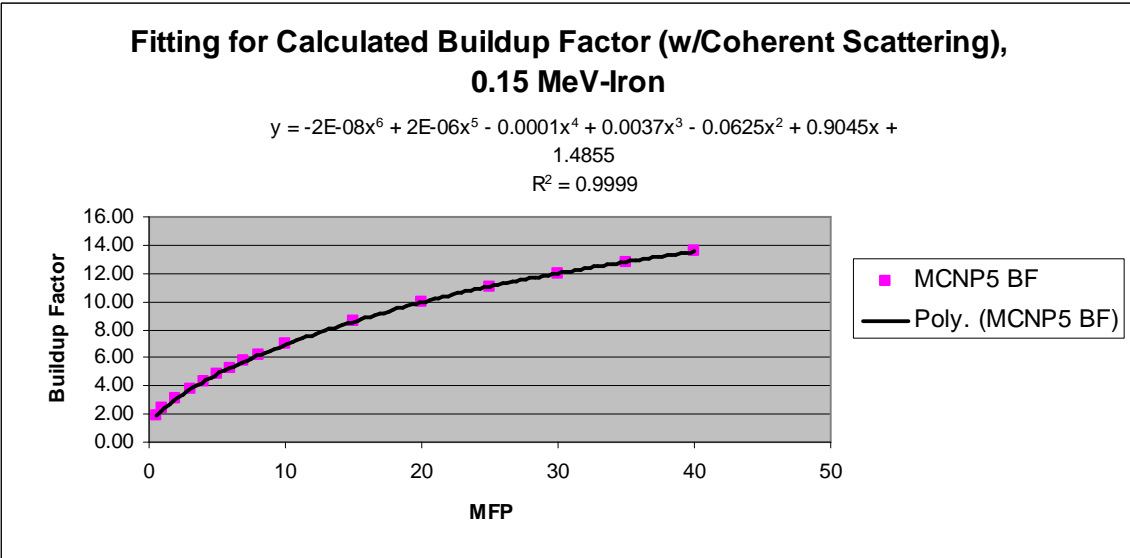


Figure 14r. Fitting Function for Buildup Factor w/Coherent Scattering, Iron-0.15 MeV

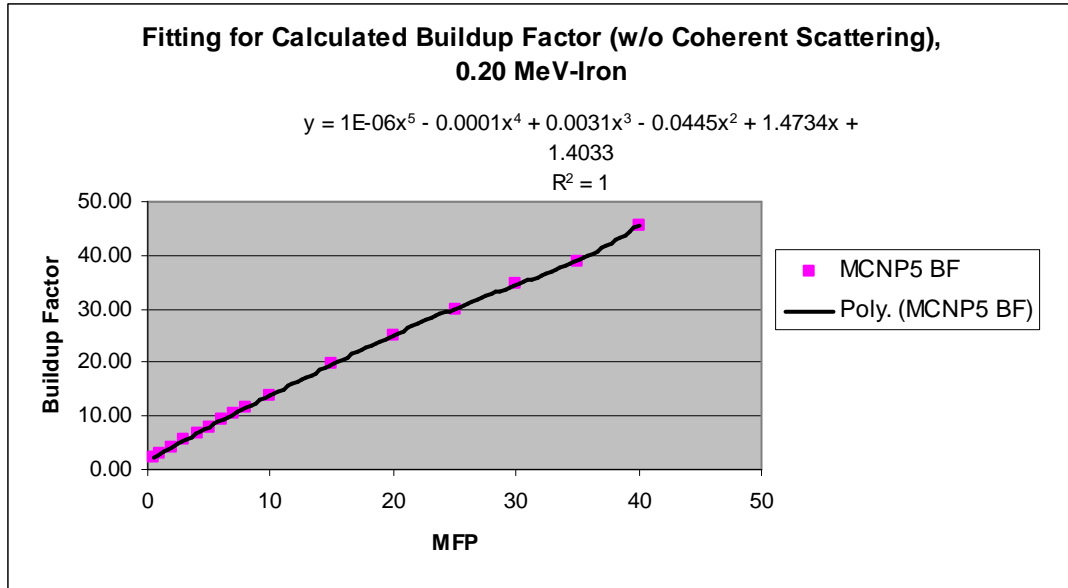


Figure 14s. Fitting Function for Buildup Factor w/o Coherent Scattering, Iron-0.20 MeV

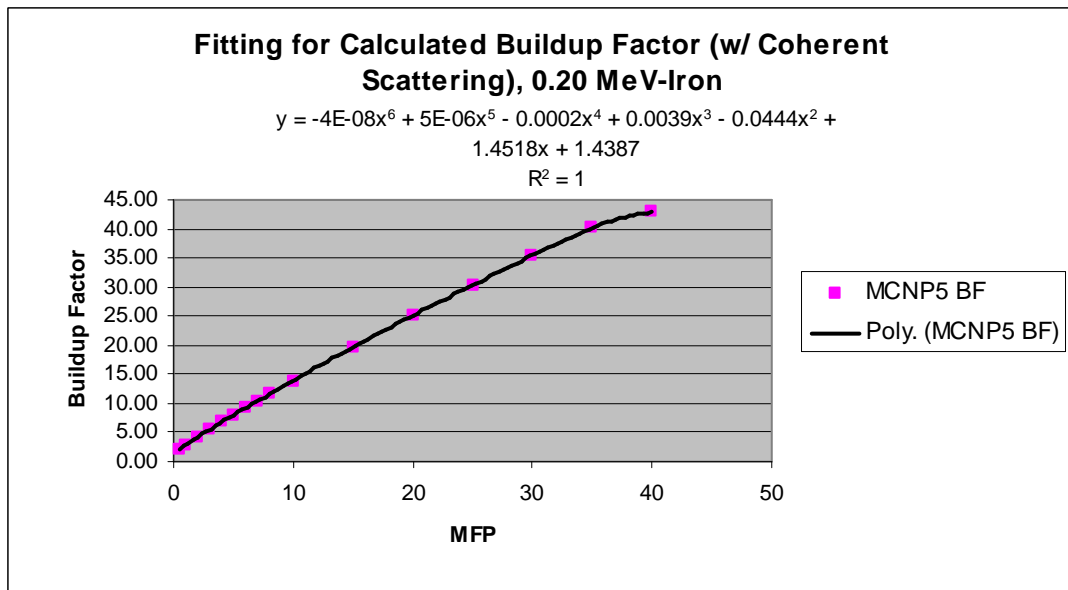


Figure 14t. Fitting Function for Buildup Factor w/Coherent Scattering, Iron-0.20 MeV

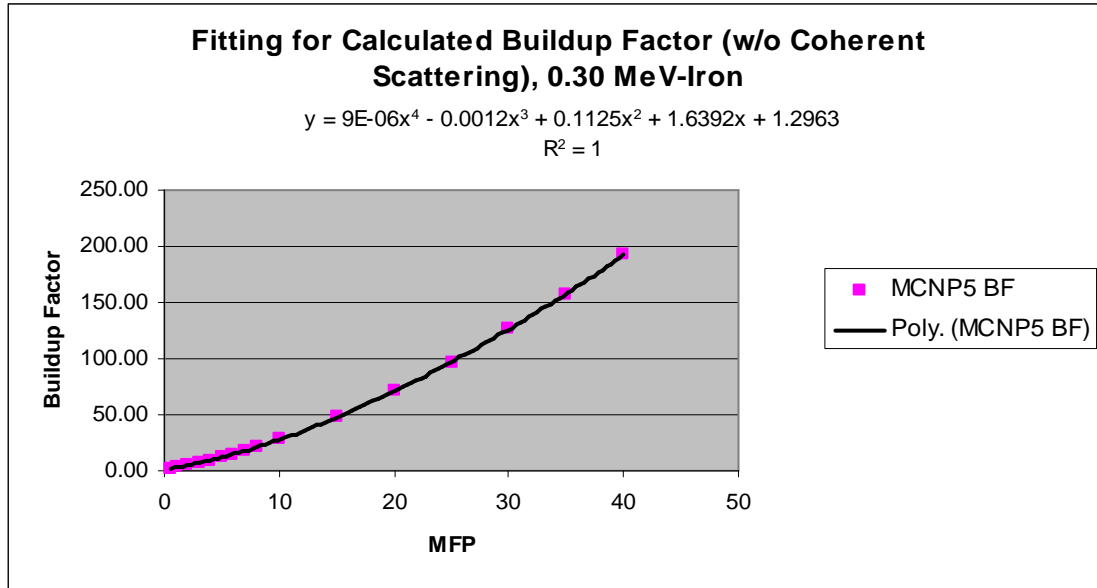


Figure 14u. Fitting Function for Buildup Factor w/o Coherent Scattering, Iron-0.30 MeV

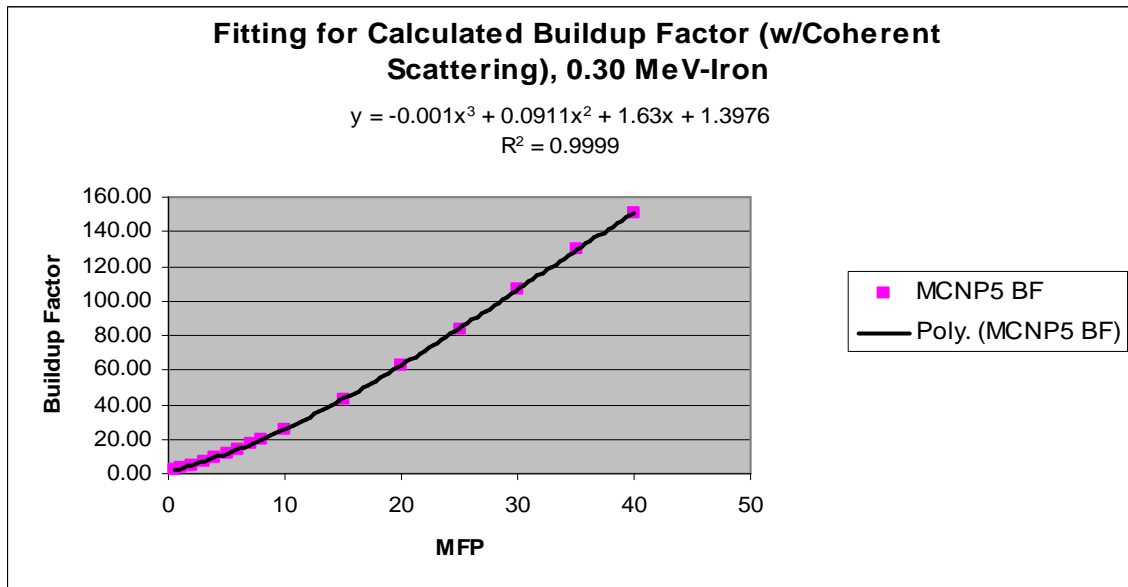


Figure 14v. Fitting Function for Buildup Factor w/Coherent Scattering, Iron-0.30 MeV

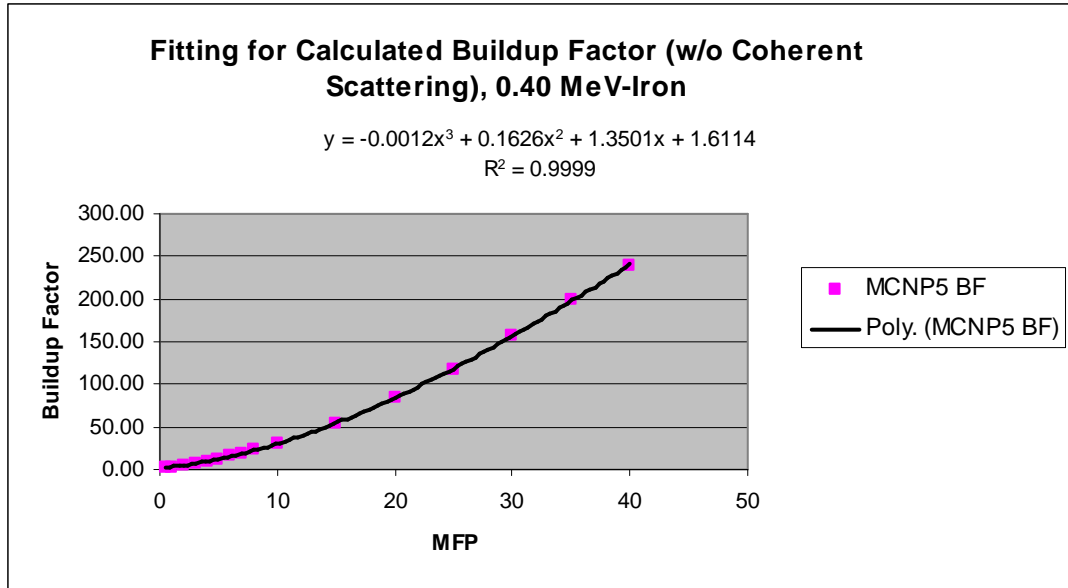


Figure 14w. Fitting Function for Buildup Factor w/o Coherent Scattering, Iron-0.40 MeV

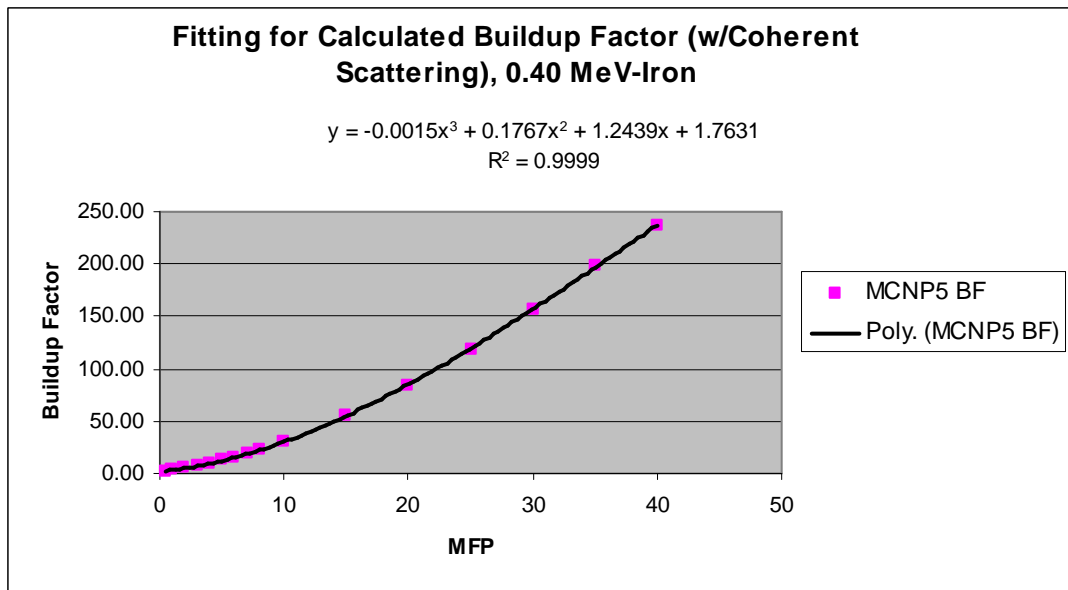


Figure 14x. Fitting Function for Buildup Factor w/Coherent Scattering, Iron-0.40 MeV

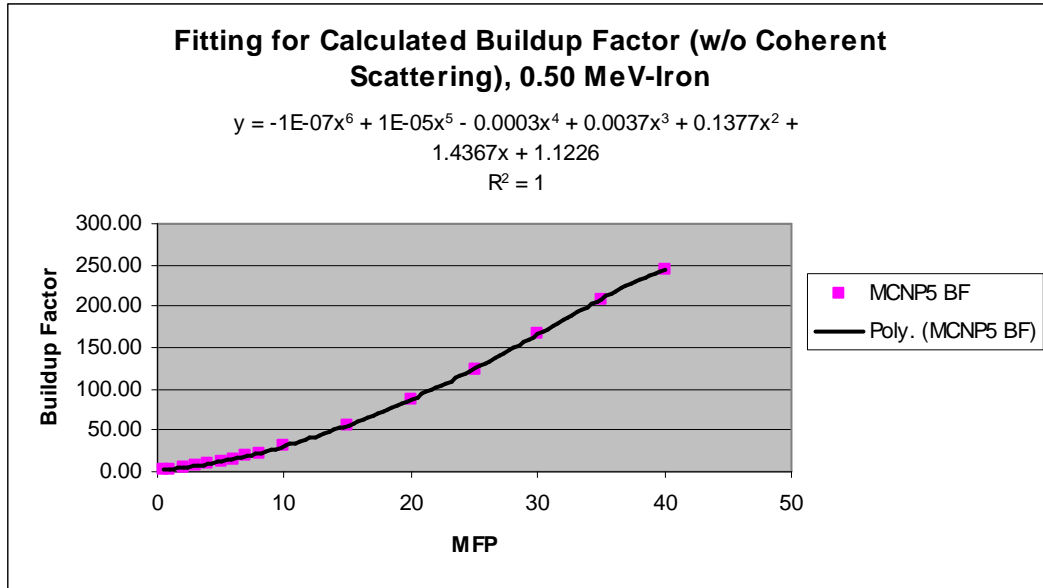


Figure 14y. Fitting Function for Buildup Factor w/o Coherent Scattering, Iron-0.50 MeV

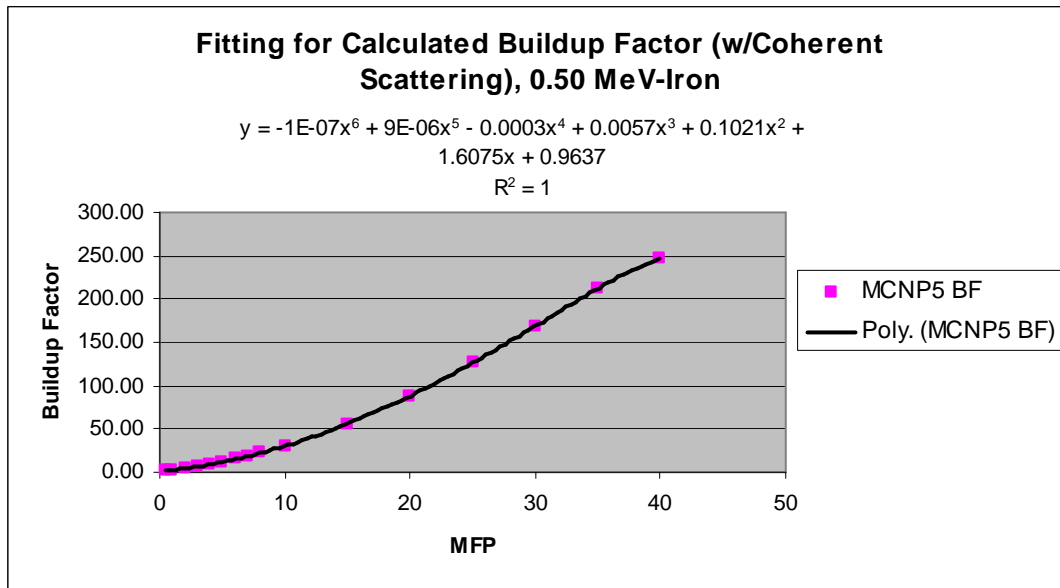


Figure 14z. Fitting Function for Buildup Factor w/Coherent Scattering, Iron-0.50 MeV

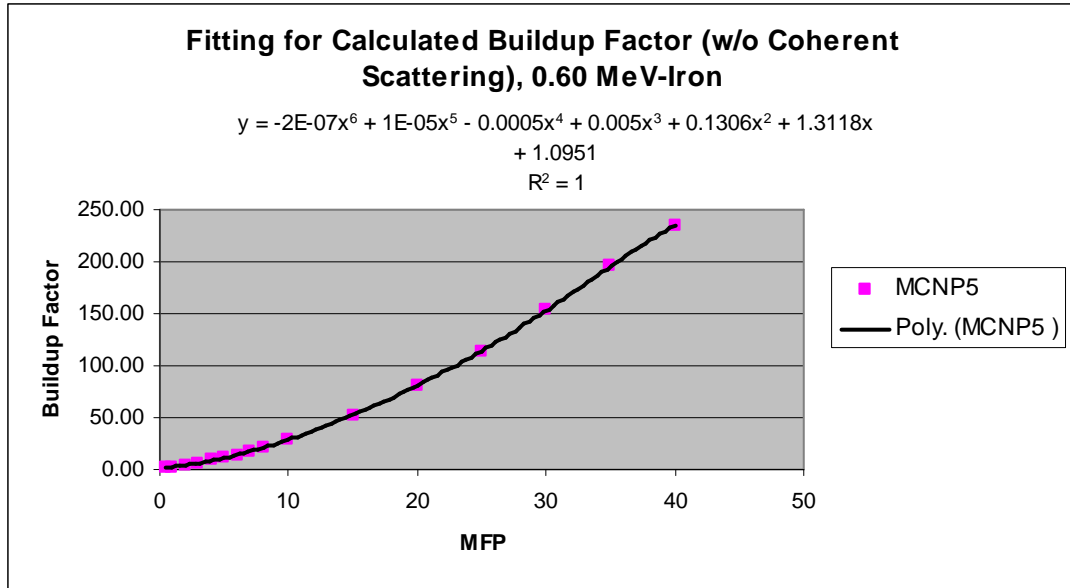


Figure 14aa. Fitting Function for Buildup Factor w/o Coherent Scattering, Iron-0.60 MeV

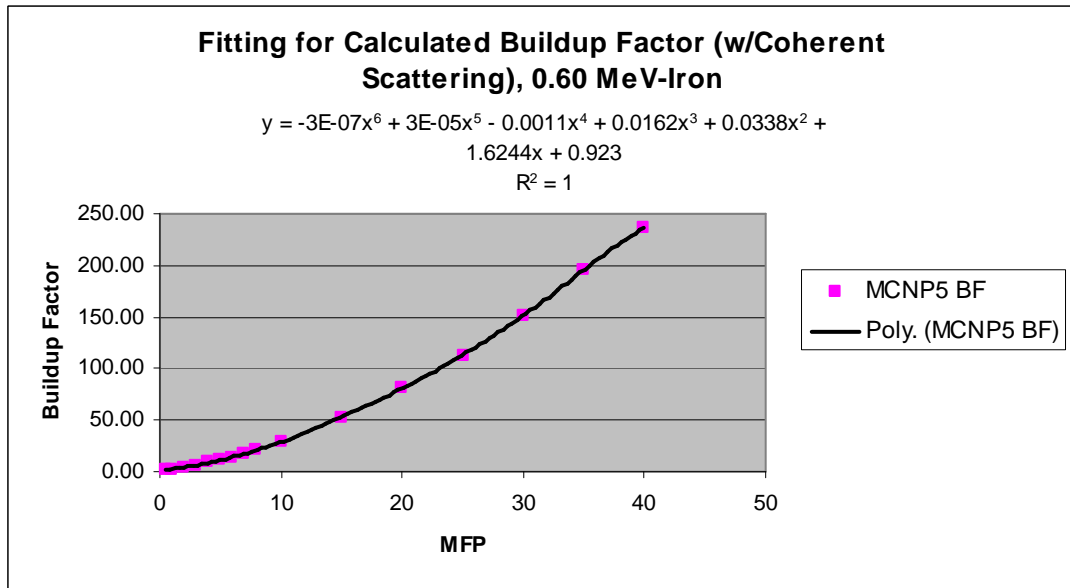


Figure 14bb. Fitting Function for Buildup Factor w/Coherent Scattering, Iron-0.60 MeV

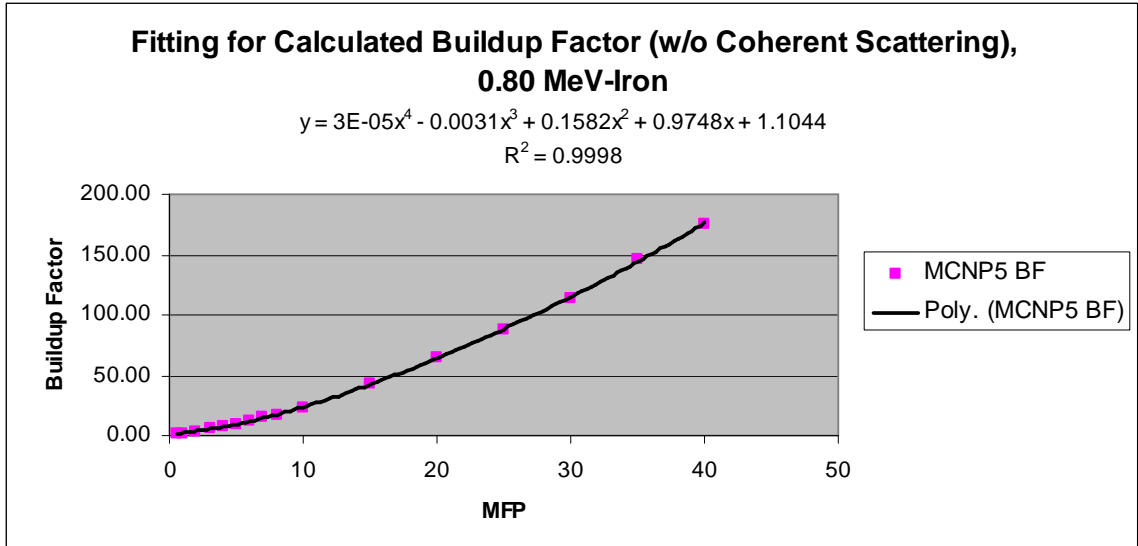


Figure 14cc. Fitting Function for Buildup Factor w/o Coherent Scattering, Iron-0.80 MeV

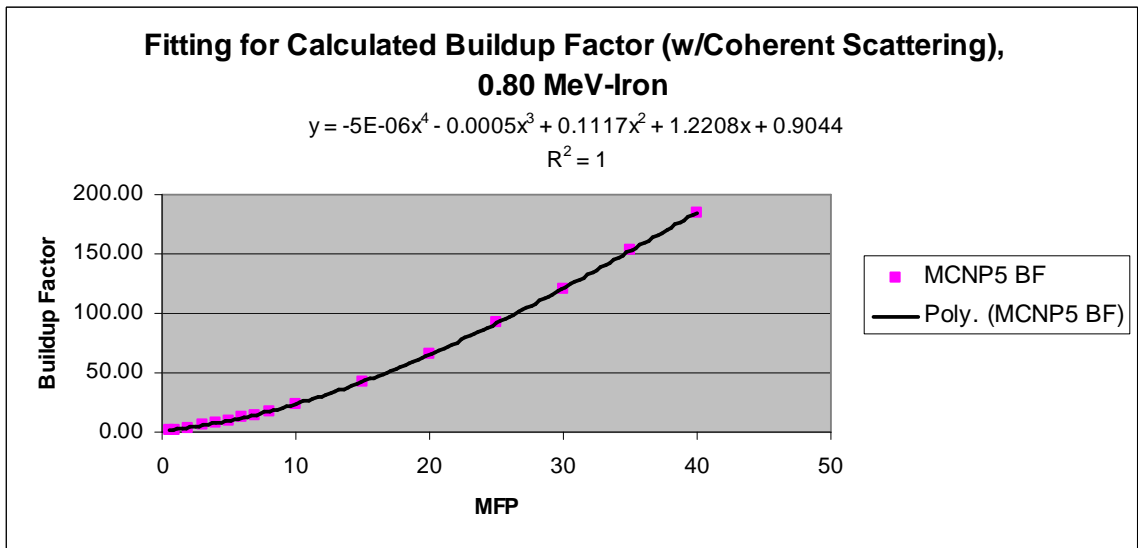


Figure 14dd. Fitting Function for Buildup Factor w/Coherent Scattering, Iron-0.80 MeV



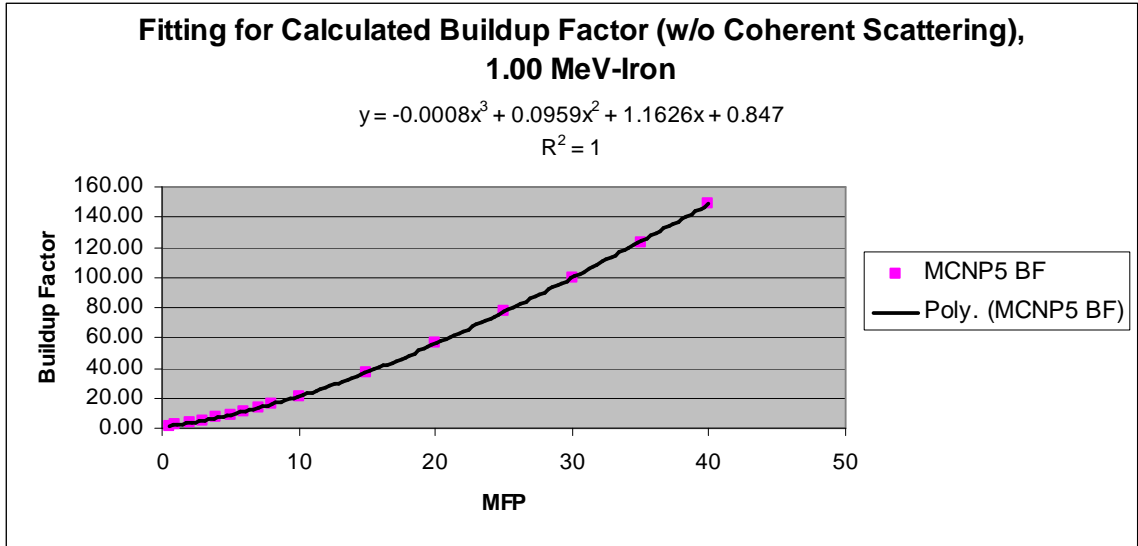


Figure 14ee. Fitting Function for Buildup Factor w/o Coherent Scattering, Iron-1.00 MeV

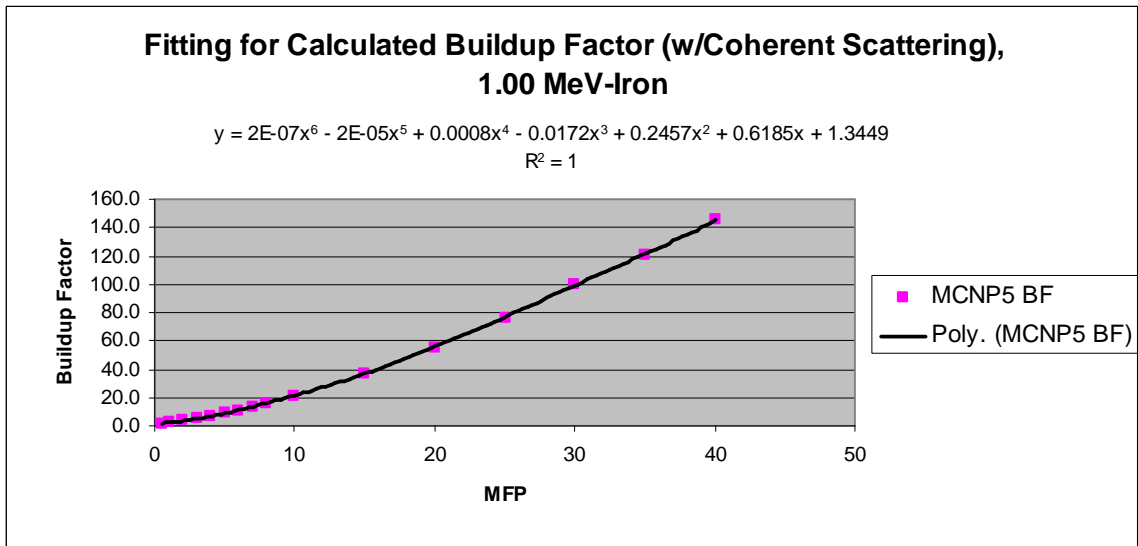


Figure 14ff. Fitting Function for Buildup Factor w/Coherent Scattering, Iron-1.00 MeV

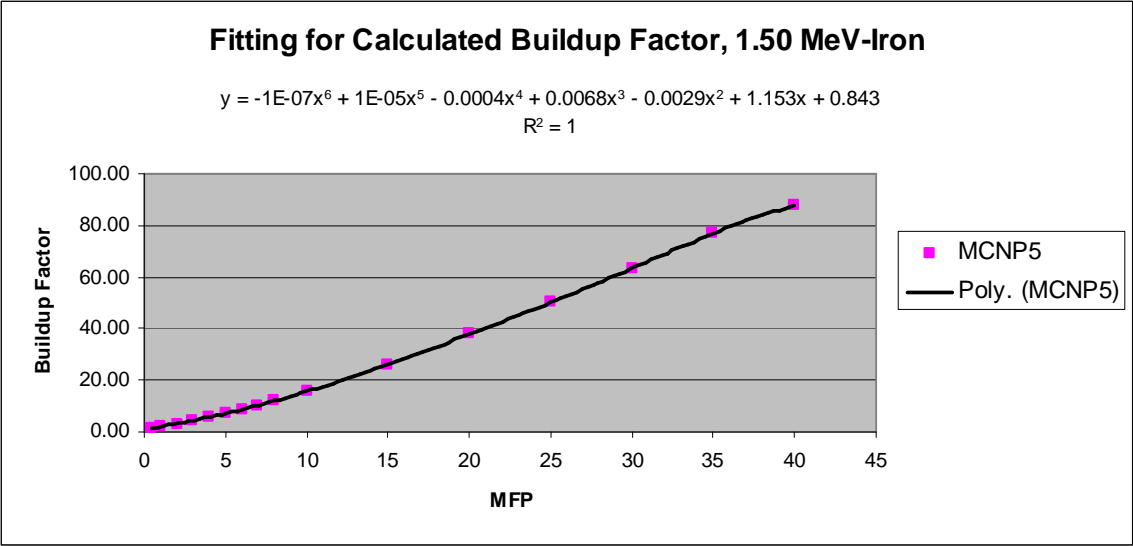


Figure 14gg. Fitting Function for Buildup Factor, Iron-1.50 MeV

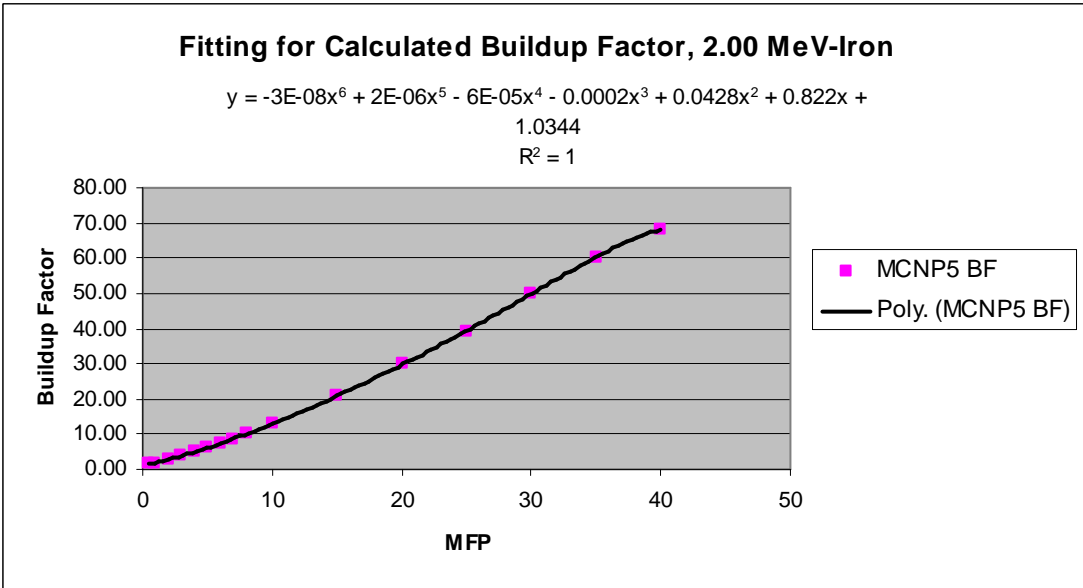


Figure 14hh. Fitting Function for Buildup Factor, Iron-2.00 MeV

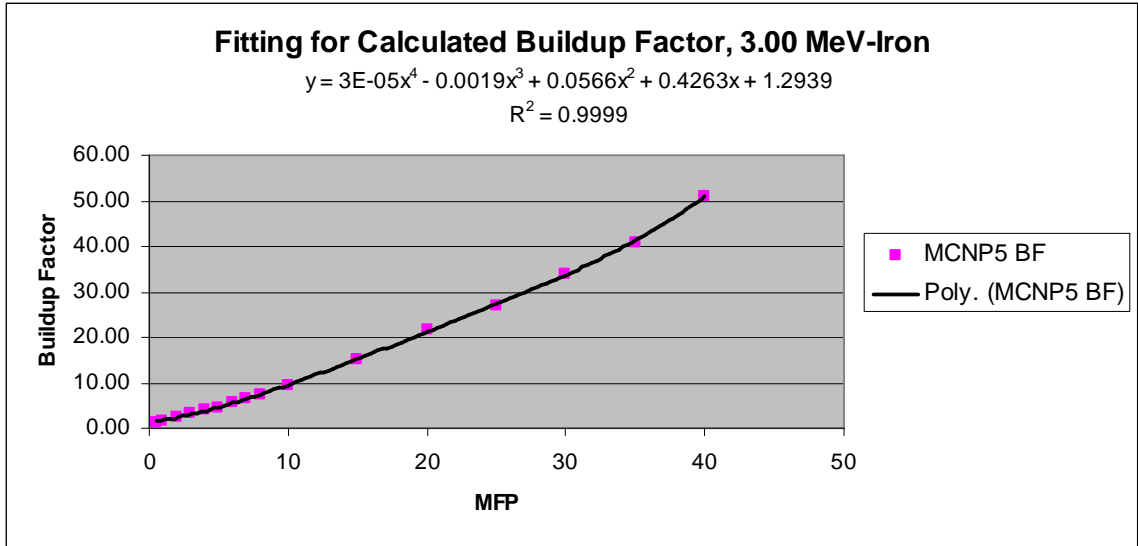


Figure 14ii. Fitting Function for Buildup Factor, Iron-3.00 MeV

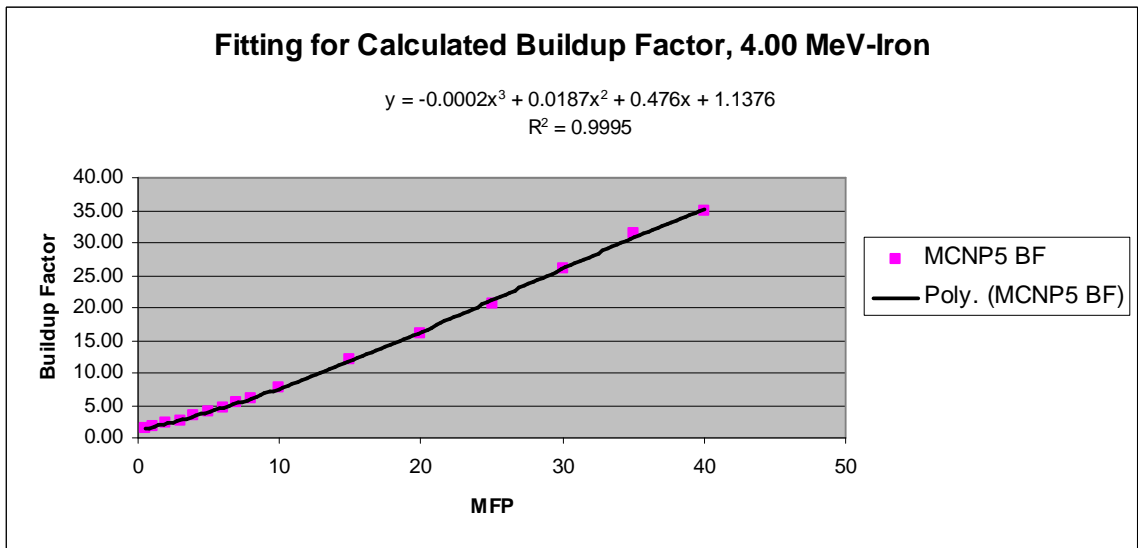


Figure 14jj. Fitting Function for Buildup Factor, Iron-4.00 MeV

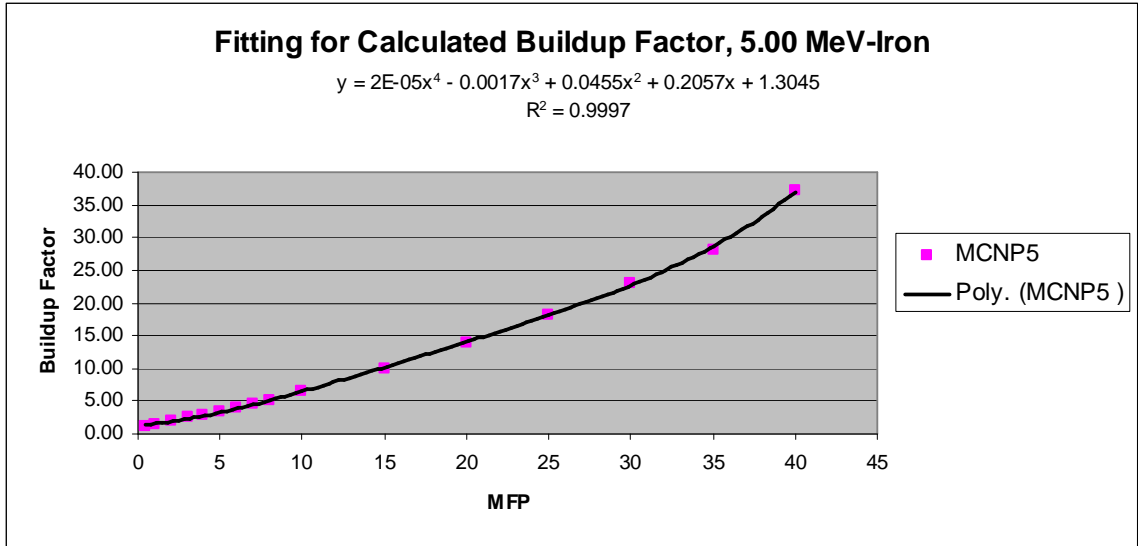


Figure 14kk. Fitting Function for Buildup Factor, Iron-5.00 MeV

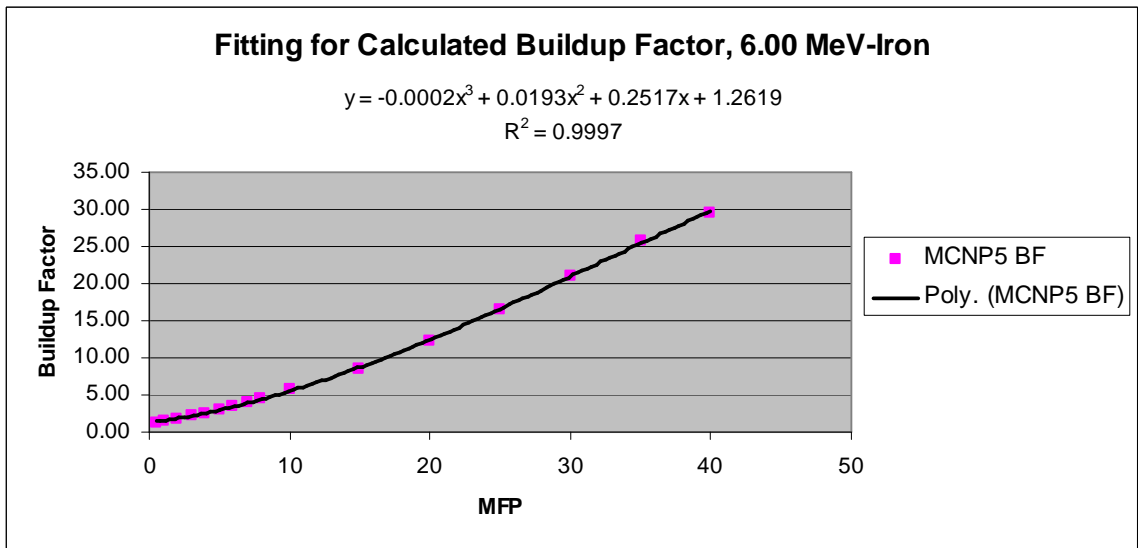


Figure 14ll. Fitting Function for Buildup Factor, Iron-6.00 MeV

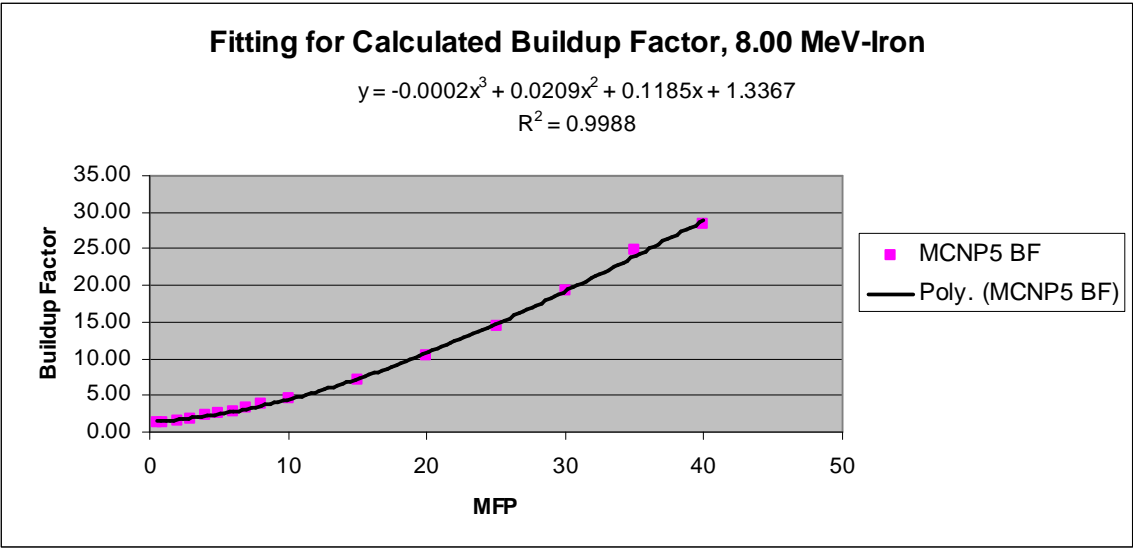


Figure 14mm. Fitting Function for Buildup Factor, Iron-8.00 MeV

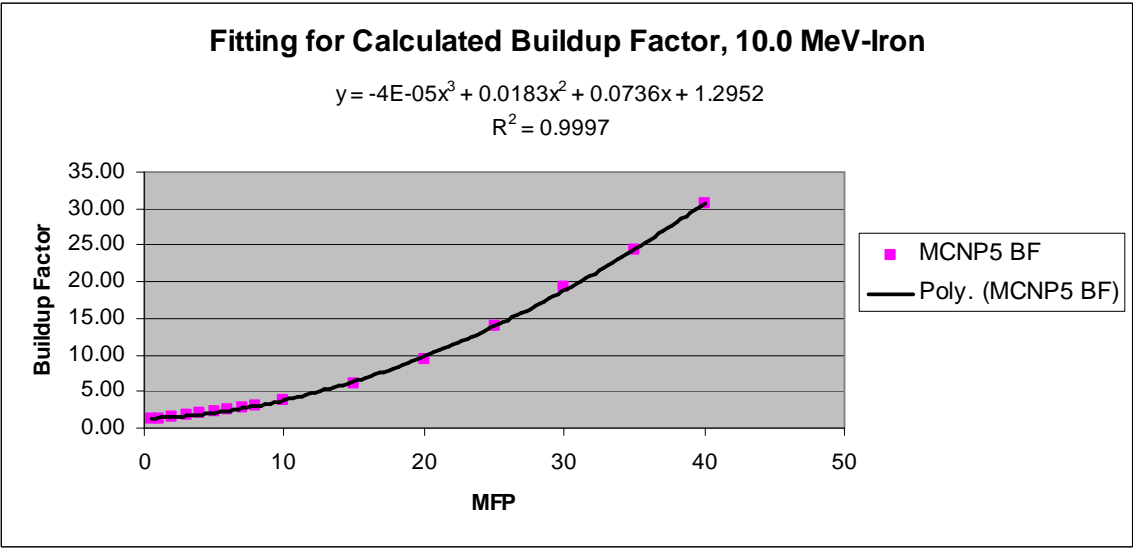


Figure 14nn. Fitting Function for Buildup Factor, Iron-10.0 MeV

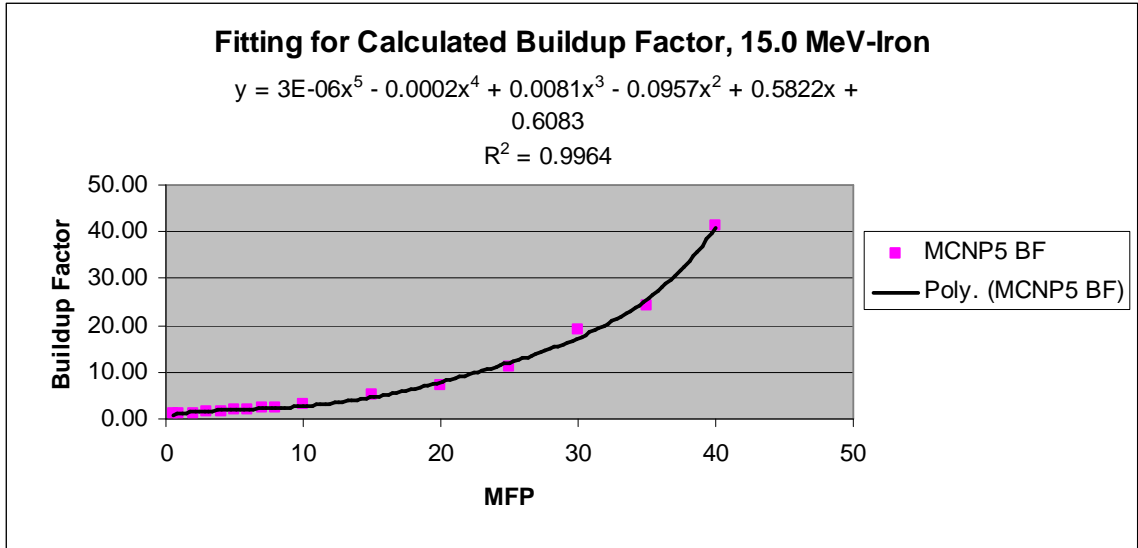


Figure 14oo. Fitting Function for Buildup Factor, Iron-3.00 MeV

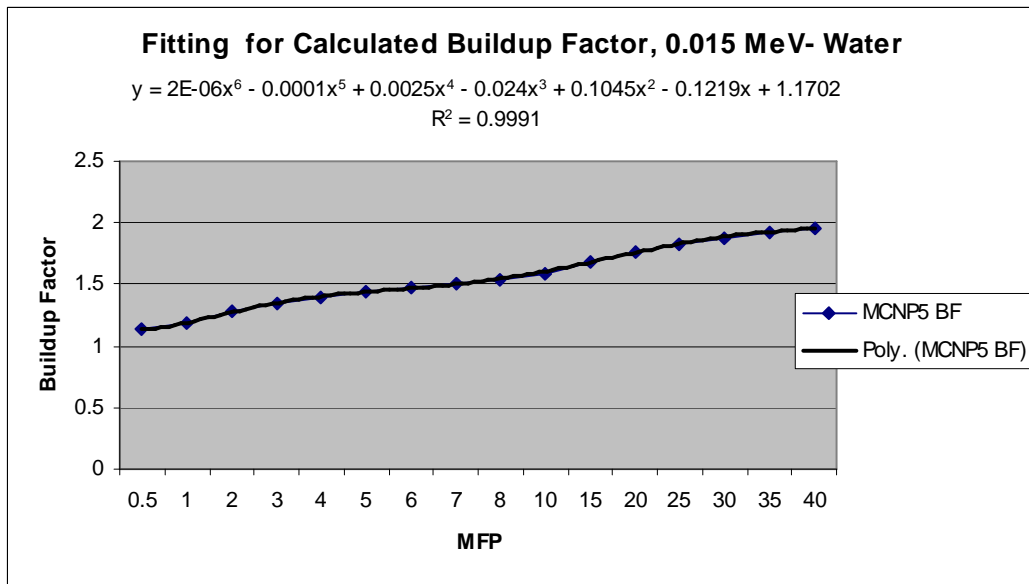


Figure 14pp. Fitting Function for Buildup Factor, Water-0.015 MeV

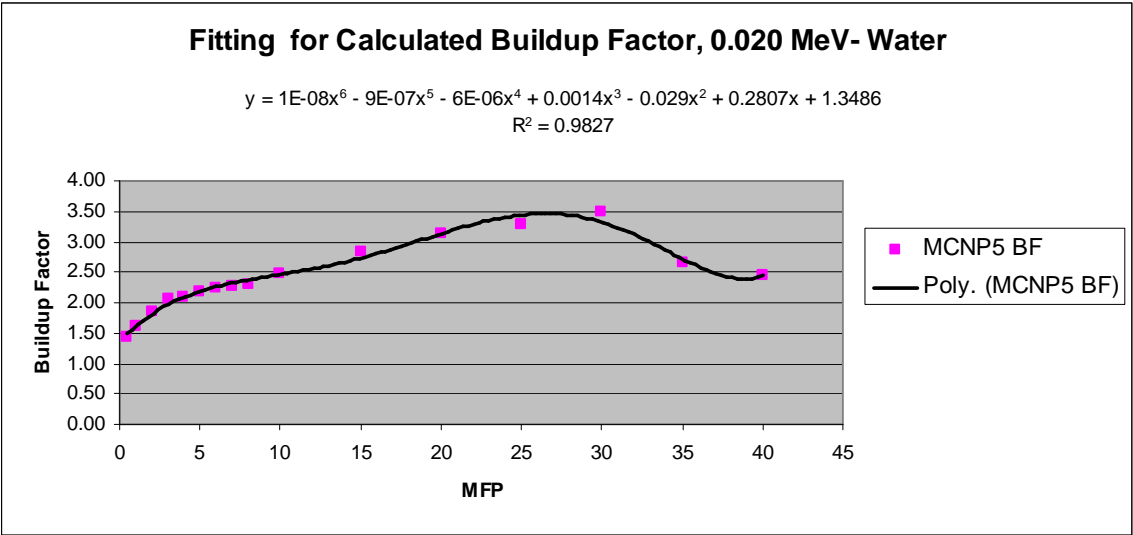


Figure 14qq. Fitting Function for Buildup Factor, Water-0.020 MeV

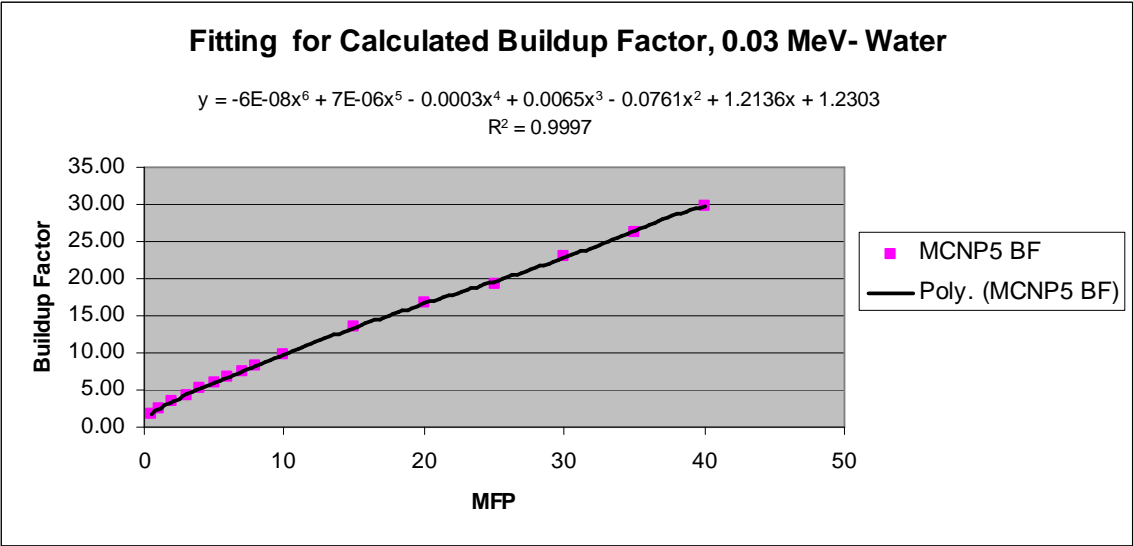


Figure 14rr. Fitting Function for Buildup Factor, Water-0.030 MeV

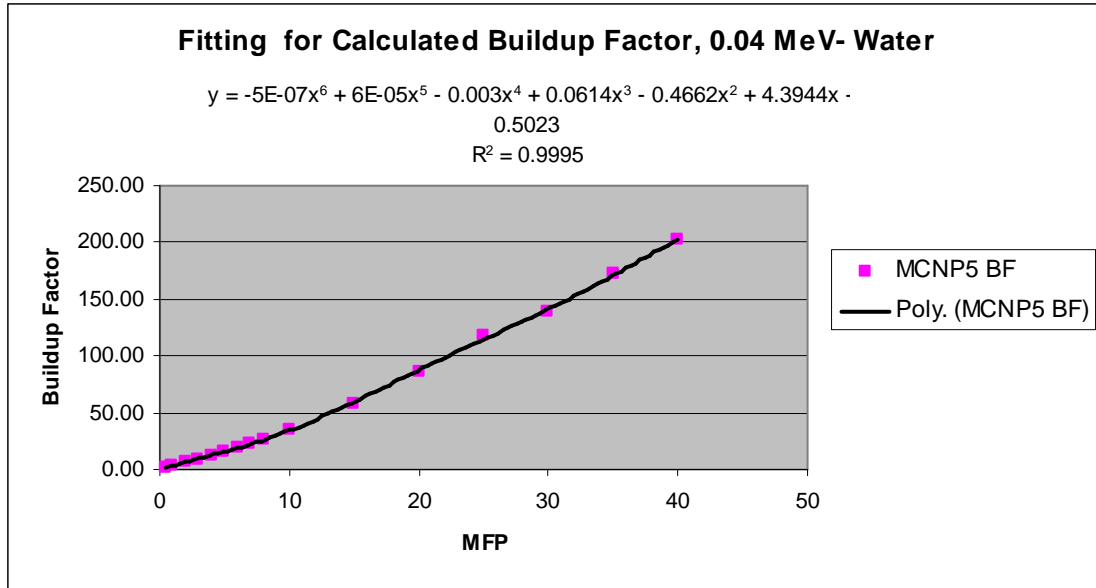


Figure 14ss. Fitting Function for Buildup Factor, Water-0.040 MeV

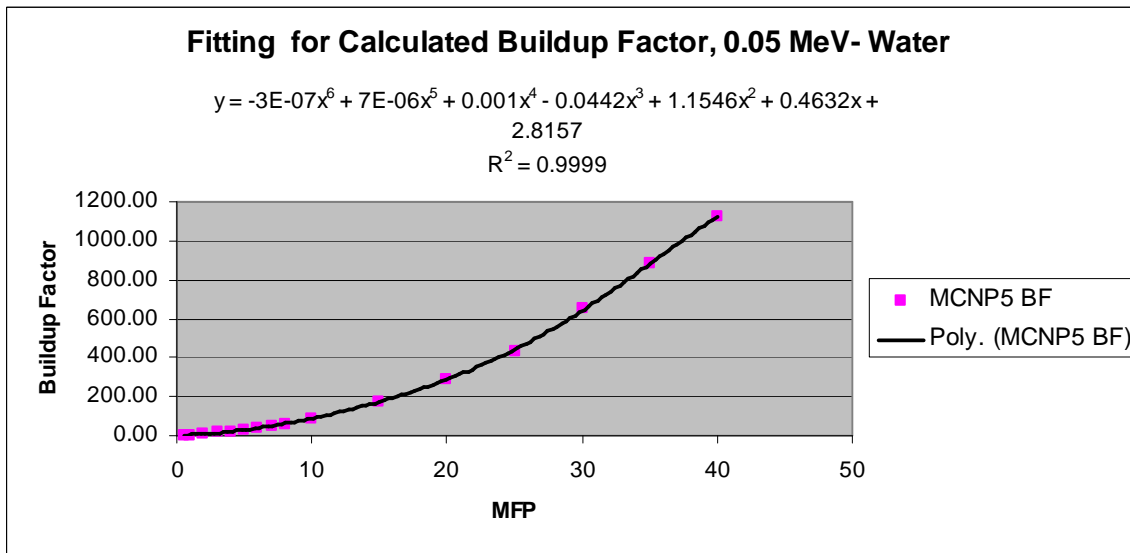


Figure 14tt. Fitting Function for Buildup Factor, Water-0.050 MeV



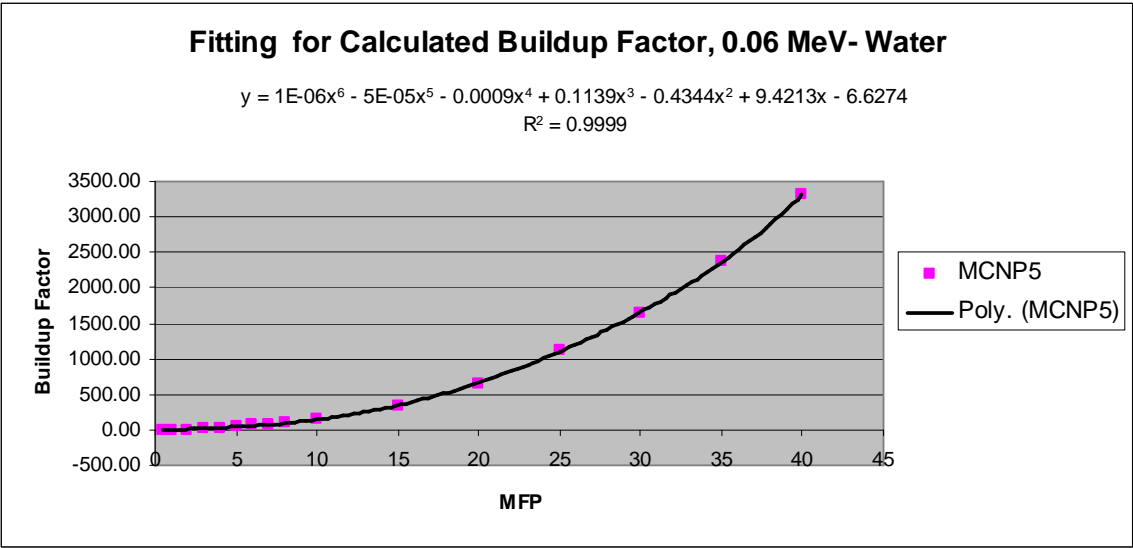


Figure 14uu. Fitting Function for Buildup Factor, Water-0.060 MeV

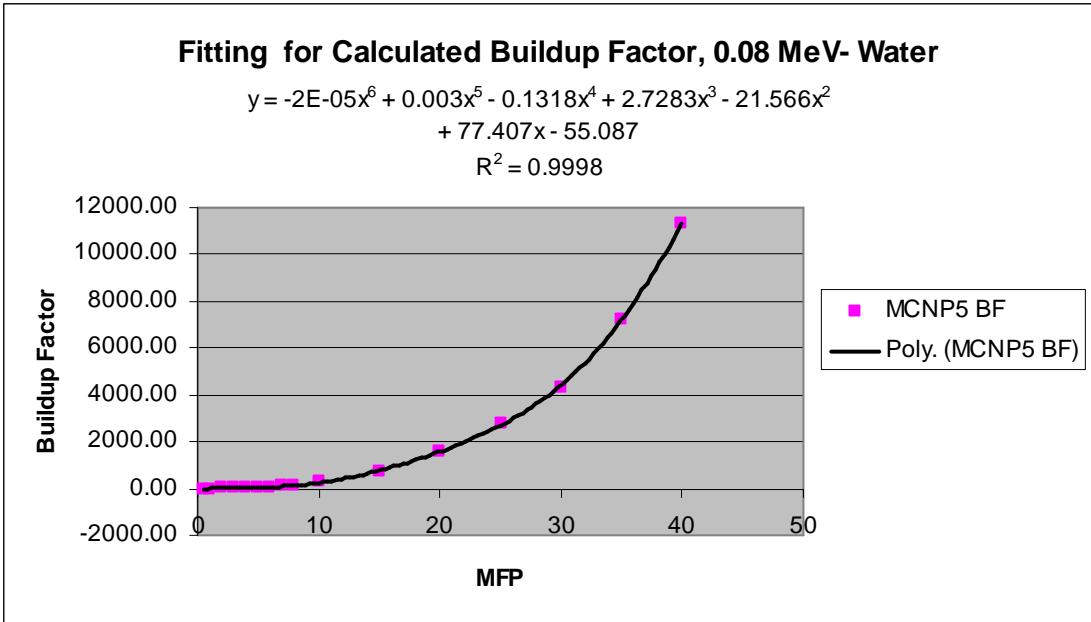


Figure 14vv. Fitting Function for Buildup Factor, Water-0.080 MeV

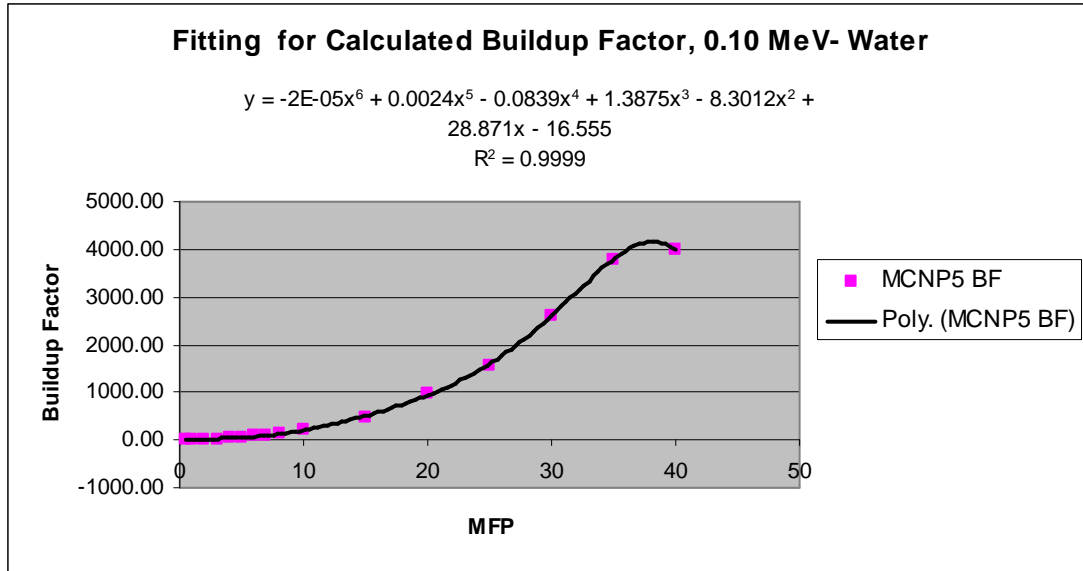


Figure 14ww. Fitting Function for Buildup Factor, Water-0.10 MeV

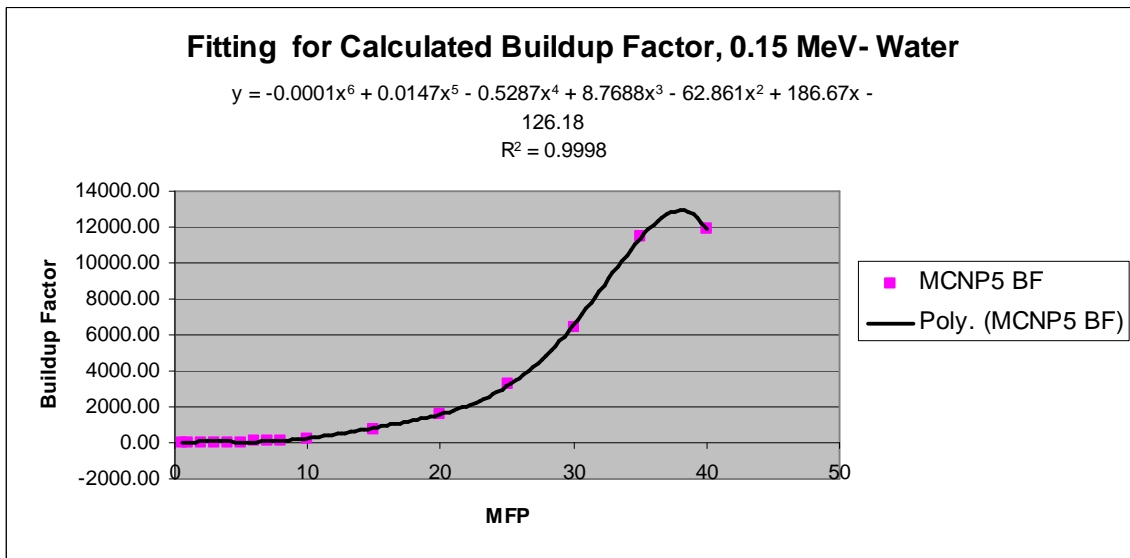


Figure 14xx. Fitting Function for Buildup Factor, Water-0.150 MeV

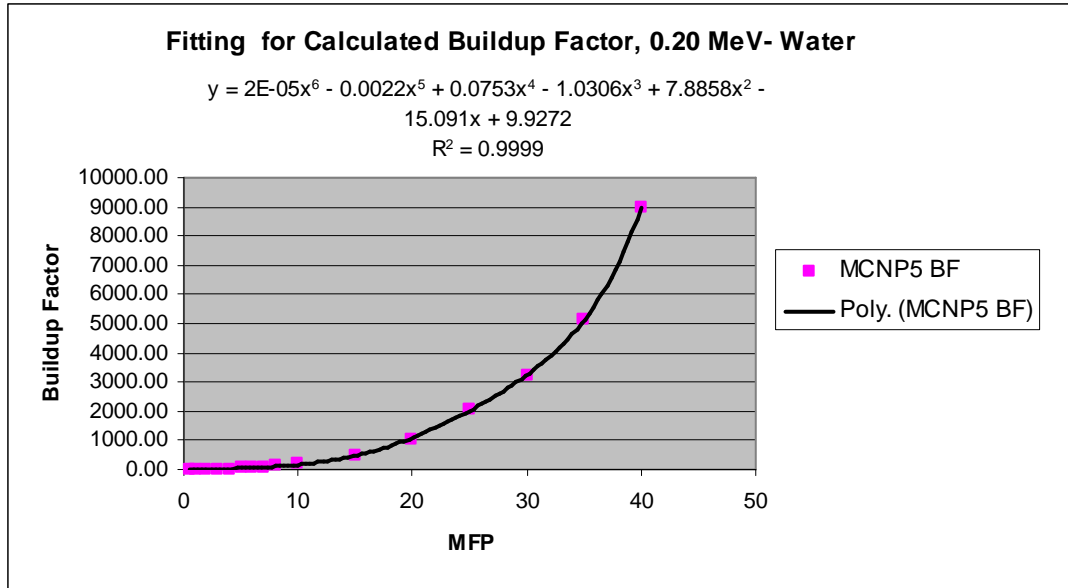


Figure 14yy. Fitting Function for Buildup Factor, Water-0.20 MeV

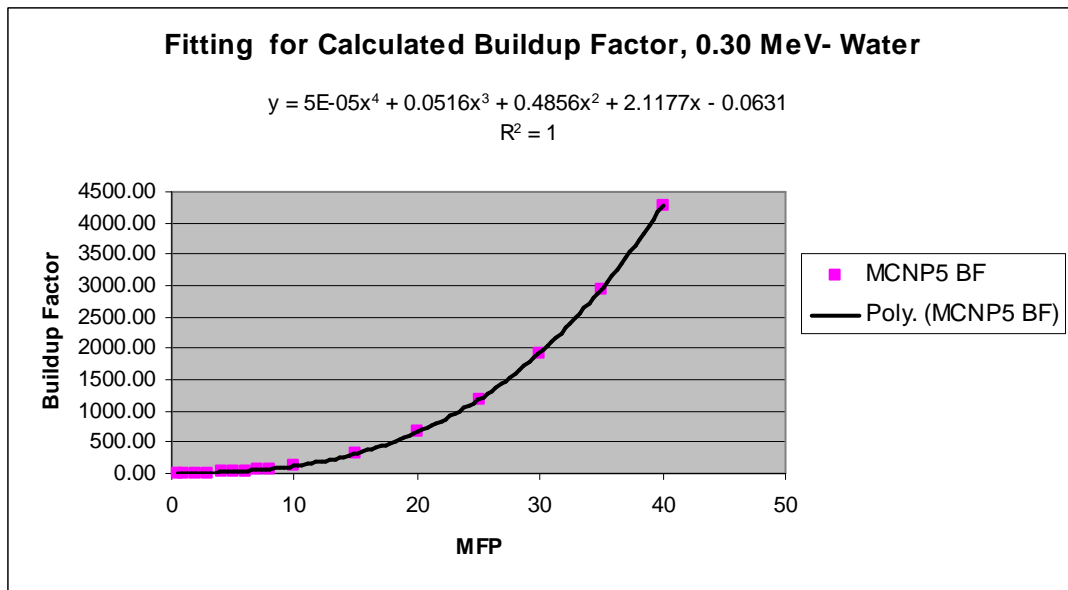


Figure 14zz. Fitting Function for Buildup Factor, Water-0.30 MeV

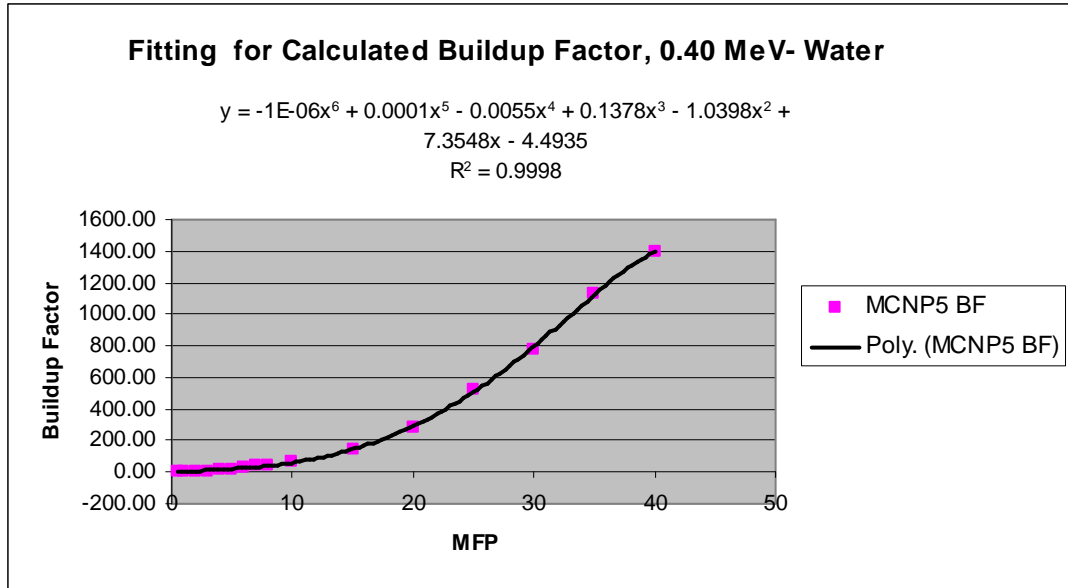


Figure 14ab. Fitting Function for Buildup Factor, Water-0.40 MeV

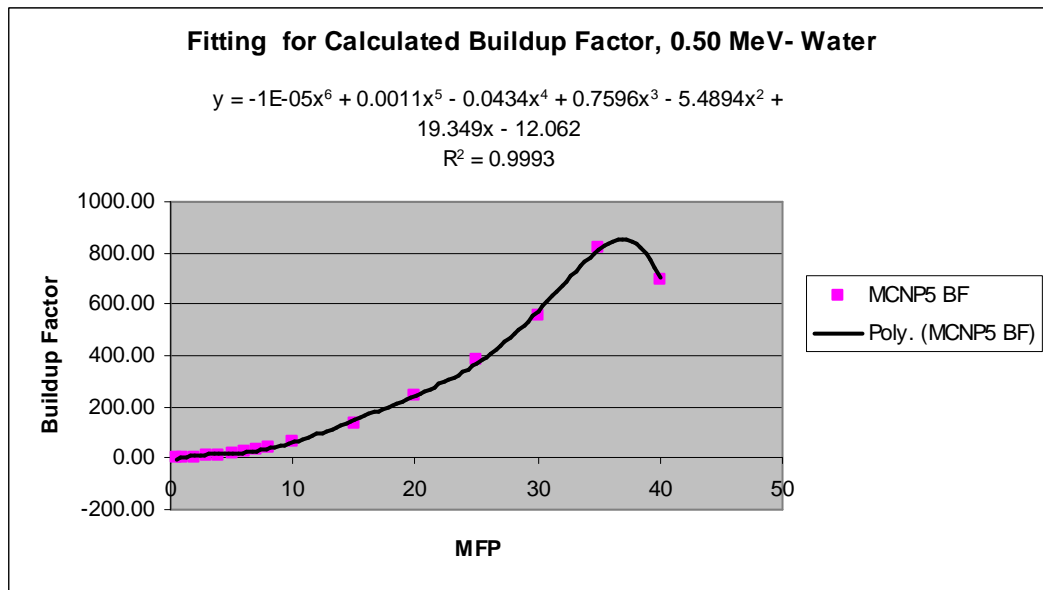


Figure 14ac. Fitting Function for Buildup Factor, Water-0.50 MeV

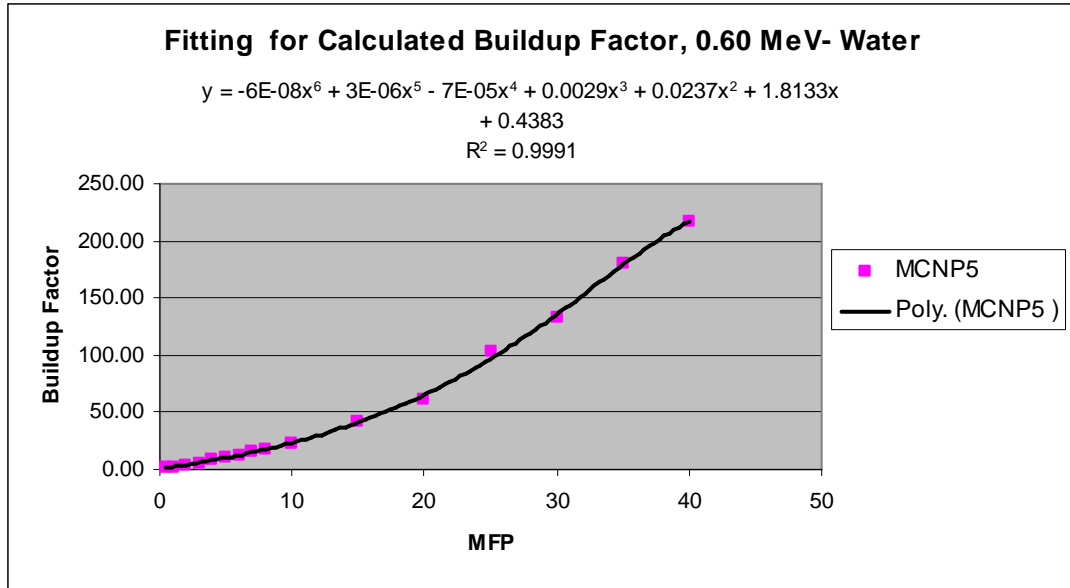


Figure 14ad. Fitting Function for Buildup Factor, Water-0.60 MeV

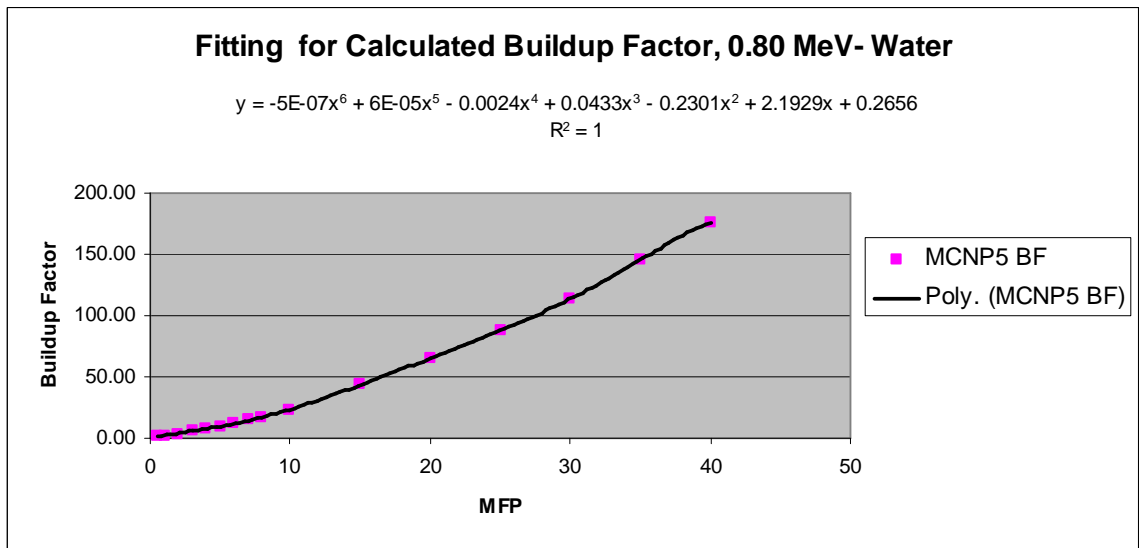


Figure 14ae. Fitting Function for Buildup Factor, Water-0.80 MeV

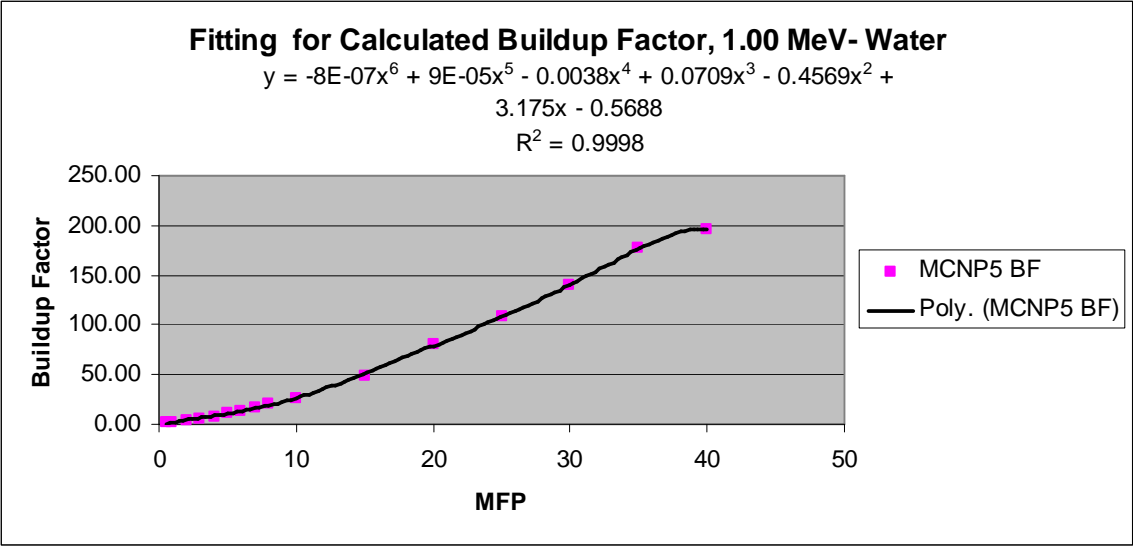


Figure 14af. Fitting Function for Buildup Factor, Water-1.00 MeV

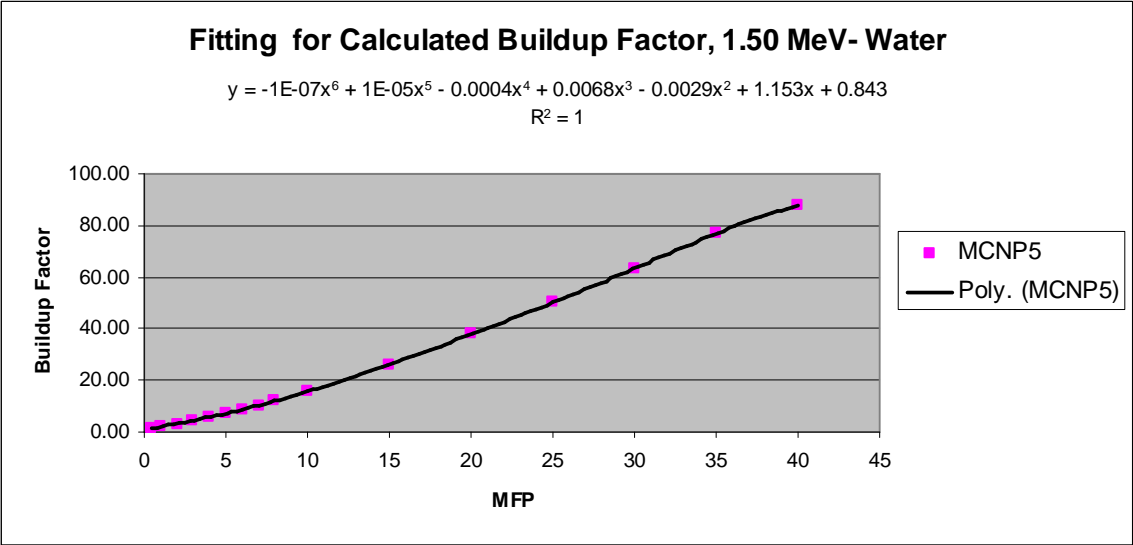


Figure 14ag. Fitting Function for Buildup Factor, Water-1.50 MeV

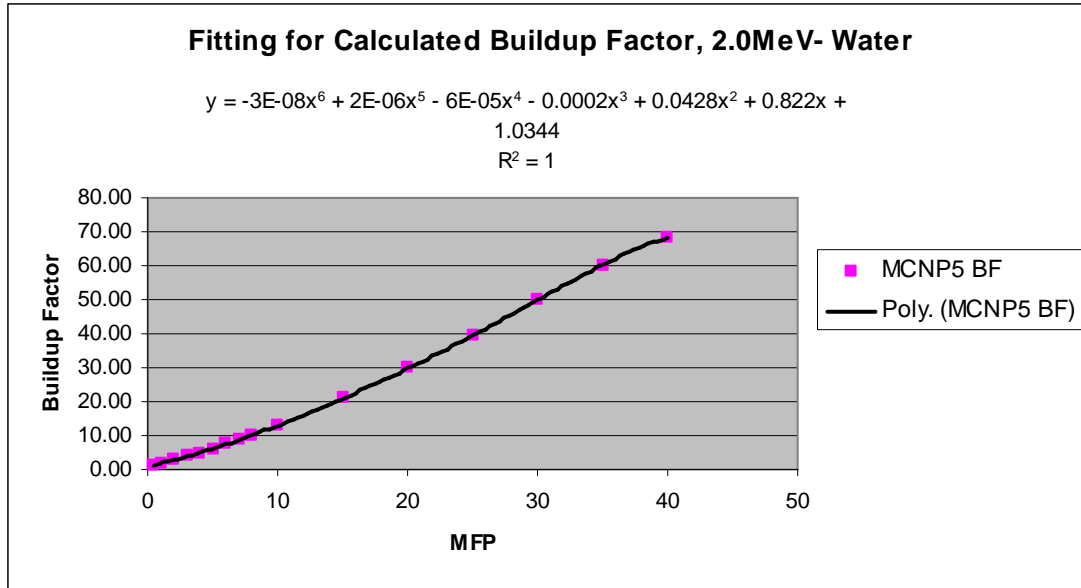


Figure 14ah. Fitting Function for Buildup Factor, Water-2.00 MeV

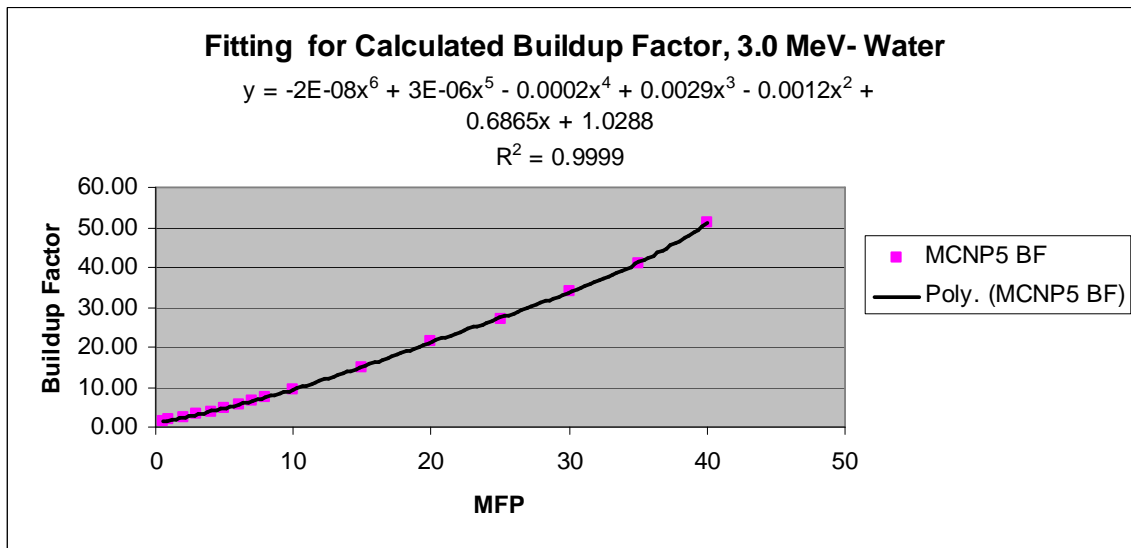


Figure 14ai. Fitting Function for Buildup Factor, Water-3.00 MeV

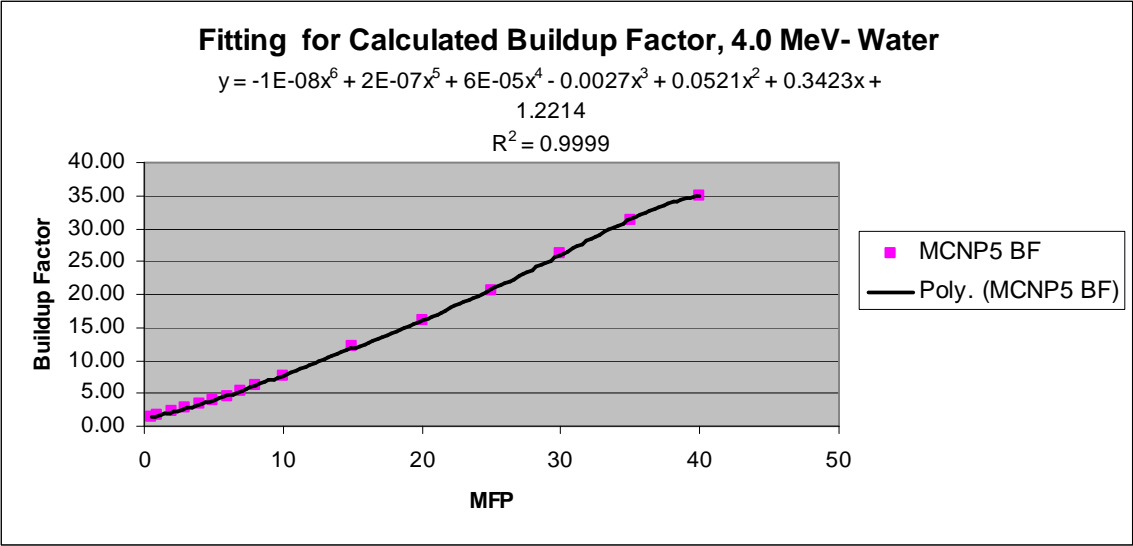


Figure 14aj. Fitting Function for Buildup Factor, Water-4.00 MeV

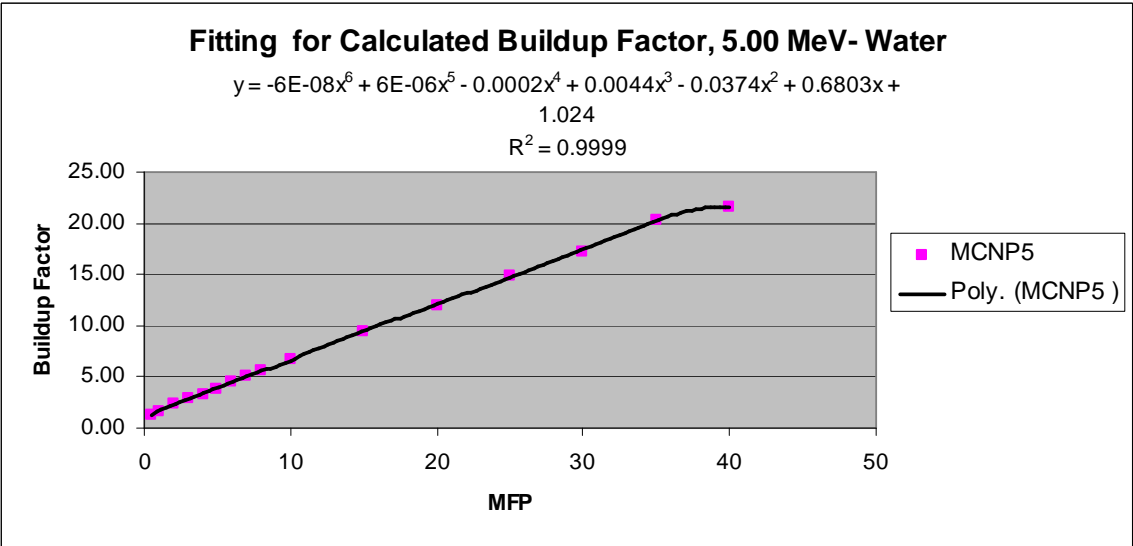


Figure 14ak. Fitting Function for Buildup Factor, Water-5.00 MeV



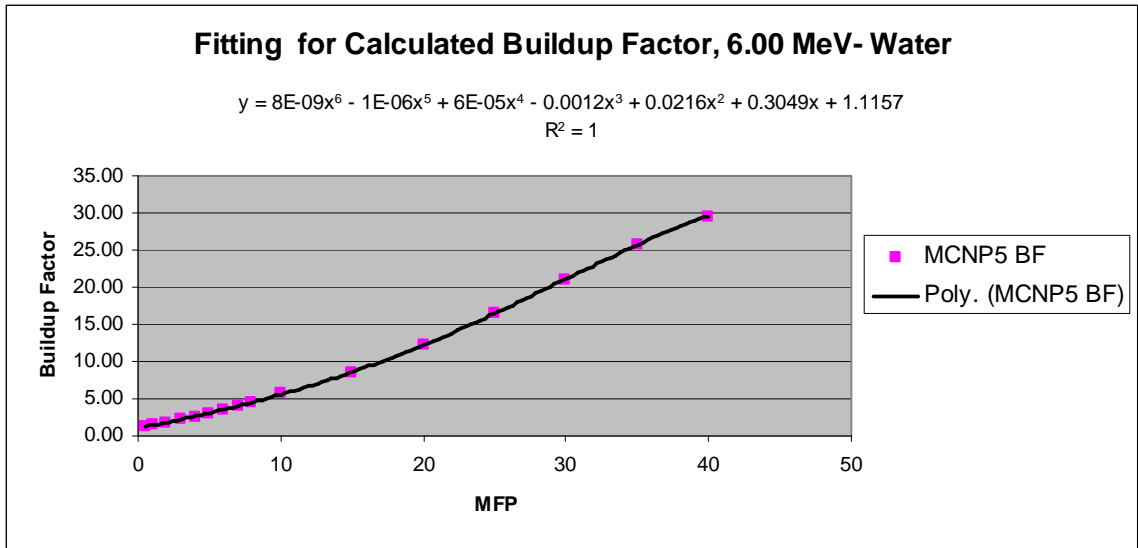


Figure 14al. Fitting Function for Buildup Factor, Water-6.00 MeV

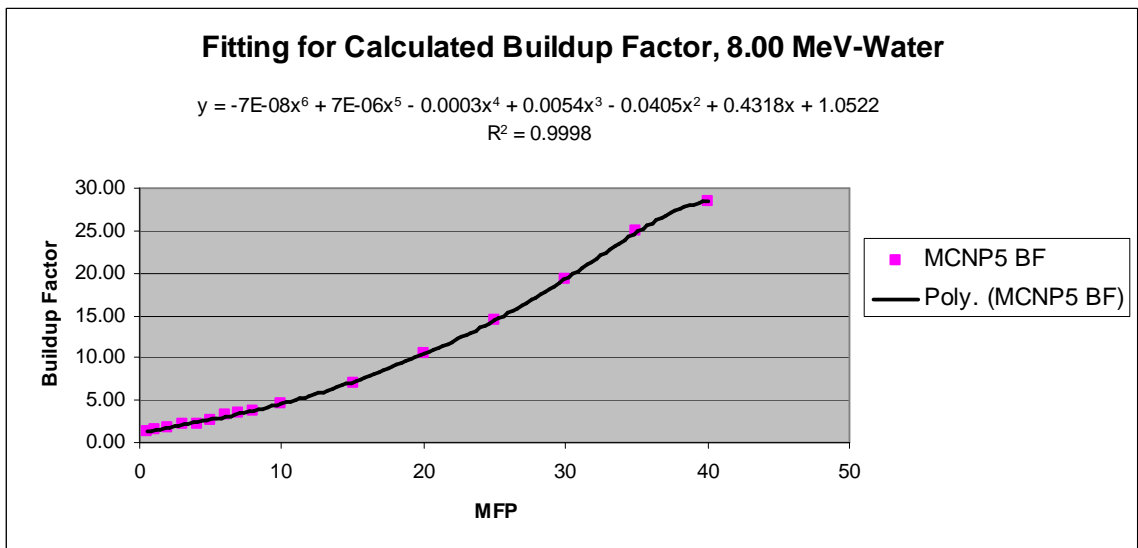


Figure 14am. Fitting Function for Buildup Factor, Water-8.00 MeV

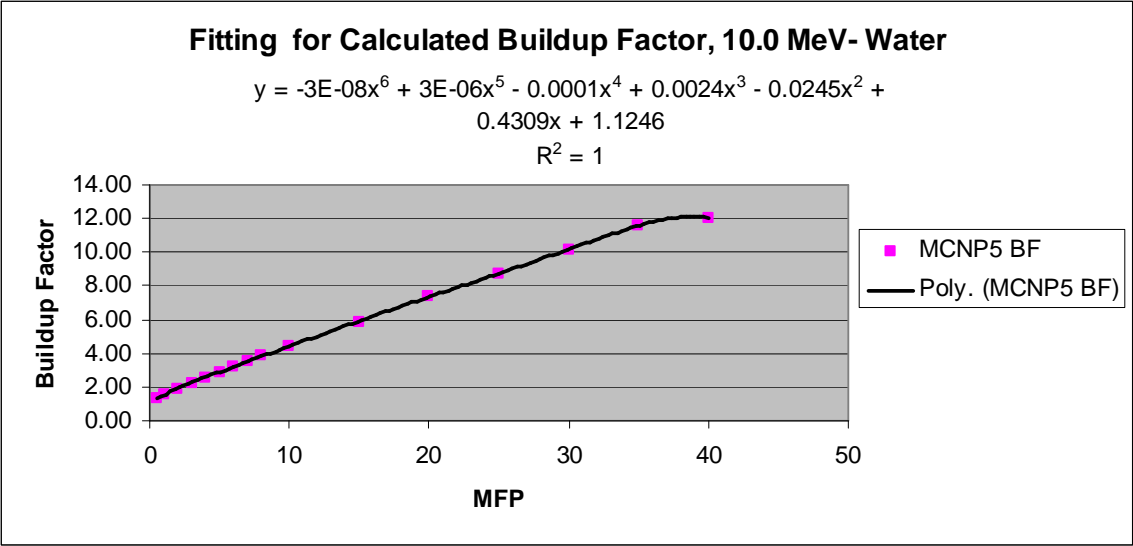


Figure 14an. Fitting Function for Buildup Factor, Water-10.0 MeV

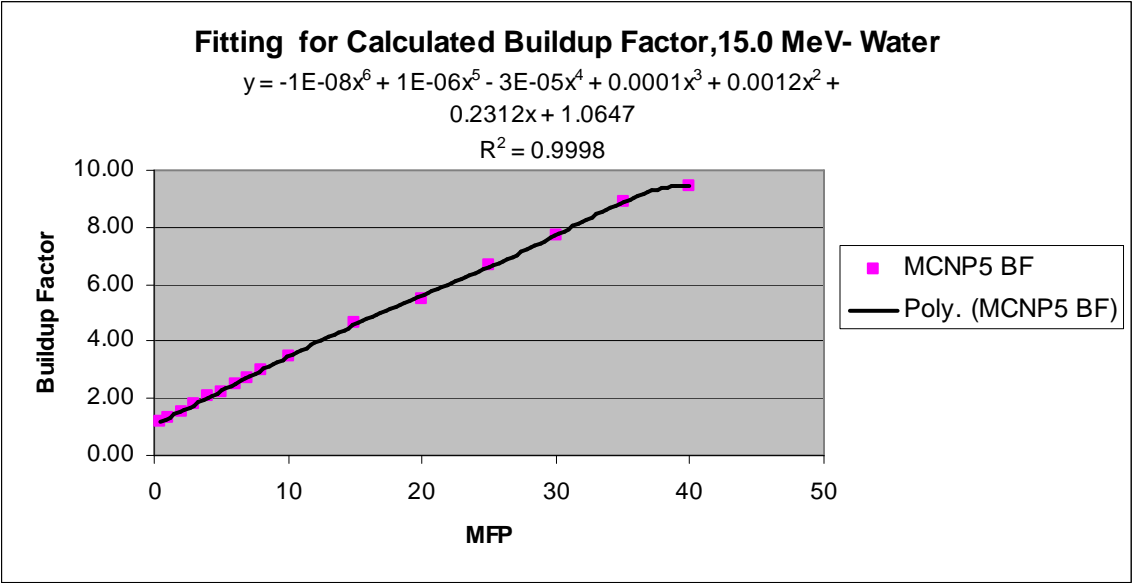


Figure 14ao. Fitting Function for Buildup Factor, Water-15.0 MeV

APPENDIX X

CALCULATION OF MFP- SAMPLE

Table 12. Calculation of MFP

Avogadro's Number, NA=	6.02E+23	(NST)	Density of Fe=	7.87	g/cm <sup>3</sup>	NST	
			Atomic Weight of Fe=	55.87	amu=g/mol	Fundamentals Book, Table II.3	
Energy (MeV)	mfp	Total microscopic cross-sections (barns) (ENDF VI)	Total microscopic cross-sections (cm <sup>2</sup> )	Photon Total Linear Attenuation Coefficients (cm <sup>-1</sup> )	Photon Mass Energy-Absorption Coefficient (cm <sup>2</sup> )	Photon Mass Energy-Absorption Coefficient (cm <sup>2</sup> /g) (NST)	r (cm)
1000	0.50	2.77	2.77E-24	0.24	0.17	0.02	2.13
1000	1.00	2.77	2.77E-24	0.24	0.17	0.02	4.25
1000	2.00	2.77	2.77E-24	0.24	0.17	0.02	8.50
1000	3.00	2.77	2.77E-24	0.24	0.17	0.02	12.75
1000	4.00	2.77	2.77E-24	0.24	0.17	0.02	17.00
1000	5.00	2.77	2.77E-24	0.24	0.17	0.02	21.25
1000	6.00	2.77	2.77E-24	0.24	0.17	0.02	25.50
1000	7.00	2.77	2.77E-24	0.24	0.17	0.02	29.76
1000	8.00	2.77	2.77E-24	0.24	0.17	0.02	34.01
1000	10.00	2.77	2.77E-24	0.24	0.17	0.02	42.51
1000	15.00	2.77	2.77E-24	0.24	0.17	0.02	63.76
1000	20.00	2.77	2.77E-24	0.24	0.17	0.02	85.02
1000	25.00	2.77	2.77E-24	0.24	0.17	0.02	106.27
1000	30.00	2.77	2.77E-24	0.24	0.17	0.02	127.52
1000	35.00	2.77	2.77E-24	0.24	0.17	0.02	148.78
1000	40.00	2.77	2.77E-24	0.24	0.17	0.02	170.03

APPENDIX XI

CALCULATED BUILDUP FACTOR WITHOUT BREHMSSTRAHLUNG

Table 13a. Calculated Buildup Factor w/o Bremsstrahlung, 0.10 MeV-Iron

<b>0.10 MeV Buildup Factors w/o Bremsstrahlung-Iron</b>			
<b>MFP</b>	<b>ANS Standard</b>	<b>Calculated BF</b>	<b>% Difference</b>
0.5	1.38	1.43	3.64%
1	1.6	1.62	1.19%
2	1.94	1.88	3.23%
3	2.13	2.09	1.95%
4	2.31	2.23	3.53%
5	2.48	2.42	2.55%
6	2.63	2.58	1.76%
7	2.77	2.78	0.44%
8	2.9	2.97	2.31%
10	3.13	3.15	0.71%
15	3.61	3.59	0.46%
20	4	3.92	2.01%
25	4.34	4.30	0.99%
30	4.63	4.56	1.46%
35	4.85	4.70	3.16%
40	4.98	4.89	1.86%

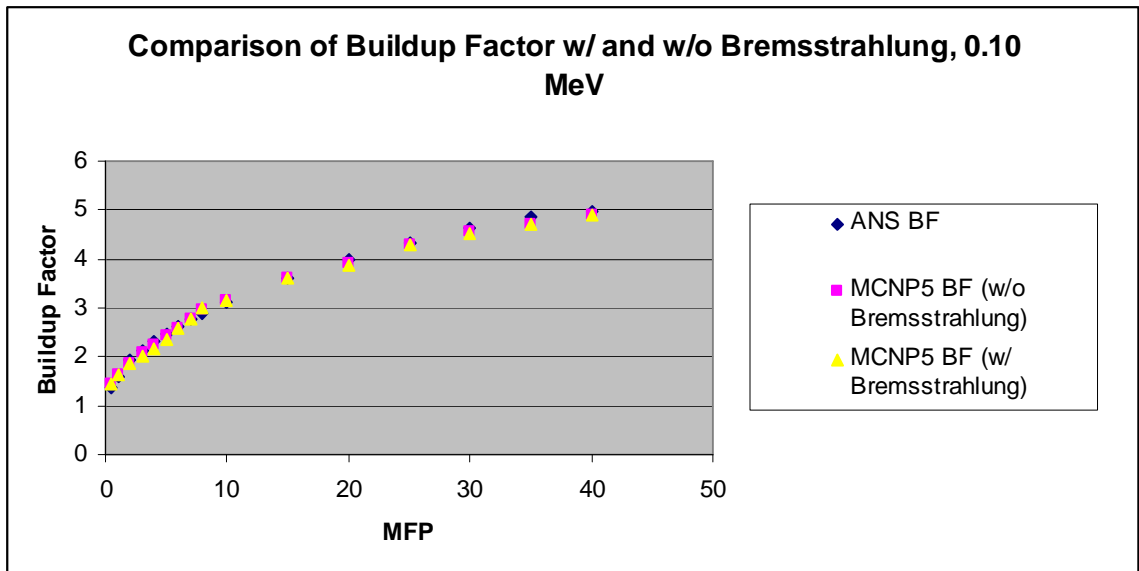


Figure 15a. Comparison of Buildup Factor w/ and w/o Bremsstrahlung, 0.10 MeV-Iron

Table 13b. Calculated Buildup Factor w/o Bremsstrahlung, 1.5 MeV-Iron

1.5 MeV Buildup Factors w/o Bremsstrahlung-Iron			
MFP	ANS Standard	Calculated BF	% Difference
0.5	1.45	1.47	1.47%
1	1.95	1.98	1.52%
2	3.03	3.07	1.42%
3	4.23	4.29	1.45%
4	5.54	5.61	1.33%
5	6.95	7.04	1.27%
6	8.47	8.58	1.32%
7	10.1	10.21	1.06%
8	11.8	11.92	1.00%
10	15.3	15.53	1.47%
15	25.4	25.47	0.29%
20	36.8	36.70	0.27%
25	49.2	48.45	1.55%
30	62.6	61.12	2.42%
35	76.8	75.42	1.83%
40	91.6	89.19	2.70%

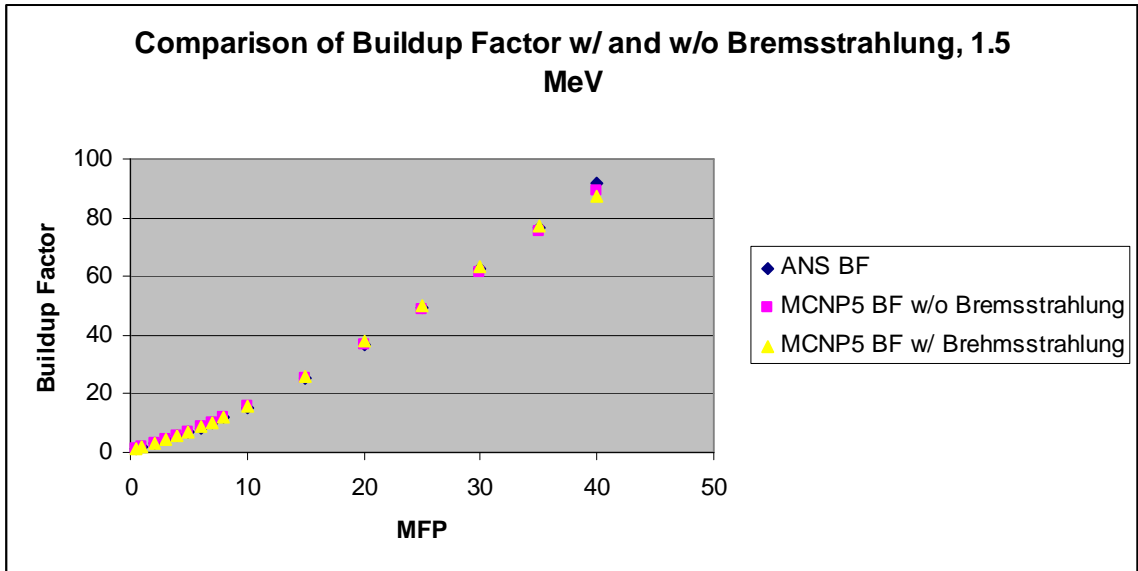


Figure 15b. Comparison of Buildup Factor w/ and w/o Bremsstrahlung, 1.5 MeV-Iron

Table 13c. Calculated Buildup Factor w/o Bremsstrahlung, 5.00 MeV-Iron

5.00 MeV Buildup Factors w/o Bremsstrahlung-Iron			
MFP	ANS Standard	Calculated BF	% Difference
0.5	1.26	1.27	0.43%
1	1.49	1.50	0.95%
2	1.93	1.93	0.24%
3	2.39	2.41	0.64%
4	2.86	2.85	0.20%
5	3.37	3.34	0.90%
6	3.91	3.89	0.51%
7	4.47	4.45	0.45%
8	5.07	5.12	0.93%
10	6.33	6.36	0.49%
15	9.92	9.98	0.60%
20	14.1	13.92	1.29%
25	18.7	18.45	1.36%
30	23.7	23.55	0.64%
35	28.9	28.38	1.84%
40	34	33.43	1.70%

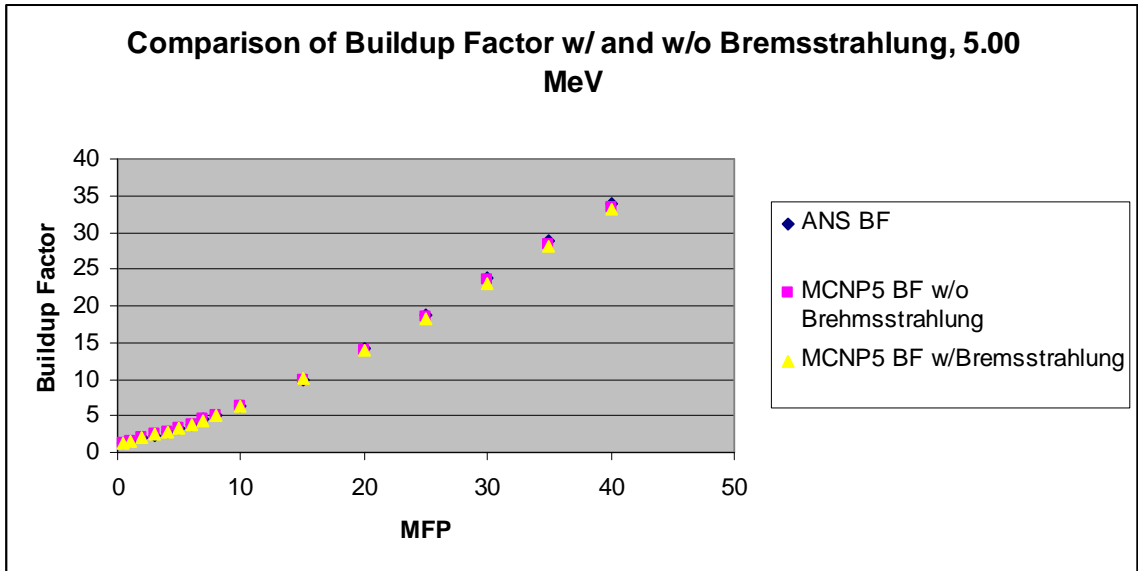


Figure 15c. Comparison of Buildup Factor w/ and w/o Bremsstrahlung, 5.00 MeV-Iron

Table 13d. Calculated Buildup Factor w/o Bremsstrahlung, 10.0 MeV-Iron

10.0 MeV Buildup Factors w/o Bremsstrahlung-Iron			
MFP	ANS Standard	Calculated BF	% Difference
0.5	1.15	1.15	0.40%
1	1.27	1.29	1.88%
2	1.48	1.49	0.67%
3	1.69	1.70	0.59%
4	1.93	1.96	1.64%
5	2.19	2.20	0.53%
6	2.47	2.47	0.04%
7	2.78	2.80	0.67%
8	3.12	3.14	0.64%
10	3.87	3.79	2.02%
15	6.29	6.25	0.59%
20	9.59	9.52	0.72%
25	14	13.87	0.94%
30	19.6	19.18	2.18%
35	26.7	26.30	1.54%
40	35.4	34.52	2.55%

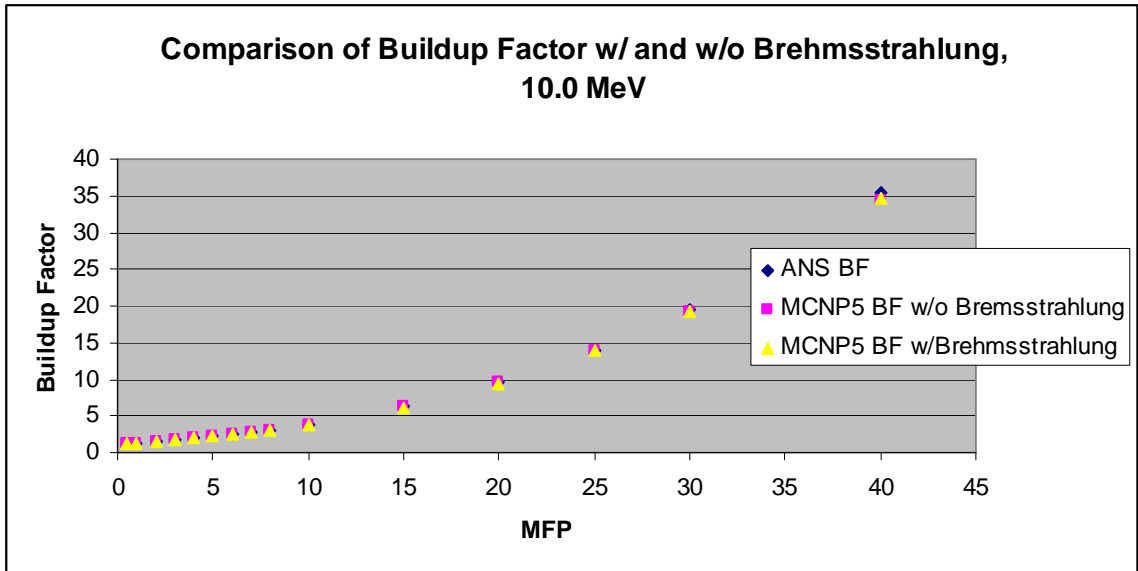


Figure 15d. Comparison of Buildup Factor w/ and w/o Bremsstrahlung, 10.0 MeV-Iron

Table 13e. Calculated Buildup Factor w/o Bremsstrahlung, 15.0 MeV-Iron

<b>15.0 MeV Buildup Factors w/o Bremsstrahlung-Iron</b>			
<b>MFP</b>	<b>ANS Standard</b>	<b>Calculated BF</b>	<b>% Difference</b>
0.5	1.1	1.11	0.45%
1	1.18	1.20	1.67%
2	1.31	1.32	0.86%
3	1.44	1.46	1.59%
4	1.59	1.61	0.96%
5	1.76	1.77	0.81%
6	1.96	1.98	1.17%
7	2.17	2.17	0.16%
8	2.42	2.47	1.92%
10	2.99	3.09	3.21%
15	5.06	5.11	0.98%
20	8.44	8.31	1.54%
25	13.8	13.57	1.67%
30	22.2	21.92	1.27%
35	35	34.53	1.36%
40	54.1	52.43	3.18%

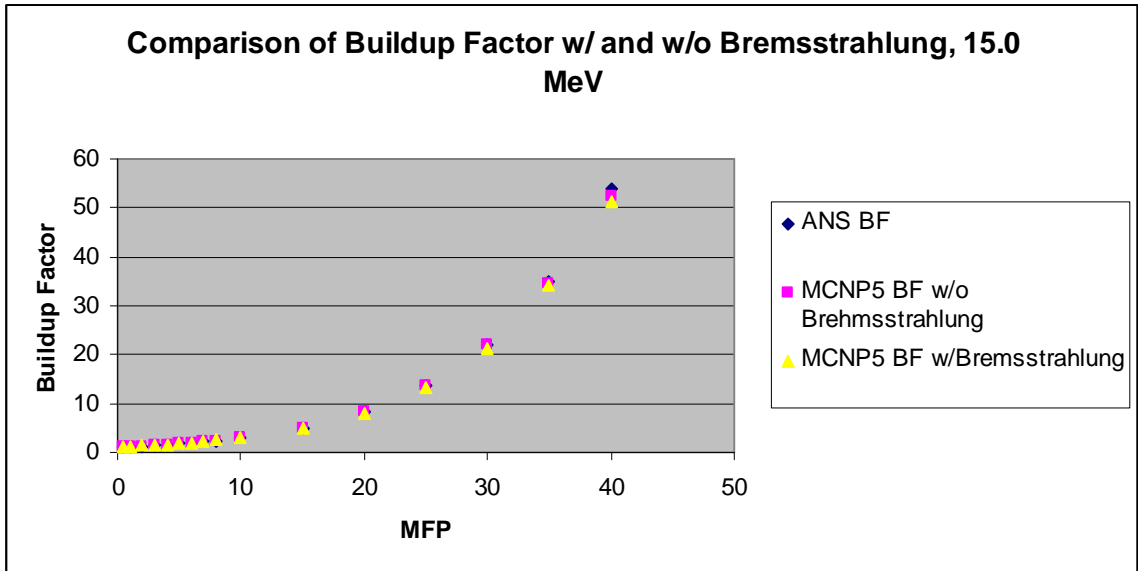


Figure 15e. Comparison of Buildup Factor w/ and w/o Bremsstrahlung, 15.0 MeV-Iron



Table 13f. Calculated Buildup Factor w/o Bremsstrahlung, 0.10 MeV-Water

<b>0.10 MeV Buildup Factors-w/o Bremsstrahlung-H<sub>2</sub>O</b>			
<b>MFP</b>	<b>ANS Standard</b>	<b>Calculated BF</b>	<b>% Difference</b>
0.5	2.36	2.34	0.68%
1	4.52	4.48	0.88%
2	11.70	11.09	5.21%
3	23.50	22.40	4.68%
4	40.60	38.81	4.41%
5	64.00	60.83	4.95%
6	94.80	89.43	5.66%
7	134.00	127.43	4.90%
8	183.00	177.02	3.27%
10	314.00	290.02	7.64%
15	917.00	893.23	2.59%
20	2120.00	2004.93	5.43%
25	4260.00	3976.21	6.66%
30	7780.00	7176.13	7.76%
35	13100.00	11996.72	8.42%
40	20300.00	18902.82	6.88%

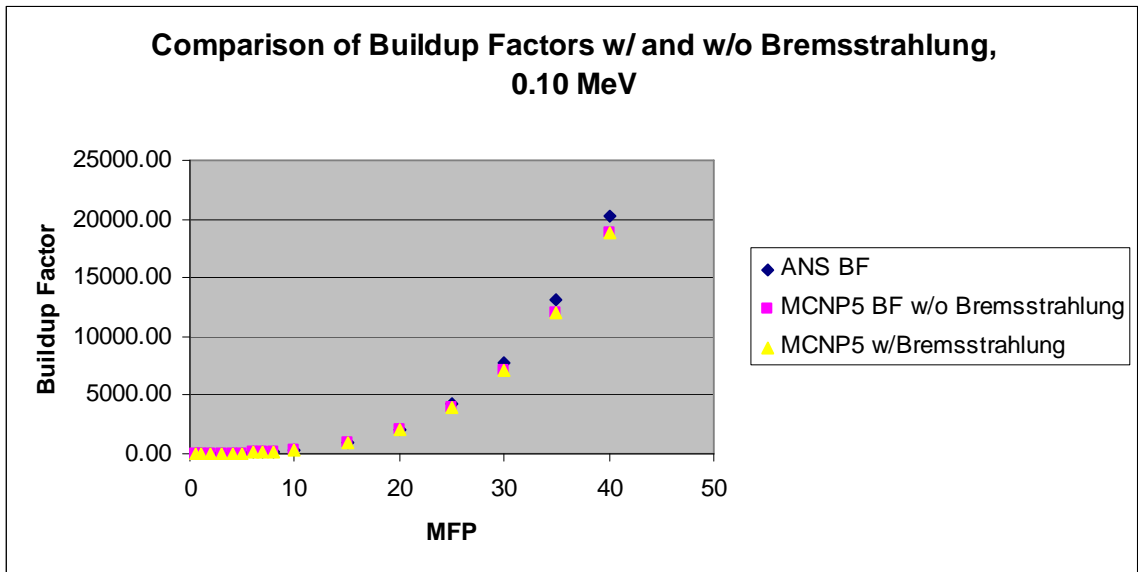


Figure 15f. Comparison of Buildup Factor w/ and w/o Bremsstrahlung, 0.10 MeV-Water

Table 13g. Calculated Buildup Factor w/o Bremsstrahlung, 1.50 MeV-Water

1.5 MeV Buildup Factors-w/o Bremsstrahlung-H <sub>2</sub> O			
MFP	ANS Standard	Calculated BF	% Difference
0.5	1.42	1.45	2.07%
1	1.93	1.98	2.75%
2	3.11	3.12	0.28%
3	4.44	4.39	1.16%
4	5.9	5.72	3.13%
5	7.47	7.21	3.61%
6	9.14	8.71	4.94%
7	10.9	10.42	4.60%
8	12.8	12.31	3.98%
10	16.8	15.75	6.64%
15	27.9	26.12	6.81%
20	40.4	38.12	5.98%
25	54.1	50.02	8.16%
30	68.8	64.61	6.49%
35	84.4	78.12	8.04%
40	101	89.32	13.08%

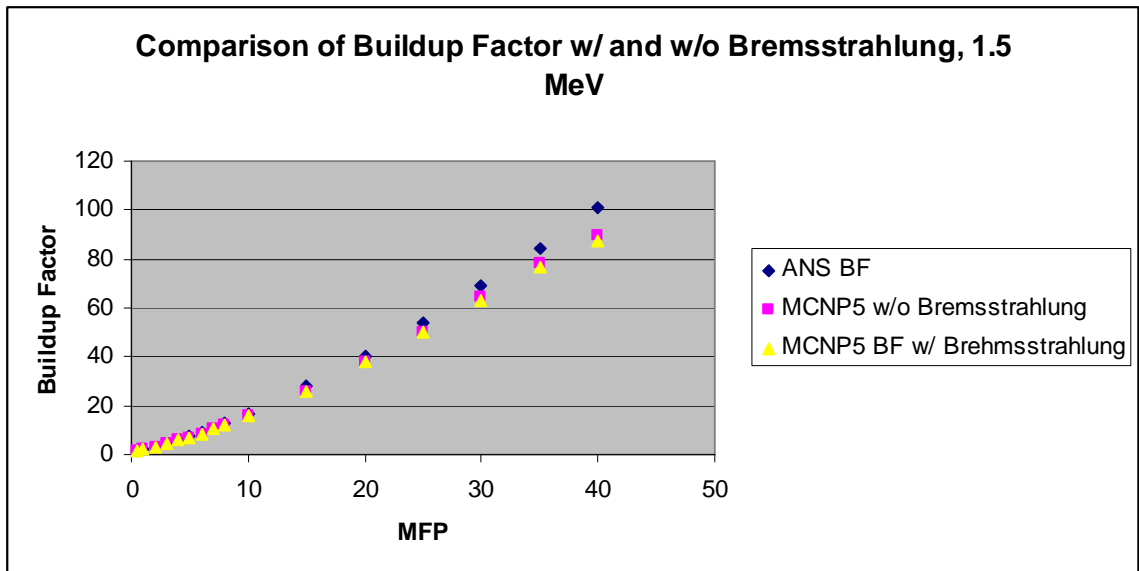


Figure 15g. Comparison of Buildup Factor w/ and w/o Bremsstrahlung, 1.50 MeV-Water

Table 13h. Calculated Buildup Factor w/o Bremsstrahlung, 5.00 MeV-Water

5.00 MeV Buildup Factors w/o Bremsstrahlung-H <sub>2</sub> O			
MFP	ANS Standard	Calculated BF	% Difference
0.5	1.29	1.30	0.93%
1	1.57	1.62	3.09%
2	2.1	2.16	2.92%
3	2.62	2.73	4.17%
4	3.12	3.21	2.81%
5	3.63	3.71	2.16%
6	4.14	4.18	0.96%
7	4.64	4.88	4.98%
8	5.14	5.34	3.80%
10	6.14	6.34	3.19%
15	8.62	9.02	4.43%
20	11.1	11.54	3.84%
25	13.5	14.18	4.80%
30	15.9	16.43	3.24%
35	18.3	19.08	4.09%
40	20.7	21.18	2.28%

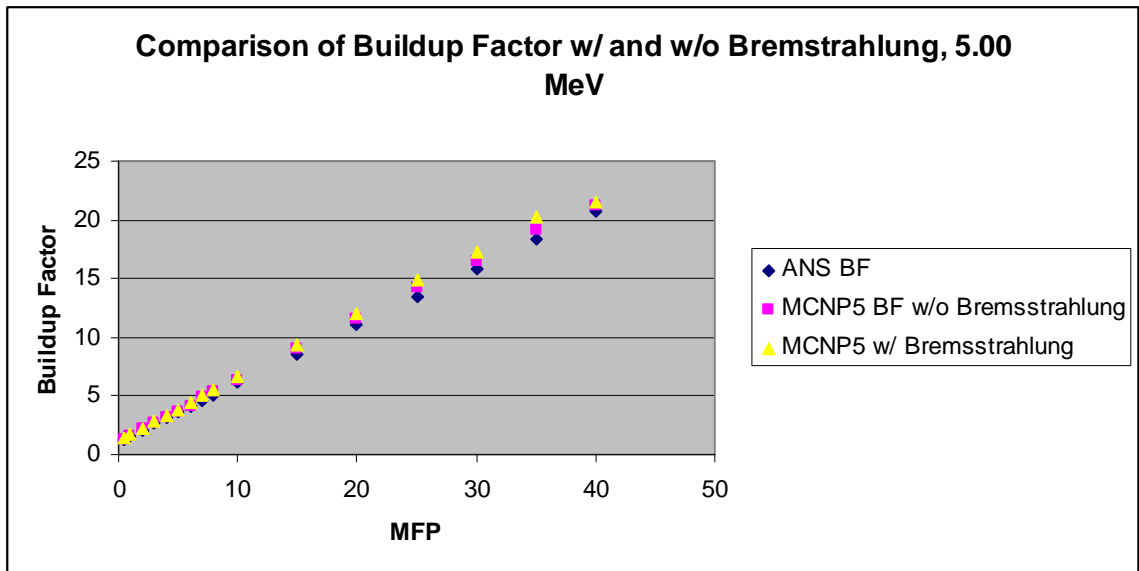


Figure 15h. Comparison of Buildup Factor w/ and w/o Bremsstrahlung, 5.00 MeV-Water

Table 13i. Calculated Buildup Factor w/o Bremsstrahlung, 10.0 MeV-Water

10.0 MeV Buildup Factors-w/o Bremsstrahlung-H <sub>2</sub> O			
MFP	ANS Standard	Calculated BF	% Difference
0.5	1.21	1.22	0.66%
1	1.38	1.42	2.89%
2	1.7	1.73	1.99%
3	2	2.06	2.77%
4	2.29	2.32	1.34%
5	2.57	2.64	2.65%
6	2.85	2.88	1.04%
7	3.13	3.19	1.95%
8	3.4	3.53	3.74%
10	3.94	4.11	4.14%
15	5.24	5.39	2.73%
20	6.51	6.73	3.33%
25	7.75	7.92	2.16%
30	8.97	9.32	3.77%
35	10.2	10.72	4.85%
40	11.3	11.82	4.40%

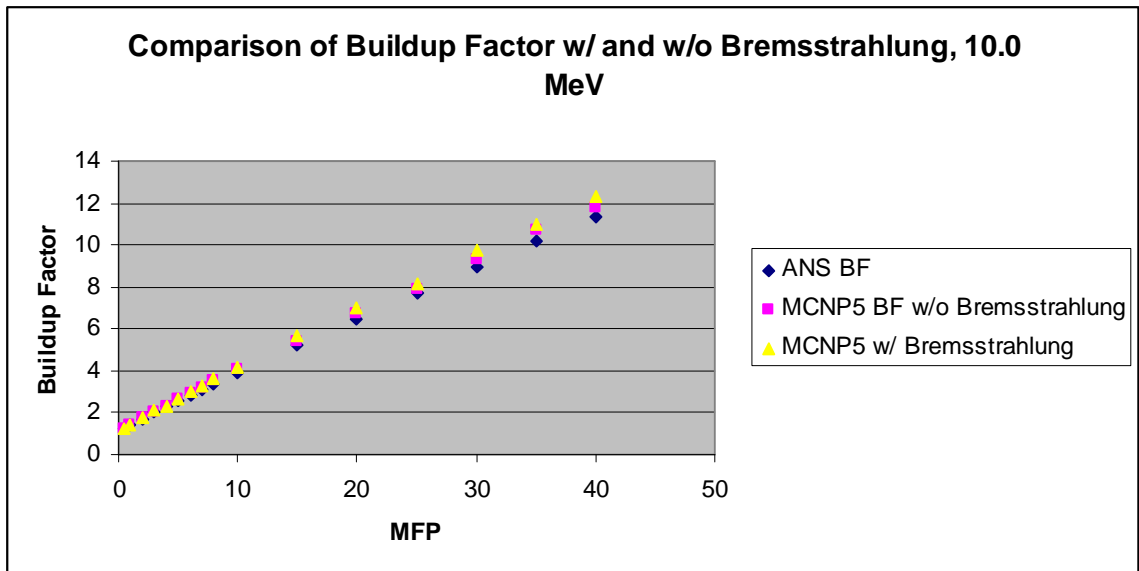


Figure 15i. Comparison of Buildup Factor w/ and w/o Bremsstrahlung, 10.0 MeV-Water

Table 13j. Calculated Buildup Factor w/o Bremsstrahlung, 15.0 MeV-Water

15.0 MeV Buildup Factors- w/o Bremsstrahlung-H <sub>2</sub> O			
MFP	ANS Standard	Calculated BF	% Difference
0.5	1.16	1.14	1.85%
1	1.29	1.30	0.92%
2	1.51	1.53	1.18%
3	1.72	1.76	2.27%
4	1.93	1.98	2.62%
5	2.14	2.20	2.64%
6	2.34	2.38	1.60%
7	2.53	2.64	4.24%
8	2.73	2.84	3.97%
10	3.11	3.18	2.20%
15	4.04	4.10	1.42%
20	4.93	4.98	1.00%
25	5.81	5.91	1.73%
30	6.64	6.75	1.56%
35	7.42	7.67	3.31%
40	8.09	8.53	5.18%

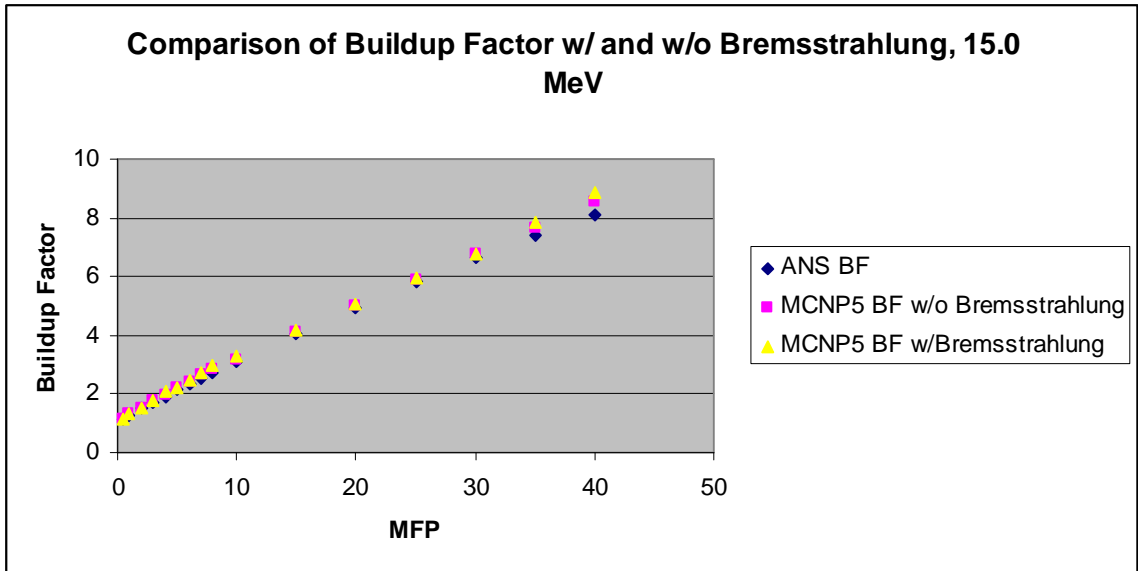


Figure 15j. Comparison of Buildup Factor w/ and w/o Bremsstrahlung, 15.0 MeV-Water

APPENDIX XII

ASFIT AND MCNP5 SAMPLE INPUT FILES

ASFIT-VARI Sample Input File

```
$CARD 1
$ IGRP KS KE KGM
   00  00  00  00
$
$CARD 2
$ NMAX MAXANG KG IG JRG
   06    10    60 16  01
$
$CARD 3
$ ISINDX ISPACE IFLORO IPAIR IBREM IPOINT
   02     01     00    01    01     01
$
$CARD 4
$ TITLE
"BUILDUP FACTOR FOR WATER @ 1.50 MEV"
$
$CARD 5
$ JB(I)
   01
$
$CARD 6
$ IP1 IP2 IP3 IP4 IP5 IP6 IP7 IP8
   01  00  00  01  01  01  00  00
$
$CARD 7
$ NGENR
   01
$
$CARD 8
$ SPEC (K)
  1.500
$
$CARD 9
$ XM(I)
  0.5 1.0 2.0 3.0 4.0 5.0 6.0 7.0 8.0 10.0 15.0 20.0 25.0 30.0 35.0 40.0
$
$CARD 10
$ CROSS SECTION INPUT
$ WATER REGION
```

\$  
 \$CARD 11  
 \$ IEL(I)  
   01  
 \$  
 \$CARD 12  
 \$ RHO(I)  ZE(I)  A(I)  
   1.00    1.0   18.0  
 \$  
 \$CARD 13  
 \$ NOE(I)  
   25  
 \$  
 \$CARD 14  
 \$ EN(I,N)  
 1.500-2 2.000-2 3.000-2 4.000-2 5.000-2 6.000-2 8.000-2 1.000-1 1.500-1 2.000-1  
 3.000-1 4.000-1 5.000-1 6.000-1 8.000-1 1.00000 1.50000 2.00000 3.00000 4.00000  
 5.00000 6.00000 8.00000 10.0000 15.0000  
 \$  
 \$CARD 15  
 \$ STE (I,N)  
 1.27000 5.050-1 1.380-1 5.480-2 2.670-2 1.500-1 5.950-3 2.850-3 7.760-4 3.110-4  
 8.860-5 3.780-5 2.040-5 1.280-5 6.420-6 3.980-6 1.860-6 1.180-6 6.620-7 4.510-7  
 3.440-7 2.750-7 1.970-7 1.540-7 1.109-7  
 \$  
 \$CARD 16  
 \$ ST(I,N)  
 0.00000 0.00000 0.00000 0.00000 0.00000 0.00000 0.00000 0.00000 0.00000 0.00000  
 0.00000 0.00000 0.00000 0.00000 0.00000 0.00000 9.860-5 3.930-4 1.130-3 1.830-3  
 2.430-3 3.000-3 3.930-3 4.690-3 6.110-3  
 \$  
 \$CARD 17  
 \$ EABS(I,N)  
 1.480+0 7.110-1 3.380-1 2.480-1 2.140-1 1.970-1 1.790-1 1.680-1 1.490-1 1.360-1  
 1.180-1 1.060-1 9.670-2 8.950-2 7.860-2 7.070-2 5.750-2 4.940-2 3.970-2 3.400-2  
 3.030-2 2.770-2 2.430-2 2.220-2 1.940-2  
 0.00,0.000,0.000,0.000  
 4.70000 1.28000 0.51200 0.14900 0.06780 0.04190 0.03200 0.02620 0.02560 0.02770  
 0.02970 0.03190 0.03280 0.03300 0.03290 0.03210 0.03110 0.02850 0.02640 0.02340  
 0.02140 0.02000 0.01900 0.01760 0.01680  
 0.50000 0.00000 0.00000 0.00000 0.00000 0.00000 0.00000 0.00000 0.00000 0.00000  
 0.00000 0.00000 0.00000 0.00000 0.00000 0.00000 0.00000 0.02620 0.02290 0.02090  
 0.01950 0.01850 0.01700 0.01570 0.01450  
 0.50000 0.00000 0.00000 0.00000 0.00000 0.00000 0.00000 0.00000 0.00000 0.00000  
 0.00000 0.00000 0.00000 0.00000 0.00000 0.03090 0.02820 0.02600 0.02270 0.02060  
 0.01910 0.01800 0.01660 0.01570 0.01480

MCNP5 Sample Input File

**C IRON INFINITE MEDIUM 2.00 MEV UP TO 40 MFP**

1 1 -7.874 -1 \$INNER SPHERE 1  
2 1 -7.874 1 -2 \$\$HELL 2  
3 1 -7.874 2 -3 \$\$HELL 3  
4 1 -7.874 3 -4 \$\$HELL 4  
5 1 -7.874 4 -5 \$\$HELL 5  
6 1 -7.874 5 -6 \$\$HELL 6  
7 1 -7.874 6 -7 \$\$HELL 7  
8 1 -7.874 7 -8 \$\$HELL 8  
9 1 -7.874 8 -9 \$\$HELL 9  
10 1 -7.874 9 -10 \$\$HELL 10  
11 1 -7.874 10 -11 \$\$HELL 11  
12 1 -7.874 11 -12 \$\$HELL 12  
13 1 -7.874 12 -13 \$\$HELL 13  
14 1 -7.874 13 -14 \$\$HELL 14  
15 1 -7.874 14 -15 \$\$HELL 15  
16 1 -7.874 15 -16 \$\$HELL 16  
17 1 -7.874 16 -17 \$\$HELL 17  
18 1 -7.874 17 -18 \$\$HELL 18  
19 1 -7.874 18 -19 \$\$HELL 19  
20 1 -7.874 19 -20 \$\$HELL 20  
21 1 -7.874 20 -21 \$\$HELL 21  
22 1 -7.874 21 -22 \$\$HELL 22  
23 1 -7.874 22 -23 \$\$HELL 23  
24 1 -7.874 23 -24 \$\$HELL 24  
25 1 -7.874 24 -25 \$\$HELL 25  
26 1 -7.874 25 -26 \$\$HELL 26  
27 1 -7.874 26 -27 \$\$HELL 27  
28 1 -7.874 27 -28 \$\$HELL 28  
29 1 -7.874 28 -29 \$\$HELL 29  
30 1 -7.874 29 -30 \$\$HELL 30  
31 1 -7.874 30 -31 \$\$HELL 31  
32 1 -7.874 31 -32 \$\$HELL 32  
33 1 -7.874 32 -33 \$\$HELL 33  
34 1 -7.874 33 -34 \$\$HELL 34  
35 1 -7.874 34 -35 \$\$HELL 35  
36 1 -7.874 35 -36 \$\$HELL 36  
37 1 -7.874 36 -37 \$\$HELL 37  
38 1 -7.874 37 -38 \$\$HELL 38  
39 1 -7.874 38 -39 \$\$HELL 39  
40 1 -7.874 39 -40 \$\$HELL 40  
41 0 40 -41 \$OUTSIDE OF MATERIAL BUT WITHIN LIMIT OF SPACE  
42 0 41 \$OUTSIDE SPACE LIMIT



**C ALL MFP @ 2.00 MEV IN FE**

1 SO 1.4923 \$0.5 MFP  
2 SO 2.9846 \$1 MFP  
3 SO 4.5000 \$  
4 SO 5.9692 \$2 MFP  
5 SO 7.9692 \$  
6 SO 8.9538 \$3 MFP  
7 SO 9.4575 \$  
8 SO 11.9384 \$ 4 MFP  
9 SO 13.4500 \$  
10 SO 14.9230 \$5 MFP  
11 SO 16.500 \$  
12 SO 17.9076 \$6 MFP  
13 SO 18.9000 \$  
14 SO 19.9500 \$  
15 SO 20.8922 \$7 MFP  
16 SO 21.8500 \$  
17 SO 22.8500 \$  
18 SO 23.8768 \$8 MFP  
19 SO 25.5000 \$  
20 SO 27.7500 \$  
21 SO 29.8460 \$10 MFP  
22 SO 33.5000 \$  
23 SO 37.3450 \$  
24 SO 41.5000 \$  
25 SO 44.7690 \$15 MFP  
26 SO 52.5000 \$  
27 SO 59.6920 \$20 MFP  
28 SO 64.5000 \$  
29 SO 69.5000 \$  
30 SO 74.6150 \$25 MFP  
31 SO 79.5000 \$  
32 SO 84.7500 \$  
33 SO 89.5380 \$30 MFP  
34 SO 94.7500 \$  
35 SO 99.9500 \$  
36 SO 104.461 \$35 MFP  
37 SO 109.570 \$  
38 SO 114.750 \$  
39 SO 119.384 \$40 MFP  
40 SO 120.000 \$  
41 SO 125.000 \$LIMIT OF SPACE  
C

MODE P

IMP:P 1 1 12 15 20 31 39 46 82 121 179 275 400 526 706

924 1215 1618 2207 3579 6882 13128 39098  
124636 436431 1240827 13509002 130152027 571718517  
2825636379 13765920821 59494929562 311014873159  
1326386959059 4509715660800 18038862643200 180388626432000  
1443109011456000 2886218022912000 5772436045824000 0 0

C

M1 26000.04P 1.

C M1 26000 1.

C

SDEF POS 0 0 0 ERG 2.00

C

FC2 DOSE AT MFP

C

F2:P 1 2 4 6 8 10 12 15 18 21 25 27 30 33 36 39

C

FT2 INC \$DETERMINE WHICH PARTICLES HAVE COLLIDED

FU2 0 10E6 T \$DISCRIMINATE PARTILCES BY COLLISIONS

FQ2 F U

FC12 UNCOLLIDED DOSE

F12:P 1 2 4 6 8 10 12 15 18 21 25 27 30 33 36 39

E12 1.999 2.00 T

FQ12 F U

C

C GAMMA DOSE FUNCTION CARDS SPREADSHEET, CALCULATED

DE 0.01 0.02 0.03 0.05 0.08 0.10 0.15

0.20 0.30 0.35 0.40 0.45 0.50 0.55

0.60 0.65 0.70 0.80 1.00 1.40 1.80

2.20 2.60 2.80 3.25 3.75 4.25 4.75

5.00 5.25 5.50 6.31 6.75 7.00 9.00

11.0 13.0 15.0 20.0

C

DF 2.19-9 7.24-10 3.48-10 1.31-10 5.26-11 3.49-11 1.91-11

1.55-11 1.62-11 1.79-11 1.95-11 2.14-11 2.33-11 2.53-11

2.73-11 2.92-11 3.11-11 3.48-11 4.17-11 5.38-11 6.51-11

7.62-11 8.73-11 9.28-11 1.06-11 1.20-11 1.35-11 1.51-11

1.59-11 1.67-11 1.75-11 2.03-11 2.18-11 2.27-11 3.00-11

3.76-11 4.54-11 5.34-11 7.34-11

C

PRDMP 2J -1

PRINT

NPS 1000000

APPENDIX XIII

ASFIT USER'S GUIDE

Table 14. Description of Cards

CARD #	CARD DESCRIPTION
<b>CARD 1</b>	
IGRP	00 REFERS TO POINT CROSS SECTION, 01 IS GROUP CROSS SECTION DATA
KS	STARTING ENERGY OF WHICH CALCULATIONS WILL BE DONE, MEV
KE	ENDING ENERGY OF WHICH CALCULATIONS WILL BE DONE, MEV
KGM	OMIT IF IGRP=00, IF NOT THIS DIVIDES THE CROSS SECTION INTO ENERGY GROUPS
<b>CARD 2</b>	
NMAX	ORDER OF LEGENDRE POLYNOMIAL EXPANSION OF THE FLUX
MAXANG	NUMBER OF ANGULAR NODES IN GAUSSIAN ANGULAR FLUX
KG	NUMBER OF ENERGY NODES
IG	NUMBER OF SPACE NODES
JRG	NUMBER OF MATERIAL REGIONS ( $\leq 4$ )
<b>CARD 3</b>	
ISINDX	SPECIFICATION OF SOURCE TYPE: 1- NORMAL INCIDENCE, 2- PLANE ISOTROPIC FLUX, 3- PLANE ISOTROPIC DISTRIBUTED SOURCE
ISPACE	SPECIFICATION FOR SYSTEM THICKNESS, 0- IN MFP, 1- IN CENTIMETERS
IFLORO	INCLUSION OF K X-RAYS, 1- INCLUDES IT, 0-NOT INCLUDED
IPAIR	INCLUSION OF ANNIHILATION PHOTONS, 1-INCLUDED, 0-NOT INCLUDED
IBREM	INCLUSION OF BREMSSTRAHLUNG, 1-INCLUDED, 0-NOT INCLUDED
IPOINT	NUMBER AT WHICH SOURCE REGION ENDS, ONLY FOR ISINDX =3
<b>CARD 4</b>	
TITLE	80 CHARACTERS ALLOWED
<b>CARD 5</b>	
JB(I)	REGION WHERE THE NODES START I=1, JRG
<b>CARD 6</b>	
IP1	INDEX, 1-PRINT, 0-NOT PRINT
IP2	INDEX FOR PRINTING PHOTON FLUX, 1-PRINT, 0-NOT PRINT
IP3	INDEX FOR PRINTING ANGULAR FLUX, 1-PRINT, 0-NOT PRINT
IP4	INDEX FOR PRINTING BUILDUP FACTOR, 1-PRINT, 0-NOT PRINT
IP5	INDEX FOR PRINTING CROSS SECTIONS OF REGIONS, 1-PRINT, 0-NOT PRINT
IP6	INDEX FOR PRINTING WAVELENGTH NODES, 1-PRINT, 0-NOT PRINT
IP7	INDEX FOR PRINTING FIRST COLLISION FLUX, IF ISINDX =1

IP8	INDEX FOR PRINTING VIRGIN FLUX, IF ISINDX =3
<b>CARD 7</b>	
NGENR	NUMBER OF GAMMA-RAY ENERGIES FOR THIS CALCULATION, REQUIRED IF IGRP=0
<b>CARD 8</b>	
SPEC (K)	SOURCE GAMMA-RAY ENERGIES, MEV
<b>CARD 9</b>	
XM(I)	SPACE NODE LOCATIONS IN MFP AT SOURCE ENERGY
<b>CARD 10</b>	
TITLE	TITLE FOR THE CROSS SECTION
<b>CARD 11</b>	
IE(L)	PAIR PRODUCTION CROSS-SECTION, 1-BARNS/ATOMS, 2-CM <sup>2</sup> /G
<b>CARD 12</b>	
RHO(I)	DENSITY OF REGION
ZE(I)	ATOMIC NUMBER OF REGION
A(I)	ATOMIC WEIGHT OF REGION
<b>CARD 13</b>	
NOE(I)	NUMBER OF GAMMA-RAY ENERGY POINTS @WHICH CROSS SECTIONS ARE GIVEN, < 36
<b>CARD 14</b>	
EN(I,N)	GAMMA-RAY ENERGY POINTS OF CROSS SECTIONS, MEV
<b>CARD 15</b>	
STE(I,N)	PHOTOELECTRIC CROSS SECTIONS OF REGION, B/ATOM
<b>CARD 16</b>	
ST(I,N)	TOTAL X-SECTION (W/OUT COHERENT SCATTERING)
<b>CARD 17</b>	
EABS (I,N)-	ENERGY ABSORPTION COEFFICIENTS, 3 SETS; M <sub>A</sub> /P, M <sub>K</sub> /P, M <sub>EN</sub> /P

## VITA

Graduate College  
University of Nevada, Las Vegas

Luis A. Durani

### Local Address:

11344 Altura Vista Dr.  
Las Vegas, NV 89138

### Home Address:

1003 Misty Mountain Rd. Unit 512  
Lynchburg, Va 24502

### Degrees:

Bachelor of Science, Mechanical Engineering, *Cum Laude* 2008  
University of Nevada, Las Vegas  
Bachelor of Arts, Political Science, *Cum Laude* 2008  
University of Nevada, Las Vegas

### Special Honors and Awards:

Highest GPA, Mechanical Engineering, Spring 2006-2007  
2<sup>nd</sup> Place Award, Fred and Harriet Cox Senior Design Competition, Spring 2008  
Dean's Honors List

### Publications:

Update to ANSI/ANS-6.4.3-1991 Gamma-ray Buildup Factors for Low-Z  
Engineering Materials and Compound.

Thesis Title: Update to ANSI/ANS-6.4.3-1991 for Low-Z and Compound Materials and  
Review of Particle Transport Theory

### Thesis Examination Committee:

Co-Chairperson, Dr. Charlotta Sanders, Ph.D., P.E.  
Co-Chairperson, Dr. Brendan O'Toole, Ph.D.  
Committee Member, Dr. Robert Boehm, Ph.D.  
Graduate Faculty Representative, Dr. Ralf Sudowe, Ph.D.